ECHOLCATION IN PREGANT AND LACTATING BIG BROWN BATS

SPECTRAL AND TEMPORAL CHARACTERISTICS OF ECHOLOCATION CALLS IN PREGNANT AND LACTATING BIG BROWN BATS

By

ALEXA CLARKE, Hons. BSc

A Thesis Submitted in Partial Fulfillment of the Requirements for the

Degree of Masters of Science

in the Department of Psychology, Neuroscience & Behaviour

Faculty of Science

McMaster University MASTER OF SCIENCE (2023) Hamilton, Ontario (Psychology)

TITLE: Spectral and temporal characteristics of echolocation calls in pregnant and lactating big brown bats

AUTHOR: Alexa Clarke, Hons. BSc (McMaster University)

SUPERVISORS: Dr. Paul A. Faure and Dr. John M. Ratcliffe (University of Toronto)

NUMBER OF PAGES: xvii, 221

Lay Abstract

The goals of this study were to see if big brown bats change the way that they echolocate while they are pregnant and/or nursing pups, and what changes occur. We did this by recording the vocal sounds bats made while they were pregnant and after they had given birth, and looking to see if there were any changes in the duration of echolocation calls, the time between individual sounds, the range of sound frequencies in each call, the central sound frequency in each call, and each call's sound pressure level over this time and compared to non-pregnant/nursing female big brown bats. We found that echolocation call duration increases over pregnancy and nursing pups, while frequency range and the centre frequency decreases.

Abstract

While they are pregnant and rearing pups, bats continue to leave their roosts to forage for food. Many bats use echolocation vocalizations as part of this process. Other mammalian species including primates experience changes in vocal characteristics during pregnancy and lactation. As echolocation is a vital tool for spatial navigation and prey detection in most bats, investigating echolocation characteristics during pregnancy through lactation may provide new insight into how reproduction, pregnancy and pup rearing influence vocalizations. We measured changes in mass and recorded echolocation calls of pregnant (n = 21) and non-pregnant (n = 2) female wild-caught big brown bats (*Eptesicus fuscus*) released by hand into roost emergence-like flight. Recording began ~15 days prepartum and ended when the last bat reached 34 days postpartum, when pups were expected to be weaned. Analyses were completed using MATLAB and R, primarily with repeated measures ANOVAs focused on echolocation calls present in the ~562 ms before and ~562 ms after take-off. Based on vocal changes experienced by humans during pregnancy and post-birth, correlations found between bat echolocation call characteristics and the effects of differences in mass on bat echolocation, we predicted that female bats in late-stage pregnancy would emit calls of shorter duration, longer pulse interval, narrower bandwidth, and lower centroid frequency compared to calls emitted by the same bat post-parturition and compared to non-pregnant bats, while source level remained unchanged. We found that pulse interval and source level did not change while pregnant/lactating or control bats were in flight, and that increases in call duration and decreases in centroid frequency and bandwidth in flight began in pregnancy and continued through the lactation period while remaining unchanged for the control bats.

Acknowledgments

First and foremost, thank you to my supervisors Dr. Paul Faure and Dr. John Ratcliffe for their guidance and support during this project, and to the other members of my supervisory committee, Dr. Sigal Balshine and Dr. Katrina Choe, for their valuable insights. I would also like to acknowledge the financial support of the Natural Sciences and Engineering Research Council of Canada Discovery Grants awarded to Dr. Faure and Dr. Ratcliffe that made conducting this research possible.

Immense gratitude to Dr. Lasse Jakobsen of the University of Southern Denmark for collaborating with us on data analyses and lending your MATLAB skills to this project. Also, thank you to Dr. Kazuma Hase and Dr. Katrina Deane for their help with learning to use MATLAB.

Data collection could not have happened without help from Sufal Deb and the other summer 2021 and 2022 members of the McMaster BatLab. You all put in so much work and I am so grateful for your help and support. Additional thanks to Renata Soljmosi and Shane Seheult for their help with editing this thesis.

Thanks to my friend Jack for the bat memes, book recommendations and reminders to take breaks. And thanks to my parents, aunts and uncles for their support while applying to master's programs.

Finally, thank you to Dr. Tim Ryan, Dr. Kathleen Delaney, Dawn Graham and the rest of the bat care staff at McMaster University's Central Animal Facility for their veterinary and animal care support. The McMaster captive bat colony could not function without you.

Table of Contents

List of Figures and Tables

List of Abbreviations and Symbols

ANOVA = analysis of variance

CF = constant frequency; a sound frequency that remains the same

dB = decibel; a logarithmic relative unit of sound level, one-tenth of a bel

F_0 = fundamental frequency; the lowest frequency element in a sound with multiple harmonics

FM = frequency modulated; a sound frequency that changes

ICC = intraclass correlation coefficient; a measure of association strength for a mixed-effects model denoting how much population variance the random effect(s) is responsible for (Maxwell et al., 2018, p.565); similarity between measurements in the same group from zero (no similarity) to one (complete similarity) for a mixed-effects model (Lüdecke et al., 2021)

IPI = interpulse interval; the time from the end of an echolocation call to the start of the next

PND = post-natal day; a day after being born

μ = mean

σ = standard deviation

Declaration of Academic Achievement

Alexa Clarke and Paul Faure designed the experiments, and Alexa Clarke conducted the experiments in June and July 2022 with help from the undergraduate students in the McMaster BatLab, particularly Sufal Deb. Alexa Clarke, John Ratcliffe (University of Toronto) and Lasse Jakobsen (Syddansk Universitet/University of Southern Denmark) analyzed the data. Lasse Jakobsen created the MATLAB program (Moonshine) used to extract information from the audio recordings. Alexa Clarke wrote and edited the thesis text, and created the figures and tables included. Renata Soljmosi and Shane Seheult provided suggested edits to the text.

Introduction

Bat Echolocation

Bats are unique in that they are the only mammals capable of flight. Another distinctive feature of many bat species is echolocation, though they share this skill with other mammals, such as toothed whales (Madsen & Surlykke, 2013). Echolocating bats emit sounds from their mouths or nostrils and use the resulting echoes to determine the physical characteristics of the surrounding environment, helping them to navigate, locate food and avoid predators (Jakobsen, Brinkløv, & Surlykke, 2013; Madsen & Surlykke, 2013). The sounds used in bat echolocation are frequency-modulated (FM) and/or constant-frequency (CF) depending on the species (Jones, 1999). For example, big brown bats (*Eptesicus fuscus*) echolocate using downward FM sweeps, where each call starts at a high frequency (~48 kHz) and ends at a relatively lower frequency (~27 kHz) while hitting all of the frequencies in between (Kurta & Baker, 1990). Other species that incorporate CF components into their echolocation, such as great Himalayan leaf-nosed bats (*Hipposideros armiger*), have echolocation calls that remain the same frequency for their entire duration (Fenton et al., 2011). The source of echolocation calls also varies between bat species. Most bats, including *E. fuscus*, are laryngeal echolocators, which means that they produce sounds for echolocation in their larynxes (Veselka et al., 2010; Mayberry & Faure, 2015). Other echolocating bats, such as Egyptian fruit bats (*Rousettus aegyptiacus*), use tongue clicks to produce echolocation sounds (Veselka et al., 2010).

Along with the aforementioned range of frequencies covered by each call (i.e., signal bandwidth), important temporal (time-related) and spectral (frequency-related) characteristics of bat echolocation include the duration of each call, the amount of time

separating each call (referred to as interpulse interval [IPI] when measured from the end of one call to the start of the next, and pulse interval when measured from the start of one call to the start of the next), fundamental frequency (F_0) when calls contain multiple harmonics, and measures of central tendency for a call's frequency range such as the spectral centroid/centroid frequency (Petrites et al., 2009; Jakobsen, Brinkløv, & Surlykke, 2013; Luo & Wiegrebe, 2016; Madsen & Surlykke, 2013). These characteristics of echolocation calls can be modified by bats. The temporal parameters (call duration and IPI/pulse interval) can be lengthened or shortened by a bat as needed for navigation and prey capture (Moss & Surlykke, 2001; Surlykke & Moss, 2000). For instance, insectivorous bats drastically shorten IPI/pulse interval by increasing their call repetition rate to up to 200 calls per second right before prey capture (Moss & Surlykke, 2001; Surlykke & Moss, 2000). Bats also modify IPI/pulse interval to create strobe groups, which are groups of at least two echolocation calls separated by similar IPIs/pulse intervals that are shorter than the IPIs/pulse intervals surrounding the group. Criteria that can be used to identify strobe groups were named the island and stability criteria by Kothari et al. (2014). The island criterion refers to the IPIs/pulse intervals directly before and after the strobe group being at least 1.2 times the duration of the IPIs/pulse intervals within the strobe group (Kothari et al., 2014). The stability criterion applies to strobe groups containing more than two echolocation calls and requires the IPIs/pulse intervals within a strobe group to all be within ±5% of the strobe group's mean IPI/pulse interval.

The intensity or source level (the sound pressure level 1 m away from a bat's mouth/nostrils on a horizontal axis assuming no atmospheric attenuation) of each echolocation call measured in decibels (dB), and the shape and direction of an

echolocation beam are also characteristics that impact the information a bat can gather about their environment (Jakobsen, Brinkløv, & Surlykke, 2013; Koblitz et al., 2010). Spectral parameters (bandwidth, F_0 and spectral centroid/centroid frequency) can be modulated by changing the sound produced in the larynx (or by tongue clicks) or using parts of the vocal tract (e.g., vocal folds) to filter the call, and in combination with changing amplitude (loudness) can be used to modify sound intensity (Mayberry & Faure, 2015; Luo & Wiegrebe, 2016). Bats emitting echolocation calls from their mouths can modulate echolocation beam dimensions and directionality by adjusting their mouth gape (Jakobsen, Brinkløv, & Surlykke, 2013). A bat widening its mouth gape by opening the mouth wider makes an echolocation beam that is narrower and more directional, allowing for focused observation of a part of the environment. Beam dimensions can also be modified through control of sound frequency, as use of higher frequencies results in a narrower, more focused sound beam (Jakobsen, Brinkløv, & Surlykke, 2013; Jakobsen, Ratcliffe, & Surlykke, 2013).

The physical characteristics of the specific environment being navigated can affect bats' echolocation modulation (Moss & Surlykke, 2001; Surlykke & Moss, 2000). For example, the presence or absence of obstacles (i.e., clutter) such as tree branches and leaves has been show to affect echolocation. Big brown bats use shorter IPIs while flying in areas cluttered with obstacles compared to in open spaces (Petrites et al., 2009; Surlykke & Moss, 2000). They also use shorter IPIs in lab settings such as anechoic flight rooms (~88 ms) than in open fields (~134-270 ms) and wooded areas (~122 ms), indicating lab settings are more cluttered than natural environments (Surlykke & Moss, 2000). Consistent with the use of shorter IPIs/pulse intervals in more cluttered

environments, the number of sonar strobe groups big brown bats produce increases with clutter (Kothari et al., 2014; Surlykke & Moss, 2000). Tracking prey in a cluttered environment further increases the number of strobe groups produced. Bats that use FM echolocation calls also tend to shift the frequencies of their calls in cluttered environments to avoid overlapping rapidly emitted new calls with echoes of the same frequencies leading to uncertainty about which calls the echoes belong to (Hiryu et al., 2010). In situations where bats use longer IPIs, echolocation calls tend to have longer duration (~14-20 ms), which is also correlated with lower frequency and narrower bandwidth (Surlykke & Moss, 2000).

Flight energetics can also influence echolocation. Energy use is required to produce echolocation calls and may be offset during flight by syncing emission of lower intensity (below 130 dB SPL) calls with exhalation (Currie et al., 2020; Koblitz et al., 2010; Speakman et al., 1989; Speakman & Racey, 1991; Voigt & Lewanzik, 2012). The force generated by the abdominal and flight muscles creates the pressure in the lower (subglottic) part of the larynx (i.e., subglottic pressure) that is needed to emit calls and results in echolocation calls being emitted on exhalation when a bat is flapping its wings upwards (Koblitz et al., 2010; Lancaster et al., 1995; Suthers et al., 1972). Multiple calls can be emitted during the time of this wing upstroke, such as when a bat is landing or approaching prey (Koblitz et al., 2010; Moss & Surlykke, 2001; Surlykke & Moss, 2000). When approaching a landing site, *E. fuscus* modulate the source levels of their grouped echolocation calls depending on when in the upstroke of their wings each call occurs. Koblitz et al. (2010) note a difference of 4 dB on average (maximum 12 dB) between the calls of lowest and highest intensity in a call group. These changes in source level are

thought to occur due to subglottic pressure changing as the wings move (Koblitz et al., 2010).

Bat Behaviour During Pregnancy and Lactation

In spring, female big brown bats gather into maternity colonies (~25-75 individuals) that roost either in natural structures (e.g., hollow trees) or in manmade structures (e.g., attics) for the duration of pregnancy, nursing, and weaning pups (Fenton & Barclay, 1980; Kurta & Baker, 1990; Kunz et al., 1995). Early on, maternity colonies may include adult males, but they most often remain separate from females throughout the summer (Fenton & Barclay, 1980; Kurta & Baker, 1990). Thus, males do not help raise pups, nor do they provide for females they have mated with.

Female big brown bats' energetic costs (including sustaining pregnancy, producing milk and metabolic processes) increase from the later half of gestation (~48.9 kJ/day) to lactation (~105.1 kJ/day) and lead to a corresponding increase in feeding requirements from approximately 8.0 g/day to approximately 17.2g/day of insects (Kurta et al., 1990). Indeed, feeding rates in the insectivorous Mexican free-tailed bat (*Tadarida brasiliensis*) increase until late into gestation and again during lactation (Kunz et al., 1995). In little brown bats (*Myotis lucifugus*), lactating females leave their pups in the roost and stay close while foraging, returning frequently over the course of the night to care for them (Henry et al., 2002). In contrast, pregnant *M. lucifugus* forage further from their roost and usually do not return there during the night, suggesting that *M. lucifugus* change foraging behaviour between pre- and post-parturition to account for changes in energy requirements (Henry et al., 2002). Similar patterns of foraging behaviour are

found in big brown bats, such that lactating females go on shorter foraging trips more frequency throughout the night than pregnant females (Rintoul & Brigham, 2014).

Effects of Pregnancy and Lactation on the Body and Voice

Pregnancy and lactation lead to many changes in a female bat's body that could also impact echolocation in various ways. A female bat's mass increases during pregnancy influenced in part by the number of fetuses she is carrying (i.e., litter size), which varies across species (Barclay et al., 2004). For instance, many bat species of the Americas give birth to single pups (*Myotis leibii*, *M. lucifugus*, *Myotis septentrionalis*, *E. fuscus*, *Lasionycteris noctivagans*) or twins (*E. fuscus*, *L. noctivagans*, *Perimyotis subflavus*), but other species can have litters of up to four (*Lasiurus cinereus*) or five (*Lasiurus borealis*) pups (Best & Jennings, 1997; Caceres & Barclay, 2000; Fenton & Barclay, 1980; Fujita & Kunz, 1984; Kunz, 1982; Kurta & Baker, 1990; Shump Jr. & Shump, 1982a; Shump Jr. & Shump, 1982b). The length of the gestation period also varies across these species, ranging from ~44 days in *P. subflavus* to ~90 days in *L. borealis* (Fujita & Kunz, 1984; Shump Jr. & Shump, 1982a). The gestation period for *E. fuscus* is ~60 days, during which time twin fetuses grow to ~20 percent of their mother's postpartum body mass, which is ~16.5 g in the wild (Kurta & Baker, 1990). After birth, *E. fuscus* pups feed on milk that their mothers produce until they transition fully to solid food upon reaching ~70 percent of their adult body mass (Hood et al., 2006). This lactation period lasts until approximately post-natal day (PND) 35. During lactation, the bodies of mother bats adjust how they store fat to be able to meet the energy needs of themselves and their pups, but mother's body mass does not change significantly over this period (Hood et al., 2006).

Body mass increase during pregnancy and decrease after parturition should lead to a corresponding increase and decrease in wing loading (the ratio of body mass to wing area), which could impact aspects of flying such as flight speed or wing beat frequency (Hughes & Rayner, 1993; Norberg & Rayner, 1987). The square root of a bat's wing loading is related to flight speed such that a bat with higher wing loading would fly faster (Norberg & Rayner, 1987). Based on this alone we might expect that pregnant bats with higher wing loading would fly faster. However, this trend is found between different bat species, not between conspecific individuals. Within the same species, heavier (e.g., pregnant) bats have been found to have a reduction in flight speed compared to lighter (e.g., non-pregnant) bats (Hughes & Rayner, 1993; Taub et al, 2023). Slower flight speed leads to increased wing flapping to keep bats in the air, so wing loading increase during pregnancy and decrease after parturition could be correlated with corresponding increases and decreases in the frequency of wingbeat cycles (Hughes & Rayner, 1993; Koblitz et al., 2010; Norberg & Rayner, 1987). Increases in wingbeat frequency during pregnancy could lead to increases in the number of calls emitted, causing pulse interval to decrease. During lactation wingbeat frequency could decrease, leading to a corresponding decrease in the number of calls emitted.

Wing aspect ratio is a unitless ratio of wingspan squared to wing area. It impacts aerodynamic efficiency and energy loss during flight, such that between species bats with higher wing aspect ratios would be more aerodynamically efficient and use less energy in flight (Norberg & Rayner, 1987) Aspect ratio should not change over pregnancy and lactation, as it is not dependent on a bat's mass.

Pregnancy affects vocal characteristics, primarily demonstrated in humans (Cassuraga et al., 2012; Ghaemi et al., 2020; Hamdan et al., 2009; Hancock & Gross, 2015; Saltürk et al., 2016). When pregnant people are closest to giving birth (~30 to 41 weeks of pregnancy) they have significantly shorter maximum phonation times (MPT; length of time they could continuously produce a single sound) than non-pregnant people (Cassuraga et al., 2012; Hamdan et al., 2009). Their MPTs shorten during pregnancy and increase after parturition (Ghaemi et al., 2020; Hamdan et al., 2009; Saltürk et al., 2016). If bats experience a similar phenomena during pregnancy, then echolocation call duration could decrease during the gestation period and increase after bats gave birth (Cassuraga et al., 2012; Ghaemi et al., 2020; Hamdan et al., 2009; Saltürk et al., 2016). Pregnant people's voices have similar fundamental frequency (F_0) to non-pregnant controls, but higher F_0 compared to controls following parturition (Cassuraga et al., 2012; Hamdan et al., 2009). If bats experience a similar increase in the F_0 of their echolocation calls after parturition (which could also be measured as an increase in centroid frequency), then the frequency range of echolocation calls could change during lactation. Relatedly, increase in body mass during pregnancy has been found in some bats to be correlated with lower frequency echolocation calls, so pregnant bats could also use lower centroid frequencies compared to non-pregnant bats (Taub et al., 2023).

In rats, thickening and thus an increase in mass of the vocal cords during pregnancy has been observed and could explain complaints of vocal fatigue (increased effort to produce sounds) in pregnant humans (Hamdan et al., 2009; Şanal et al., 2016). If bats experience vocal cord thickening during pregnancy as rats do, then they may adjust their echolocation behaviour due to vocal fatigue (Şanal et al., 2016). This could involve

an increase in IPI/pulse interval used such that pregnant bats produce fewer calls over time compared to non-pregnant controls. Longer pulse interval would likely be correlated with longer call duration, narrower bandwidth, and lower frequency in general (Moss & Surlykke, 2001; Surlykke & Moss, 2000).

During human pregnancy the force produced by the abdominal and respiratory muscles that bats use to power echolocation remains the same as in non-pregnant humans (Lancaster et al., 1995; LoMauro et al., 2019). If this force production is similarly preserved in bats, then pregnant bats may show similar patterns of source level modulation to non-pregnant control bats, such that source level does not change significantly over pregnancy and lactation or differ significantly from controls (Lancaster et al., 1995; LoMauro et al., 2019; Koblitz et al., 2010).

The Current Study

The aforementioned findings lead us to predict that there are changes in echolocation behaviours of *E. fuscus* during pregnancy and lactation. Taub et al. (2023) recorded longer call durations and IPIs/pulse intervals in pregnant Kuhl's pipistrelles (*Pipistrellus kuhlii*) than in post-lactating, non-pregnant *P. kuhlii*. However, they were unable to follow bats through the lactation period. In this study, we look at the pulse interval, call duration, bandwidth, centroid frequency and source level of *E. fuscus* echolocation calls over the course of pregnancy and lactation. We recorded the calls of pregnant females and a control group of non-pregnant females over the course of the pregnant females' gestation and lactation periods. Bats were recorded while being released by hand into a vertical drop to mimic emergence from a roost. We compare call characteristics within individual bats (before and after parturition) and between the

pregnant/lactating and control bats to determine if there are changes in echolocation behaviour.

Our hypothesis is that echolocation will change with change in mass across these reproductive stages. We predict that pregnant bats will increase the pulse interval, shorten the duration, narrow the bandwidth, and decrease the centroid frequency of their echolocation calls through pregnancy and when compared to control bats, but not change their calls' source level (Lancaster et al., 1995; Moss & Surlykke, 2001; Surlykke & Moss, 2000). We also predict that these features will begin to rebound to pre-pregnancy/control values after bats give birth (Hamdan et al., 2009). The predicted spectral changes are based on correlations found in previous studies of bats. Weight gain during pregnancy has be correlated with lower frequency echolocation calls, and lower call frequency has been correlated with narrower bandwidth as well as longer IPI/pulse intervals (Moss & Surlykke, 2001; Surlykke & Moss, 2000; Taub et al., 2023). The predicted temporal changes are also based on the assumption that pregnant/lactating bats will be similar to other pregnant/lactating mammals, such that shortened MPTs and vocal fatigue seen in pregnant humans would translate to shortened call durations and increased effort to produce echolocation calls in pregnant bats, and the latter lead to a reduction in the number of calls produced and thus reduced IPI/pulse interval (Cassuraga et al., 2012; Ghaemi et al., 2020; Hamdan et al., 2009; Saltürk et al., 2016; Şanal et al., 2016). Similarly, preservation of abdominal and respiratory muscle activity in pregnant humans leads us to predict that if this muscle activity is also preserved in pregnant bats then the force needed for generating subglottic pressure to produce echolocation calls will not be affected by pregnancy, so call source level will be unchanged (Lancaster et al., 1995;

LoMauro et al., 2019; Koblitz et al., 2010). How bats change their echolocation calls and signaling behaviour during pregnancy and lactation will provide new insight into how reproduction, pregnancy and rearing pups influences acoustic signaling and perception.

Methods

Animal Collection

Wild big brown bats (*Eptesicus fuscus*) captured May 20 and 23, 2022 from two detached houses in Puslinch, Ontario (referred to as the Valens [May 20] and Abby [May 23] roosts) were housed in wire mesh cages in the McMaster University Psychology Animal Facility over the course of recording. The cages were generally 28 × 22 × 18 cm (length × width × height; there was some variation in cage length) and after all pregnant bats (n = 20) had given birth there were at most six bats (two mothers and four pups) per cage. Bats were given *ad libitum* access to food (mealworms, *Tenebrio molitor*) and water, and were removed from their cages during recording. After recording was completed, bats were moved to the quarantine side of a larger husbandry facility (250 × 150 × 225 cm), which was a separate cage from the pre-existing members of the captive *E. fuscus* colony. There they had the same access to food and water, as well as the ability to fly freely within their large cage.

Subjects

Our subjects were 24 female big brown bats, of which 22 were pregnant at the time of capture and two were not. Two pregnant (one pre-birth and one during birth) bats, four lactating (post successful birth) bats and one non-pregnant bat died during the recording period, so we could not collect full data sets for them. All pregnant bats (apart

from the two deceased) successfully gave birth between June 9, 2022 and June 17, 2022 (inclusive), mostly to twins (19/20 births, 95% twins). The pups of two bats (three pups total) died before recording was completed. Each of the adult female bats was identified by a coloured and numbered (e.g., Grey 53) plastic split-ring band placed on their left forearm. Grey 88 and Grey 92 were the non-pregnant control bats, of which Grey 88 passed away on July 2, 2022. Data from subsets of this group of females were used for wing loading, wing aspect ratio and echolocation call analyses, described in Table 1.

Table 1: Bats that had data analysed, which roost they were from, what type of data they had analysed, and, when applicable, recording days removed from the data set.

Bat	**Roost**	**Reproductive status**	**Wing loading/aspect ratio data analysed?**	**Recording data analysed?**	**Days re parturition removed from data set**
Grey 53	Valens	Pregnant/lactating	Yes	Yes	-6
Grey 54	Valens	Pregnant/lactating	No	Yes	None
Grey 56	Valens	Pregnant/lactating	Yes	Yes	22
Grey 58	Valens	Pregnant/lactating	Yes	No	n/a
Grey 82	Valens	Pregnant/lactating	Yes	Yes	None
Grey 83	Valens	Pregnant/lactating	No	Yes	9
Grey 85	Valens	Pregnant/lactating	Yes	Yes	28
Grey 86	Valens	Pregnant/lactating	No	Yes	None
Grey 87	Valens	Pregnant/lactating	Yes	Yes	None
Grey 88	Valens	Non-reproductive	No	Yes	None
Grey 92	Valens	Non-reproductive	No	Yes	None
Grey 93	Valens	Pregnant/lactating	Yes	No	n/a
Grey 94	Valens	Pregnant/lactating	Yes	Yes	None
Grey 95	Abby	Pregnant/lactating	Yes	No	n/a
Grey 96	Abby	Pregnant/lactating	Yes	No	n/a
Grey 97	Abby	Pregnant/lactating	Yes	Yes	16
Grey 98	Abby	Pregnant/lactating	Yes	No	n/a

Recording Setup

Recordings were conducted in the 3.48 × 3.25 × 2.76 m section of an anechoic room in which the walls were lined with approximately 3.7 cm thick Sonex Classic acoustic foam. The microphone array used for recording was positioned along one 3.48 × 2.76 m wall and consisted of two perpendicular aluminum T-slot tracks (3.5 cm wide) attached to and offset 10.5 cm from the wall to which eleven GRAS 46BE 1/4" CCP free-field microphones were attached with wooden dowels (Appendix Figure 1). There were seven microphones on the horizontal axis and five on the vertical axis (two above the horizontal, two below, and one in the centre of the array included in the pervious seven microphones), for eleven microphones and eleven recording channels total. There was approximately 40 cm between neighbouring microphones and the ends of the microphones were approximately 56 cm from the wall. The aluminum T-slot tracks were wrapped in cotton batting to minimize echoes. The wall to the left side of the array was 1.27 m long and ended at a 1.35 × 1.96 m area continuous with the rest of the room where the other recording equipment (e.g., computer with Avisoft-RECORDER software) was set up (Appendix Figure 2). A twelfth recording channel was set up to record ambient noise in the room using an Avisoft-Bioacoustics CM16/CMPA condenser ultrasound microphone, which was placed approximately 2.95 m across the room from the aluminum structure of the array and elevated about 50 cm above the floor using a retort stand. A full list of recording equipment can be found in Appendix Table 1.

Recording Procedure

Echolocating bats were recorded individually with no other bats in the room. One handler and one note-taker were present during recording. If pups were attached to their

mother's teat at the time she was to be recorded, they were detached using a blunt probe inserted into the pup's mouth. Pups remained in a separate room during recordings and were reattached to their mother after she had been recorded. The mass of each adult bat in grams was taken before they were recorded. Bats were released about 1.41 m from the centre of the microphone array at about 1.80 m above the floor by allowing them to hang from the handler's hand until they took flight, prodding them into take-off if needed. Each recording was manually triggered when a bat left the handler's hand. Recordings were taken with Avisoft-RECORDER software using a 375 kHz sampling rate and 8-bit format and saved as .wav files. Each recording lasted for seven seconds total, with a pre-trigger time of two seconds and a hold time of five seconds, regardless of how long the bat was in flight. Each bat was released and recorded at least three times per recording session, with additional recordings taken until the bat had flown in the direction of the array for three recordings. The exception to this was when recording sessions were terminated early due to concerns for the bat's health observed before or during recording. Before each day of recordings, the microphone array was calibrated by placing a GRAS 42AB sound calibrator over the grid of a microphone and recording five seconds of audio from the sound calibrator, repeating for each of the eleven microphones. The calibration audio was recorded starting at the microphone on the far left (microphone 1) of the array and ending at the microphone on the bottom of the array (microphone 11), going from left to right and then top to bottom (Appendix Figure 1). Microphone grids were removed during recording.

The recording period was from June 1, 2022 to July 20, 2022 (inclusive). Before pregnant bats gave birth, pregnant and non-pregnant bats were assigned to one of three

groups that were recorded on alternating weekdays (excluding June 2, 2022 due to an equipment malfunction). The earliest that pregnant bats ended up being recorded was fifteen days before they gave birth. After parturition, lactating bats were recorded every three days starting on PND4 and non-lactating bats were recorded every two to three days (excluding June 19, 2022 due to scheduling conflicts; bats who would have been recorded that day were instead recorded the day before and after). Lactating bats were recorded until PND34 and non-pregnant controls were recorded up until the last lactating bat reached the end of her recording period, barring attrition. After June 29, 2022, the control bats had their recording schedule changed to couple them with the same lactating bats for the remainder of their recording period. Grey 88 was recorded on the same days as Grey 82, Grey 85, Grey 87 and Grey 94 (Green Group), who all had the same parturition day. Similarly, Grey 92 was recorded on the same days as Grey 53, Grey 54 and Grey 86 (Blue Group). Grey 88 was only able to be recorded until PND19 for Green Group before passing away, while Grey 92 finished recordings at PND34 for Blue Group.

Recording Analysis

The pregnant/lactating bats with at least three days of prepartum recordings were initially selected to be included for analyses. Of these bats, six had wing loading data (Table 1). Also included in analysis were the two control bats (Grey 88 and Grey 92) and one pregnant/lactating bat (Grey 94) whose mass was considered to be slightly more similar to that of wild big brown bats (i.e., ~11-23 g in early pregnancy and late post-parturition) than captive bats (Kurta & Baker, 1990). In total, recordings from twelve bats (ten pregnant/lactating and two control) were chosen to be analysed. The selected recordings were run through a custom MATLAB program (Moonshine, created by Dr.

Lasse Jakobsen, University of Southern Denmark) to generate echolocation call duration, pulse interval, centroid frequency, minimum frequency, maximum frequency and source level values for each recording, as well as to map each bats' flight path. A custom script in MATLAB version 9.13.0 (R2022b) was used on each recording to mark what was judged by eye to be the call number of the take-off call in each flight path (The MathWorks Inc., 2022). This was done so that we would know which calls occurred in flight.

Another custom MATLAB script was used to extract the previously listed call characteristics and the take-off call numbers into Microsoft Excel spreadsheets. Minimum and maximum frequencies were used to calculate and extract bandwidth (maximum frequency minus minimum frequency). Some bats had multiple usable recordings (i.e., detectable echolocation calls) per day. In those cases, the recording taken earliest in the day was used for analyses. Call characteristics were organized by bat, recording date and recording day in relation to parturition day (for pregnant/lactating bats), with a separate spreadsheet for each characteristic. The call number for each data point was labeled and the take-off call number included in a separate column in each spreadsheet. At this stage, Grey 83 (a pregnant/lactating bat) was removed from the data set due to only having one usable day of recordings. The tables in these spreadsheets were then transformed into long format tables in R version 4.2.3 (R Core Team, 2023). They were imported into R using the read_excel() function in the *readxl* package, transformed using the pivot_longer() function in the *tidyr* package, and finally exported into a new Excel file with a separate spreadsheet for each call characteristic using the write_xlsx() function in the *writexl* package (Ooms, 2023; Wickham & Bryan, 2023;

Wickham, Vaughan & Girlich, 2023). Hereafter, only data from these long format tables were used.

Line plots were created in MATLAB version 9.14.0 (R2023a) of each call characteristic over time within each recording (The MathWorks Inc., 2023). To do this, first time points had to be added to the data tables in Excel. The first call in each recording was set to have occurred at the time point of zero milliseconds, then the first pulse interval was added to get the time point of the second call, the second pulse interval added to get the time point of the third call, and so on for all remaining calls in the recording. The total time did not up to seven seconds for every recording due to calls not always being present at the very start and end of recordings. The data tables were then imported into MATLAB. To create line plots for each call characteristic, two separate custom MATLAB functions were written for the pregnant/lactating bats and the control bats. This was so that pregnant/lactating bat plots could be labeled with bat ID and recording day in terms of parturition day (with parturition day set to zero), while control bat plots were labeled with bat ID and the date they were recorded. The corresponding functions were run for each bat and the resulting line plots saved as PNG files (Appendix Figures 4-8). The line plots for each call characteristic were arranged on Excel spreadsheets in rows by bat ID and in columns by recording day so they could be referred to easily. To compare pregnant/lactating bats to control bats, control bats were matched with pregnant/lactating bats recorded on the same date such that control bat data were in a temporal order that spanned pre-birth and post-birth for the pregnant/lactating bats. When matching a control bat with a pregnant/lactating bat was not possible (i.e., it placed

multiple dates of recordings on the same day), control bat data was assigned recording days based on the amount of time between recording dates.

To standardize the length of time from which echolocation calls to analyse were selected, the mean ($\mu \approx 562.10$ ms) and standard deviation ($\sigma \approx 135.37$ ms) of the length of time where echolocation calls were present after take-off for all bats on all days were calculated in R version 4.2.3 (R Core Team, 2023). The mean was used as the length of time before and after take-off to include in analyses. Where the length of time of the mean stretched to before the time point of zero milliseconds or after the time point of the last call in the recording, standard deviations were subtracted from the start and the end of the total time frame (Table 2) so that there was an equal length of time before and after take-off that fell within the time where echolocation calls were present. Grey 53 on day -6, Grey 56 on day 22, Grey 85 on day 28 and Grey 97 on day 16 did not have enough echolocation calls within the calculated time frames to identify strobe groups before and after take-off (i.e., less than three calls), and so had these days removed from the data set (Table 1).

Table 2: Bats for which a time frame of less than ~1124 ms was analyzed on the given days relative to parturition. All bats were pregnant/lactating bats. The number of standard deviations ($\sigma \approx 135.37$ ms) subtracted from the start and end of the ~1124 ms time frame to get the time frame used is represented as σ multiplied by the number of standard deviations.

Bat	**Day**	**Number of Standard Deviations**	**Time Frame Analyzed**
Grey 53	-9	3σ	311.75 ms
Grey 56	16	2σ	582.50 ms
Grey 82	28	3σ	311.75 ms
Grey 85	25	3σ	311.75 ms
Grey 87	4	2σ	582.50 ms
	8	3σ	311.75 ms
	10	3σ	311.75 ms
	28	2σ	582.50 ms

Strobe groups were identified with Kothari et al.'s (2014) island and stability criteria using a custom R script, manual calculations and manual observation of the pulse interval line plots created previously (Appendix Figure 2). Each pulse interval was labeled as belonging to a doublet (two calls) or higher-order (more than two calls) strobe group, or as not belonging to a strobe group if it did not meet the criteria (Kothari et al., 2014). Stacked bar plots (Figure 8) were created of the number of each type of pulse interval in each bat's recordings per day using the *ggplot2* package in R (Wickham, 2016). The percentage of strobe groups in relation to the total number of pulse intervals, and the number of strobe groups before and after take-off were calculated per day for each bat.

Statistical analyses were performed using the *lmerTest* and *performance* packages in R (Kuznetsova et al., 2017; Lüdecke et al., 2021). Recording data were imported into R using the *readxl* package (Wickham & Bryan, 2023). Linear mixed models were created for pre and post take-off rather than the entire recording period by using the filter() function from the *dplyr* package to split the data sets by call number at the take-off call number we determined for each recording (Wickham, François et al., 2023). Using *lmerTest*, day was modeled as a fixed factor, bat ID as a random factor allowed to vary by day, and echolocation call characteristic (call duration, pulse interval, centroid frequency or bandwidth) as the response variable (Kuznetsova et al., 2017). The linear mixed models were used to generate Type III analysis of variance tables with Satterthwaite's method and ANOVA-like tables for random-effects (using single term deletions) for before and after bats took flight. The same method was used to compare strobe group number and strobe group percentage between bats, with models using day as

the fixed factor, bat ID as the random factor, and strobe group number/percentage as the response variable.

Source level was analyzed differently from the other call characteristics due to the requirements for detecting source level (i.e., that a bat must be directly facing the microphone array to measure source level) resulting in there being many fewer data points compared to the other characteristics (Appendix Figure 5). Linear mixed models were created for the entire recording period as well as for before and after take-off. These models had day and call duration as fixed factors, bat ID as the random factor, and source level as the response variable. Another linear mixed model was used to compare mean source levels across days for each bat, with day as a fixed factor, bat ID as a random factor, and mean source level as the response variable. Mean source levels were not divided into before and after take-off.

Adjusted and unadjusted intraclass correlation coefficients (ICC) were calculated for each ANOVA using the icc() function in the *performance* package to see how similar each call characteristic was within and between the groups of pregnant/lactating and control bats (Lüdecke et al., 2021). Each characteristic within the same bat was more similar between days when ICCs were closer to one, whereas ICCs closer to zero indicated that characteristics were less similar within the same bat, and thus more similar between bats. Cohen's f was calculated for each ANOVA as a measure of effect size using the cohens_f() functions in the *effectsize* package (Ben-Shachar et al., 2020). The magnitude of Cohen's f corresponded with the magnitude of the standard deviation of echolocation call characteristic means. A Cohen's f of around 0.1 was considered small, of around 0.25 medium/moderate and of around 0.4 large (Maxwell et al., 2018, p. 126).

Wing Loading Estimation

On July 19, 2022, July 20, 2022 and August 23, 2022, the outlines of the right wing and the right half of the tail membrane were traced onto 0.5 cm grid paper for twelve pregnant/lactating bats (Table 1) that were not still being recorded. The wings and tail membrane for each bat were traced separately on the same piece of grid paper due to bat movement making tracing them together difficult, so the pages were digitized and Microsoft Paint or Paint 3D (if the tail membrane tracing needed to be rotated) were used to move the outline of the tail membrane so that it connected with the wing. The outline of the right half of the body was approximated using a rectangle drawn in Paint/Paint 3D from the tip of the tail membrane to the right shoulder, with the top left corner of the rectangle positioned at approximately the base of the neck. The part of the rectangle that fell outside the wing and tail membrane outlines was excluded from the estimated area (Appendix Figure 3). The area where the head would have been was also excluded. The number of 0.5 × 0.5 cm grid squares inside the outlines was counted and used to estimate the area of the right wing and the right halves of the tail membrane and body by multiplying the number of squares by 0.25 cm^2. This area was then doubled to get the total surface area and converted into metres squared (m^2) for use in calculations. This procedure was based on Norberg and Rayner's (1987) paper. Grey 88, a control bat, had its right wing and tail membrane traced on August 28, 2023, having been frozen since it passed away. The estimation of area described previously was done on paper rather than digitally for this bat, but followed the same procedure apart from the tail membrane tracing not being moved to line up with the wing tracing. Instead, the wing and the tail membrane were traced together, and when the tail membrane from that tracing was too

stretched out to use in the area estimate the retraced tail membrane had where it attached to the wing marked so that overlapping areas were not counted.

To calculate wing loading (WL) we used the equation from Norberg and Rayner's (1987) paper such that the mass (M) of a bat collected from the day it was caught until between PND34 to PND37 (inclusive) was converted from grams into kilograms (kg), multiplied by acceleration due to gravity ($g = 9.81\ m/s^2$) and divided by the total surface area (SA) in metres squared:

$$WL = \frac{M \times g}{SA}$$

Calculations of wing loading were done using a custom script in R version 4.2.3 (R Core Team, 2023). The package *readxl* was used to import bat mass data from an Excel spreadsheet (Wickham & Bryan, 2023).

Wing Loading Analysis

One-way within-subjects analysis of variance (ANOVA) was used to compare the wing loadings over pregnancy and lactation, over pregnancy only (ending at parturition), and over lactation only (beginning at parturition) for all twelve bats. The R package *lmerTest* was used to create linear mixed models with bat ID modeled as the random factor, day (from -23 to 37 in terms of parturition day set to zero) modeled as the within-subjects factor and wing loading as the response variable (Kuznetsova et al., 2017). These were used to generate Type III analysis of variance tables with Satterthwaite's method and ANOVA-like tables for random-effects (using single term deletions) for each period of time.

Aspect Ratio Estimation

The same wing tracings as for estimating wing loading were used to estimate wing aspect ratio. Aspect ratio (A) is the square of the wingspan (S^2) divided by the wing surface area (SA):

$$A = \frac{S^2}{SA}$$

The same wing surface areas as for estimating wing loading were used when calculating aspect ratio. To get the wing spans, MS Paint was used to place a straight line from the tip of the wing to the far edge of the "body" rectangle added to the wing tracings while estimating the surface area. The number of 0.5 × 0.5 cm grid squares that would lie along that line was estimated by measuring the length of the line and the length of one side of a grid square using a clear ruler while the image was set to a level of magnification for which the whole page of grid paper was visible (53% - 100%), and then dividing the length of the line by the length of the grid square to get the number of squares. The number of squares was multiplied by 0.5 cm to get the actual length of the line and then doubled to get the wingspan. For Grey 88, a line was physically drawn across the wing tracing in the same way as for the digitized wing tracings, measured with a ruler and that length doubled to get Grey 88's wingspan. Calculated aspect ratios are presented in Table 3.

Aspect Ratio Analysis

The mean and standard deviation of the twelve pregnant/lactating wing aspect ratios were calculated using the base R functions mean() and sd().

Results

Wing Loading Increases During Pregnancy

The wing loading of the 12 pregnant/lactating bats increased significantly during pregnancy ($F = 128.7$, $p = 2.071 \times 10^{-7}$) and decreased significantly during lactation ($F = 4.8662$, $p = 0.04971$). The increase in wing loading during pregnancy was larger than the decrease after the bats gave birth (Figure 1). Grey 88 (control bat) had a continuous increase in wing loading over a comparable time that was not as steep as the pregnant/lactating bats' increase or decrease in wing loading.

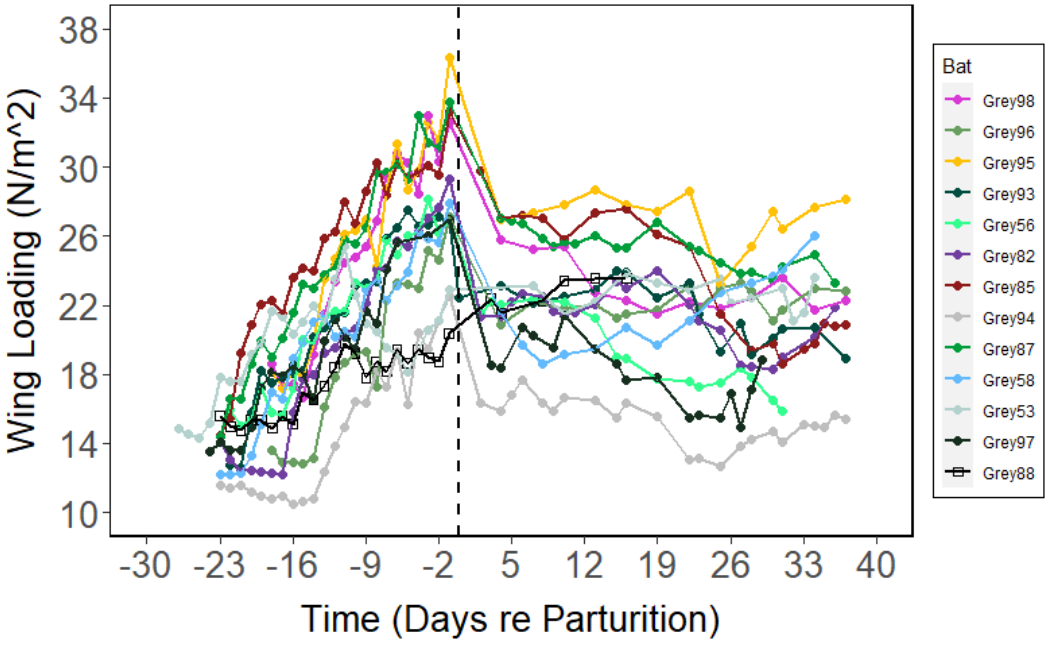

Figure 1: Wing loading over pregnancy and lactation as a function of days relative to parturition (dashed vertical line) for thirteen individual bats (Grey 98, Grey 96, Grey 95, Grey 93, Grey 56, Grey 82, Grey 85, Grey 94, Grey 87, Grey 58, Grey 53, Grey 97 and Grey 88 [control]).

Aspect Ratio Remains Unchanged During Pregnancy and Lactation

The aspect ratios presented in Table 3 were assumed to remain the same throughout the pregnancy and lactation periods due to aspect ratio being unaffected by changes in mass. The aspect ratios for the pregnant/lactating bats ($\mu = 7.48$, $\sigma = 1.01$) and for the control bat are higher than the aspect ratio of 6.40 reported by Norburg and Rayner (1987) for *E. fuscus*.

Table 3: Wing aspect ratios for 12 pregnant/lactating bats ($\mu = 7.48$, $\sigma = 1.01$) and one control bat (Grey 88).

Bat	**Aspect Ratio**
Grey 53	6.66
Grey 56	7.55
Grey 58	9.75
Grey 82	8.22
Grey 85	6.73
Grey 87	7.11
Grey 93	6.77
Grey 94	6.68
Grey 95	7.19
Grey 96	9.02
Grey 97	7.33
Grey 98	6.75
Grey 88	6.54

Call Duration in Flight Increases During Pregnancy and Lactation

There was a significant difference in echolocation call durations over the recording days between bats both before ($p < 0.05$) and after ($p < 0.001$) take-off (Table 4). The ICCs were closer to one after take-off (adjusted ICC = 0.545, unadjusted ICC = 0.522) than before take-off (adjusted ICC = 0.316, unadjusted ICC = 0.310). Cohen's f was 0.23 before take-off and 0.31 after take-off, both indicating that a moderate amount of the variance in call durations could be explained by the day. The call durations used by pregnant/lactating bats increased significantly across pregnancy and lactation ($p < 0.001$) and during the lactation period alone ($p < 0.01$), both only after bats had taken flight (Figures 2 to 5). There was no significant change during lactation before flight or during pregnancy alone. The control bats had a significant increase in call duration before flight ($p < 0.01$) but not during flight. Pregnant/lactating bats also used longer call durations on average than control bats while bats were in flight (Figure 5). Consistent with the ICCs close to zero, pregnant/lactating and control bats before take-off used calls of similar durations on average (Figure 3).

Table 4: F- and p-values for call duration repeated measures ANOVAs used to test change in call duration over time. A p-value ≤ 0.05 is considered significant

	Before Take-off			**After Take-off**		
Group	**Fixed Effects**	**Random Effects**		**Fixed Effects**	**Random Effects**	
	Day	**Day:Bat**	**Bat**	**Day**	**Day:Bat**	**Bat**
All bats	F = 6.6647 p = 0.01101	$p < 2 \times 10^{-16}$	p = 0.01135	F = 11.667 p = 0.0008585	$p < 2 \times 10^{-16}$	p = 0.0006649
Pregnant and lactating	F = 3.8852 p = 0.05144	$p < 2 \times 10^{-16}$	p = 0.08532	F = 11.69 p = 0.0008987	$p < 2 \times 10^{-16}$	p = 0.0183
Pregnant	F = 0.0287 p = 0.8671	p = 4.782×10^{-5}	p = 0.2754	F = 0.7313 p = 0.4051	p = 3.057×10^{-8}	p = 0.003942
Lactating	F = 1.7545 p = 0.1893	$p < 2.2 \times 10^{-16}$	p = 0.003361	F = 8.4428 p = 0.004788	$p < 2 \times 10^{-16}$	p = 0.01151
Control	F = 14.774 p = 0.001159	p = 0.04707	p = 4.283×10^{-5}	F = 0.1148 p = 0.7382	p = 0.0002018	p = 0.0028331

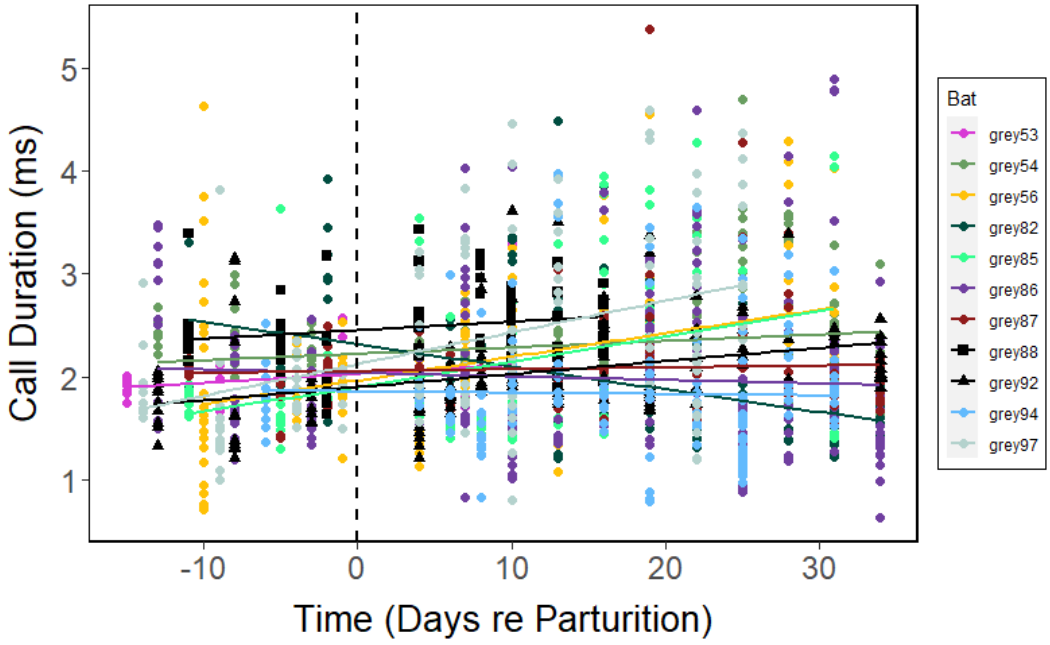

Figure 2: Call duration before take-off over pregnancy and lactation as a function of days relative to parturition (dashed vertical line) for nine pregnant/lactating and two control (Grey 88 and Grey 92) bats with linear trend lines.

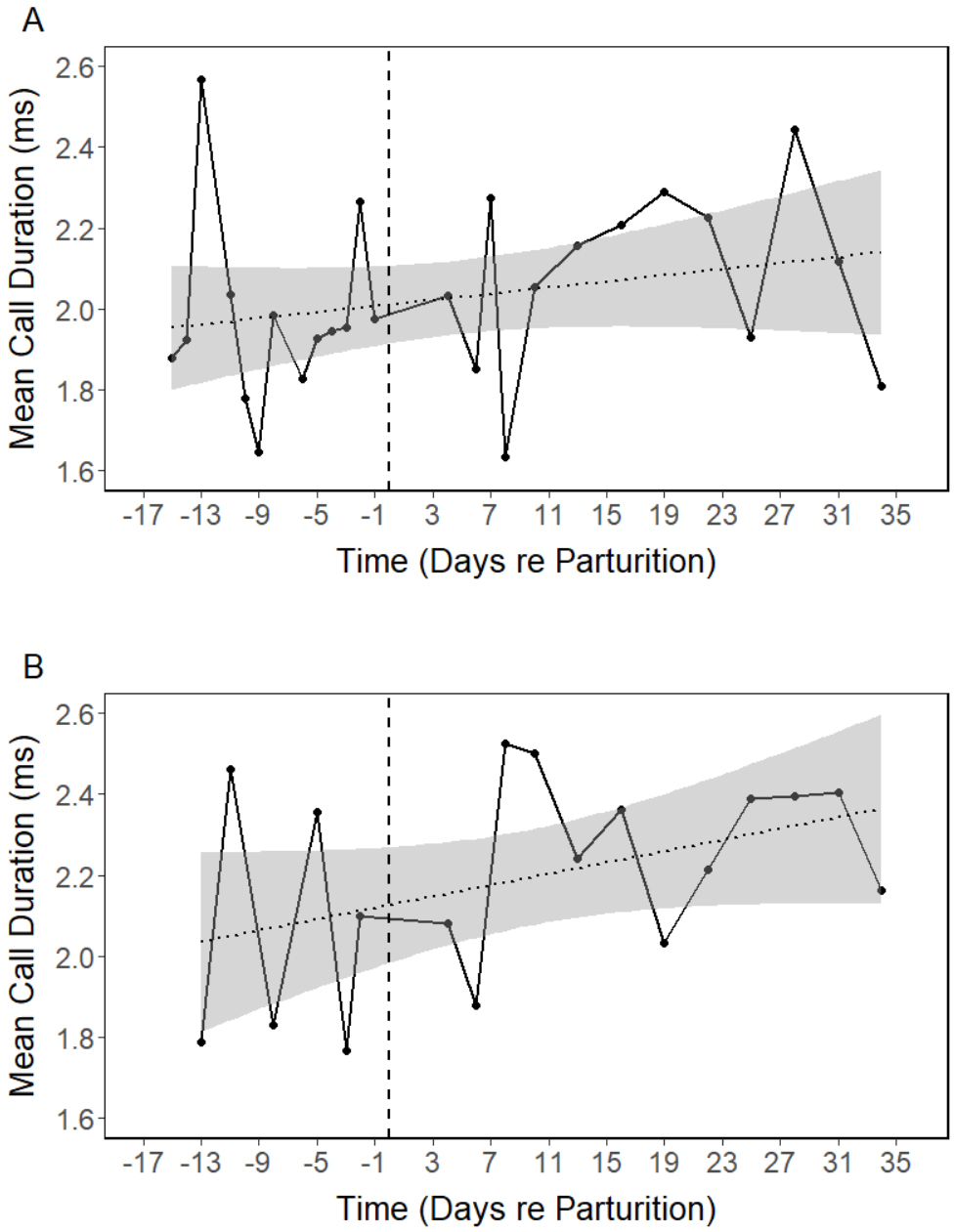

Figure 3: Mean call duration before take-off over pregnancy and lactation as a function of days relative to parturition (dashed vertical line) for A) nine pregnant/lactating and B) two control bats with linear trend lines (dotted lines) and shaded 95% confidence intervals. A significant increase occurred over time for the control bats.

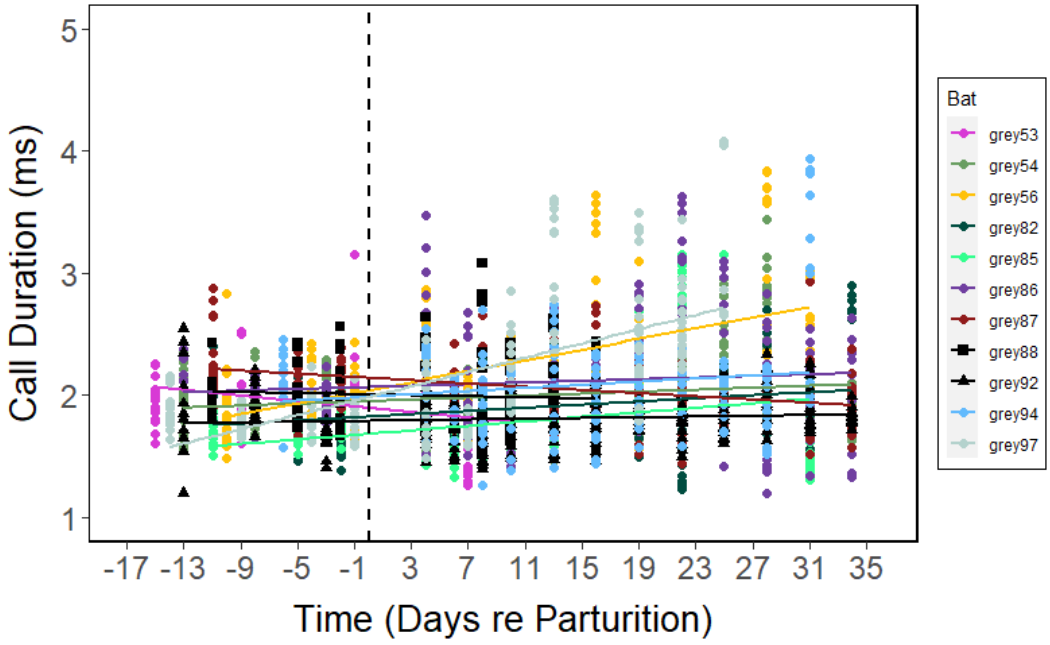

Figure 4: Call duration after take-off over pregnancy and lactation as a function of days relative to parturition (dashed vertical line) for nine pregnant/lactating and two control (Grey 88 and Grey 92) bats with linear trend lines.

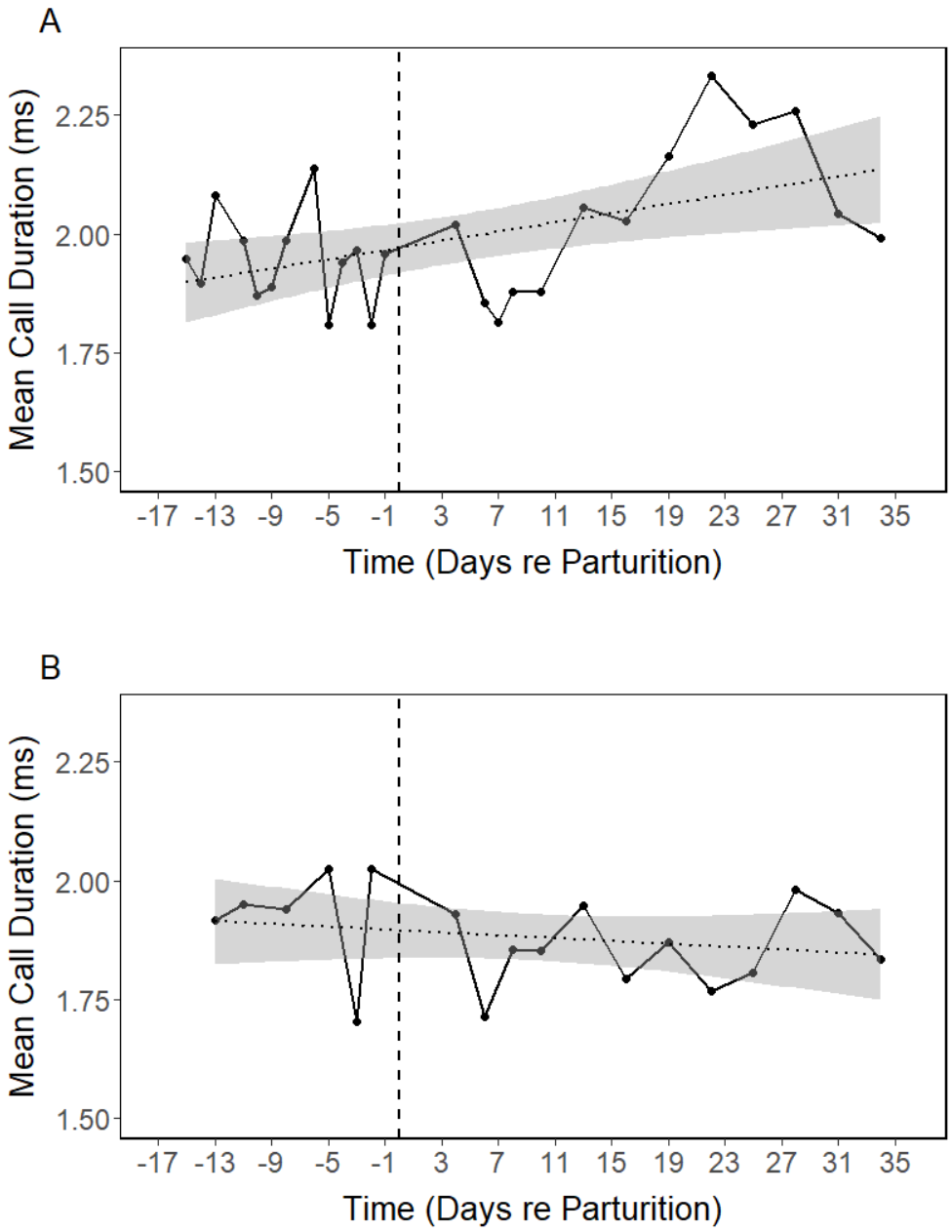

Figure 5: Mean call duration after take-off over pregnancy and lactation as a function of days relative to parturition (dashed vertical line) for A) nine pregnant/lactating and B) two control bats with linear trend lines (dotted lines) and shaded 95% confidence intervals. A significant increase occurred over time for the pregnant/lactating bats.

Pulse Interval in Flight Undergoes No Significant Change

There were significant changes in pulse interval based on random effects but not on fixed effects for both before and after all bats took flight, so the recording day did not affect pulse interval when pregnant/lactating and control bat data were tested together (Table 5). The ICCs were close to zero both before (adjusted ICC = 0.176, unadjusted ICC = 0.175) and after (adjusted ICC = 0.113, unadjusted ICC = 0.113) take-off, so pulse interval was similar between pregnant/lactating and control bats, which can be seen in Figure 6 and Figure 8 with how all of the linear trend lines are in the same range of pulse intervals. Cohen's f was 0.15 before take-off and 4.16×10^{-3} after take-off, both indicating that very little of the variance in pulse intervals could be explained by the day. Pulse interval had a significant decrease before take-off over pregnancy and lactation ($p < 0.05$), a significant increase before take-off during lactation alone ($p < 0.05$), and a significant increase before take-off for control ($p < 0.05$) bats (Figure 6, Figure 7). There were no other significant changes during pregnancy and lactation after take-off, during lactation after take-off, during pregnancy, or in control bats after take-off (Figure 8, Figure 9). The longest duration pulse intervals used are lower after bats take flight than before (Figure 6, Figure 8).

Table 5: F- and p-values for pulse interval repeated measures ANOVAs used to test change in pulse interval over time. A p-value ≤ 0.05 is considered significant.

	Before Take-off			**After Take-off**		
Group	**Fixed Effects**	**Random Effects**		**Fixed Effects**	**Random Effects**	
	Day	**Day:Bat**	**Bat**	**Day**	**Day:Bat**	**Bat**
All bats	$F = 2.0171$ $p = 0.1592$	$p = 3.5 \times 10^{-14}$	$p = 0.002966$	$F = 0.0018$ $p = 0.9666$	$p = 2.084 \times 10^{-7}$	$p = 3.314 \times 10^{-7}$
Pregnant and lactating	$F = 5.3677$ $p = 0.02358$	$p = 6.891 \times 10^{-13}$	$p = 0.01499$	$F = 0.0039$ $p = 0.9505$	$p = 1.211 \times 10^{-9}$	$p = 7.902 \times 10^{-6}$
Pregnant	$F = 2.2056$ $p = 0.166$	$p = 1.238 \times 10^{-5}$	$p = 0.5778$	$F = 0.1875$ $p = 0.6729$	$p = 0.30047$	$p = 0.05922$
Lactating	$F = 6.6002$ $p = 0.0125$	$p = 2.049 \times 10^{-9}$	$p = 0.2725$	$F = 1.3372$ $p = 0.2519$	$p = 3.944 \times 10^{-8}$	$p = 0.0003405$
Control	$F = 7.4761$ $p = 0.01278$	$p = 0.3483$	$p = 0.5457$	$F = 0.0624$ $p = 0.8047$	$p = 0.9996$	$p = 0.5042$

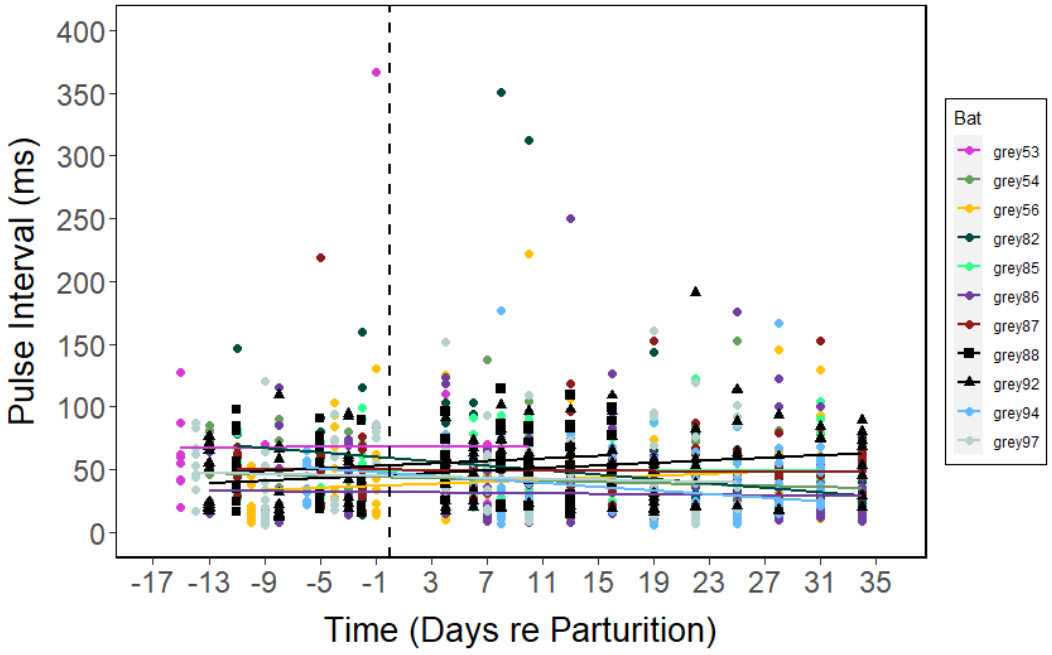

Figure 6: Pulse interval before take-off over pregnancy and lactation as a function of days relative to parturition (dashed vertical line) for nine pregnant/lactating and two control (Grey 88 and Grey 92) bats with linear trend lines.

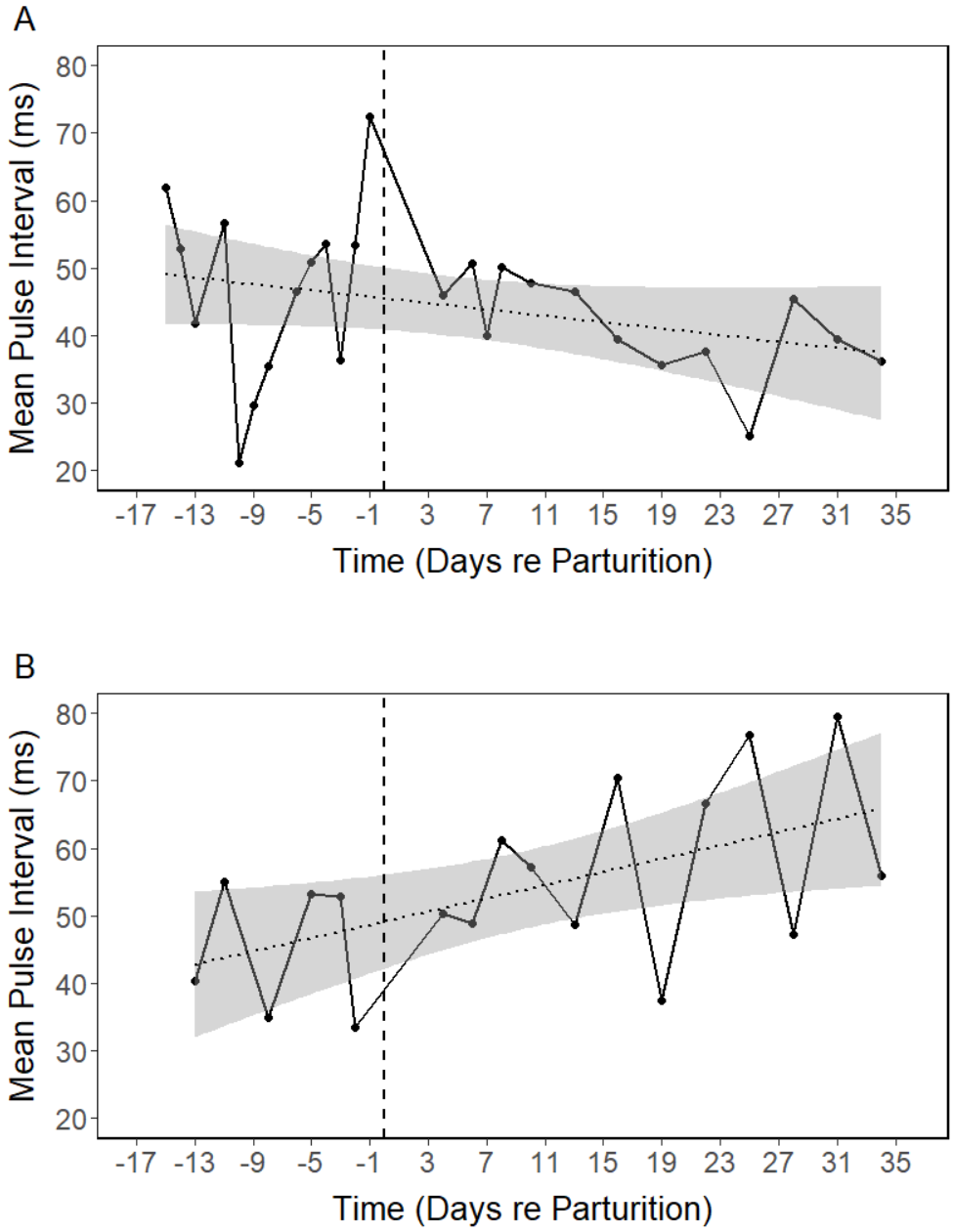

Figure 7: Mean pulse interval before take-off over pregnancy and lactation as a function of days relative to parturition (dashed vertical line) for A) nine pregnant/lactating and B) two control bats with linear trend lines (dotted lines) and shaded 95% confidence intervals. There was a significant decrease for pregnant/lactating bats and a significant increase for control bats.

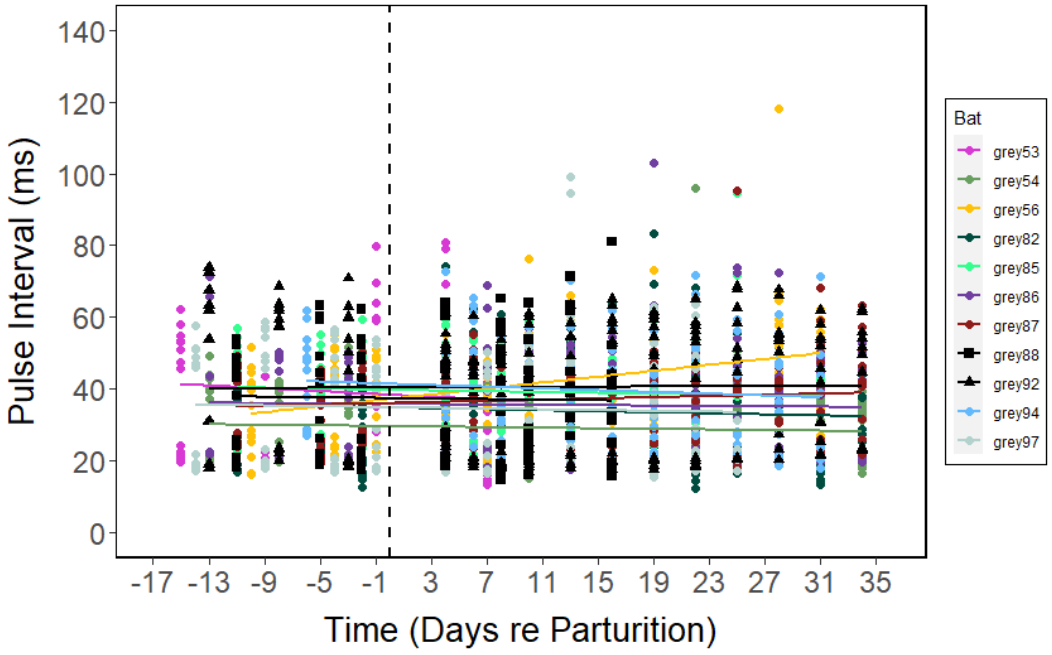

Figure 8: Pulse interval after take-off over pregnancy and lactation as a function of days relative to parturition (dashed vertical line) for nine pregnant/lactating and two control (Grey 88 and Grey 92) bats with linear trend lines.

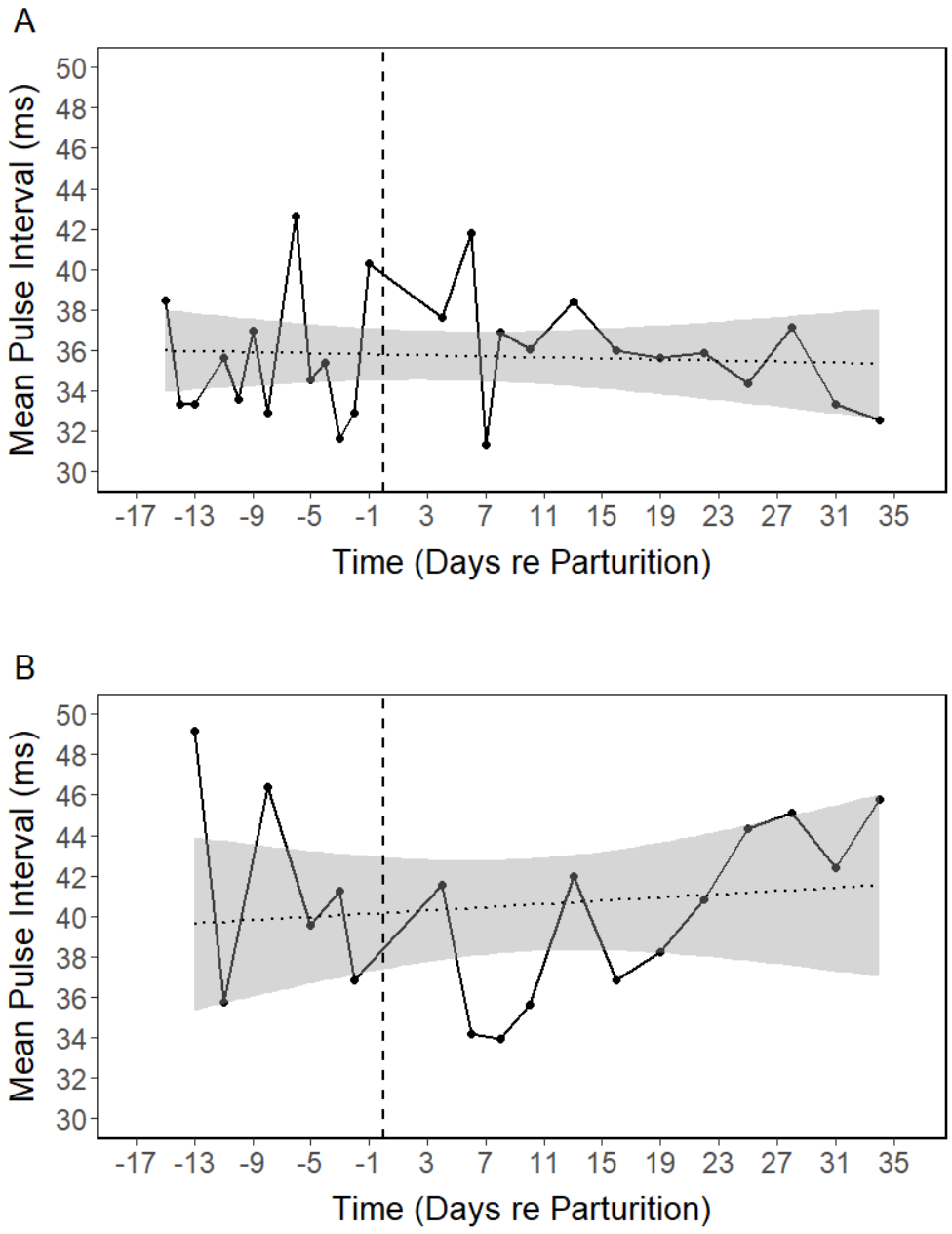

Figure 9: Mean pulse interval after take-off over pregnancy and lactation as a function of days relative to parturition (dashed vertical line) for A) nine pregnant/lactating and B) two control bats with linear trend lines (dotted lines) and shaded 95% confidence intervals. There were no significant changes for pregnant/lactating or control bats.

Number of Strobe Groups Increases During Pregnancy and Lactation

We classified pulse intervals by the type of call grouping they belonged to (doublet, higher-order sonar strobe group, or not a sonar strobe group) as seen in Figure 10. There were significant changes in the number of pulse intervals belonging to sonar strobe groups before and after take-off due to random effects but not fixed effects when pregnant/lactating and control bat data were tested together, so some bats produced more strobe groups than others unaffected by recording day (Table 6). The ICCs were close to zero both before (adjusted ICC = 0.113, unadjusted ICC = 0.111) and after take-off (adjusted ICC = 0.281, unadjusted ICC = 0.279) for all bats. Cohen's f was 0.13 before take-off and 0.10 after take-off, both indicating that little of the variance in the number of sonar strobe groups could be explained by the day. The number of strobe groups increased significantly during pregnancy and lactation before bats had taken flight ($p < 0.05$) but not at any point when considering pregnancy and lactation individually (Figure 11, Figure 12). There was also no significant change during pregnancy and lactation after take-off (Figure 13, Figure 14). Control bats had a significant decrease in number of strobe groups before take-off ($p < 0.01$) but not after take-off (Figures 11 to 14).

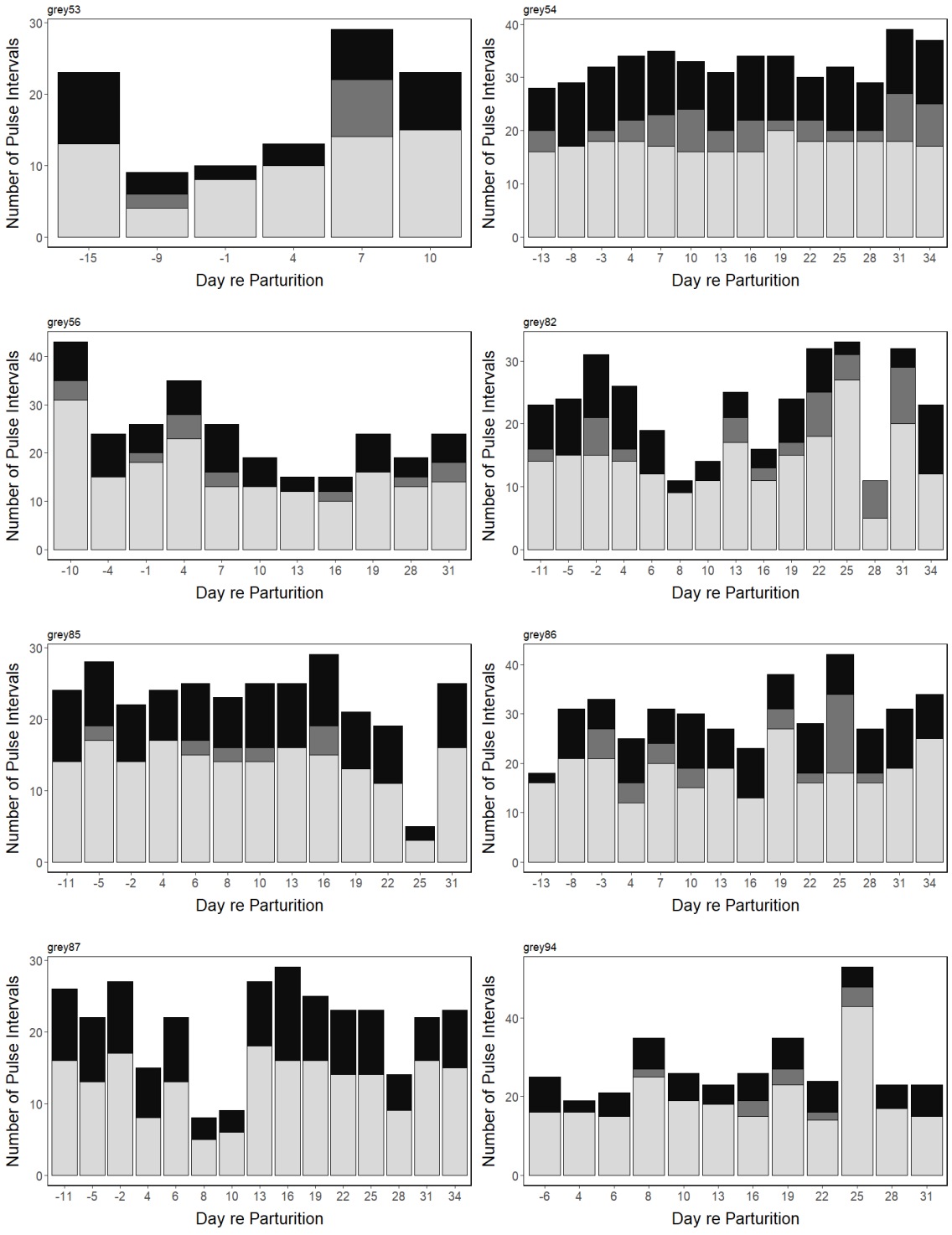
grey53
grey54
grey56
grey82
grey85
grey86
grey87
grey94
Number of Pulse Intervals
Day re Parturition

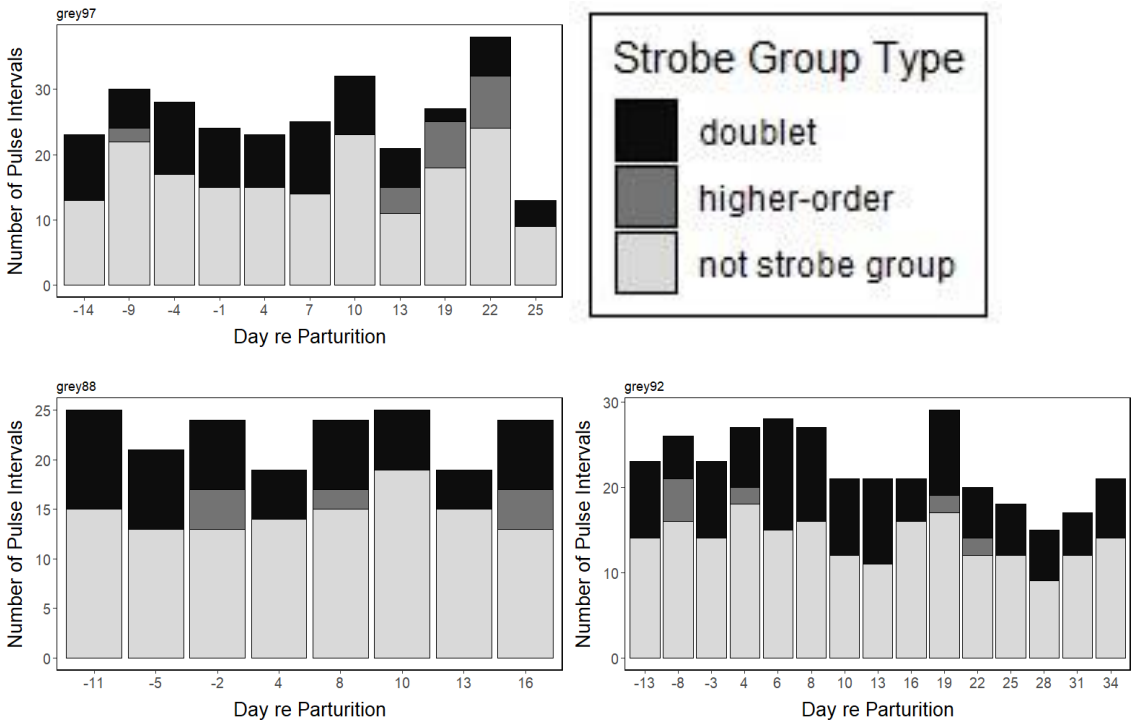

Figure 10: Stacked bar plots of the number of pulse intervals within each strobe group type (doublet, higher-order strobe group, or not a strobe group) per day with respect to parturition day (set to 0) for pregnant/lactating bat and for control bats (Grey 88 and Grey 92) using the days assigned to control bats for comparison with pregnant/lactating bats

Table 6: F- and p-values for strobe group number repeated measures ANOVAs used to test change in the number of strobe groups used over time. A p-value ≤ 0.05 is considered significant.

	Before Take-off		**After Take-off**	
Group	**Fixed Effects**	**Random Effects**	**Fixed Effects**	**Random Effects**
	Day	**Bat**	**Day**	**Bat**
All bats	F = 2.1864 p = 0.1417	p = 0.02334	F = 1.3331 p = 0.2504	p = 3.389×10^{-7}
Pregnant and lactating	F = 5.2413 p = 0.02403	p = 0.04332	F = 1.0717 p = 0.303	p = 5.172×10^{-7}
Pregnant	F = 0.358 p = 0.5567	p = 0.9288	F = 1×10^{-4} p = 0.9909	p = 0.1821
Lactating	F = 1.6629 p = 0.201	p = 0.06935	F = 6×10^{-4} p = 0.9802	p = 5.241×10^{-7}
Control	F = 9.9782 p = 0.004826	p = 0.07533	F = 0.4226 p = 0.5227	p = 1

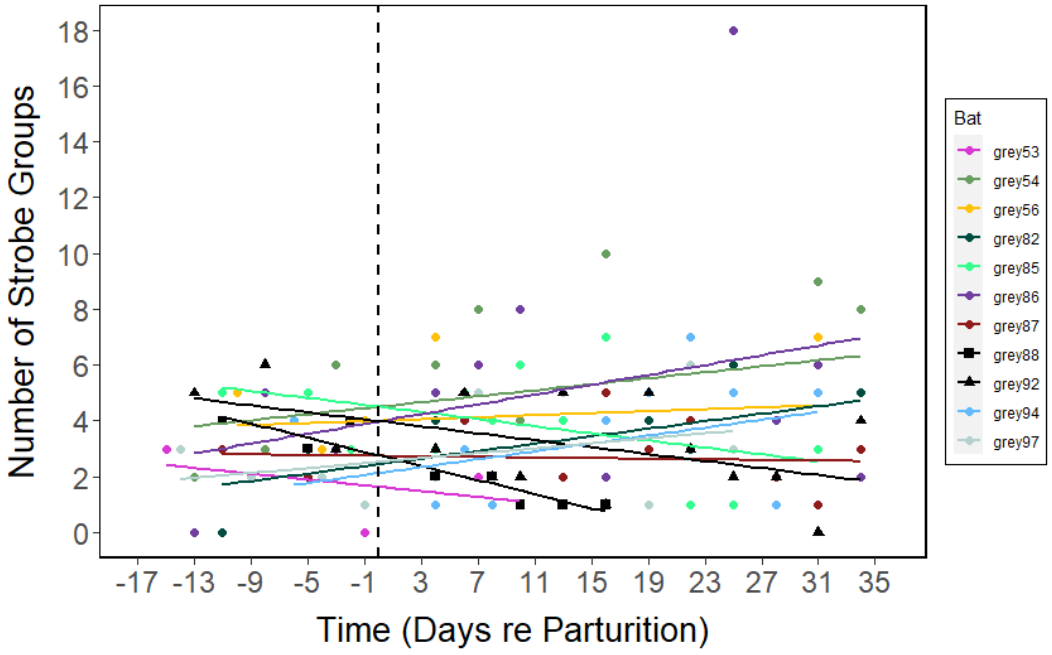

Figure 11: Number of strobe groups before take-off over pregnancy and lactation as a function of days relative to parturition (dashed vertical line) for nine pregnant/lactating and two control (Grey 88 and Grey 92) bats with linear trend lines.

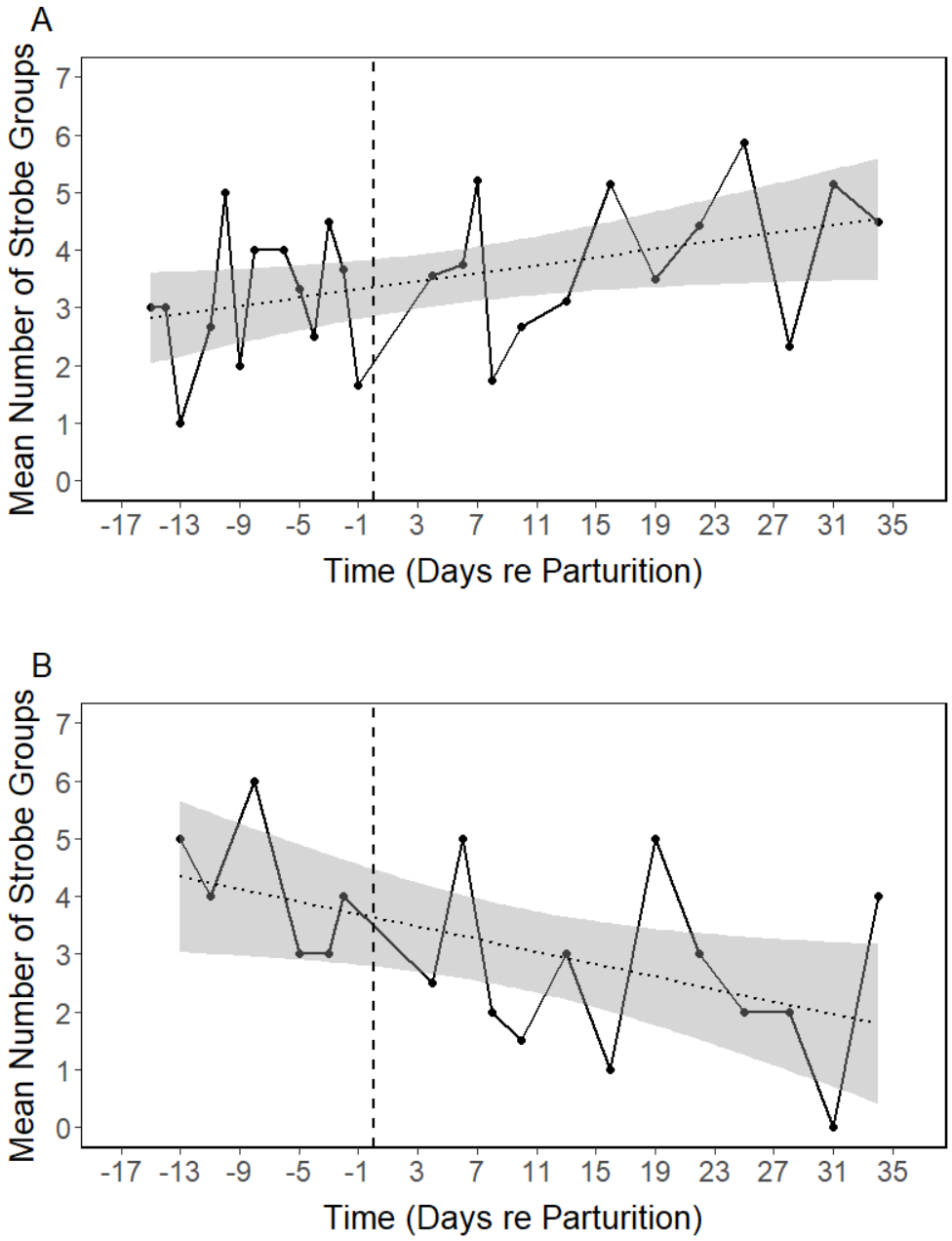

Figure 12: Mean strobe group number before take-off over pregnancy and lactation as a function of days relative to parturition (dashed vertical line) for A) nine pregnant/lactating and B) two control bats with linear trend lines (dotted lines) and shaded 95% confidence intervals. There was a significant increase for pregnant/lactating bats and a significant decrease for control bats.

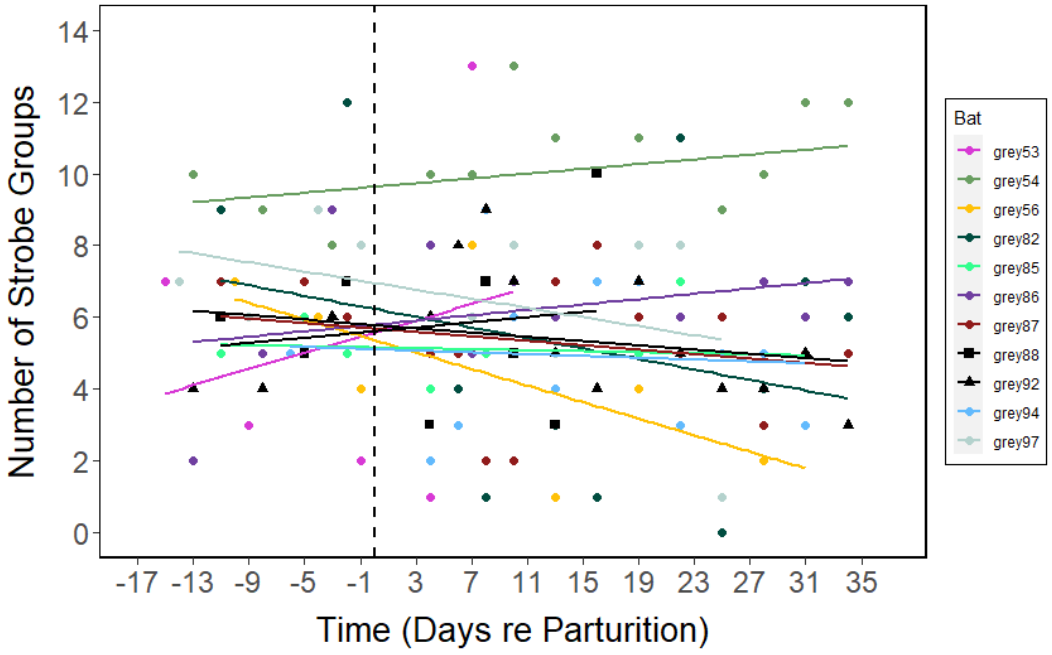

Figure 13: Number of strobe groups after take-off over pregnancy and lactation as a function of days relative to parturition (dashed vertical line) for nine pregnant/lactating and two control (Grey 88 and Grey 92) bats with linear trend lines.

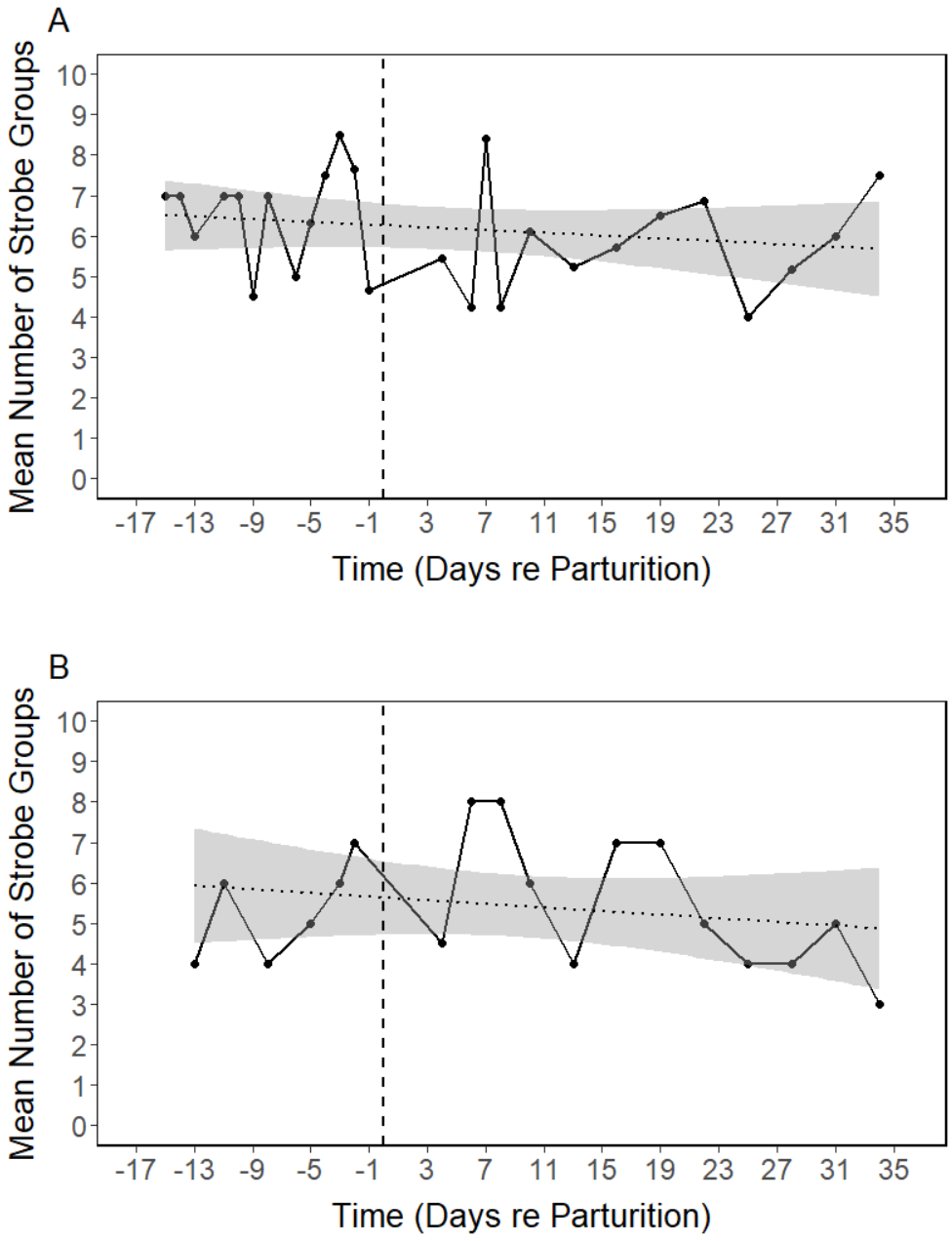

Figure 1: Mean strobe group number after take-off over pregnancy and lactation as a function of days relative to parturition (dashed vertical line) for A) nine pregnant/lactating and B) two control bats with linear trend lines (dotted lines) and shaded 95% confidence intervals. There was no significant change in pregnant/lactating or control bats.

Percentage of Strobe Groups Decreases During Pregnancy

The percentage of pulse intervals belonging to sonar strobe groups changed significantly due to random effects but not fixed effects only after take-off when pregnant/lactating and control bat data were tested together (Table 7). The ICCs were closer to zero before take-off (adjusted ICC = 0.080, unadjusted ICC = 0.079) than after take-off (adjusted ICC = 0.204, unadjusted ICC = 0.201). Cohen's f was 0.09 before take-off and 0.14 after take-off, both indicating that little of the variance in the percentage of pulse intervals that were part of sonar strobe groups could be explained by the day. Strobe group percentage decreases significantly during pregnancy after take-off ($p < 0.05$) but not before take-off (Table 7; Figure 15; Figure 16). There are also no significant changes seen during pregnancy and lactation, during lactation alone, or in the control bats (Table 7; Figure 16). The decrease during pregnancy would have resulted in a steep linear trend line on Figure 16 in the pregnancy section of the plot, but produces a shallower downward slope when combined with the lactation section.

Table 7: F- and p-values for strobe group percentage repeated measures ANOVAs used to test change in the percentage of strobe groups used over time. A p-value ≤ 0.05 is considered significant.

	Before Take-off		**After Take-off**	
Group	**Fixed Effects**	**Random Effects**	**Fixed Effects**	**Random Effects**
	Day	**Bat**	**Day**	**Bat**
All bats	F = 1.1424	p = 0.0939	F = 2.5512	p = 0.0001097
	p = 0.2871		p = 0.1127	
Pregnant and lactating	F = 2.5675	p = 0.07559	F = 1.8978	$p = 8.906 \times 10^{-5}$
	p = 0.112		p = 0.1713	
Pregnant	F = 0.0838	p = 0.9836	F = 4.7105	p = 0.2576
	p = 0.7753		p = 0.0439	
Lactating	F = 0.1349	p = 0.08442	F = 0.0235	p = 0.0008657
	p = 0.7144		p = 0.8787	
Control	F = 1.5327	p = 0.1914	F = 0.9026	p = 1
	p = 0.2295		p = 0.3529	

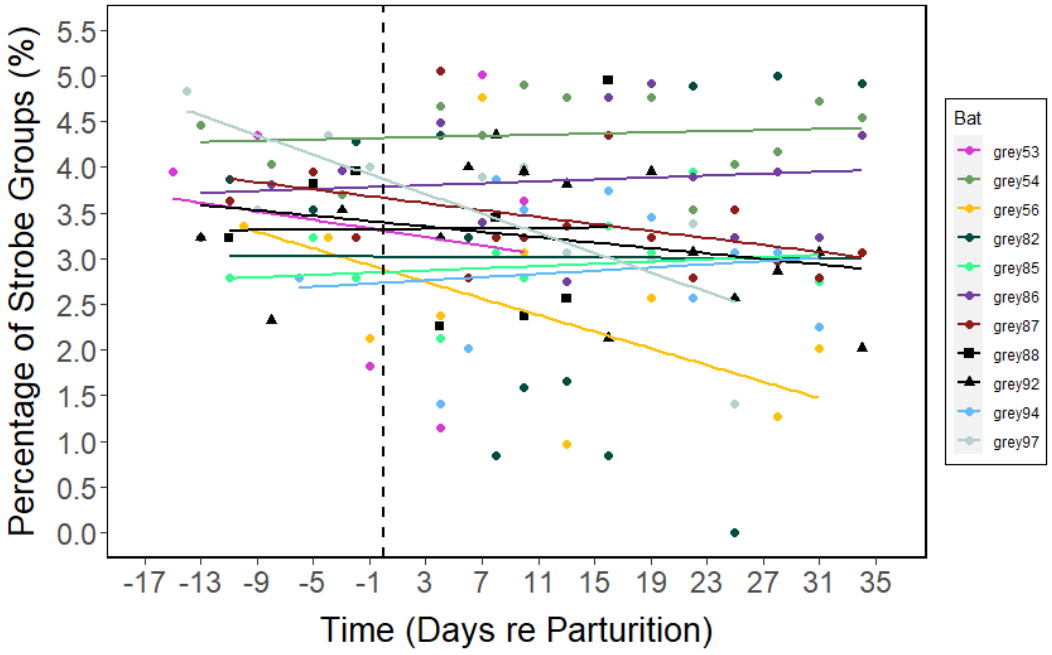

Figure 15: Percentage of strobe groups after take-off over pregnancy and lactation as a function of days relative to parturition (dashed vertical line) for nine pregnant/lactating and two control (Grey 88 and Grey 92) bats with linear trend lines.

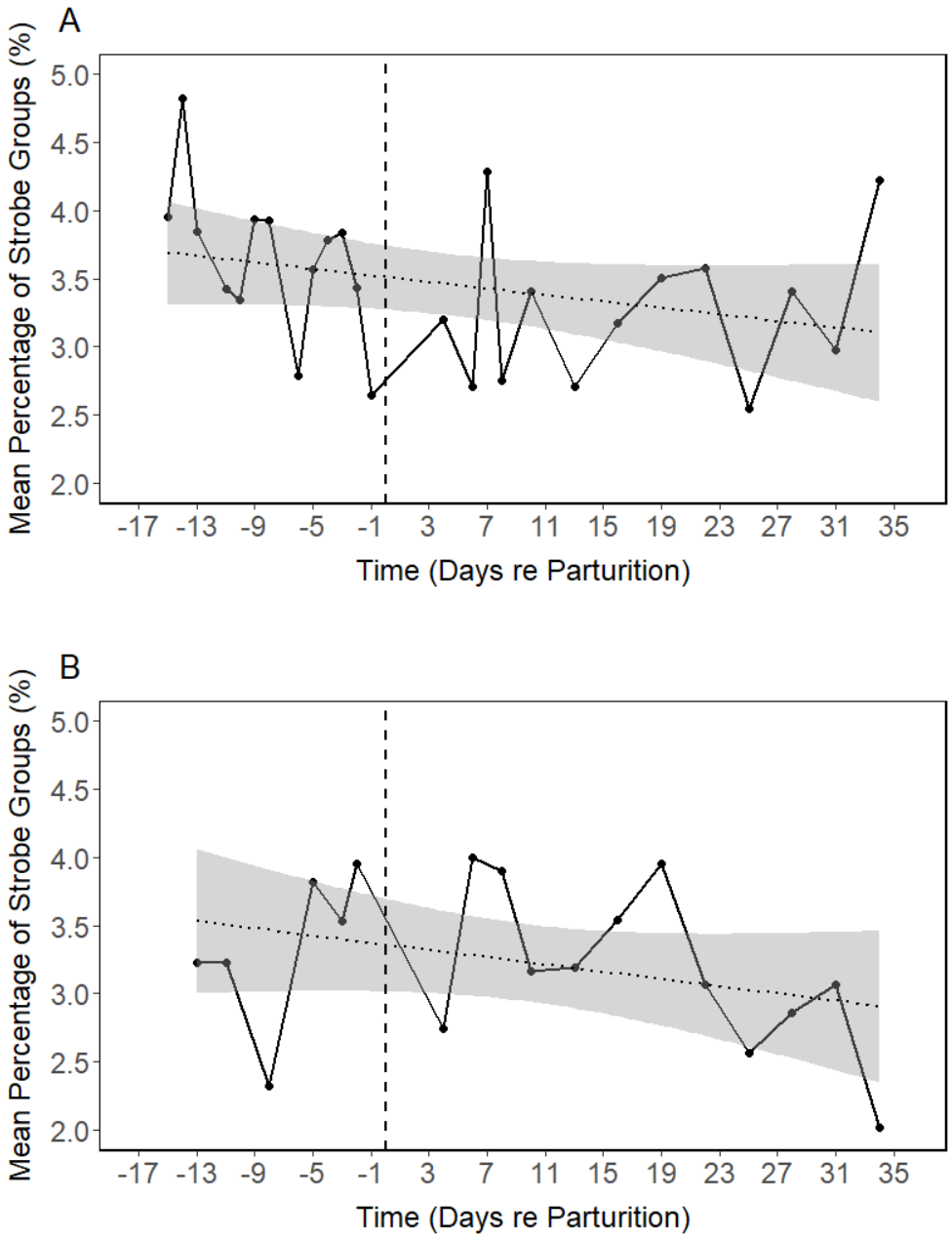

Figure 2: Mean percentage of strobe groups after take-off over pregnancy and lactation as a function of days relative to parturition (dashed vertical line) for A) nine pregnant/lactating and B) two control bats with linear trend lines (dotted lines) and shaded 95% confidence intervals. There is a significant decrease during pregnancy only.

Bandwidth in Flight Narrows During Pregnancy and Lactation

There was a significant difference in echolocation call bandwidth between days after ($p < 0.01$) but not before take-off when pregnant/lactating and control bat data were considered together (Table 8; Figure 17). The ICCs were slightly closer to one than to zero both before (adjusted ICC = 0.615, unadjusted ICC = 0.613) and after (adjusted ICC = 0.569, unadjusted ICC = 0.554) bats took flight. Cohen's f was 0.09 before take-off and 0.25 after take-off, indicating that before take-off little of the variance in the bandwidths could be explained by day, while after take-off a moderate amount of the variance could be explained by day. Bandwidth decreased significantly during pregnancy and lactation after ($p < 0.01$) but not before take-off (Figure 18A). It also decreased significantly during lactation alone only after take-off ($p < 0.01$). There were no significant changes in bandwidth during pregnancy alone or in the control bats. On average, pregnant/lactating bats in flight used echolocation calls of narrower bandwidths than control bats in flight (Figure 18).

Table 8: F- and p-values for bandwidth repeated measures ANOVAs used to test change in the bandwidth used over time. A p-value $\leqslant 0.05$ is considered significant.

	Before Take-off			**After Take-off**		
Group	**Fixed Effects**	**Random Effects**		**Fixed Effects**	**Random Effects**	
	Day	**Day:Bat**	**Bat**	**Day**	**Day:Bat**	**Bat**
All bats	F = 1.0185 p = 0.3148	$p < 2.2 \times 10^{-16}$	$p = 4.676 \times 10^{-8}$	F = 7.7094 p = 0.006339	$p < 2.2 \times 10^{-16}$	$p = 1.667 \times 10^{-6}$
Pregnant and lactating	F = 2.4091 p = 0.1236	$p < 2.2 \times 10^{-16}$	$p = 5.404 \times 10^{-7}$	F = 7.548 p = 0.007085	$p < 2.2 \times 10^{-16}$	p = 0.0003215
Pregnant	F = 0.0061 p = 0.9382	$p < 2 \times 10^{-16}$	p = 1	F = 0.0192 p = 0.891	$p < 2 \times 10^{-16}$	p = 1
Lactating	F = 1.715 p = 0.1941	$p < 2.2 \times 10^{-16}$	$p = 2.36 \times 10^{-6}$	F = 8.5404 p = 0.004552	$p < 2.2 \times 10^{-16}$	p = 0.0001568
Control	F = 1.2451 p = 0.2773	$p < 2 \times 10^{-16}$	p = 0.05668	F = 0.0619 p = 0.806	$p < 2 \times 10^{-16}$	p = 0.2716

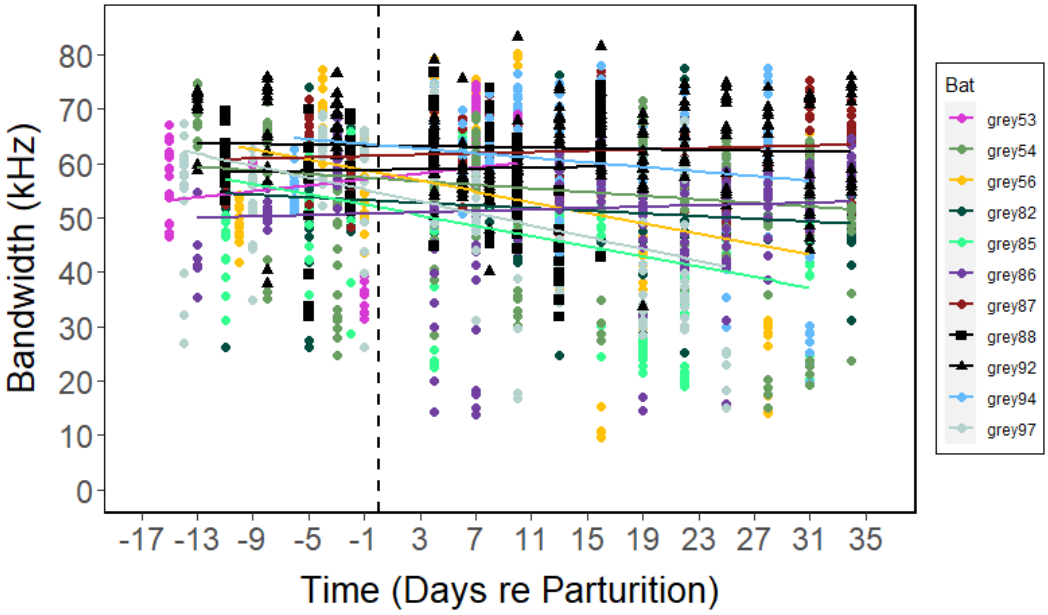

Figure 3: Echolocation call bandwidth after take-off over pregnancy and lactation as a function of days relative to parturition (dashed vertical line) for nine pregnant/lactating and two control (Grey 88 and Grey 92) bats with linear trend lines.

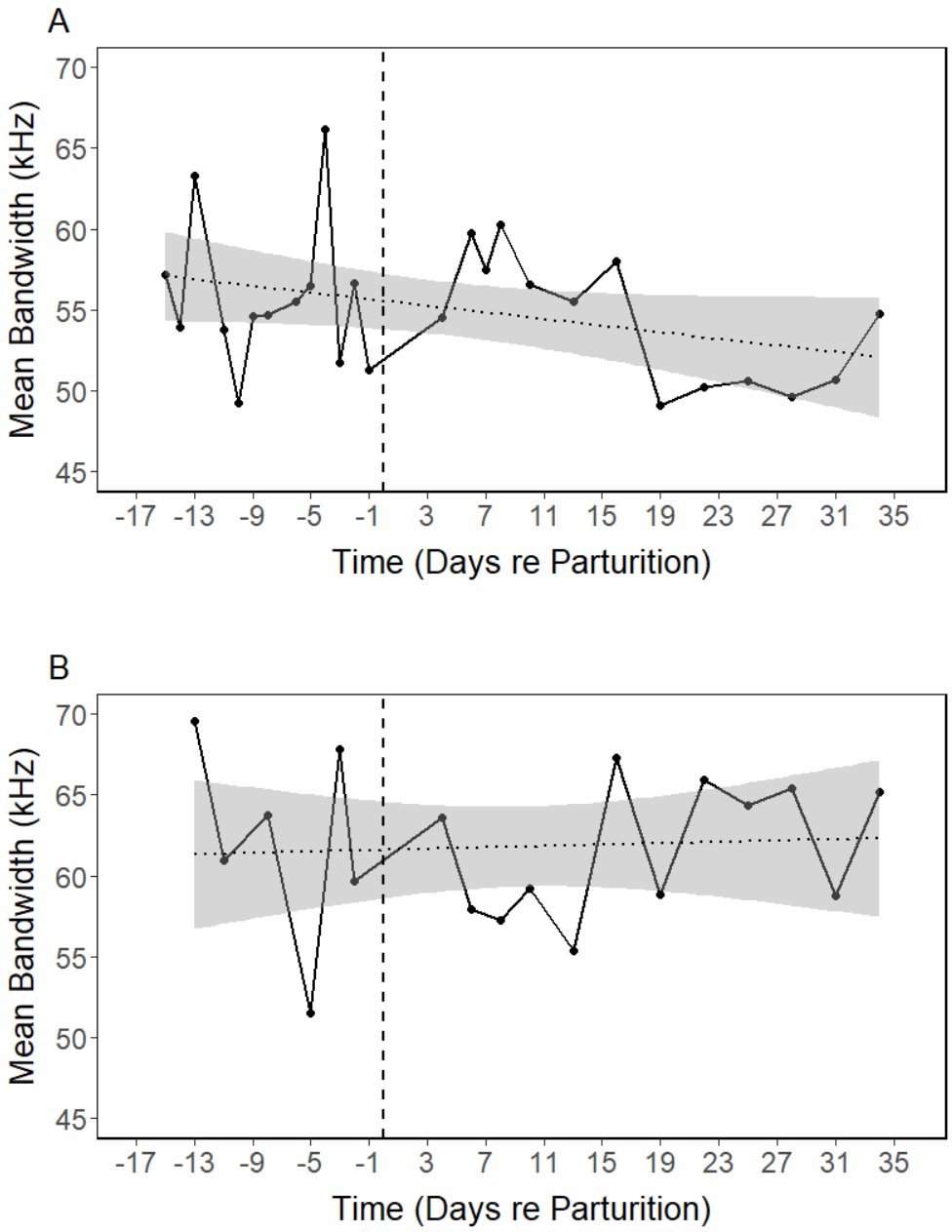

Figure 4: Mean echolocation call bandwidth after take-off over pregnancy and lactation as a function of days relative to parturition (dashed vertical line) for A) nine pregnant/lactating and B) two control bats with linear trend lines (dotted lines) and shaded 95% confidence intervals. There was a significant decrease in bandwidth for pregnant/lactating bats but not for control bats.

Centroid Frequency Decreases During Pregnancy and Lactation

There was a significant change in centroid frequency between days both before ($p < 0.05$) and after ($p < 0.01$) take-off when considering pregnant/lactating and control bat data together (Table 9). The ICCs were close to one both before (adjusted ICC = 0.737, unadjusted ICC = 0.724) and after (adjusted ICC = 0.697, unadjusted ICC = 0.677) take-off. Cohen's f was 0.18 before take-off and 0.25 after take-off, both indicating that a moderate amount of the variance in the centroid frequencies could be explained by day. The centroid frequency decreased significantly during pregnancy and lactation before ($p < 0.05$) and after ($p < 0.01$) bats took flight (Figure 19; Figure 21). It also decreased significantly during lactation alone before ($p < 0.05$) and after ($p < 0.01$) take-off (Figure 20A; Figure 22A). There were no significant changes in centroid frequency during pregnancy alone or in the control bats. Pregnant/lactating bats in flight used slightly lower centroid frequencies on average than control bats in flight (Figure 22).

Table 9: F- and p-values for centroid frequency repeated measures ANOVAs used to test change in the centroid frequency used over time. A p-value ≤ 0.05 is considered significant.

	Before Take-off			**After Take-off**		
Group	**Fixed Effects**	**Random Effects**		**Fixed Effects**	**Random Effects**	
	Day	**Day:Bat**	**Bat**	**Day**	**Day:Bat**	**Bat**
All bats	$F = 4.1428$ $p = 0.04388$	$p < 2.2 \times 10^{-16}$	$p = 1.222 \times 10^{-7}$	$F = 7.9042$ $p = 0.005725$	$p < 2.2 \times 10^{-16}$	$p = 8.776 \times 10^{-9}$
Pregnant and lactating	$F = 5.9316$ $p = 0.01655$	$p < 2.2 \times 10^{-16}$	$p = 1.29 \times 10^{-7}$	$F = 6.935$ $p = 0.009747$	$p < 2.2 \times 10^{-16}$	$p = 1.317 \times 10^{-7}$
Pregnant	$F = 0.0112$ $p = 0.9165$	$p < 2 \times 10^{-16}$	$p = 1$	$F = 0.0186$ $p = 0.8927$	$p < 2 \times 10^{-16}$	$p = 1$
Lactating	$F = 6.0585$ $p = 0.01601$	$p < 2.2 \times 10^{-16}$	$p = 1.516 \times 10^{-7}$	$F = 9.1143$ $p = 0.003436$	$p < 2.2 \times 10^{-16}$	$p = 6.265 \times 10^{-8}$
Control	$F = 0.8447$ $p = 0.3682$	$p < 2 \times 10^{-16}$	$p = 1$	$F = 0.67$ $p = 0.4222$	$p < 2 \times 10^{-16}$	$p = 0.3764$

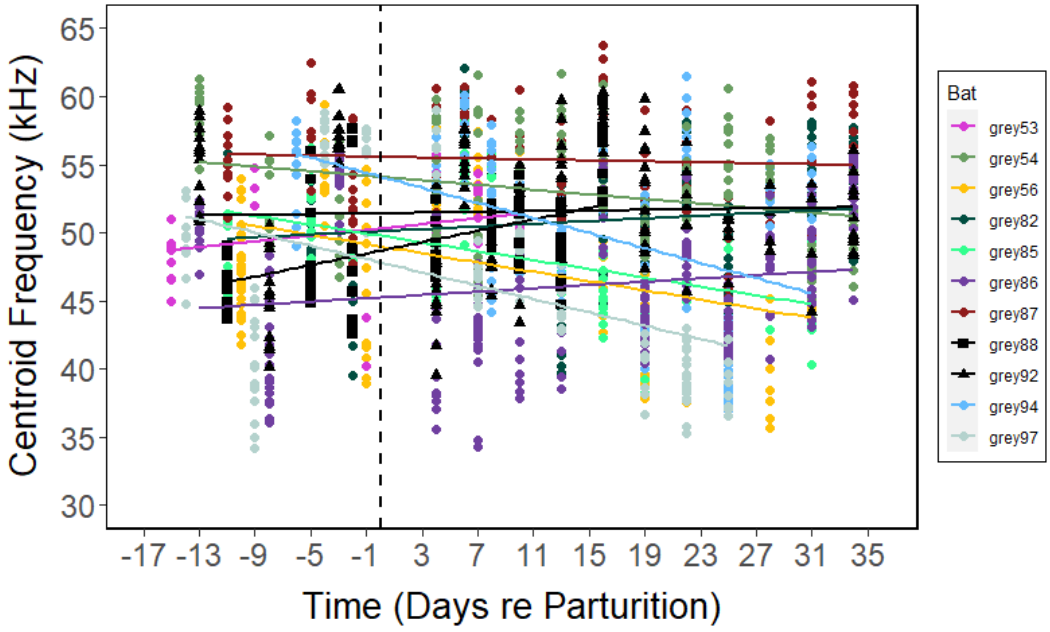

Figure 5: Echolocation call centroid frequency before take-off over pregnancy and lactation as a function of days relative to parturition (dashed vertical line) for nine pregnant/lactating and two control (Grey 88 and Grey 92) bats with linear trend lines. The significant decrease in centroid frequency for pregnant/lactating bats is visible on this graph.

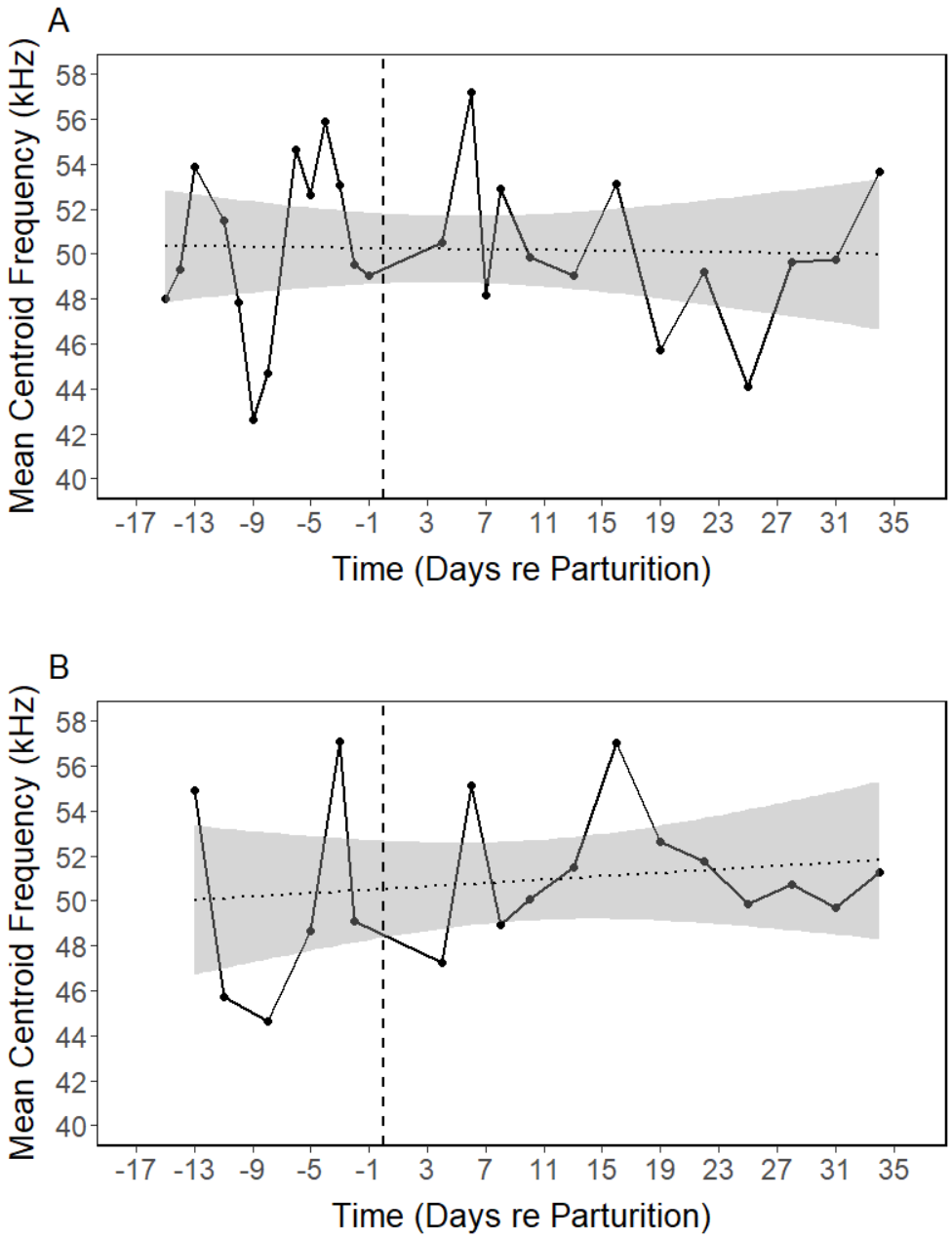

Figure 6: Mean echolocation call centroid frequency before take-off over pregnancy and lactation as a function of days relative to parturition (dashed vertical line) for A) nine pregnant/lactating and B) two control bats with linear trend lines (dotted lines) and shaded 95% confidence intervals.

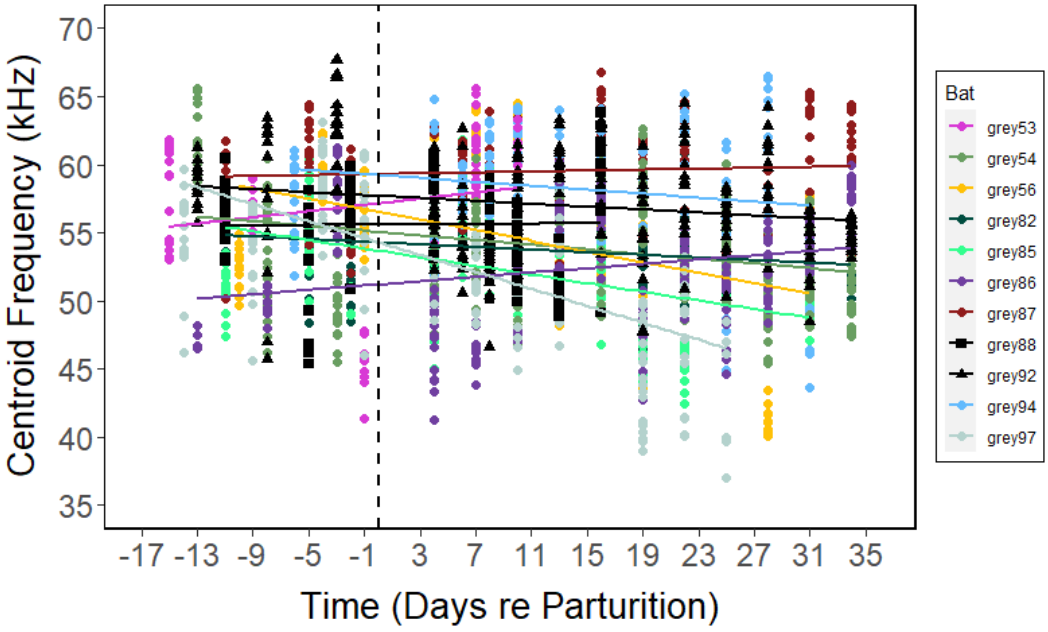

Figure 21: Echolocation call centroid frequency after take-off over pregnancy and lactation as a function of days relative to parturition (dashed vertical line) for nine pregnant/lactating and two control (Grey 88 and Grey 92) bats with linear trend lines.

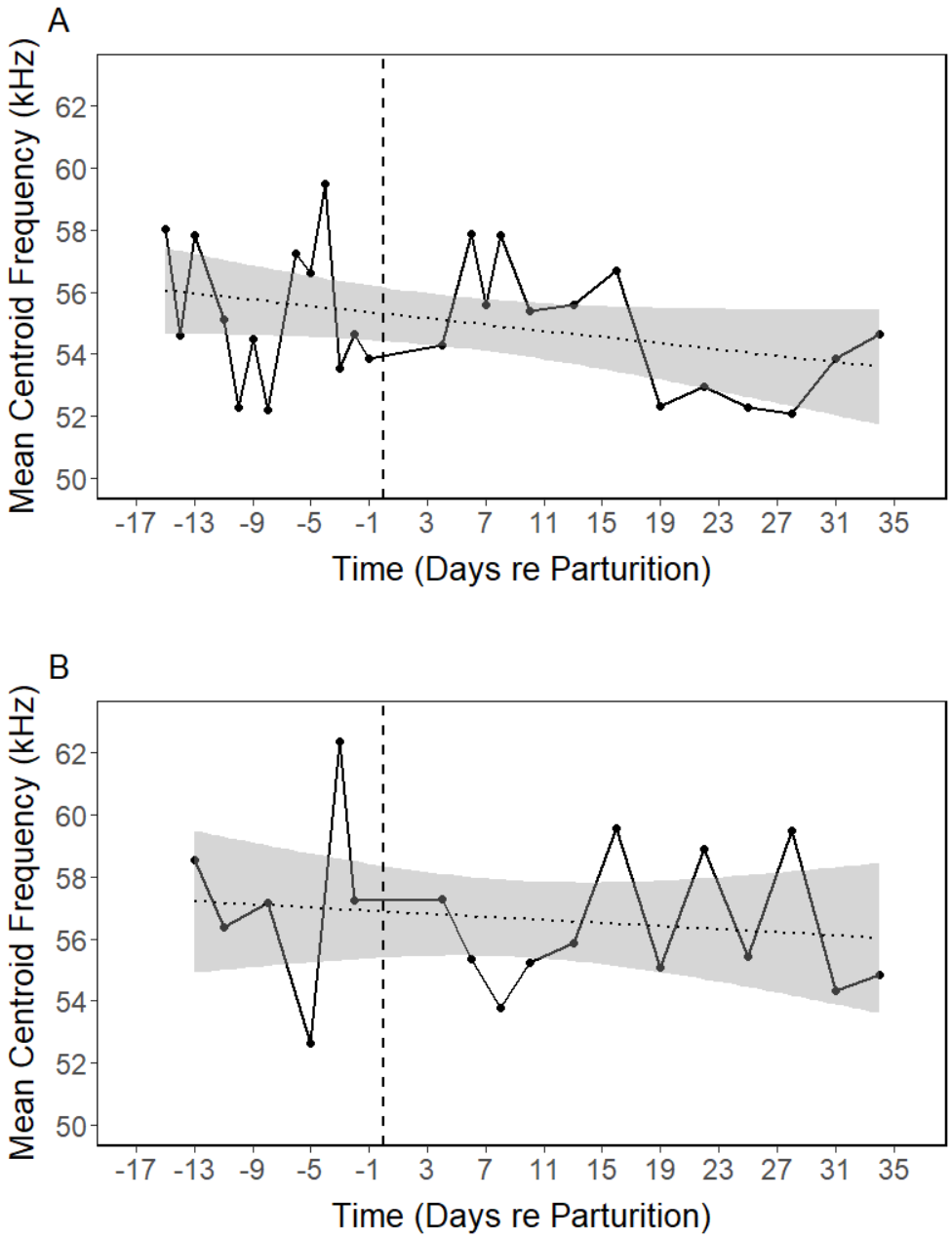

Figure 7: Mean echolocation call centroid frequency after take-off over pregnancy and lactation as a function of days relative to parturition (dashed vertical line) for A) nine pregnant/lactating and B) two control bats with linear trend lines (dotted lines) and shaded 95% confidence intervals. There was a significant decrease for pregnant/lactating bats.

Mean Source Level Remains Unchanged During Pregnancy and Lactation

Source level changed significantly between days ($p < 0.01$) but not with call duration only when including data from both before and after take-off for pregnant/lactating and control bats (Table 10; Figure 23 to 25). The ICCs for this model were close to zero (adjusted ICC = 0.207, unadjusted ICC = 0.203), indicating similarity in source level between bats, and the Cohen's f was small (0.14) for variance due to day and very small (5.27×10^{-3}) for variance due to call duration, indicating that neither was greatly responsible for the variance in source level. When data was divided into before ($p < 0.01$) and after ($p < 0.01$) take-off, source level changed significantly with call duration but not between days (Figure 23). The ICCs for these models were also close to zero, again indicating more similarity in source levels used between bats that within individual bats. The Cohen's f was 0.06 for variance due to day and 0.56 for variance due to call duration before take-off, indicating that a large amount of the variance in source level was due to the call duration while little was due to the day. After take-off, Cohen's f was 0.11 for variance due to day and 0.55 for variance due to call duration, also indicating that a large amount of the variance in source level was due to the call duration. There was no significant change in mean source level per bat between days and the ICCs were close to zero (adjusted ICC = 0.121, unadjusted ICC = 0.119) for this model, indicating that the mean source levels the bats used were similar between pregnant/lactating and control bats (Figure 26).

Table 10: F- and p-values for source level repeated measures ANOVAs used to test change in the source level used over time. A p-value ≤ 0.05 is considered significant.

	Fixed Effects		**Random Effects**	**Intraclass**
Group	**Day**	**Call Duration**	**Bat**	**Correlation Coefficients**
All bats before and after take-off	F = 8.1189 p = 0.004602	F = 0.0113 p = 0.915434	$p = 1.02 \times 10^{-14}$	Adjusted = 0.207 Unadjusted = 0.203
All bats before take-off	F = 0.294 p = 0.5891	F = 27.113 $p = 1.276 \times 10^{-6}$	$p = 5.037 \times 10^{-5}$	Adjusted = 0.259 Unadjusted = 0.203
All bats after take-off	F = 3.5362 p = 0.06098	F = 94.5660 $p < 2 \times 10^{-16}$	$p = 1.438 \times 10^{-12}$	Adjusted = 0.226 Unadjusted = 0.170

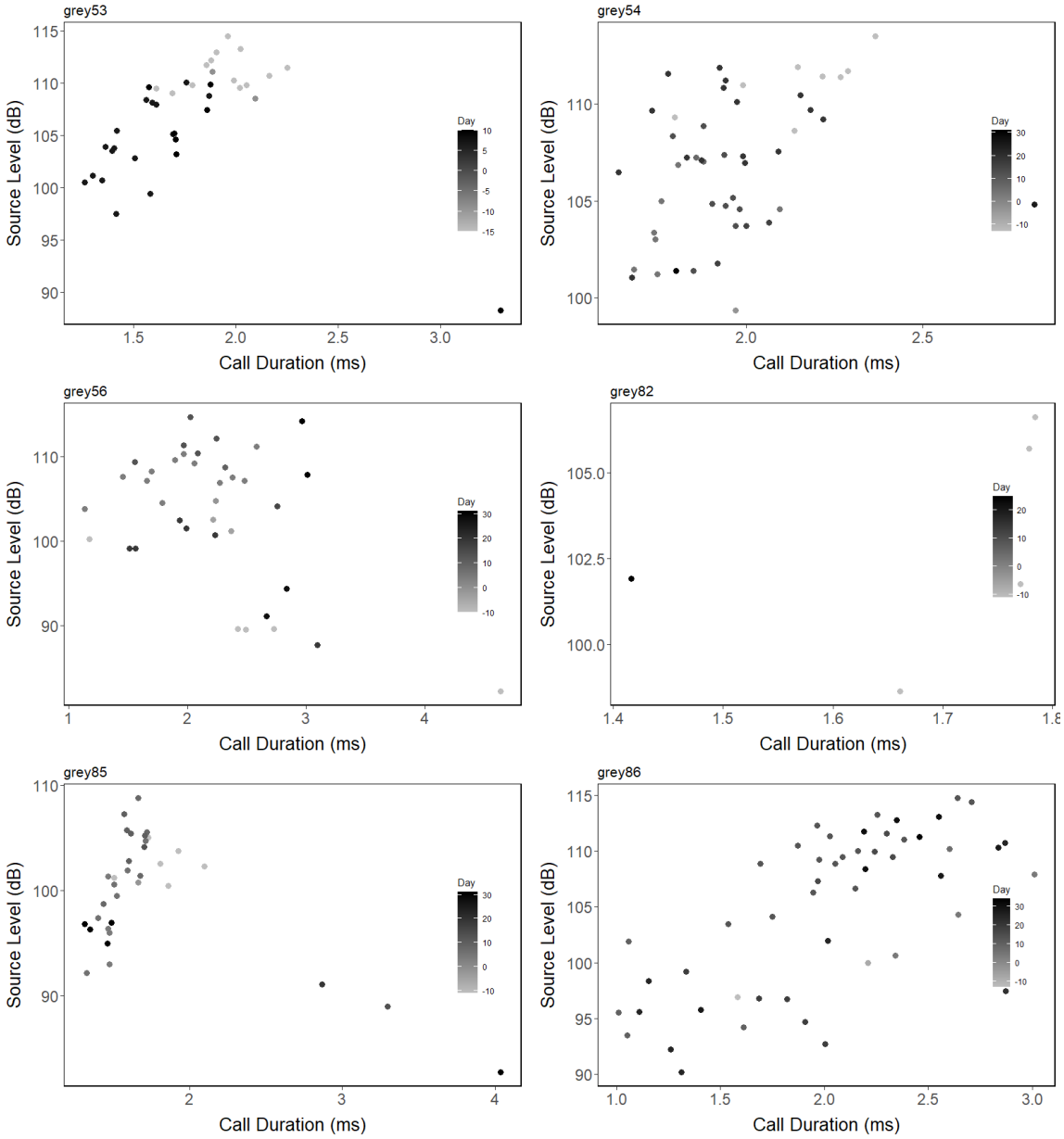
grey53
grey54
grey56
grey82
grey85
grey86
Source Level (dB)
Call Duration (ms)
Day

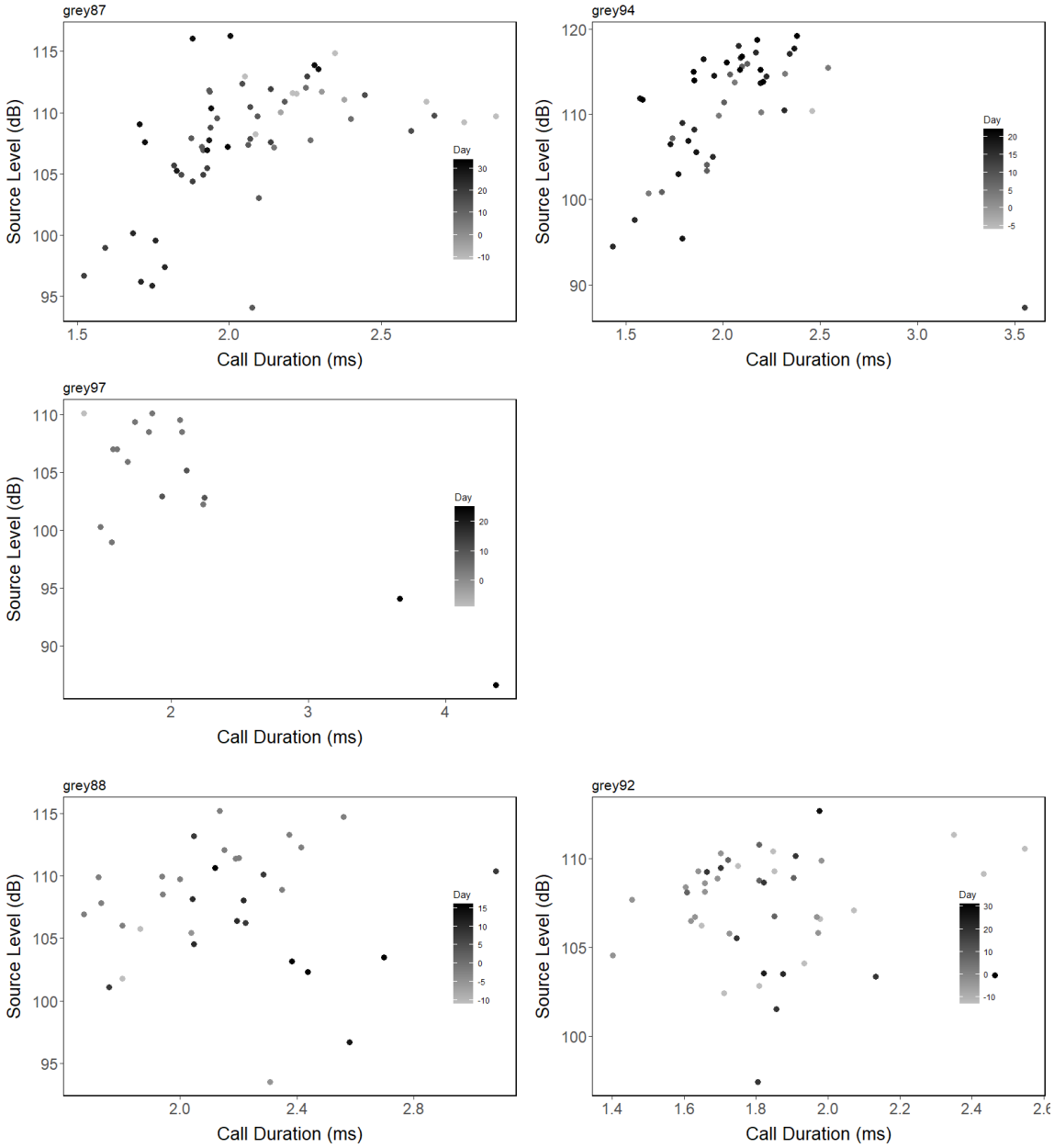

Figure 8: Source level across echolocation call duration for nine pregnant/lactating and two control (Grey 88 and Grey 92) bats. The data points are coloured with respect to days relative to parturition such that lighter points are earlier in the gestation period (maximum 15 days before parturition) and darker points are later in the lactation period (maximum 34 days after parturition).

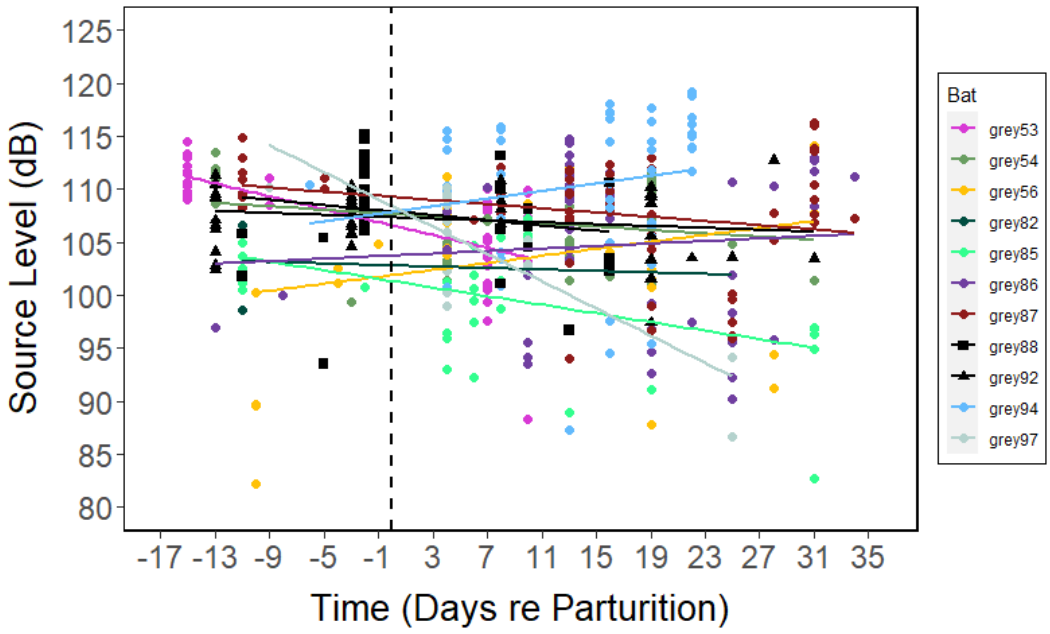

Figure 9: Source level before and after take-off over pregnancy and lactation as a function of days relative to parturition (dashed vertical line) for each of nine pregnant/lactating and two control (Grey 88 and Grey 92) bats with linear trend lines.

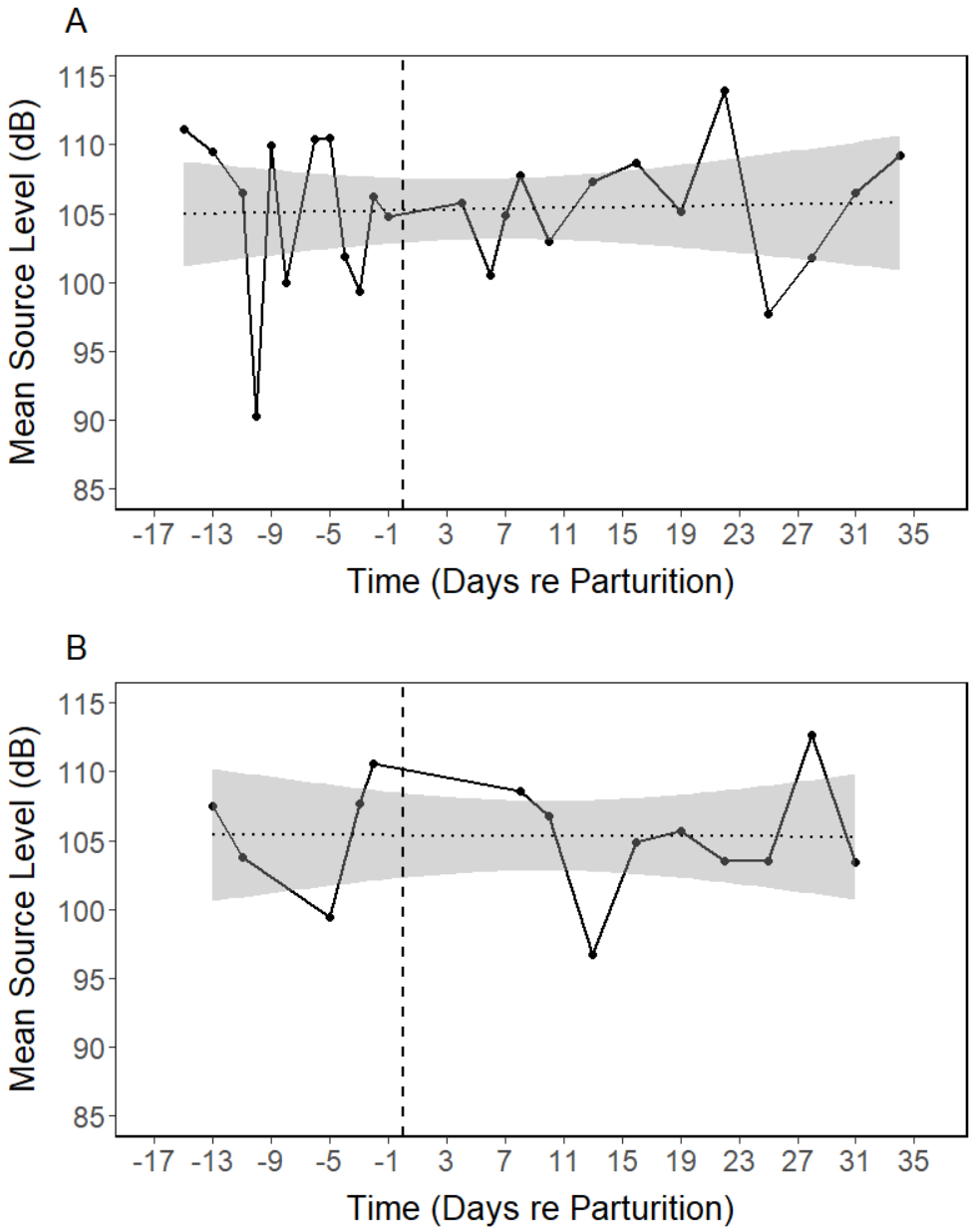

Figure 10: Mean echolocation call source level before and after take-off over pregnancy and lactation as a function of days relative to parturition (dashed vertical line) for A) nine pregnant/lactating and B) two control bats with linear trend lines (dotted lines) and shaded 95% confidence intervals. There was no significant change for pregnant/lactating or control bats.

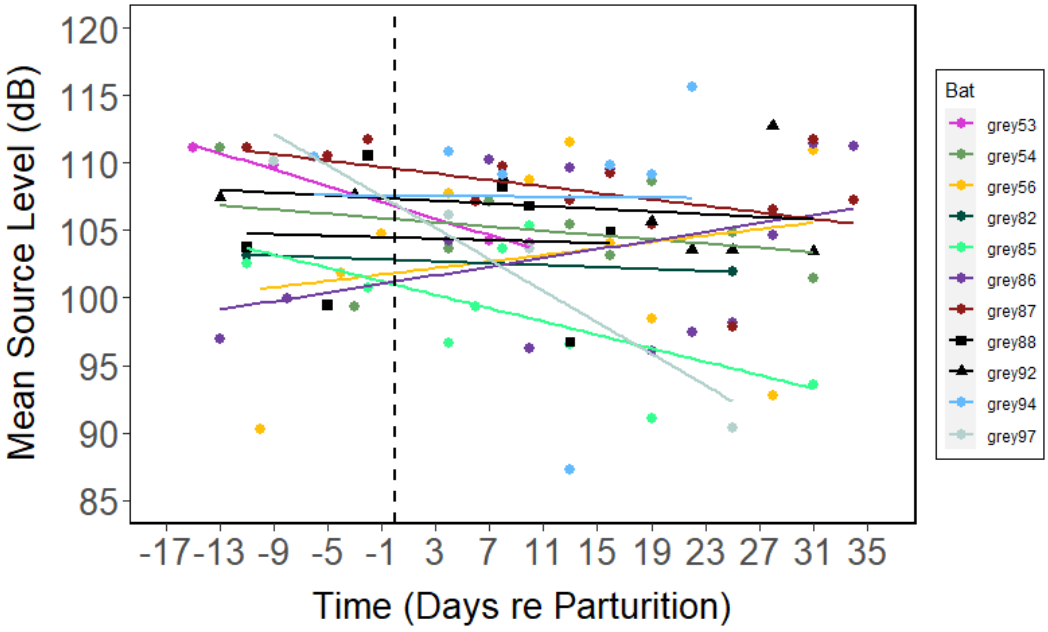

Figure 11: Mean source levels before and after take-off over pregnancy and lactation as a function of days relative to parturition (dashed vertical line) for each of nine pregnant/lactating and two control (Grey 88 and Grey 92) bats with linear trend lines.

Discussion

With our captive colony of big brown bats we were able to follow the same individuals through pregnancy and lactation, and thus observe changes in echolocation over this time. During recordings bats were released in a manner that we believe mimics their emergence from a roost. In this way, the results of our study cover the effects of pregnancy and lactation on echolocation in the first few seconds after a female bat has left the roost.

In their study on echolocation in wild Kuhl's pipistrelles (*Pipistrellus kuhlii*), Taub et al. (2023) found that the echolocation calls of pregnant bats completing a foraging task had longer call durations and interpulse intervals than female bats after the lactation period. If we focus on the time after 'roost emergence' when our bats were in flight, we find that over the course of pregnancy and lactation female *E. fuscus* used increasingly longer call durations, but the pulse intervals they used did not change significantly. Longer call durations would result in longer duration echoes, which would carry more information than shorter echoes. The number of strobe groups emitted during this time were similar for pregnant/lactating and control bats (ICCs close to zero). Therefore the pregnant/lactating bats were not significantly changing how many strobe groups were used to navigate the recording room but were changing the duration of their echolocation calls. Kothari et al. (2014) noted that big brown bats produce more sonar strobe groups when they need to accurately track movement and separate objects from a background, such as when they are navigating or foraging in a cluttered environment. This suggests that the use of strobe groups helps bats to gather more information about complex environments. Because the room that we recorded *E. fuscus* in did not become

more or less cluttered over time, then it makes sense that we did not observe a significant change in the number of strobe groups that bats emitted.

Taub et al. (2023) also found no significant differences in echolocation frequency and intensity between their groups of pregnant and post-lactating bats, but noted that bats with higher body mass indexes (i.e., pregnant bats) used lower frequency calls. This is consistent with the general decrease in centroid frequency that we found during the gestation and lactation periods, the lack of change in mean source level over the same time, and the change in source level between days that was similar between pregnant/lactating and control *E. fuscus* (ICCs close to zero). We also found that the female bats emitted calls with a narrower signal bandwidth while in flight throughout pregnancy and lactation. These results do not entirely match our predictions, as pulse interval did not change during flight when comparing pregnant/lactating and control bats, and the changes in call duration, centroid frequency and bandwidth continued in the same directions through the lactation period rather than reversing.

The decrease in echolocation call centroid frequency that we found over pregnancy and lactation suggests that pregnant/lactating bats would produce echolocation beams that grew gradually wider and less directional over this time (Jakobsen, Brinkløv, & Surlykke, 2013; Jakobsen, Ratcliffe, & Surlykke, 2013). Due to pregnant/lactating bats also not significantly changing their echolocation call source levels during this period, the functional operating distance of their echolocation beams would remain practically the same. In conjunction with the increase in call duration over the gestation and lactation periods, pregnant/lactating bats would be gathering more information from a wider area but not closer to or further away from them (Jakobsen, Brinkløv, & Surlykke, 2013;

Jakobsen, Ratcliffe, & Surlykke, 2013; Surlykke & Moss, 2000). This means that pregnant/lactating bats would be more aware of what was happening in their direct vicinity, which could allow them to navigate their environment with a reduced likelihood of having to make quick changes to their flight paths that would necessarily be more difficult while carrying the extra mass of fetuses during pregnancy or pups that may be attached to them during lactation (Hood et al., 2006; Hughes & Rayner, 1993; Taub et al, 2023).

Increasing call duration, lowering call frequency and narrowing call bandwidth have been correlated in previous studies of the echolocation behaviour of big brown bats that (Moss & Surlykke, 2001; Surlykke & Moss, 2000). We can assume that the *E. fuscus* recorded in these studies were not pregnant or lactating owing to the reported time of year (late August) and/or lack of mention of any pups (Moss & Surlykke, 2001; Surlykke & Moss, 2000). However, the aforementioned echolocation call changes have also been correlated with increasing IPI, which we did not find when the other three changes occurred (Moss & Surlykke, 2001; Surlykke & Moss, 2000). This may suggest that IPI/pulse interval is less strongly correlated with call duration, frequency and bandwidth during pregnancy and lactation. It may also be due to our bats being flown in a confined space, as *E. fuscus* have been found to emit signals with shorter IPIs/pulse intervals in the laboratory compared to the wild (Surlykke & Moss, 2000). Since the gestation period of big brown bats is around 60 days, our echolocation data only cover the last quarter (15 days) of pregnancy (Kurta & Baker, 1990). Future studies should consider colleting data from earlier in pregnancy to see if this would change the trends we found in echolocation call characteristics. For instance, if the IPI/pulse interval does increase during pregnancy

and lactation our data set might not reveal this because we did not record for enough days for such a trend to become visible.

As predicted, wing loading increased with increasing mass during pregnancy and began decreasing immediately after bats give birth. The increase in wing loading during pregnancy was larger than the decrease after parturition and did not return to starting (i.e., early pregnancy) values. There are at least two reasons for this. First, because captive pregnant bats did not have to fly to eat and had *ad libitum* access to food, they likely gained more mass compared to bats in the wild. Second, because lactation is expensive energetically female bats needed to continue consuming extra food during lactation to maintain milk production for their pups (Hood et al., 2006). Pulse interval, which we suspected could change with wing loading, did not differ significantly between pregnant/lactating and control bats or over pregnancy and lactation while bats were in flight. Given that wingbeat frequency has been found to increase with increased mass, it would be interesting to use video recordings to determine if the distribution of sonar strobe groups emitted throughout the wingbeat cycle changed, particularly over the course of pregnancy but also during lactation (Hughes & Rayner, 1993; Koblitz et al., 2010; Moss et al., 2006).

Although there were some significant changes in echolocation call characteristics over time before bats took flight—increased call durations in control bats, decreases in pulse interval in pregnant/lactating bats but increases in control bats, increased number of strobe groups in pregnant/lactating bats but decreased in control bats, and decreased centroid frequency in pregnant/lactating bats—these may not perfectly translate to the behaviour of bats in the process of emerging from a roost because bats were initially

handled before taking flight. Future studies seeking to make this comparison should consider creating a more roost-like environment (e.g., bat box, covered platform) where bats could initiate flight on their own with less human handling. One difficulty with this approach would be getting the bats to leave the 'roost' and fly towards the microphone array, especially during late pregnancy. During our study, we found it difficult to get pregnant bats to fly, particularly as their pregnancies progressed and they neared parturition. Although wild bats continue to fly and forage during pregnancy, and likely become less agile and maneuverable in flight the closer they are to giving birth, we do not know if and when late-stage pregnant female bats stop foraging (Henry et al., 2002; Rintoul & Brigham, 2014). We decided that handling all the bats—pregnant and control—was necessary to ensure that all animals were treated the same, and to encourage some bats in late-stage pregnancy who were reluctant to fly to become airborne, even if only for a short time. Requiring the bats to exit a 'roost' on their own would likely have resulted in obtaining fewer in-flight recordings during late pregnancy. This complication could possibly be avoided by using a food reward to train all bats the leave the 'roost' over the course of pregnancy and lactation.

Although the results of this study may not fully map onto the naturalistic echolocation behaviour of big brown bats because we know *E. fucus* uses echolocation differently in the confines to the laboratory than they do in the wild one interesting possibility is that the signaling changes we and Taub et al. (2023) observed could possibly be used as a basis to attempt to identify pregnant and lactating bats in the wild with bioacoustic monitoring (Surlykke & Moss, 2000). Even if the trends we observed do not exactly match the way pregnant/lactating bats echolocate in the wild, the relative

differences between pregnant/lactating and non-reproductive females may still hold. Repeating these studies with other bat species could also help to identify a bioacoustic signature of pregnancy and/or lactation in bats, as different bat species have unique echolocation call structures that could change in precise ways during pregnancy and lactation that differ between species (Fenton & Bell, 1981). Future research could also test if bats experience a loss of hearing sensitivity during pregnancy, as is reported for humans, and if so at what frequencies (Sennaroglu & Belgin, 2001). Pregnant humans have been observed to experience a loss of low frequency auditory sensitivity during the gestation period (Sennaroglu & Belgin, 2001). Testing the hearing of pregnant/lactating bats could provide insight into why the echolocation frequencies they use during pregnancy and lactation change in the way they do.

Conclusion

Our data demonstrate that there are significant changes in both temporal and spectral characteristics of echolocation calls produced by big brown bats in flight over the course of pregnancy and lactation. Specifically, our study design mimicked changes in echolocation characteristics during the time when pregnant and lactating bats would have emerged from their roost, which has not been covered by previous research. In this type of flight, echolocation call duration increased, bandwidth narrowed and centroid frequency dropped continuously for big brown bats during their gestation and lactation periods.

References

Ben-Shachar, M., Lüdecke, D., Makowski, D. (2020). effectsize: Estimation of effect size indices and standardized parameters. *Journal of Open Source Software*, *5*(56), 2815. https://doi.org/10.21105/joss.02815

Best, T.L., & Jennings, J.B. (1997). Myotis leibii, *Mammalian Species, 547,* 1–6. https://doi.org/10.2307/3504255

Caceres, M.C., & Barclay, R.M.R. (2000). Myotis septentrionalis, *Mammalian Species, 634*, 1–4. https://doi.org/10.2307/0.634.1

Cassuraga, V.L., Castellano, A.V., Abasolo, J., Abin, E.N., & Izbizky, G.H. (2012). Pregnancy and voice: Changes during the third trimester. *Journal of Voice, 26*(5), 585–586. https://doi.org/10.1016/j.jvoice.2011.10.004

Currie, S.E., Boonman, A., Troxell, S., Yovel, Y., & Voigt, C.C. (2020). Echolocation at high intensity imposes metabolic costs on flying bats. *Nature Ecology & Evolution, 4*, 1174–1177. https://doi.org/10.1038/s41559-020-1249-8

Fenton, M.B., & Barclay, R.M.R. (1980). Myotis lucifugus, *Mammalian Species, 142*, 1–8. https://doi.org/10.2307/3503792

Fenton, M. B., & Bell, G. P. (1981). Recognition of species of insectivorous bats by their echolocation calls. *Journal of Mammalogy, 62*(2), 233–243. https://doi.org/10.2307/1380701

Fenton, M.B., Skowronski, M.D., McGuire, L.P., & Faure, P.A. (2011). Variation in the use of harmonics in the calls of laryngeally echolocating bats. *Acta Chiropterologica, 13*(1), 169–178. https://doi.org/10.3161/150811011X578714

Fujita, M.S., & Kunz, T.H. (1984). Pipistrellus subflavus, *Mammalian Species, 228*, 1–6. https://doi.org/10.2307/3504021

Ghaemi, H., Dehqan, A., Mahmoodi-Bakhtiri, B., & Scherer, R.C. (2020). Voice changes during pregnancy trimesters in Iranian pregnant women. *Journal of Voice, 34*(3), 358–363. https://doi.org/10.1016/j.jvoice.2018.09.016

Hamdan, A.-L., Mahfoud, L., Sibai, A., & Seoud, M. (2009). Effect of pregnancy on the speaking voice. *Journal of Voice, 23*(4), 490–493. https://doi.org/10.1016/j.jvoice.2007.11.006

Hancock, A.B., & Gross, H.E. (2015). Acoustic and aerodynamic measures of the voice during pregnancy. *Journal of Voice, 29*(1), 53–58. https://doi.org/10.1016/j.jvoice.2014.04.005

Henry, M., Thomas, D.W., Vaudry, R., & Carrier, M. (2002). Foraging distances and home range of pregnant and lactating little brown bats (*Myotis lucifugus*). *Journal of Mammalogy, 83*(3), 767–774. https://doi.org/10.1644/1545-1542(2002)083<0767:FDAHRO>2.0.CO;2

Hood, W.R., Oftedal, O.T., & Kunz, T.H. (2006). Variation in body composition of female big brown bats (*Eptesicus fuscus*) during lactation. *Journal of Comparative Physiology B, 176*, 807–819. https://doi.org/10.1007/s00360-006-0102-y

Hiryu, S., Bates M.E., Simmons, J.A., & Riquimaroux, H. (2010). FM echolocating bats shift frequencies to avoid broadcast-echo ambiguity in clutter. *Proc. Natl Acad. Sci. USA 107,* 7048–7053. https://doi.org/10.1073/pnas.1000429107

Hughes, P., & Rayner, J.M.V. (1993). The flight of pipistrelle bats *Pipistrellus pipistrellus* during pregnancy and lactation. *Journal of Zoology, 230*(4), 541–555. https://doi.org/10.1111/j.1469-7998.1993.tb02705.x

Jakobsen, L., Brinkløv, S., & Surlykke, A. (2013). Intensity and directionality of bat echolocation signals. *Frontiers in Physiology, 4.* https://doi.org/10.3389/fphys.2013.00089

Jakobsen, L., Ratcliffe, J.M., & Surlykke, A. (2013). Convergent acoustic field of view in echolocating bats. *Nature, 493,* 93–96. https://doi.org/10.1038/nature11664

Jones, G. (1999). Scaling of echolocation call parameters in bats. *Journal of Experimental Biology, 202*(23), 3359–3367. https://doi.org/10.1242/jeb.202.23.3359

Koblitz, J.C., Stilz, P., & Schnitzler, H-U. (2010). Source levels of echolocation signals vary in correlation with wingbeat cycle in landing big brown bats (*Eptesicus fuscus*). *Journal of Experimental Biology, 213*(19), 3263–3268. https://doi.org/10.1242/jeb.045450

Kothari, N.B., Wohlgemuth, M.J., Hulgard, K., Surlykke, A., & Moss, C.F. (2014). Timing matters: Sonar call groups facilitate target localization in bats. *Frontiers in Physiology*, 5, 168. https://doi.org/10.3389/fphys.2014.00168

Kuznetsova, A., Brockhoff, P.B., Christensen, R.H.B. (2017). lmerTest package: Tests in linear mixed effects models. *Journal of Statistical Software*, *82*(13), 1–26. https://doi.org/10.18637/jss.v082.i13

Kunz, T.H. (1982). Lasionycteris noctivagans, *Mammalian Species, 172*, 1–5. https://doi.org/10.2307/3504029

Kunz, T.H., Whitaker Jr., O., & Wadanoli, M.D. (1995). Dietary energetics of the insectivorous Mexican free-tailed bat (*Tadarida brasiliensis*) during pregnancy and lactation. *Oecologia*, *101*(4), 407–415. https://doi.org/10.1007/BF00329419

Kurta, A., & Baker, R.H. (1990). Eptesicus fuscus, *Mammalian Species, 356*, 1–10. https://doi.org/10.2307/3504258

Kurta, A., Kunz, T.H., & Nagy, K.A. (1990). Energetics and water flux of free-ranging big brown bats (*Eptesicus fuscus*) during pregnancy and lactation. *Journal of Mammalogy*, *71*(1), 59–65. https://doi.org/10.2307/1381316

Lancaster, W.C., Henson, O.W., & Keating, A.W. (1995). Respiratory muscle activity in relation to vocalization in flying bats. *Journal of Experimental Biology, 198*(1), 175–191. https://doi.org/10.1242/jeb.198.1.175

LoMauro, A., Aliverti, A., Frykholm, P., Alberico, D., Persico, N., Boschetti, G., DeBellis, M., Briganti, F., Nosotti, M., & Righi, I. (2019). Adaptation of lung, chest wall, and respiratory muscles during pregnancy: preparing for birth. *Journal of Applied Physiology*, *127*(6), 1640–1650. https://doi.org/10.1152/japplphysiol.00035.2019

Luo, J., & Wiegrebe, L. (2016). Biomechanical control of vocal plasticity in an echolocating bat. *Journal of Experimental Biology, 219*(6), 878–886. https://doi.org/10.1242/jeb.134957

Lüdecke, D., Ben-Shachar, M., Patil, I., Waggoner, P., & Makowski, D. (2021). performance: an R package for assessment, comparison and testing of statistical models. *Journal of Open Source Software, 6*(60), 3139. https://doi.org/10.21105/joss.03139

Madsen, P.T., & Surlykke, A. (2013). Functional convergence in bat and toothed whale biosonars. *Physiology, 28*(5), 276–283. https://doi.org/10.1152/physiol.00008.2013

Maxwell, S.E., Delaney, H.D., & Kelley, K. (2018). *Designing experiments and analyzing data: A model comparison perspective* (3rd ed.). Routledge. https://doi.org/10.4324/9781315642956

Mayberry, H.W., & Faure, P. (2015). Morphological, olfactory, and vocal development in big brown bats. *Biology Open, 4*(1), 22–34. https://doi.org/10.1242/bio.201410181

Moss, C.F., & Surlykke, A. (2001). Auditory scene analysis by echolocation in bats. *The Journal of the Acoustical Society of America, 110*(4), 2207–2226. https://doi.org/10.1121/1.1398051

Norberg, U.M., & Rayner J.M.V. (1987). Ecological morphology and flight in bats (Mammalia; Chiroptera): wing adaptations, flight performance, foraging strategy

and echolocation. *Philosophical Transactions of the Royal Society B: Biological Sciences, 316,* 335–427. http://doi.org/10.1098/rstb.1987.0030

Ooms, J. (2023). *writexl: export data frames to excel 'xlsx' format*. R package version 1.4.2, https://CRAN.R-project.org/package=writexl

Petrites, A.E., Eng, O.S., Mowlds, D.S., Simmons, J.A., & DeLong, C.M. (2009). Interpulse interval modulation by echolocating big brown bats (*Eptesicus fuscus*) in different densities of obstacle clutter. *Journal of Comparative Physiology A, 195,* 603–617. https://doi.org/10.1007/s00359-009-0435-6

R Core Team (2023). R: A language and environment for statistical computing. R Foundation for Statistical Computing, Vienna, Austria. https://www.R-project.org/.

Rintoul, J. L., & Brigham, R. M. (2014). The influence of reproductive condition and concurrent environmental factors on torpor and foraging patterns in female big brown bats (*Eptesicus fuscus*). *Journal of Comparative Physiology B, 184*(6), 777–787. https://doi.org/10.1007/s00360-014-0837-9

Saltürk, Z., Kumral, T.L., Bekiten, G., Atar, Y., Ataç, E., Aydoğdu, İ., Yildirim, G., Kiliç, A., & Uyar, Y. (2016). Objective and subjective aspects of voice in pregnancy. *Journal of Voice, 30*(1), 70–73. https://doi.org/10.1016/j.jvoice.2015.02.013

Şanal, S.K., Biçer, Y.Ö., Kükner, A., & Tezcan, E. (2016). Effect of pregnancy on vocal cord histology: An animal experiment. *Balkan Medical Journal, 33*(4), 448–452. https://doi.org/10.5152/balkanmedj.2016.15286

Sennaroglu, G., & Belgin, E. (2001). Audiological findings in pregnancy. *The Journal of Laryngology & Otology, 115*(8), 617–621. https://doi.org/10.1258/0022215011908603

Shump Jr., K.A., & Shump, A.U. (1982a). Lasiurus borealis, *Mammalian Species, 183,* 1–6. https://doi.org/10.2307/3503843

Shump Jr., K.A., & Shump, A.U. (1982b). Lasiurus cinereus, *Mammalian Species, 185,* 1–5. https://doi.org/10.2307/3503878

Speakman, J.R., Anderson, M.E., & Racey, P.A. (1989). The energy cost of echolocation in pipistrelle bats (*Pipistrellus pipistrellus*). *Journal of Comparative Physiology A, 165,* 679–685. https://doi.org/10.1007/BF00610999

Speakman, J.R., & Racey, P.A. (1991). No cost of echolocation for bats in flight. *Nature, 350*, 421–423. https://doi.org/10.1038/350421a0

Surlykke, A., & Moss, C.F. (2000). Echolocation behaviour of big brown bats, *Eptesicus fuscus*, in the field and the laboratory. *The Journal of the Acoustical Society of America, 108*(5), 2419–2429. https://doi.org/10.1121/1.1315295

Suthers, R.A., Thomas, S.P., & Suthers, B.J. (1972). Respiration, wing-beat and ultrasonic pulse emission in an echo-locating bat. *Journal of Experimental Biology, 56*(1), 37–48. https://doi.org/10.1242/jeb.56.1.37

Taub, M., Mazar, O., & Yovel, Y. (2023). Pregnancy-related sensory deficits might impair foraging in echolocating bats. *BMC Biology, 21,* 60. https://doi.org/10.1186/s12915-023-01557-7

The MathWorks Inc. (2022). MATLAB version: 9.13.0 (R2022b), Natick, Massachusetts: The MathWorks Inc. https://www.mathworks.com

The MathWorks Inc. (2023). MATLAB version: 9.14.0 (R2023a), Natick, Massachusetts: The MathWorks Inc. https://www.mathworks.com

Veselka, N., McErlain, D.D., Holdsworth, D.W., Eger, J.L., Chhem, R.K., Mason, M.J., Brain, K.L., Faure, P.A., & Fenton, M.B. (2010). A bony connection signal laryngeal echolocation in bats. *Nature, 463*, 939–942. https://doi.org/10.1038/nature08737

Wickham, H. (2016). *ggplot2: Elegant graphics for data analysis.* R package version 3.4.2, Springer-Verlag New York. ISBN 978-3-319-24277-4, https://ggplot2.tidyverse.org.

Wickham, H., & Bryan, J. (2023). *readxl: Read excel files*. R package version 1.4.2, https://CRAN.R-project.org/package=readxl

Wickham, H., François, R., Henry, L., Müller, K., & Vaughan, D. (2023). *dplyr: A grammar of data manipulation.* R package version 1.1.2, https://CRAN.R-project.org/package=dplyr

Wickham, H., Vaughan, D., & Girlich, M. (2023). *tidyr: Tidy messy data*. R package version 1.3.0, https://CRAN.R-project.org/package=tidyr.

Appendix

Recording Setup

Appendix Table 1: Equipment used for audio recordings with the number of units of each item used.

Recording Equipment
GRAS 42AB Sound Calibrator × 1
GRAS 12AX 4-Channel CCP Power Module with Gain × 3
GRAS AA0070 3 m Microdot - BNC Cable × 11
5+ m XLR cable × 12
XLR to BNC connectors × 11
USBZ A/A 6 ft cable × 4
GRAS 46BE 1/4" CCP Free-field Standard Microphone × 11
GRAS 26CB 1/4" CCP Standard Preamplifier with Microdot Connector × 11
Condenser ultrasound microphone Avisoft-Bioacoustics CM16/CMPA × 1
Avisoft UltraSoundGate 1216H × 1
Lenovo ThinkPad T430 (Windows 10) with Avisoft-RECORDER software × 1
Power surge protector × 1
RAVPower 27000mAh Portable Power Outlet × 2

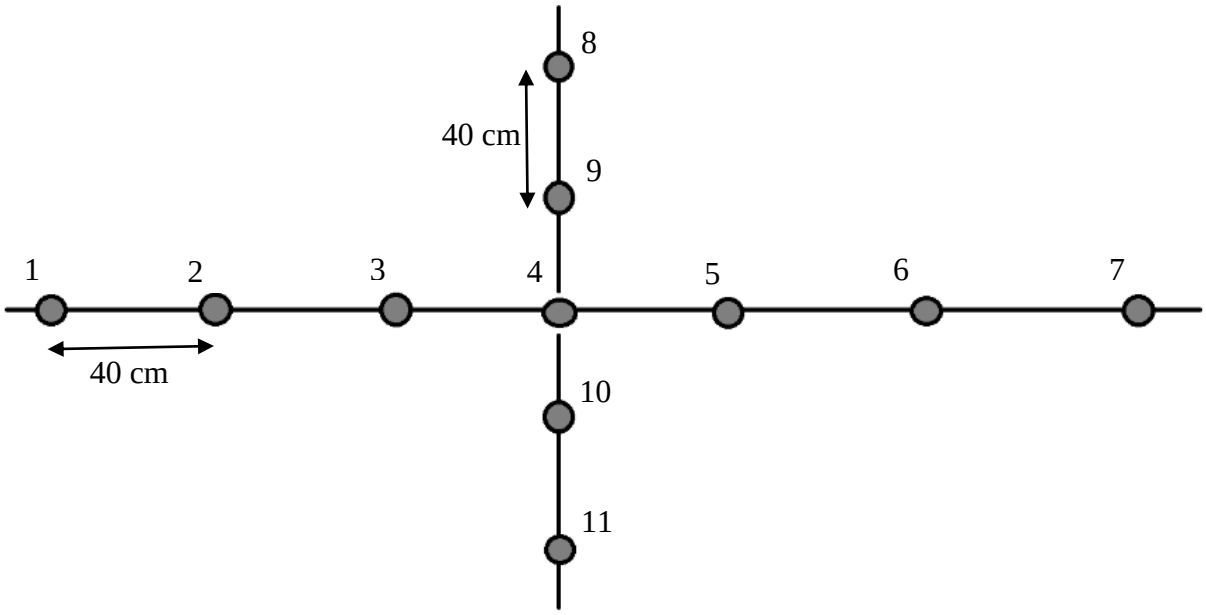

Appendix Figure 1: The dimensions (not to scale) of the eleven-microphone array used for audio recordings. Each circle represents a microphone. Microphone numbers (1 to 11) are noted above each circle. The distance between neighbouring microphones was ~40 cm for all microphones.

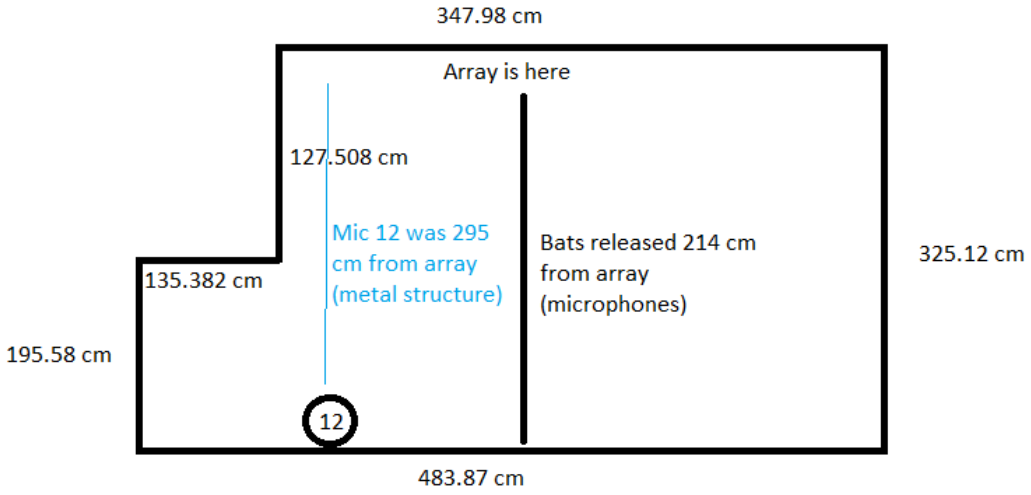

Appendix Figure 2: The dimensions of the anechoic room that audio recordings took place in. The solid vertical black line labeled 214 cm indicates the distance bats started from the array. The black circled labeled 12 indicates the location of the Avisoft-Bioacoustics CM16/CMPA ultrasound microphone used to pick up ambient noise. All other solid black lines represent the walls of the recording room.

Surface Area and Wingspan

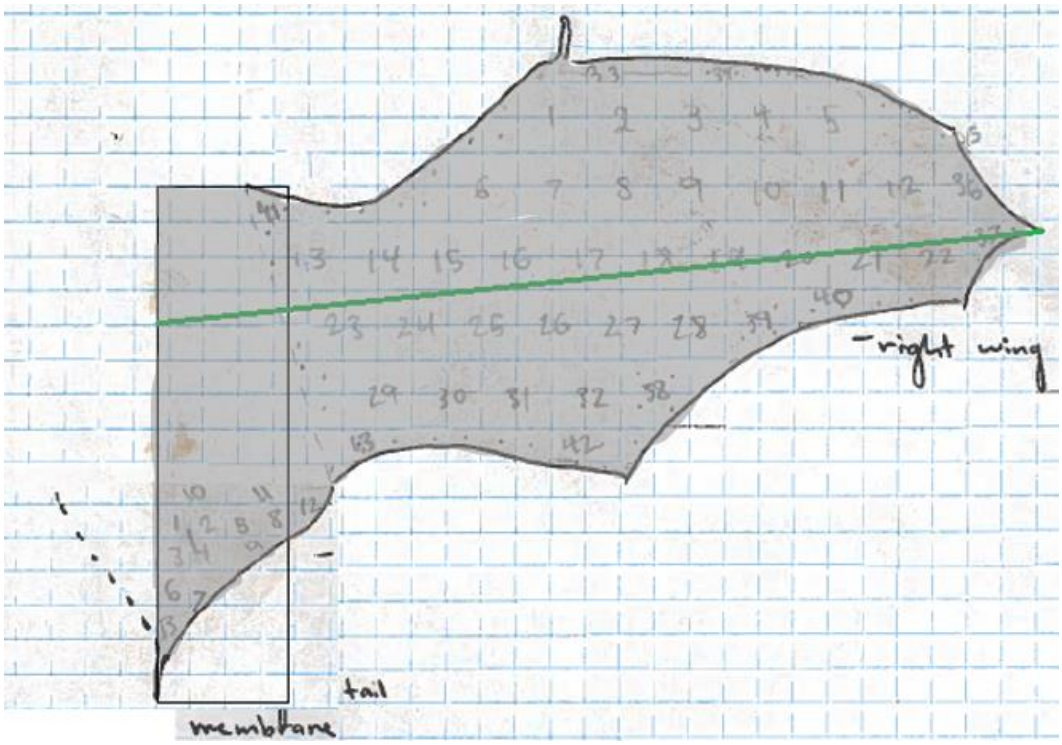

Appendix Figure 3: The surface area (SA) and wingspan (S) used to calculate wing loading and aspect ratio. The grey shaded area represents half of the total surface area (SA/2). The green line represents half of the wingspan (S/2).

Grey 53 Echolocation Call Characteristics Graphs

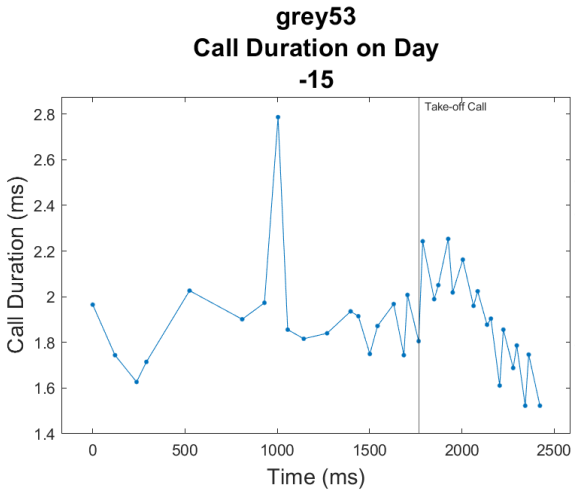

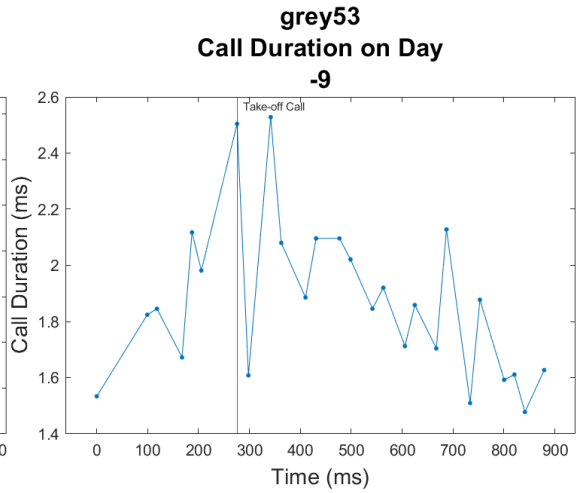

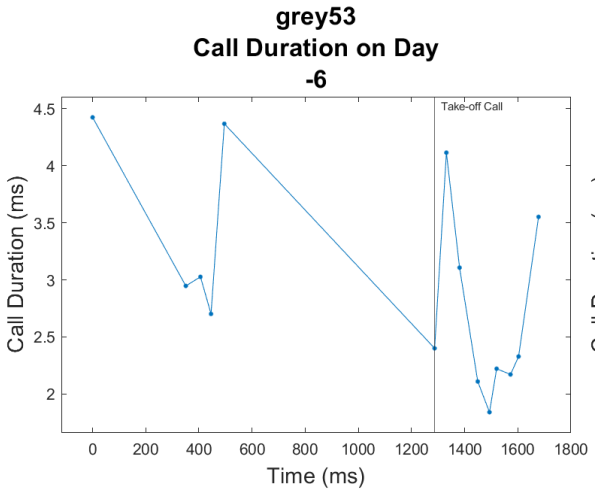

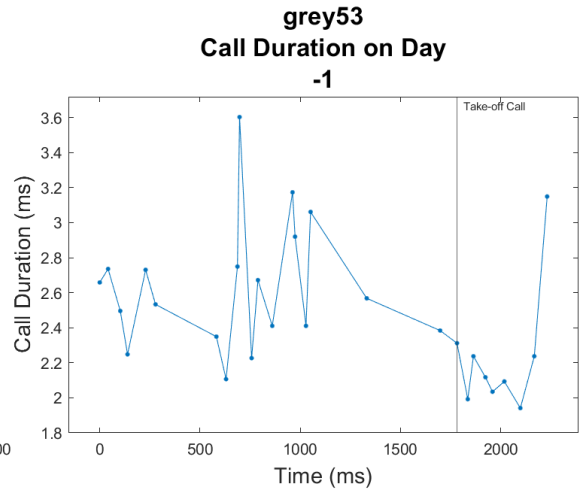

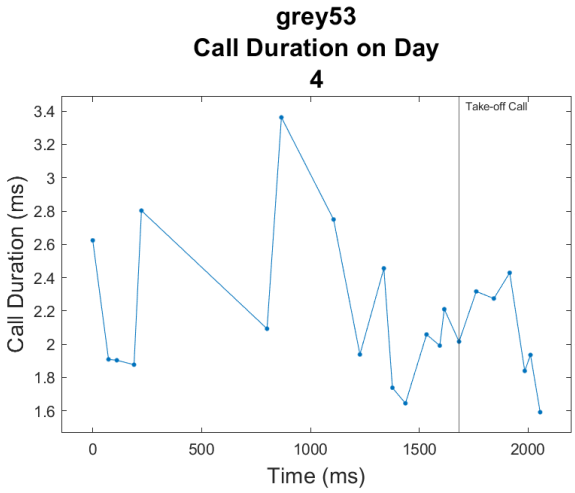

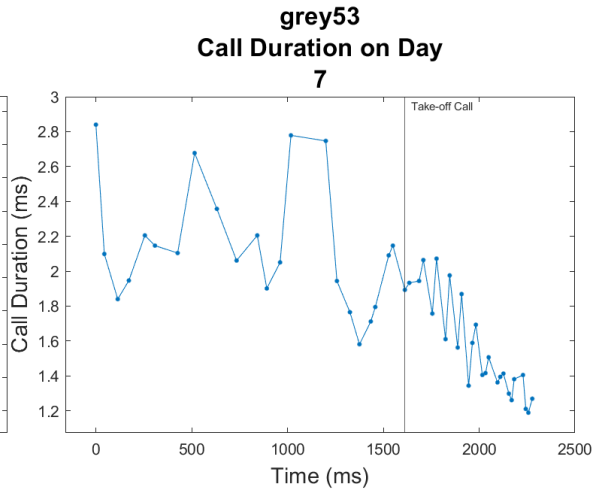

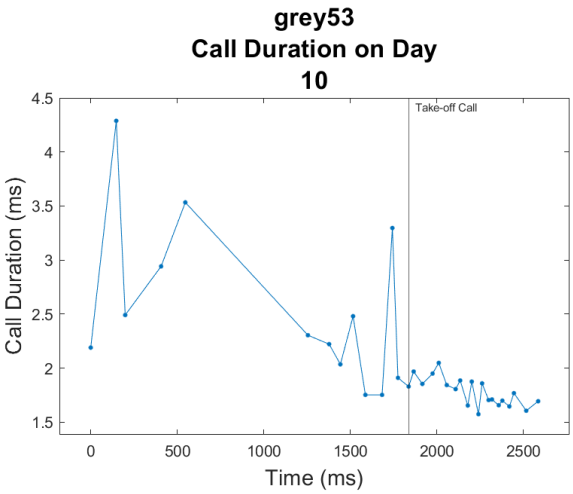

Appendix Figure 4: Grey 53 call duration plotted as a function of recording time per day. Each panel shows call durations before and after taking flight, with different panels showing data recorded on different days relative to parturition (number above panel; parturition day defined as Day 0). The take-off call is marked by a vertical line.

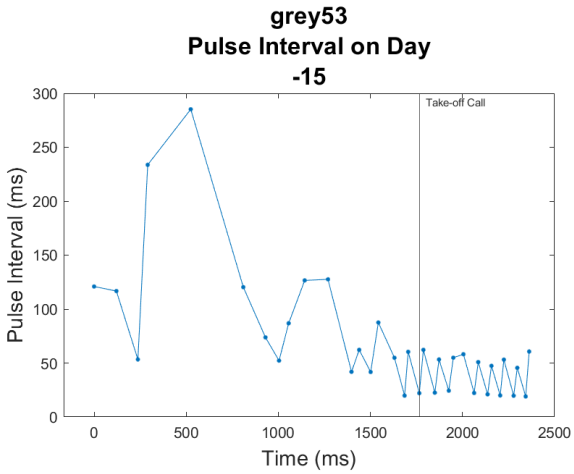
grey53
Pulse Interval on Day
-15
Take-off Call
Pulse Interval (ms)
Time (ms)

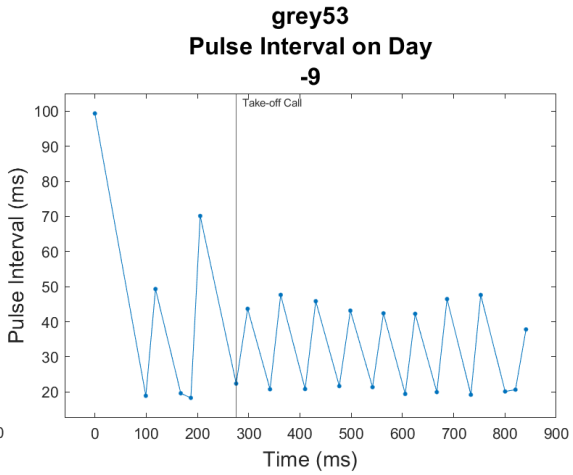
grey53
Pulse Interval on Day
-9
Take-off Call
Pulse Interval (ms)
Time (ms)

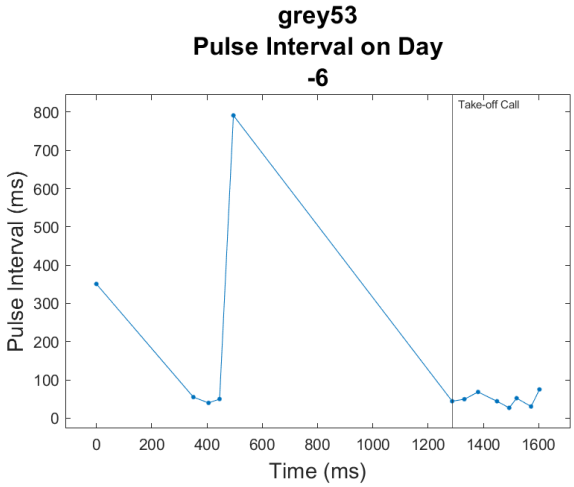
grey53
Pulse Interval on Day
-6
Take-off Call
Pulse Interval (ms)
Time (ms)

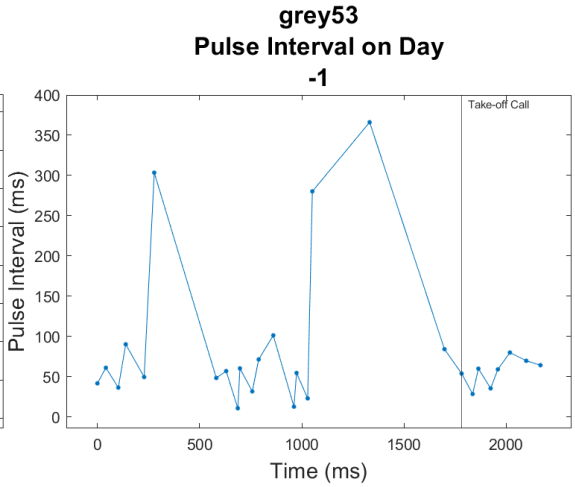
grey53
Pulse Interval on Day
-1
Take-off Call
Pulse Interval (ms)
Time (ms)

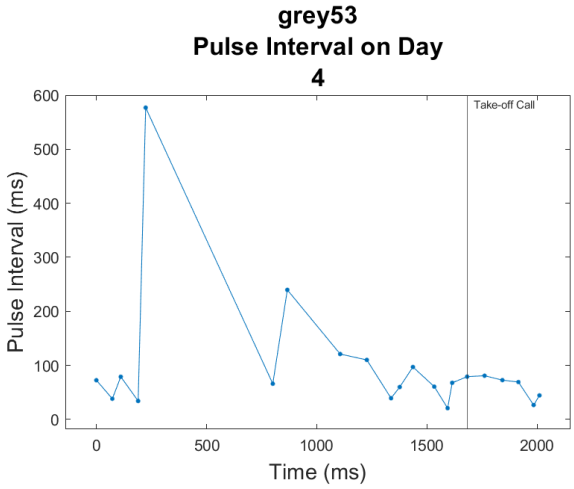
grey53
Pulse Interval on Day
4
Take-off Call
Pulse Interval (ms)
Time (ms)

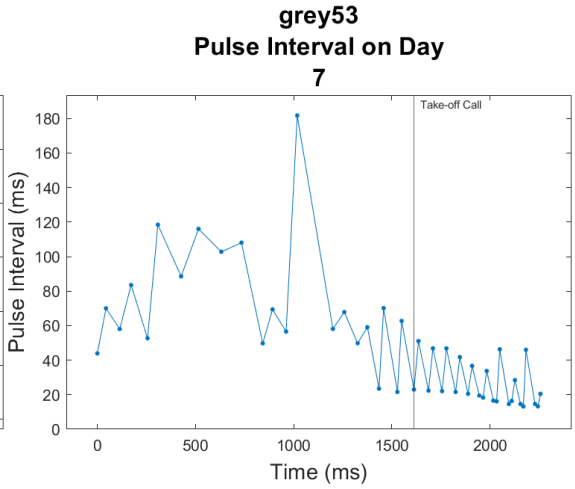
grey53
Pulse Interval on Day
7
Take-off Call
Pulse Interval (ms)
Time (ms)

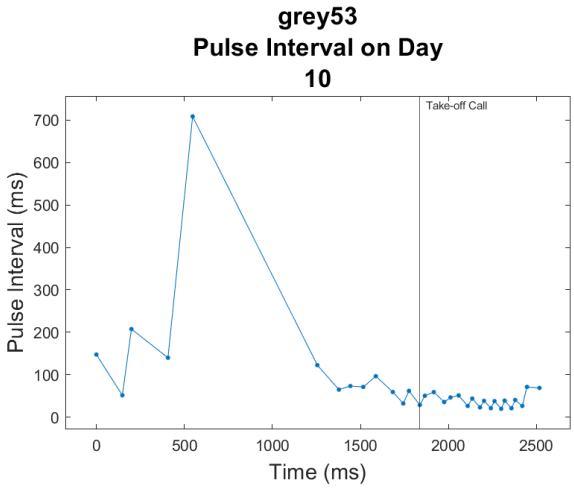

Appendix Figure 5: Grey 53 pulse interval plotted as a function of recording time per day. Each panel shows call durations before and after taking flight, with different panels showing data recorded on different days relative to parturition (number above panel; parturition day defined as Day 0). The take-off call is marked by a vertical line.

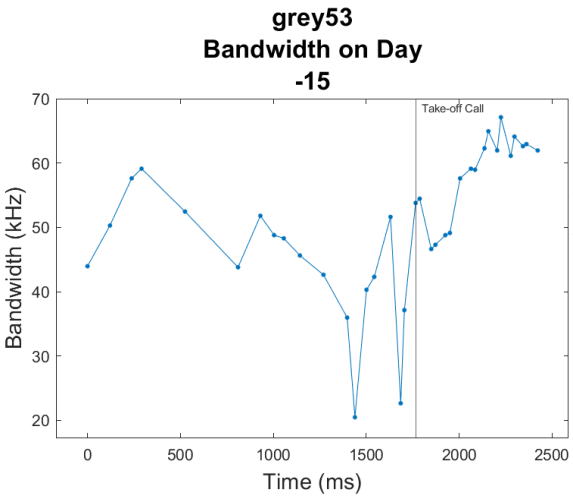
grey53
Bandwidth on Day
-15
Take-off Call
Bandwidth (kHz)
Time (ms)

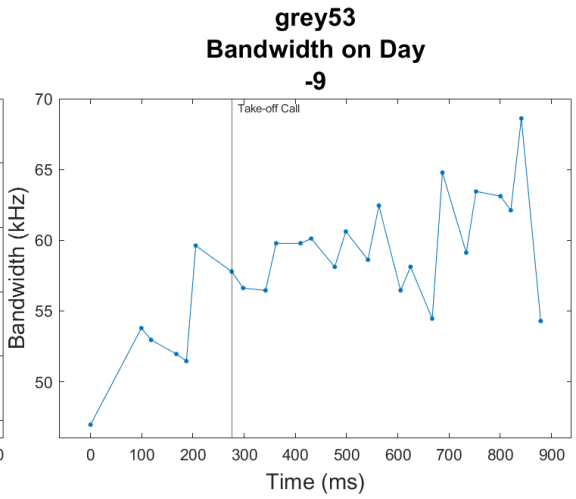
grey53
Bandwidth on Day
-9
Take-off Call
Bandwidth (kHz)
Time (ms)

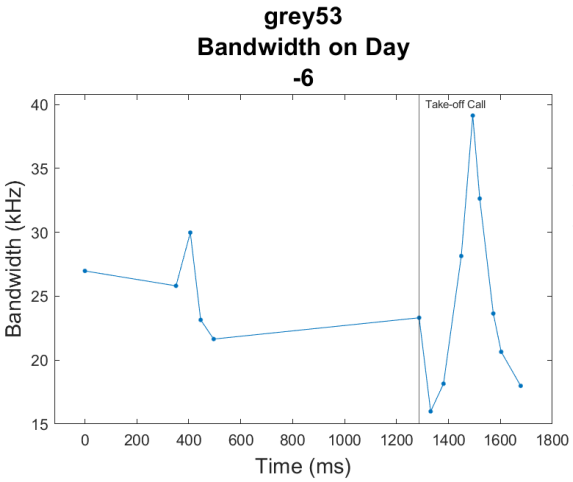
grey53
Bandwidth on Day
-6
Take-off Call
Bandwidth (kHz)
Time (ms)

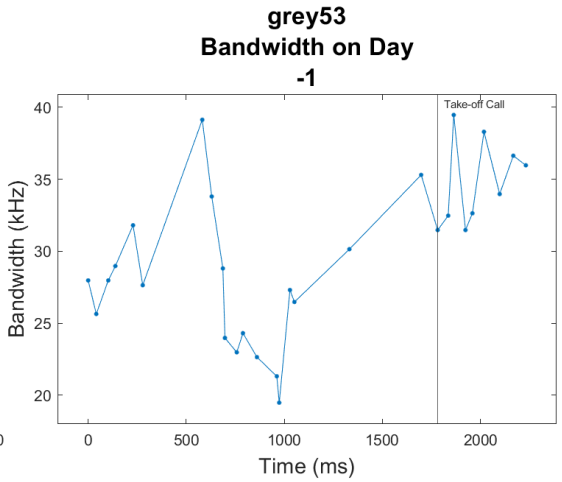
grey53
Bandwidth on Day
-1
Take-off Call
Bandwidth (kHz)
Time (ms)

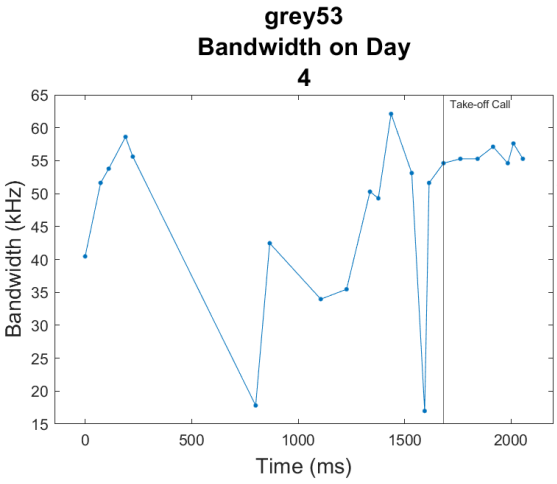
grey53
Bandwidth on Day
4
Take-off Call
Bandwidth (kHz)
Time (ms)

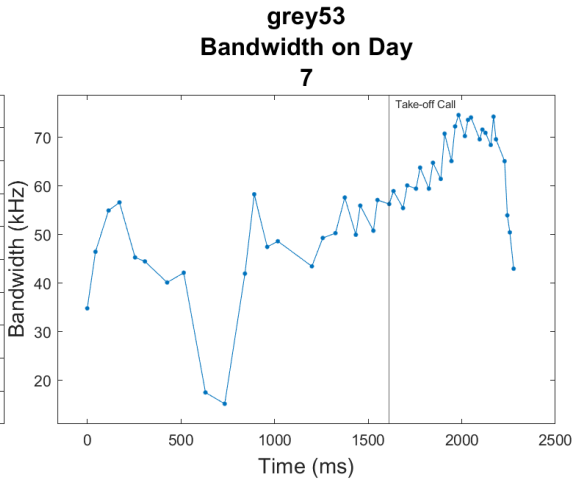
grey53
Bandwidth on Day
7
Take-off Call
Bandwidth (kHz)
Time (ms)

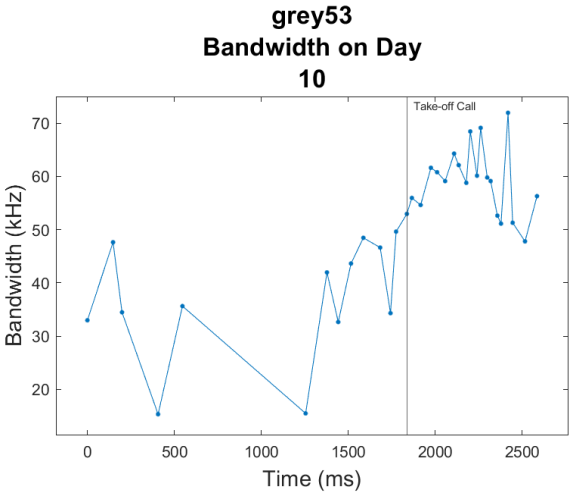

Appendix Figure 6: Grey 53 call bandwidth plotted as a function of recording time per day. Each panel shows call durations before and after taking flight, with different panels showing data recorded on different days relative to parturition (number above panel; parturition day defined as Day 0). The take-off call is marked by a vertical line.

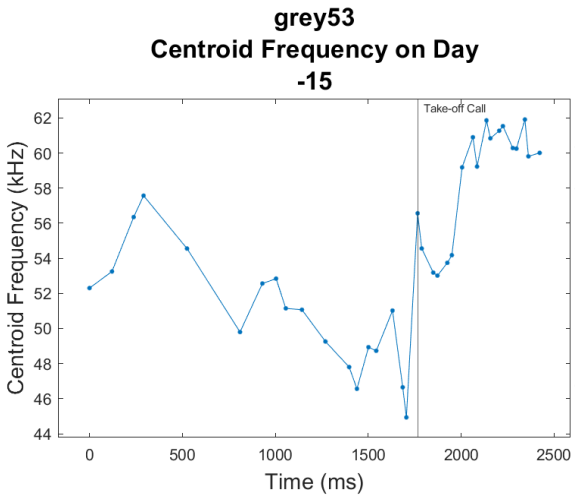
grey53
Centroid Frequency on Day
-15
Take-off Call
Centroid Frequency (kHz)
Time (ms)

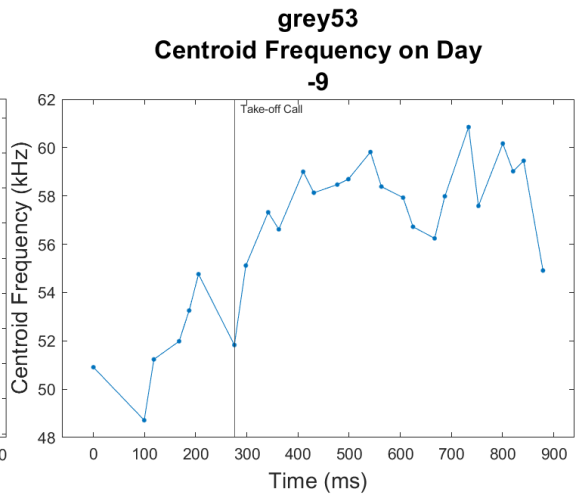
grey53
Centroid Frequency on Day
-9
Take-off Call
Centroid Frequency (kHz)
Time (ms)

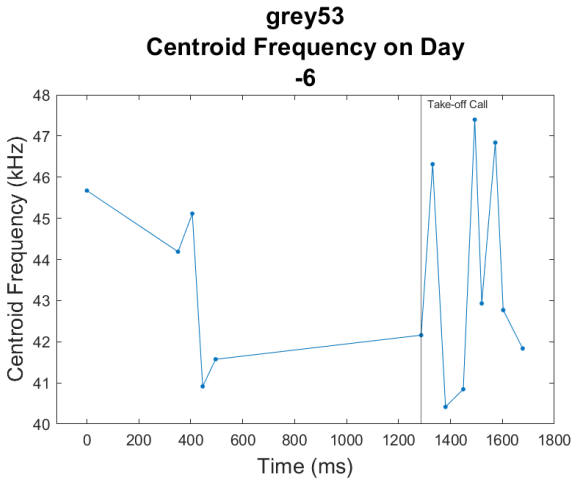
grey53
Centroid Frequency on Day
-6
Take-off Call
Centroid Frequency (kHz)
Time (ms)

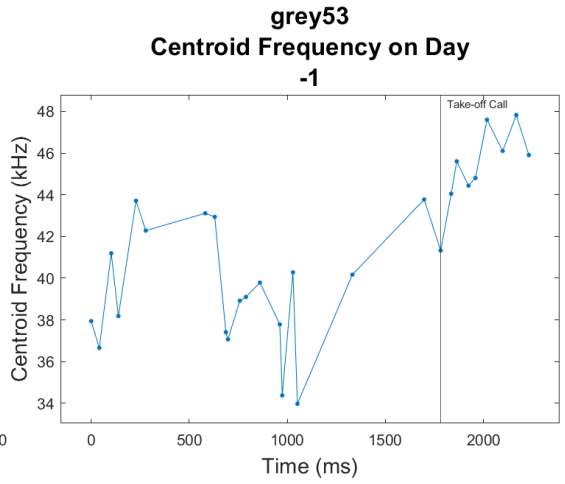
grey53
Centroid Frequency on Day
-1
Take-off Call
Centroid Frequency (kHz)
Time (ms)

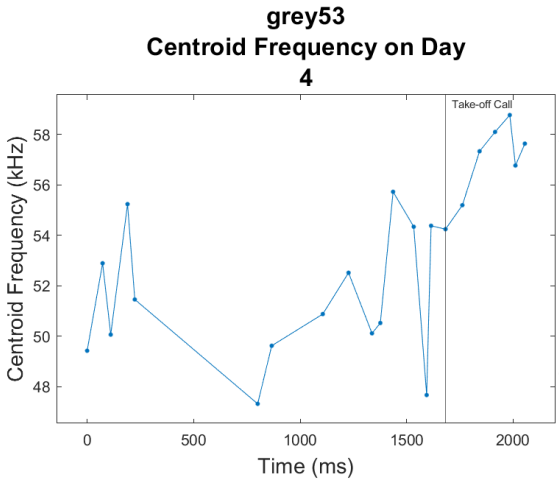
grey53
Centroid Frequency on Day
4
Take-off Call
Centroid Frequency (kHz)
Time (ms)

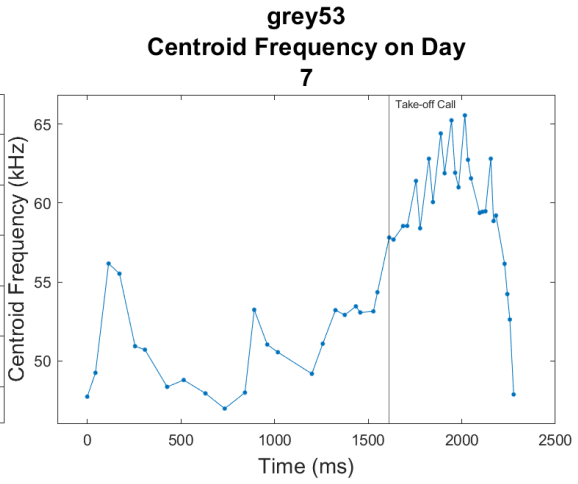
grey53
Centroid Frequency on Day
7
Take-off Call
Centroid Frequency (kHz)
Time (ms)

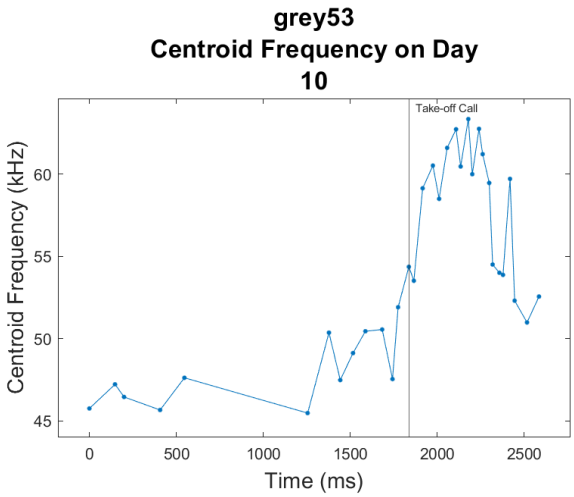

Appendix Figure 7: Grey 53 centroid frequency plotted as a function of recording time per day. Each panel shows call durations before and after taking flight, with different panels showing data recorded on different days relative to parturition (number above panel; parturition day defined as Day 0). The take-off call is marked by a vertical line.

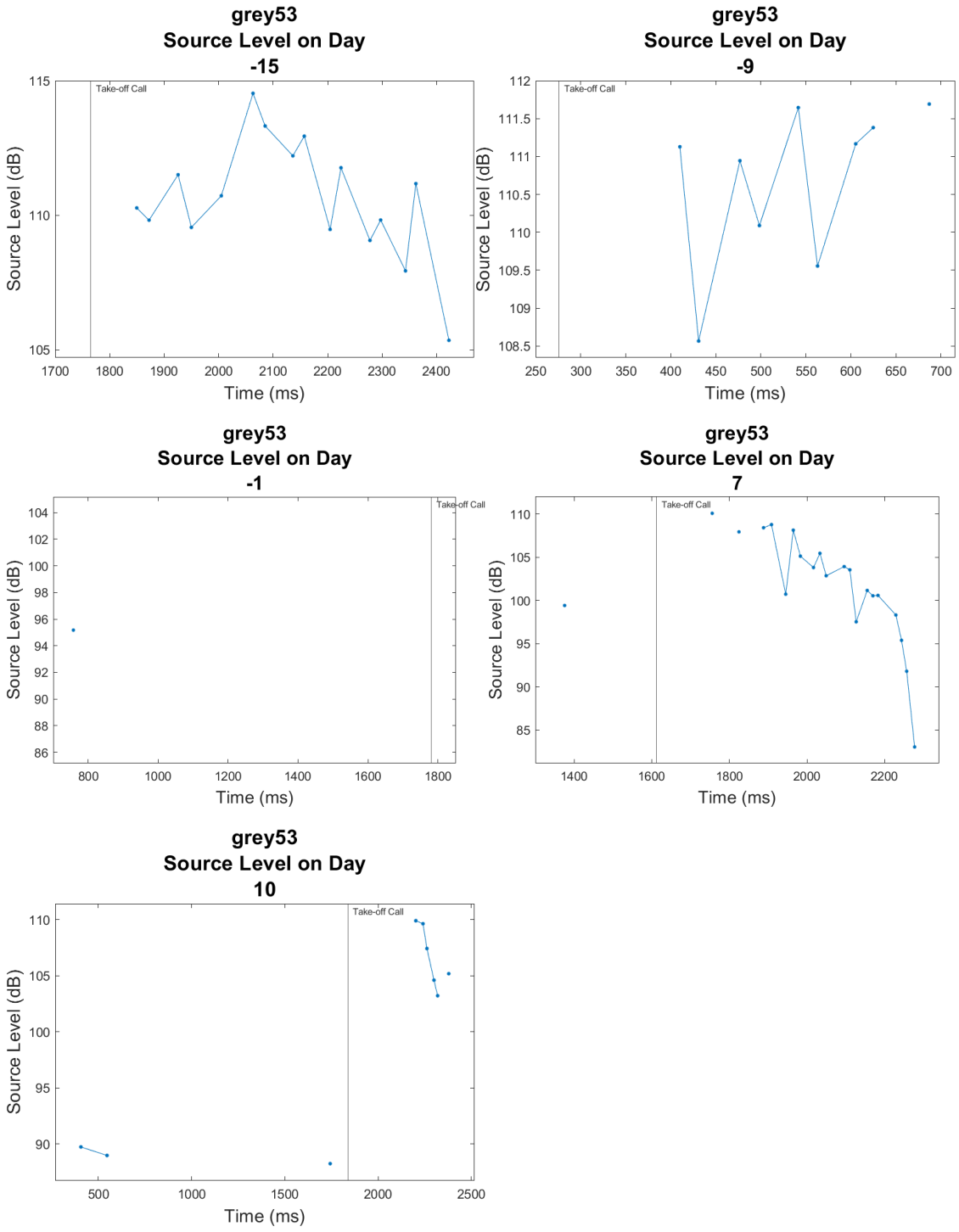

Appendix Figure 8: Grey 53 source level plotted as a function of recording time per day. Each panel shows call durations before and after taking flight, with different panels showing data recorded on different days relative to parturition (number above panel; parturition day defined as Day 0). The take-off call is marked by a vertical line.

Grey 54 Echolocation Call Characteristics Graphs

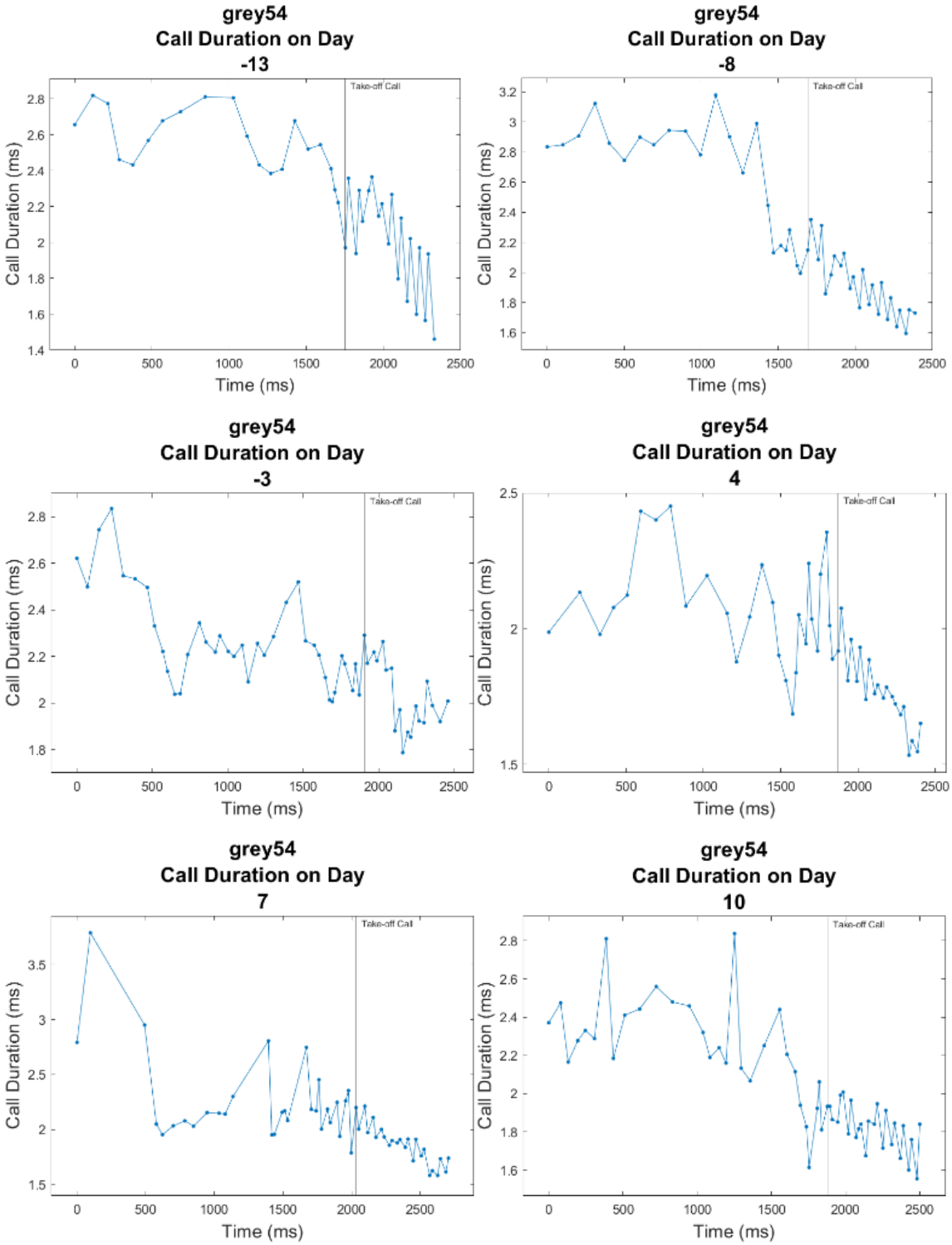

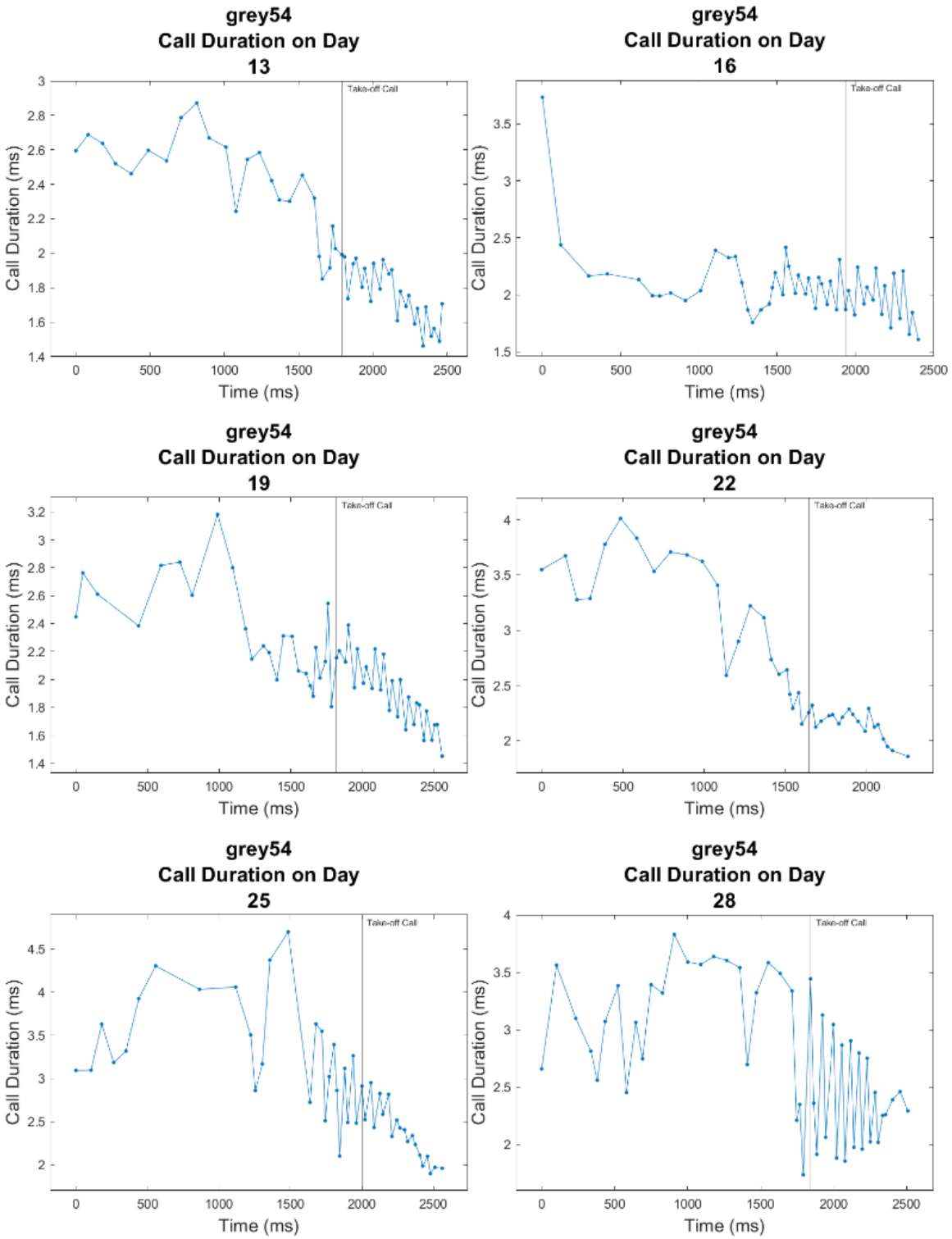
grey54
Call Duration on Day
13
grey54
Call Duration on Day
16
grey54
Call Duration on Day
19
grey54
Call Duration on Day
22
grey54
Call Duration on Day
25
grey54
Call Duration on Day
28
Take-off Call
Call Duration (ms)
Time (ms)

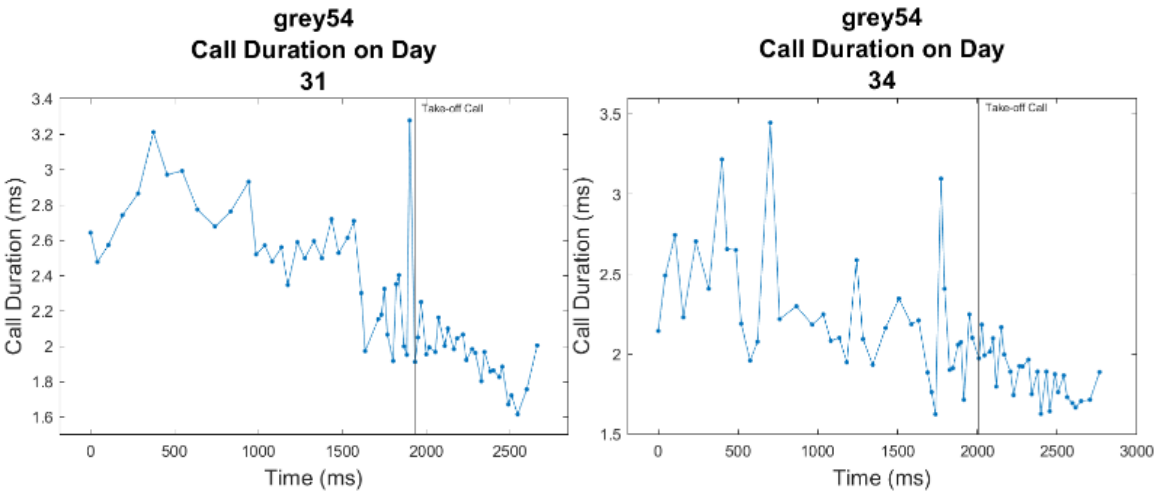

Appendix Figure 9: Grey 54 call duration plotted as a function of recording time per day. Each panel shows call durations before and after taking flight, with different panels showing data recorded on different days relative to parturition (number above panel; parturition day defined as Day 0). The take-off call is marked by a vertical line.

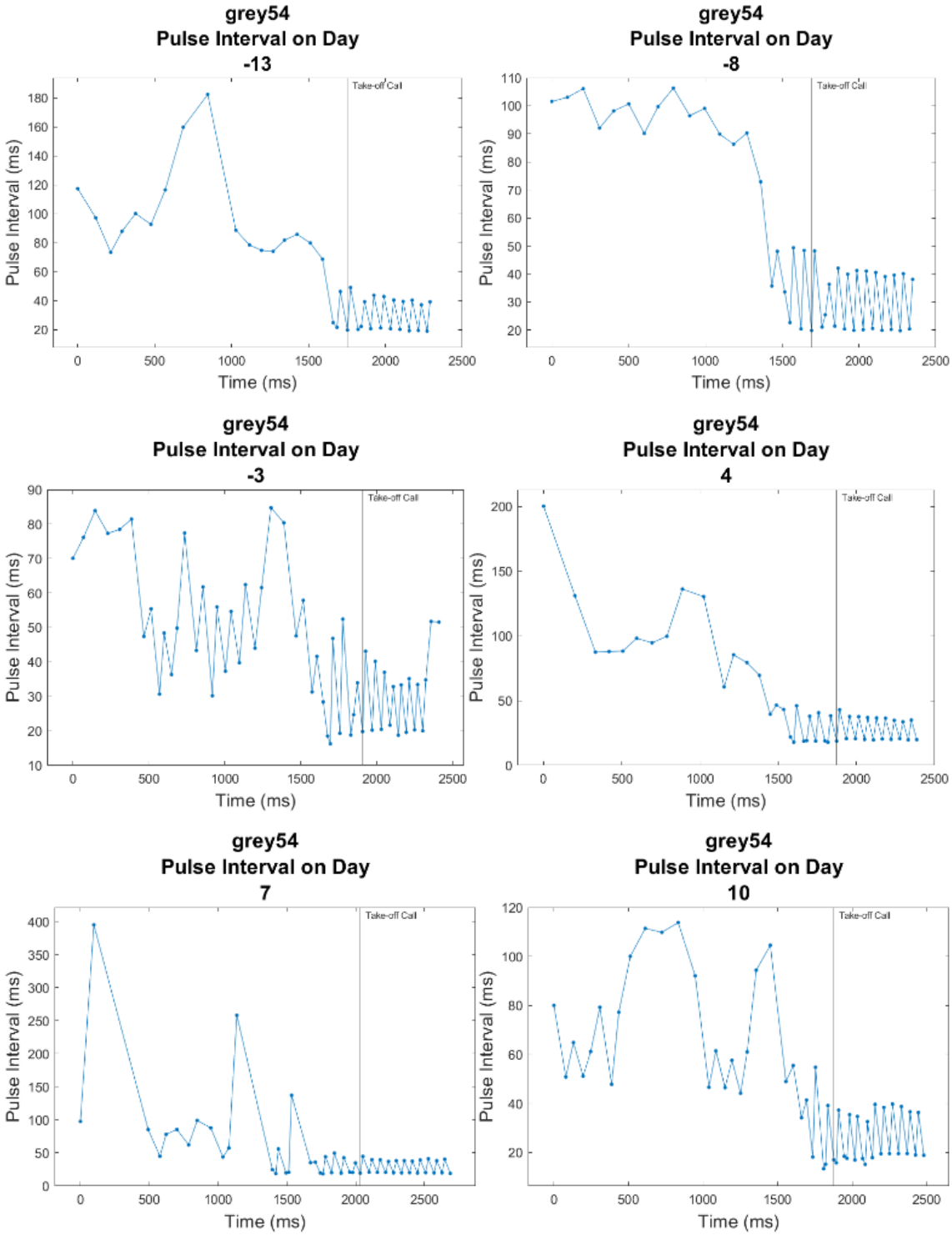
grey54
Pulse Interval on Day
-13
Take-off Call
Pulse Interval (ms)
Time (ms)
grey54
Pulse Interval on Day
-8
Take-off Call
Pulse Interval (ms)
Time (ms)
grey54
Pulse Interval on Day
-3
Take-off Call
Pulse Interval (ms)
Time (ms)
grey54
Pulse Interval on Day
4
Take-off Call
Pulse Interval (ms)
Time (ms)
grey54
Pulse Interval on Day
7
Take-off Call
Pulse Interval (ms)
Time (ms)
grey54
Pulse Interval on Day
10
Take-off Call
Pulse Interval (ms)
Time (ms)

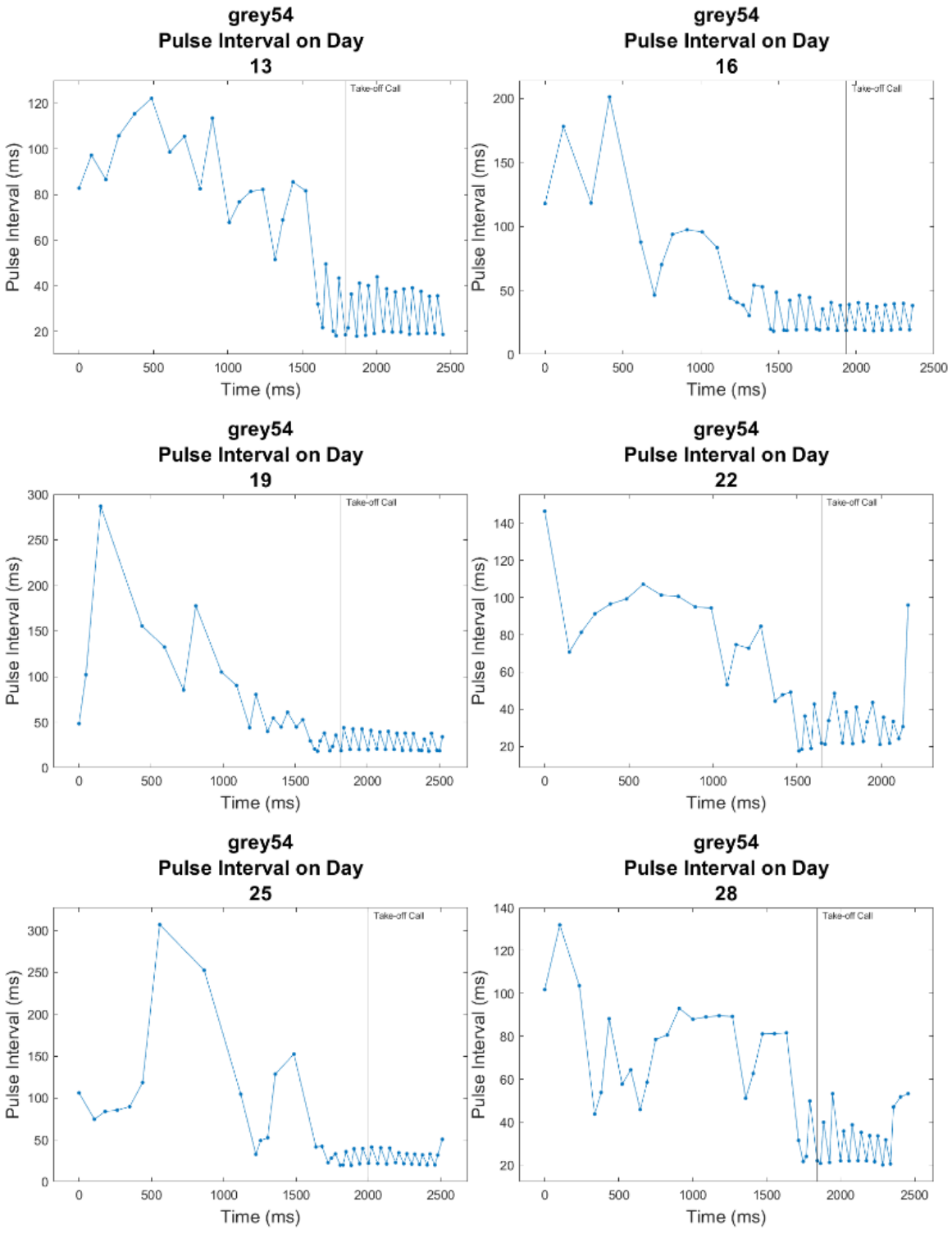
grey54
Pulse Interval on Day
13
Take-off Call
Pulse Interval (ms)
Time (ms)
grey54
Pulse Interval on Day
16
Take-off Call
Pulse Interval (ms)
Time (ms)
grey54
Pulse Interval on Day
19
Take-off Call
Pulse Interval (ms)
Time (ms)
grey54
Pulse Interval on Day
22
Take-off Call
Pulse Interval (ms)
Time (ms)
grey54
Pulse Interval on Day
25
Take-off Call
Pulse Interval (ms)
Time (ms)
grey54
Pulse Interval on Day
28
Take-off Call
Pulse Interval (ms)
Time (ms)

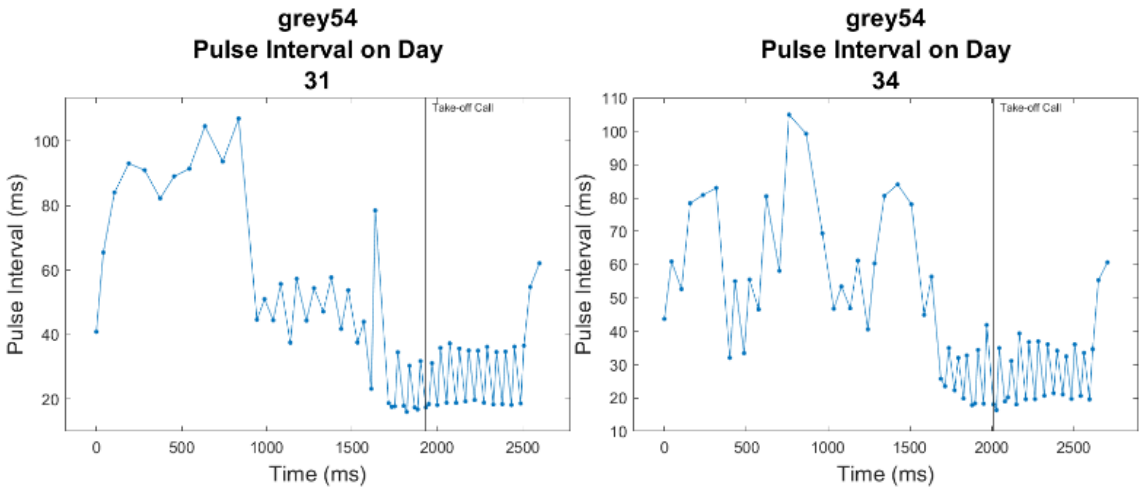

Appendix Figure 10: Grey 54 pulse interval plotted as a function of recording time per day. Each panel shows call durations before and after taking flight, with different panels showing data recorded on different days relative to parturition (number above panel; parturition day defined as Day 0). The take-off call is marked by a vertical line.

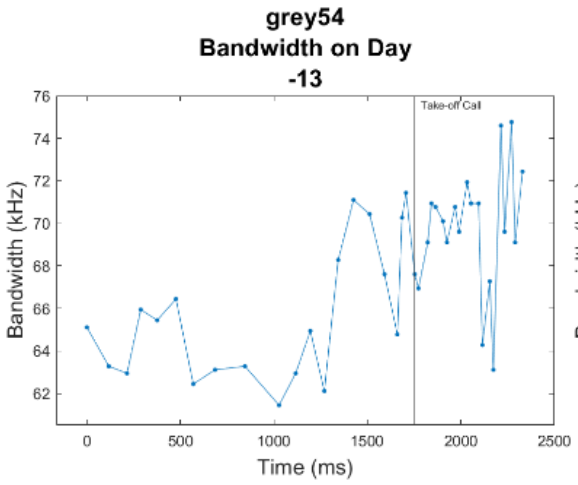
grey54
Bandwidth on Day
-13
Take-off Call
Bandwidth (kHz)
Time (ms)

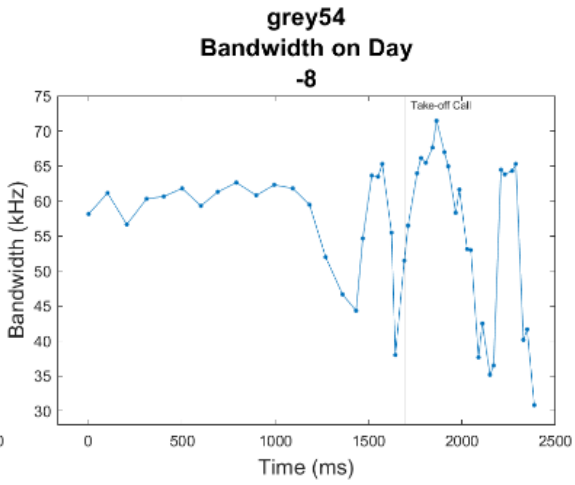
grey54
Bandwidth on Day
-8
Take-off Call
Bandwidth (kHz)
Time (ms)

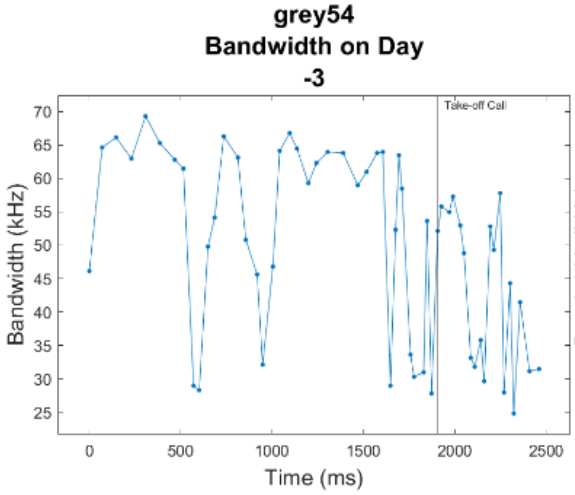
grey54
Bandwidth on Day
-3
Take-off Call
Bandwidth (kHz)
Time (ms)

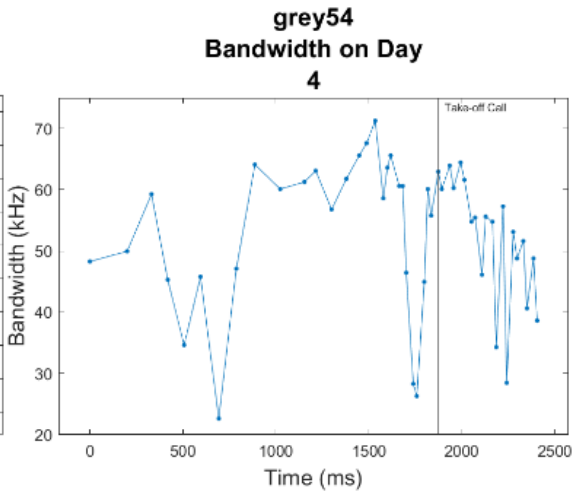
grey54
Bandwidth on Day
4
Take-off Call
Bandwidth (kHz)
Time (ms)

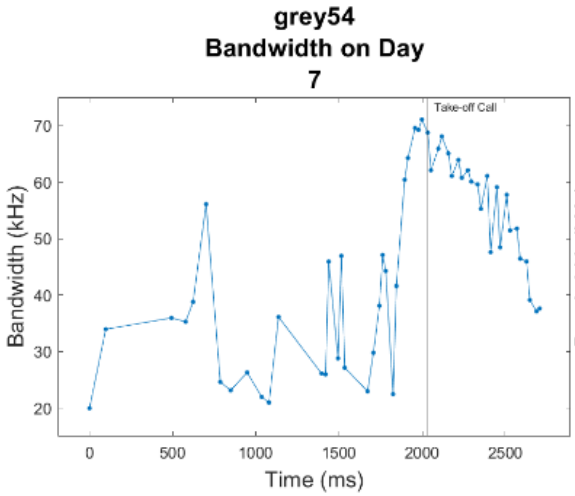
grey54
Bandwidth on Day
7
Take-off Call
Bandwidth (kHz)
Time (ms)

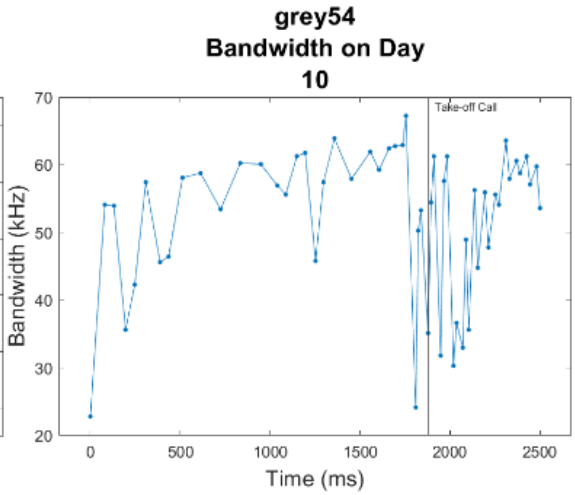
grey54
Bandwidth on Day
10
Take-off Call
Bandwidth (kHz)
Time (ms)

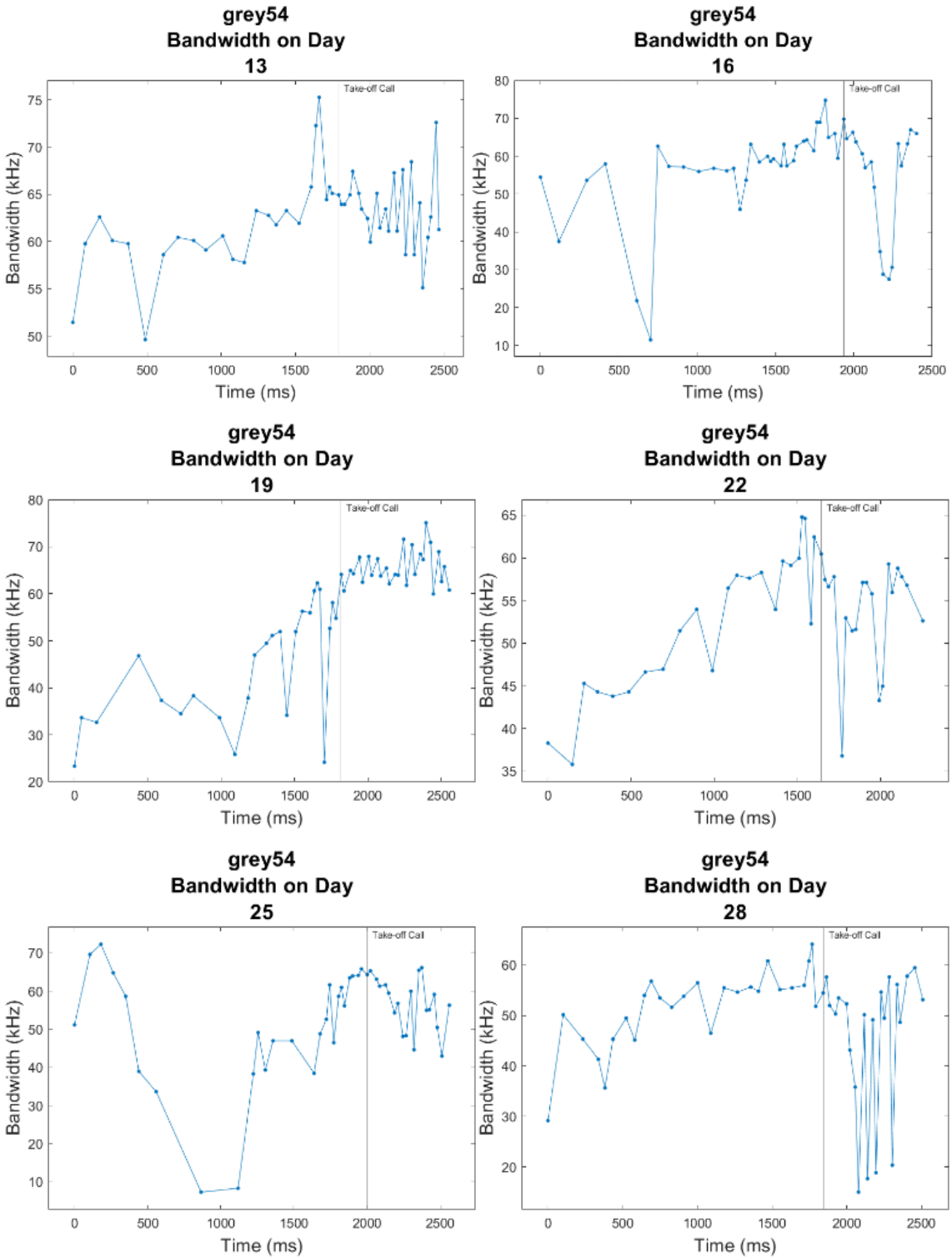
grey54
Bandwidth on Day
13
Take-off Call
Bandwidth (kHz)
Time (ms)
grey54
Bandwidth on Day
16
Take-off Call
Bandwidth (kHz)
Time (ms)
grey54
Bandwidth on Day
19
Take-off Call
Bandwidth (kHz)
Time (ms)
grey54
Bandwidth on Day
22
Take-off Call
Bandwidth (kHz)
Time (ms)
grey54
Bandwidth on Day
25
Take-off Call
Bandwidth (kHz)
Time (ms)
grey54
Bandwidth on Day
28
Take-off Call
Bandwidth (kHz)
Time (ms)

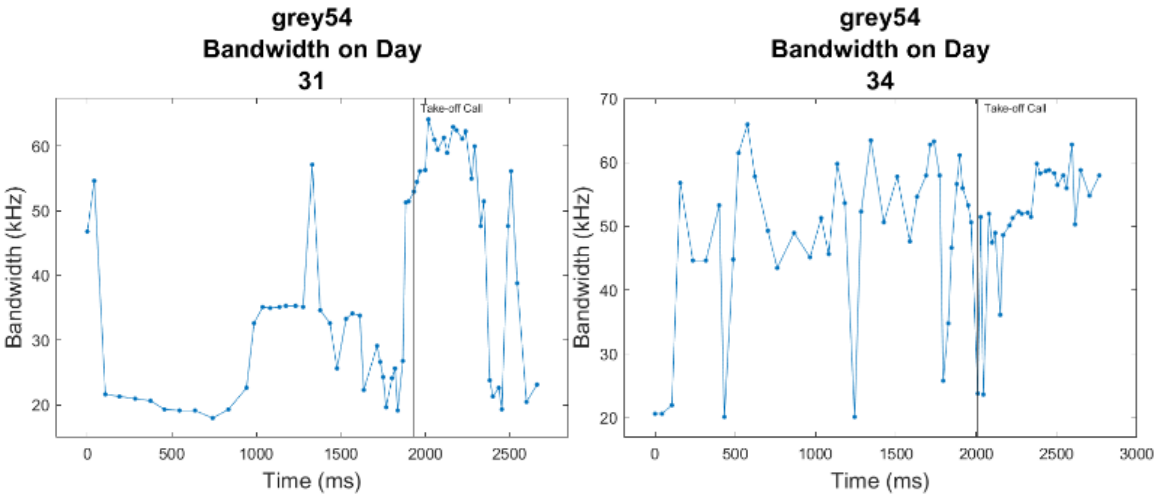

Appendix Figure 11: Grey 54 call bandwidth plotted as a function of recording time per day. Each panel shows call durations before and after taking flight, with different panels showing data recorded on different days relative to parturition (number above panel; parturition day defined as Day 0). The take-off call is marked by a vertical line.

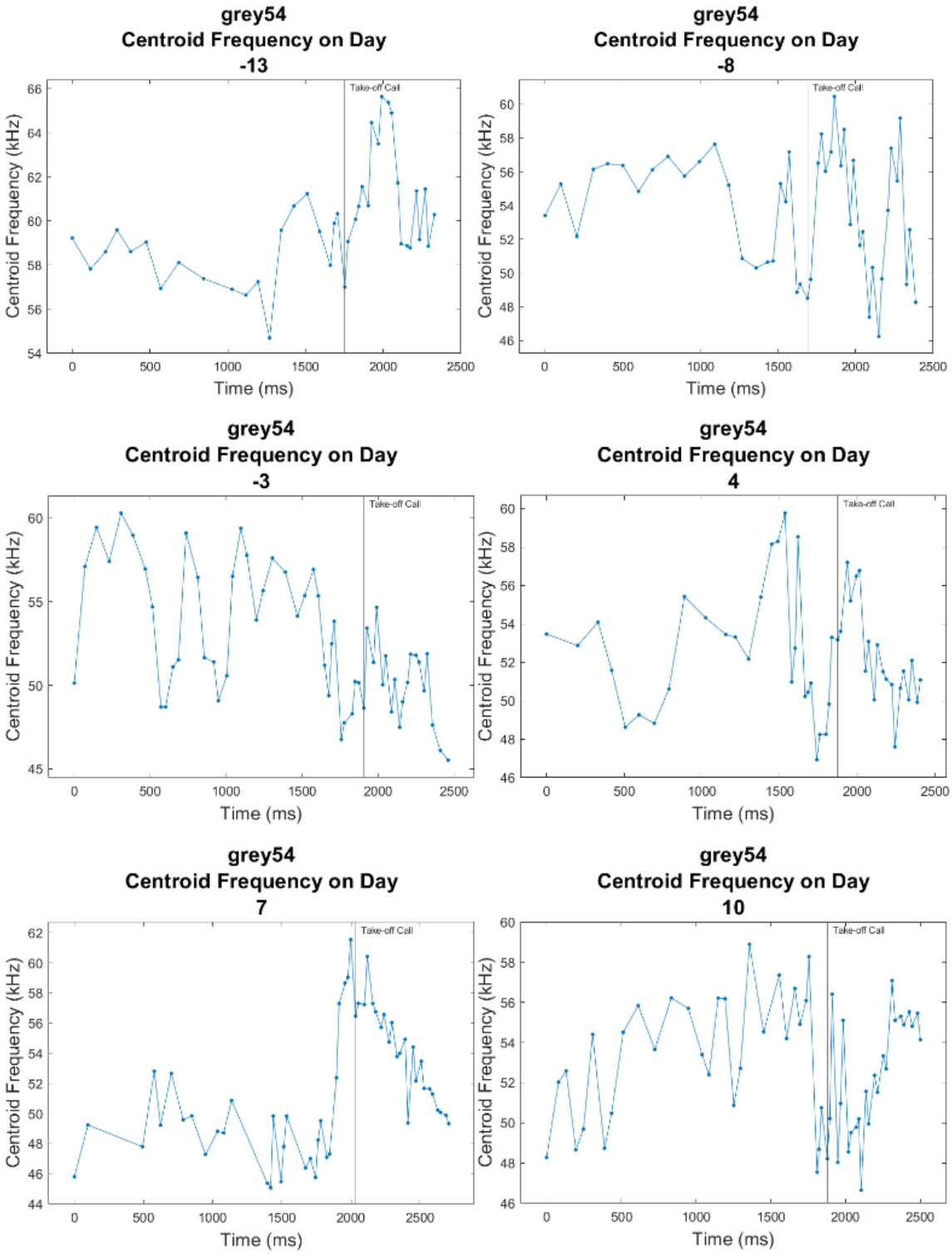
grey54
Centroid Frequency on Day
-13
grey54
Centroid Frequency on Day
-8
grey54
Centroid Frequency on Day
-3
grey54
Centroid Frequency on Day
4
grey54
Centroid Frequency on Day
7
grey54
Centroid Frequency on Day
10
Take-off Call
Centroid Frequency (kHz)
Time (ms)

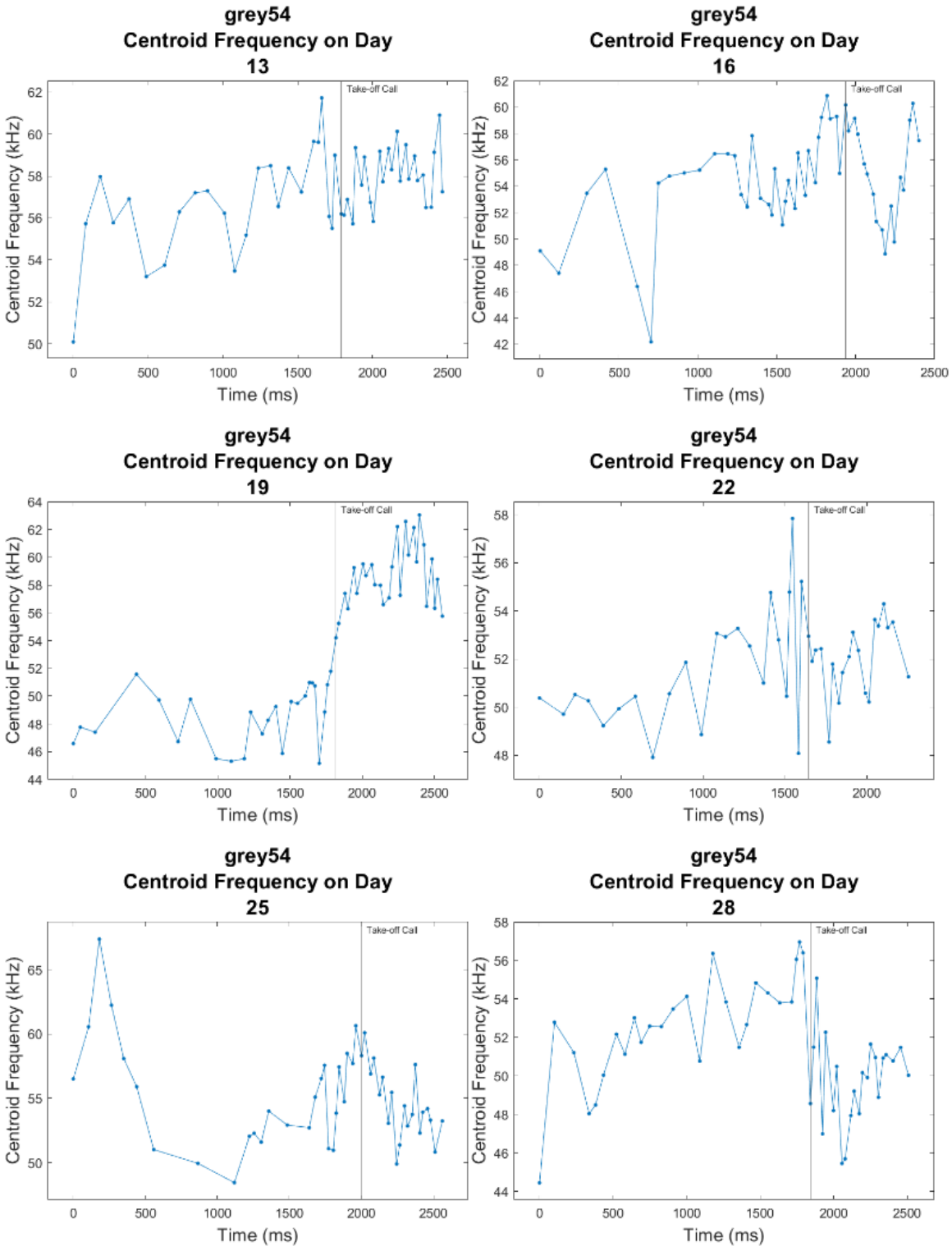
grey54
Centroid Frequency on Day 13
grey54
Centroid Frequency on Day 16
grey54
Centroid Frequency on Day 19
grey54
Centroid Frequency on Day 22
grey54
Centroid Frequency on Day 25
grey54
Centroid Frequency on Day 28
Take-off Call
Centroid Frequency (kHz)
Time (ms)

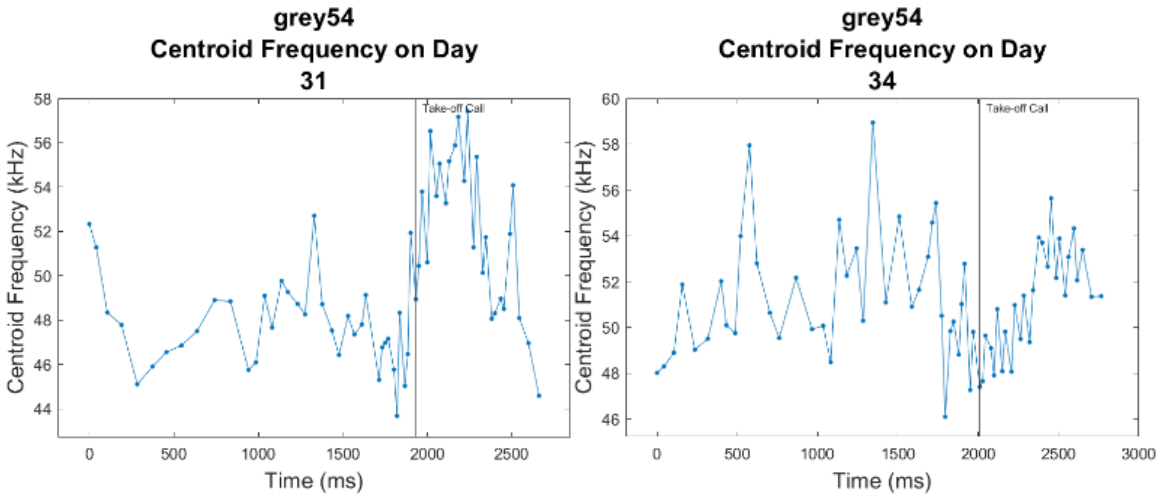

Appendix Figure 12: Grey 54 centroid frequency plotted as a function of recording time per day. Each panel shows call durations before and after taking flight, with different panels showing data recorded on different days relative to parturition (number above panel; parturition day defined as Day 0). The take-off call is marked by a vertical line.

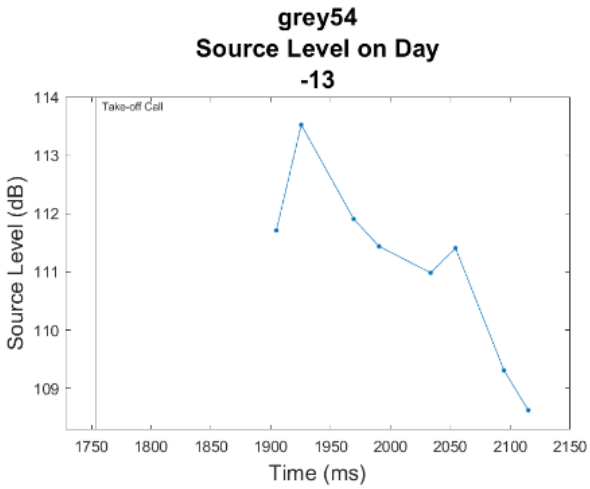
grey54
Source Level on Day
-13
Take-off Call
Source Level (dB)
Time (ms)

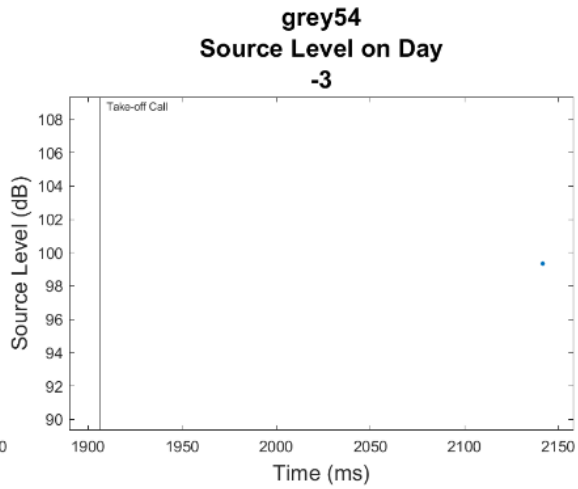
grey54
Source Level on Day
-3
Take-off Call
Source Level (dB)
Time (ms)

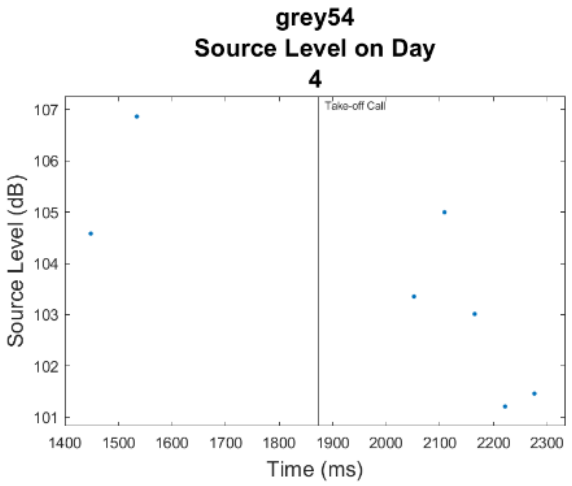
grey54
Source Level on Day
4
Take-off Call
Source Level (dB)
Time (ms)

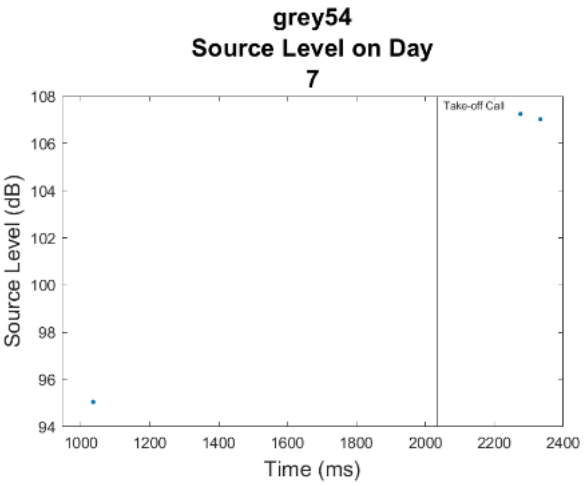
grey54
Source Level on Day
7
Take-off Call
Source Level (dB)
Time (ms)

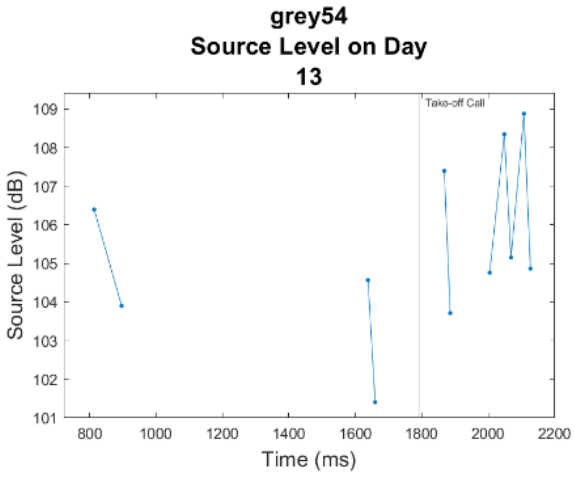
grey54
Source Level on Day
13
Take-off Call
Source Level (dB)
Time (ms)

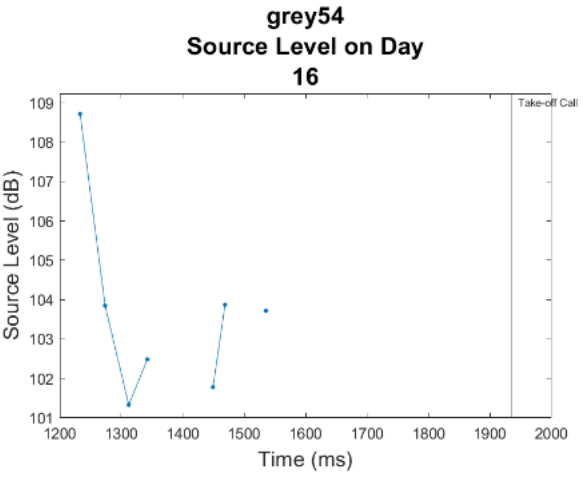
grey54
Source Level on Day
16
Take-off Call
Source Level (dB)
Time (ms)

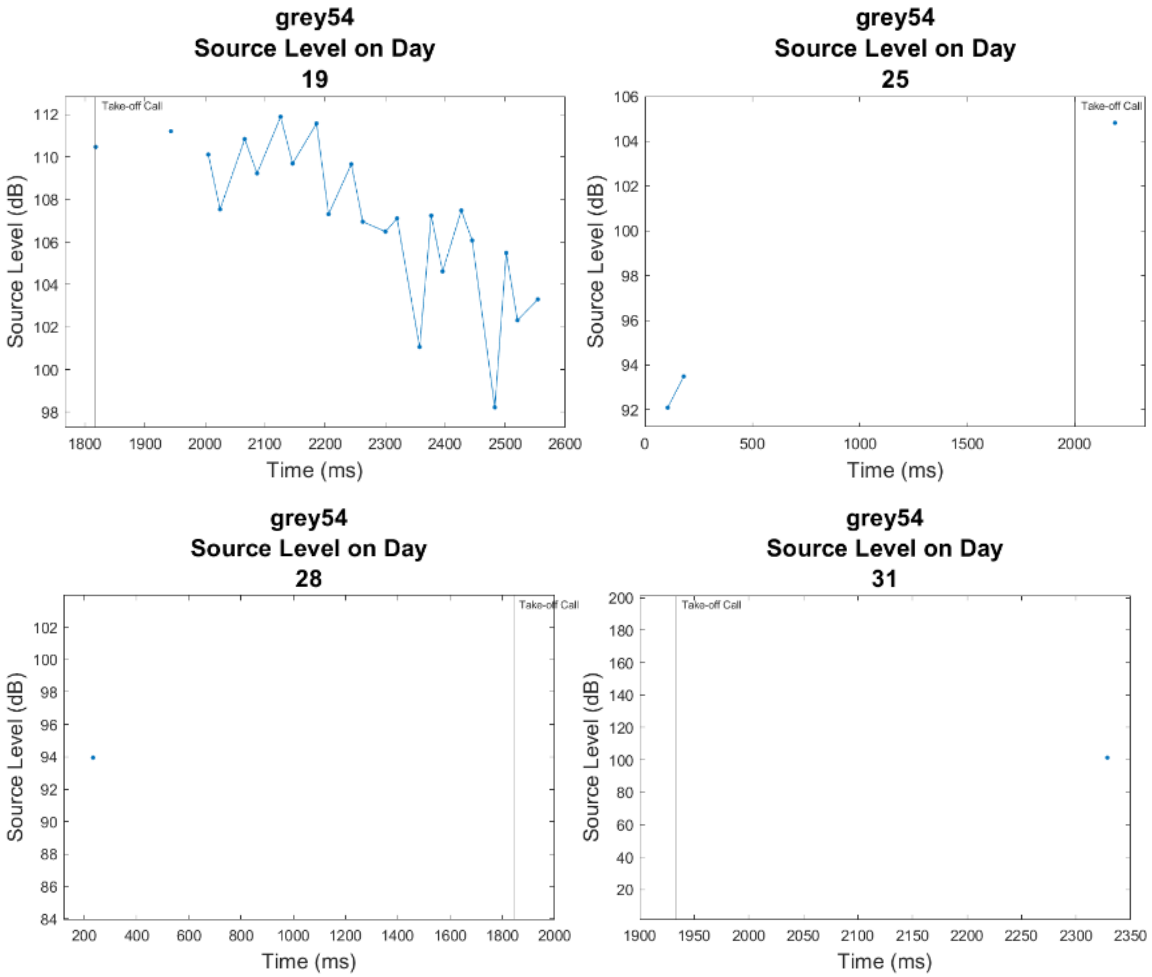

Appendix Figure 13: Grey 54 source level plotted as a function of recording time per day. Each panel shows call durations before and after taking flight, with different panels showing data recorded on different days relative to parturition (number above panel; parturition day defined as Day 0). The take-off call is marked by a vertical line.

Grey 56 Echolocation Call Characteristics Graphs

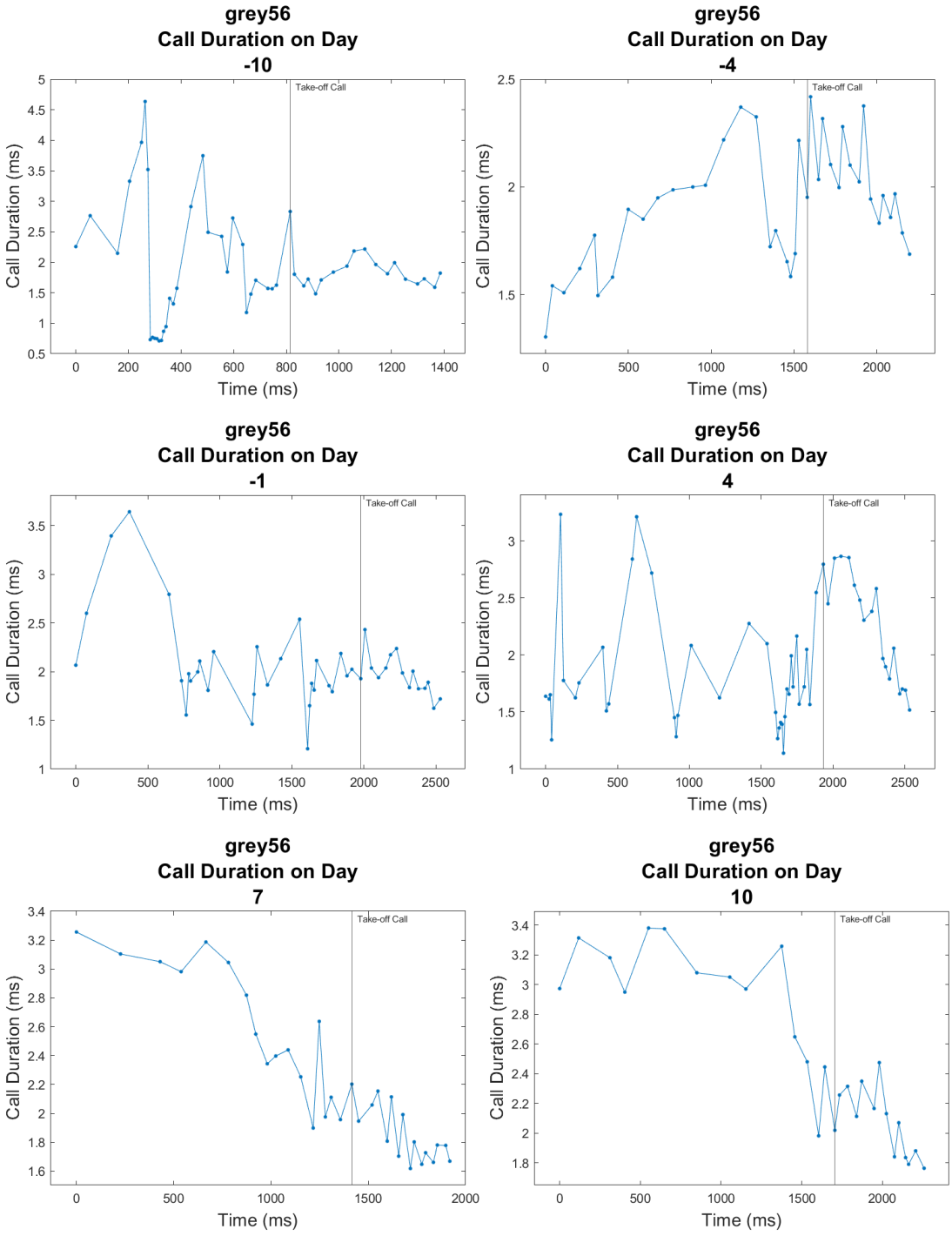

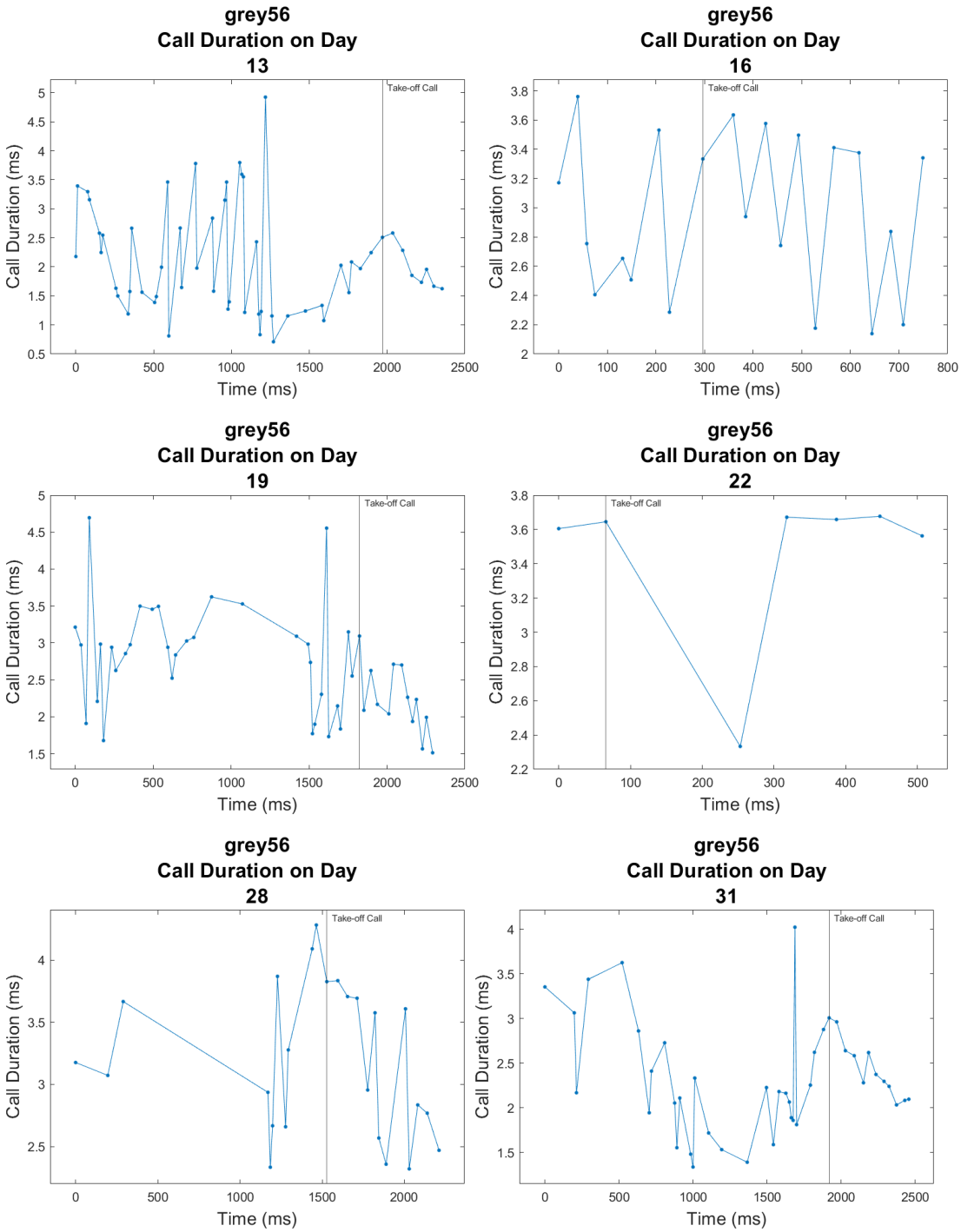

Appendix Figure 14: Grey 56 call duration plotted as a function of recording time per day. Each panel shows call durations before and after taking flight, with different panels showing data recorded on different days relative to parturition (number above panel; parturition day defined as Day 0). The take-off call is marked by a vertical line.

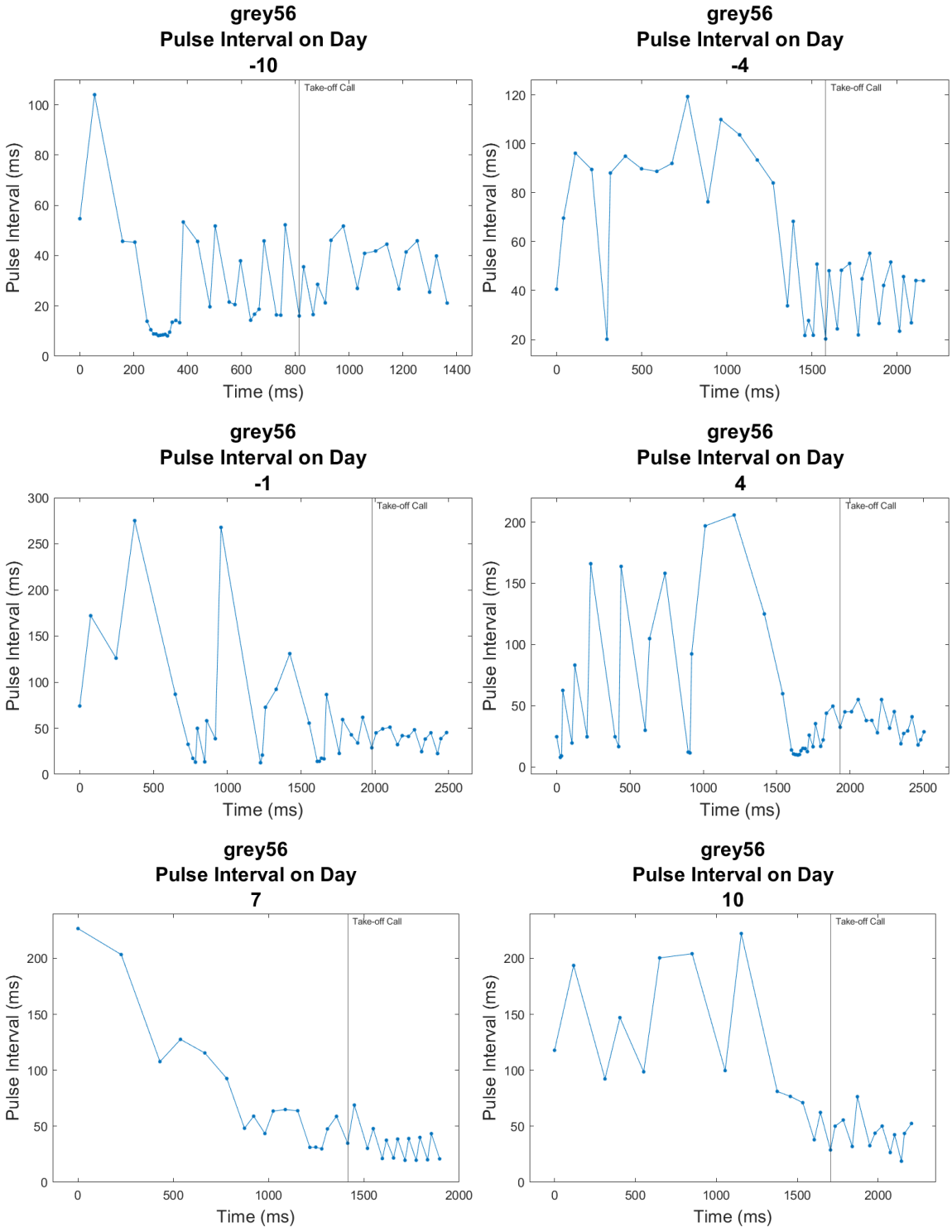
grey56
Pulse Interval on Day
-10
Take-off Call
Pulse Interval (ms)
Time (ms)
grey56
Pulse Interval on Day
-4
Take-off Call
Pulse Interval (ms)
Time (ms)
grey56
Pulse Interval on Day
-1
Take-off Call
Pulse Interval (ms)
Time (ms)
grey56
Pulse Interval on Day
4
Take-off Call
Pulse Interval (ms)
Time (ms)
grey56
Pulse Interval on Day
7
Take-off Call
Pulse Interval (ms)
Time (ms)
grey56
Pulse Interval on Day
10
Take-off Call
Pulse Interval (ms)
Time (ms)

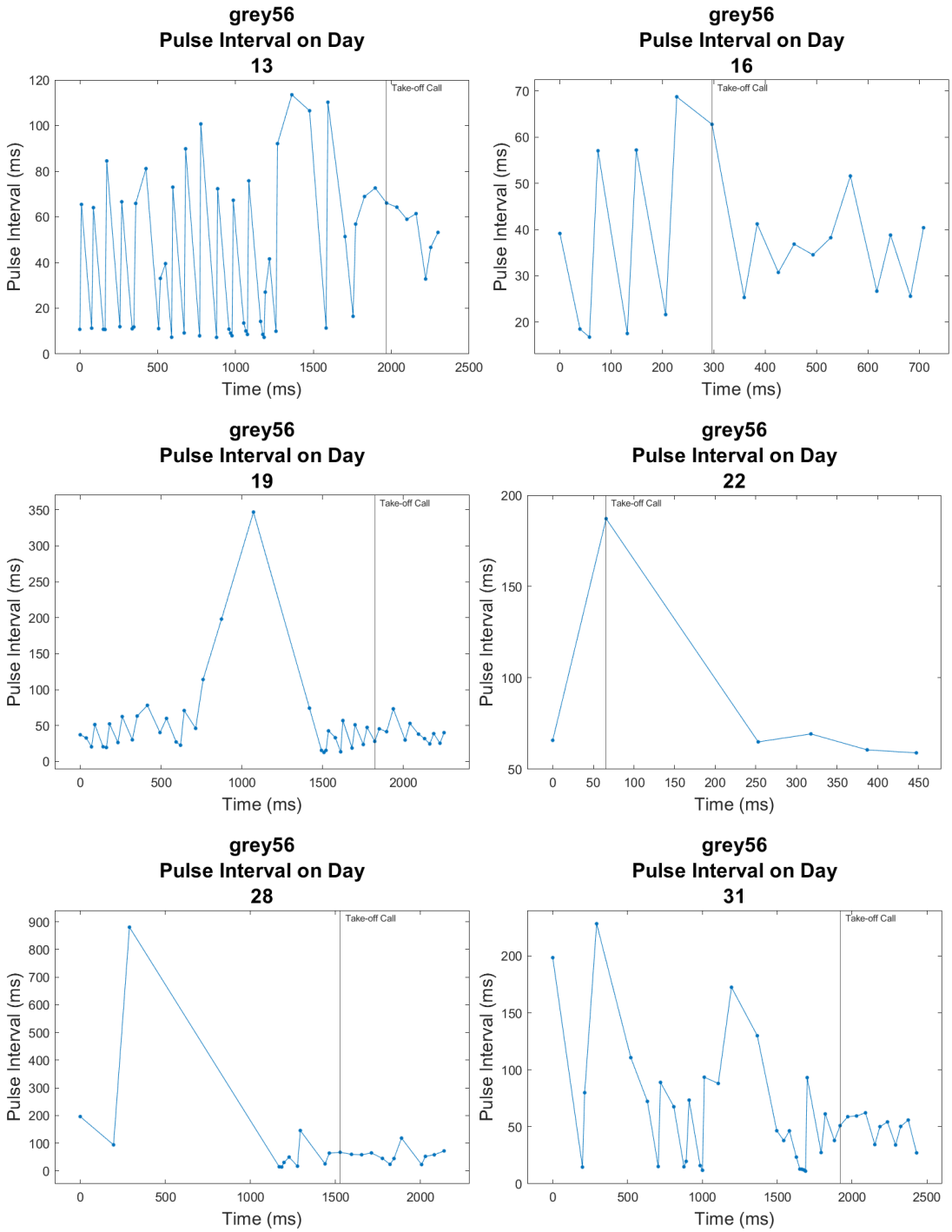

Appendix Figure 15: Grey 56 pulse interval plotted as a function of recording time per day. Each panel shows call durations before and after taking flight, with different panels showing data recorded on different days relative to parturition (number above panel; parturition day defined as Day 0). The take-off call is marked by a vertical line.

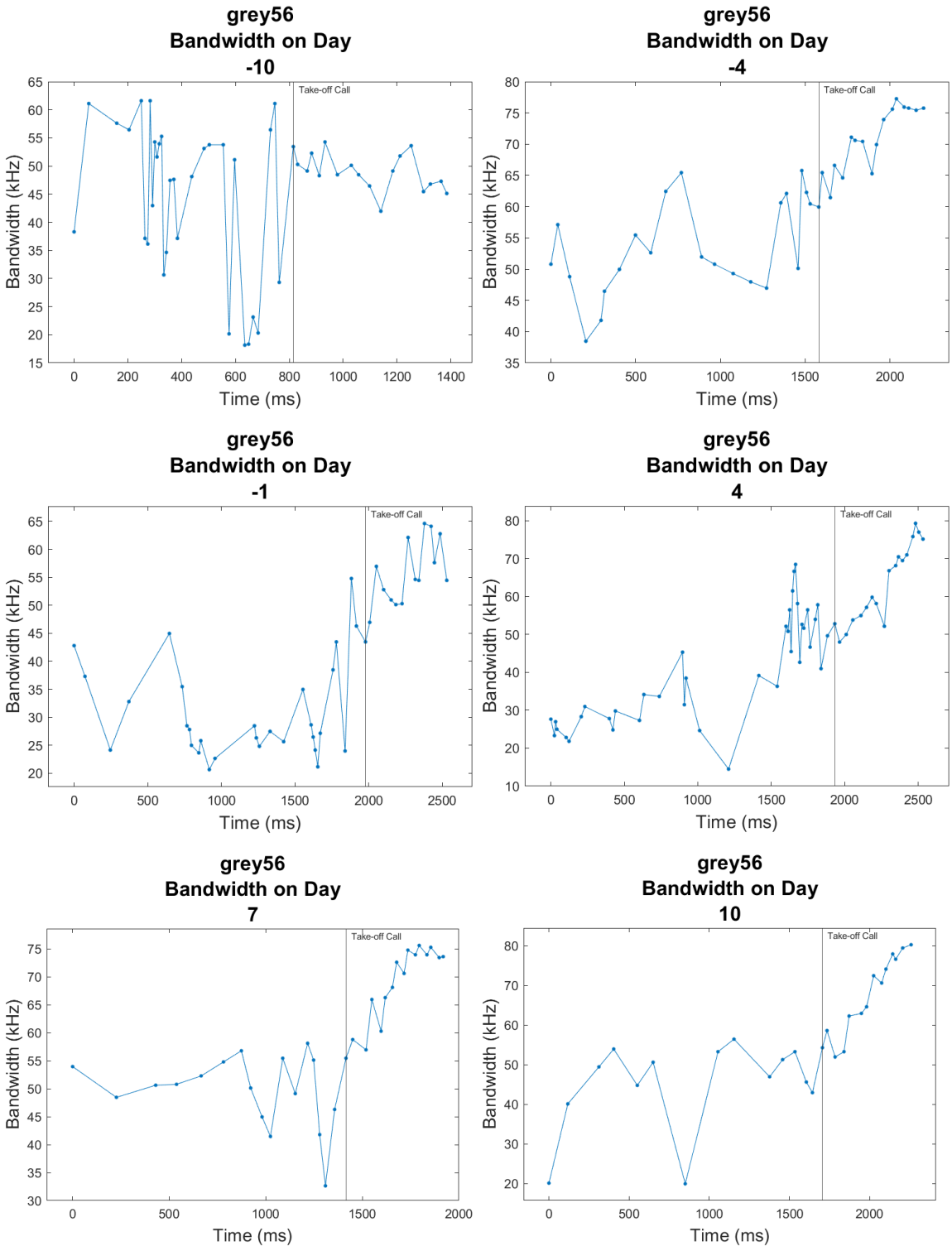
grey56
Bandwidth on Day
-10
Take-off Call
Bandwidth (kHz)
Time (ms)
grey56
Bandwidth on Day
-4
Take-off Call
Bandwidth (kHz)
Time (ms)
grey56
Bandwidth on Day
-1
Take-off Call
Bandwidth (kHz)
Time (ms)
grey56
Bandwidth on Day
4
Take-off Call
Bandwidth (kHz)
Time (ms)
grey56
Bandwidth on Day
7
Take-off Call
Bandwidth (kHz)
Time (ms)
grey56
Bandwidth on Day
10
Take-off Call
Bandwidth (kHz)
Time (ms)

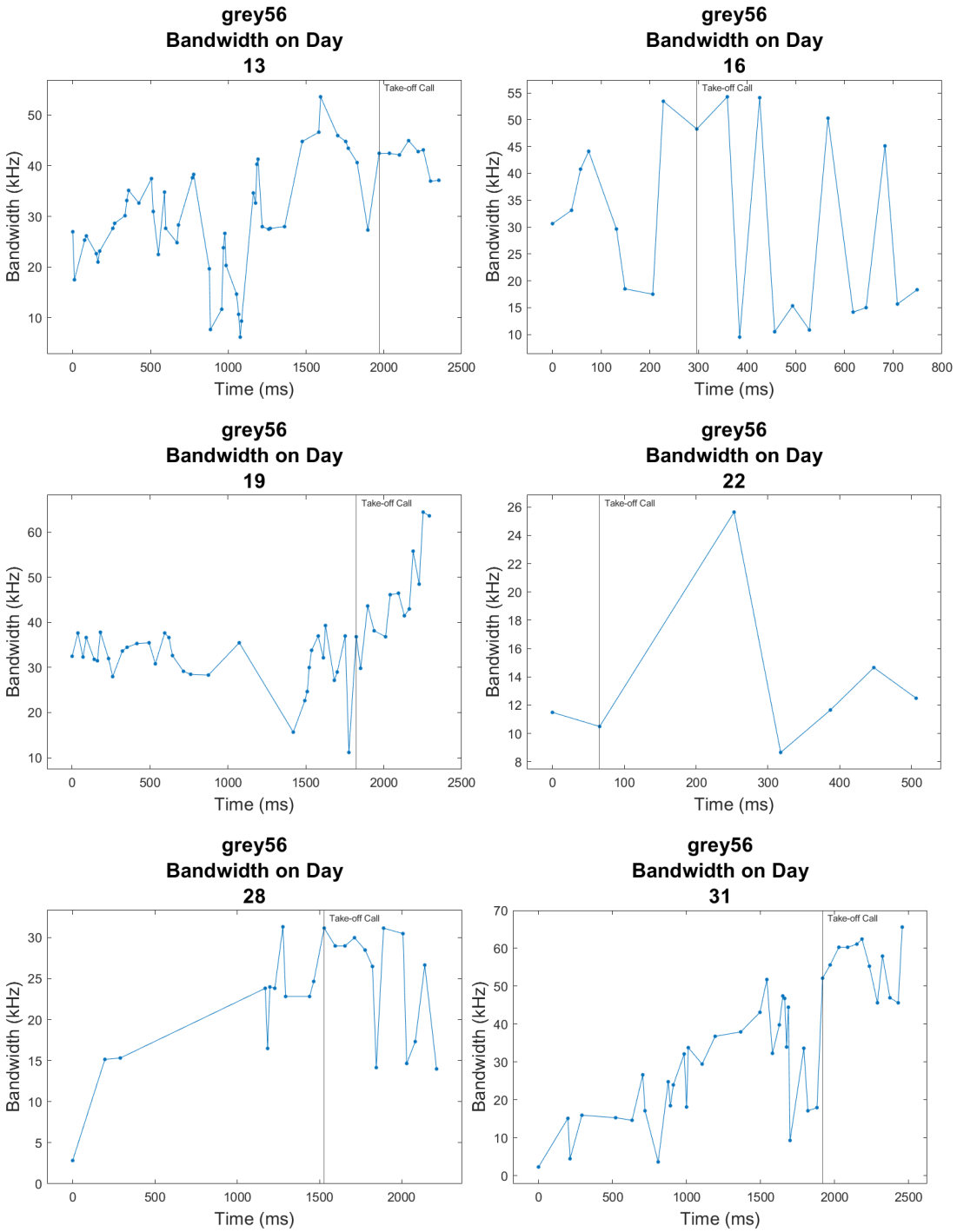

Appendix Figure 16: Grey 56 call bandwidth plotted as a function of recording time per day. Each panel shows call durations before and after taking flight, with different panels showing data recorded on different days relative to parturition (number above panel; parturition day defined as Day 0). The take-off call is marked by a vertical line..

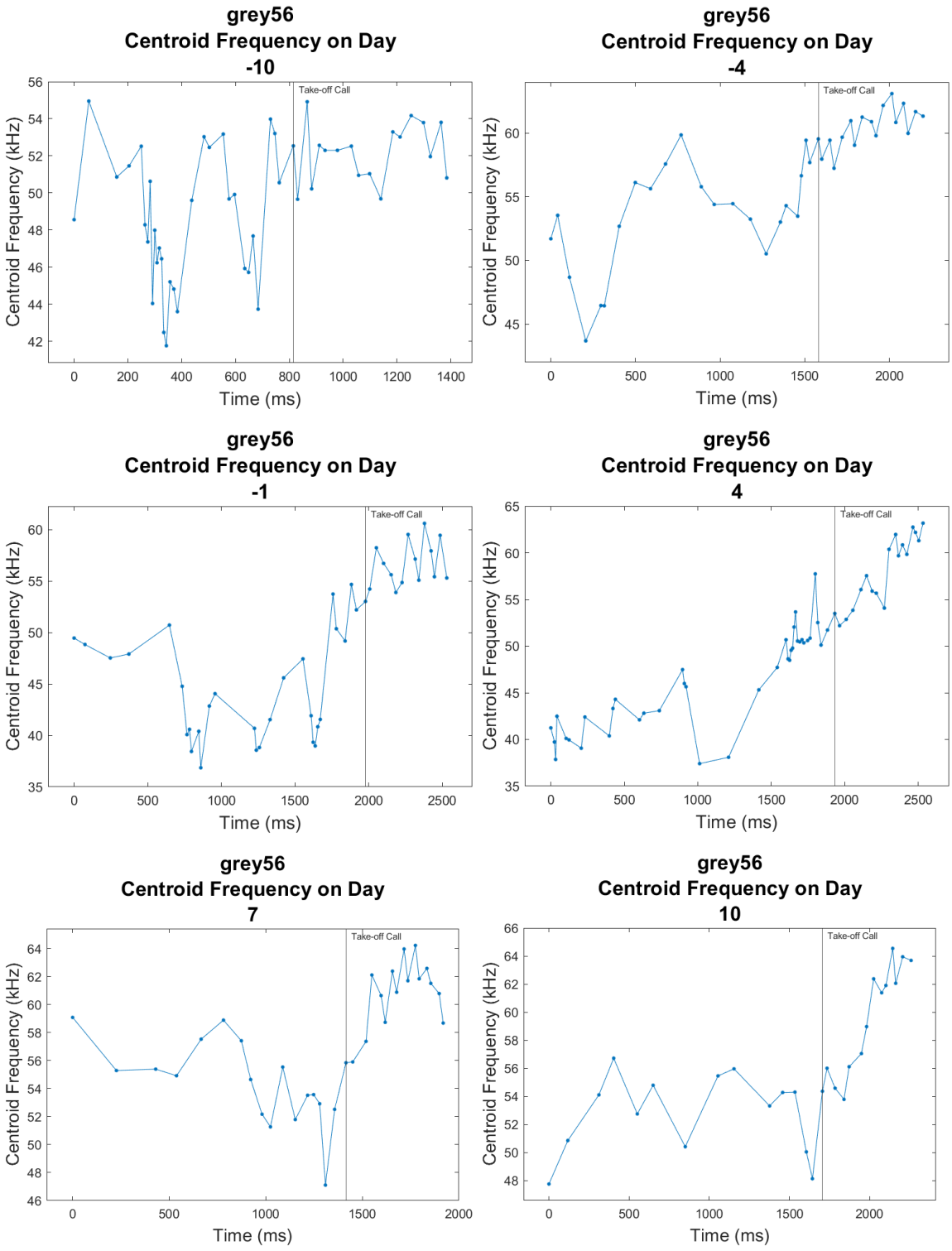
grey56
Centroid Frequency on Day
-10
Take-off Call
Centroid Frequency (kHz)
Time (ms)
grey56
Centroid Frequency on Day
-4
Take-off Call
Centroid Frequency (kHz)
Time (ms)
grey56
Centroid Frequency on Day
-1
Take-off Call
Centroid Frequency (kHz)
Time (ms)
grey56
Centroid Frequency on Day
4
Take-off Call
Centroid Frequency (kHz)
Time (ms)
grey56
Centroid Frequency on Day
7
Take-off Call
Centroid Frequency (kHz)
Time (ms)
grey56
Centroid Frequency on Day
10
Take-off Call
Centroid Frequency (kHz)
Time (ms)

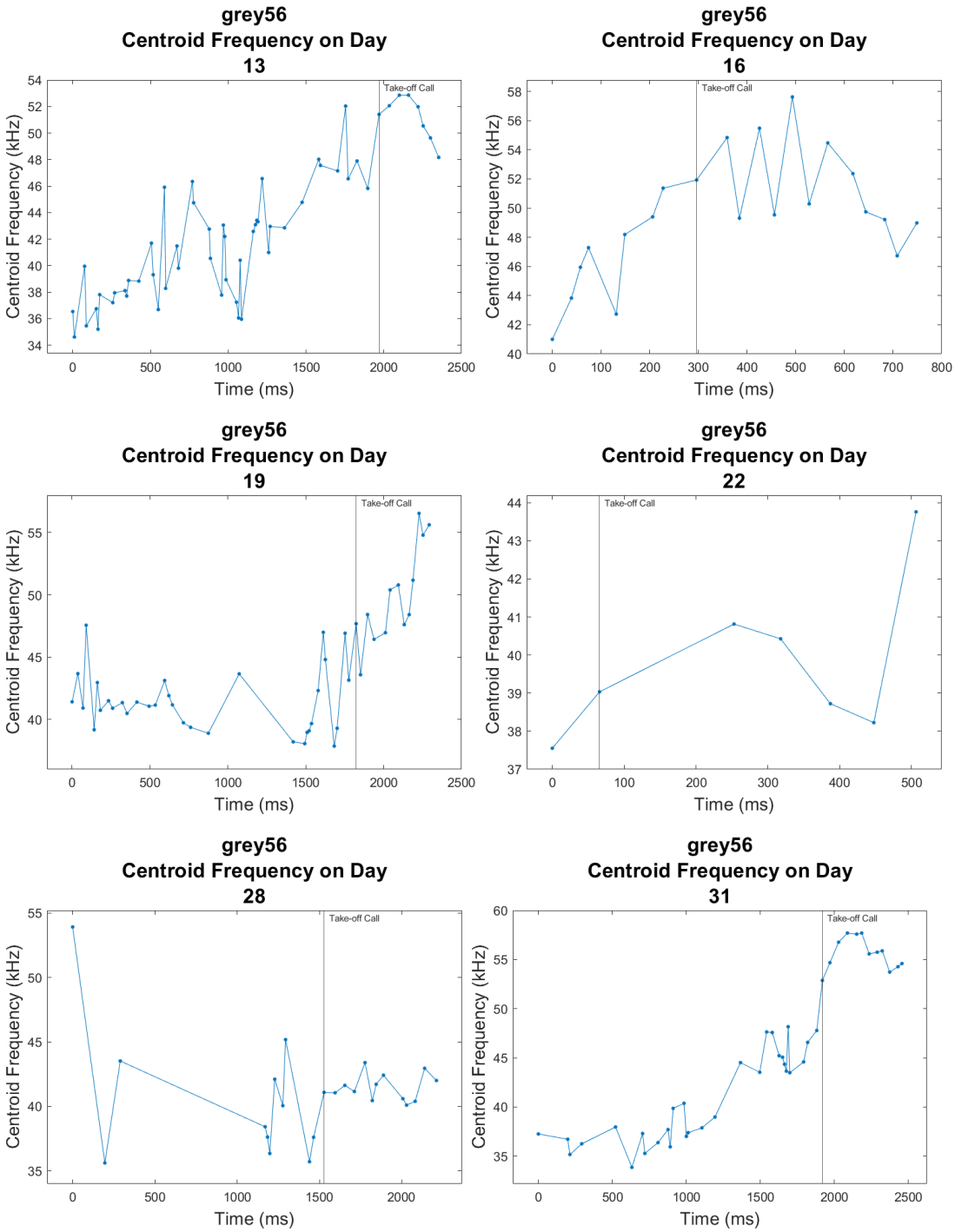

Appendix Figure 17: Grey 56 centroid frequency plotted as a function of recording time per day. Each panel shows call durations before and after taking flight, with different panels showing data recorded on different days relative to parturition (number above panel; parturition day defined as Day 0). The take-off call is marked by a vertical line.

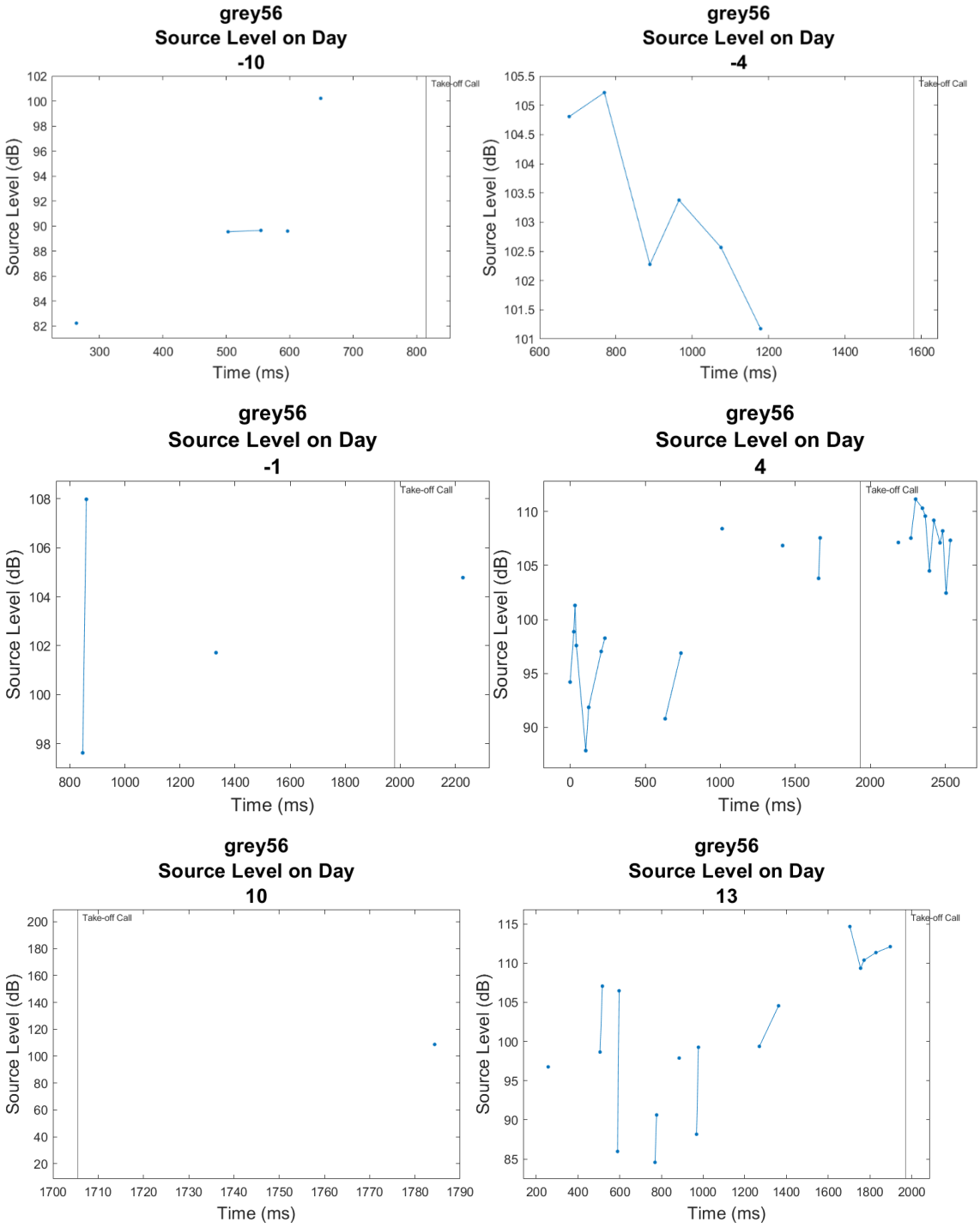
grey56
Source Level on Day
-10
Take-off Call
Source Level (dB)
Time (ms)
grey56
Source Level on Day
-4
Take-off Call
Source Level (dB)
Time (ms)
grey56
Source Level on Day
-1
Take-off Call
Source Level (dB)
Time (ms)
grey56
Source Level on Day
4
Take-off Call
Source Level (dB)
Time (ms)
grey56
Source Level on Day
10
Take-off Call
Source Level (dB)
Time (ms)
grey56
Source Level on Day
13
Take-off Call
Source Level (dB)
Time (ms)

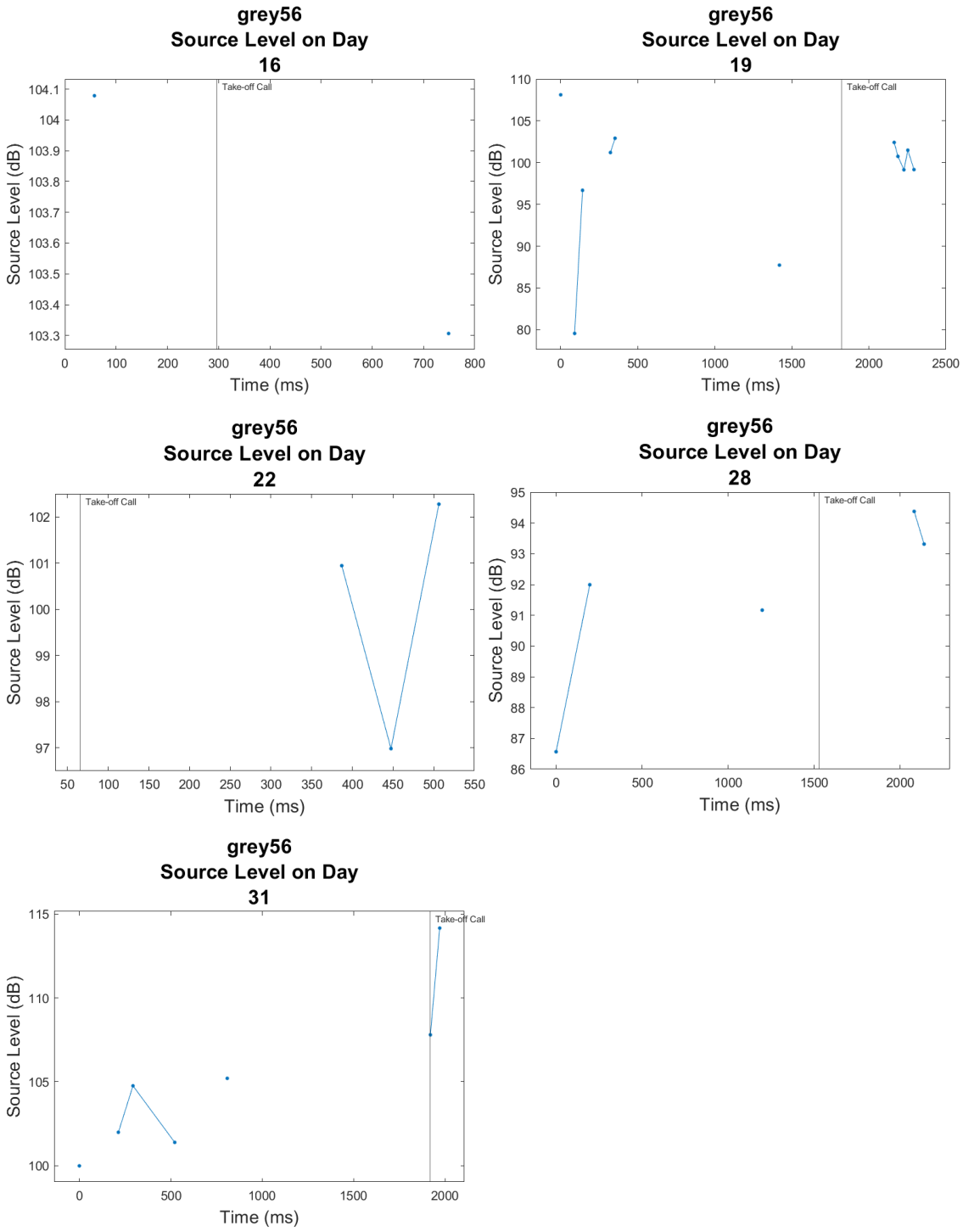

Appendix Figure 18: Grey 56 source level plotted as a function of recording time per day. Each panel shows call durations before and after taking flight, with different panels showing data recorded on different days relative to parturition (number above panel; parturition day defined as Day 0). The take-off call is marked by a vertical line.

Grey 82 Echolocation Call Characteristics Graphs

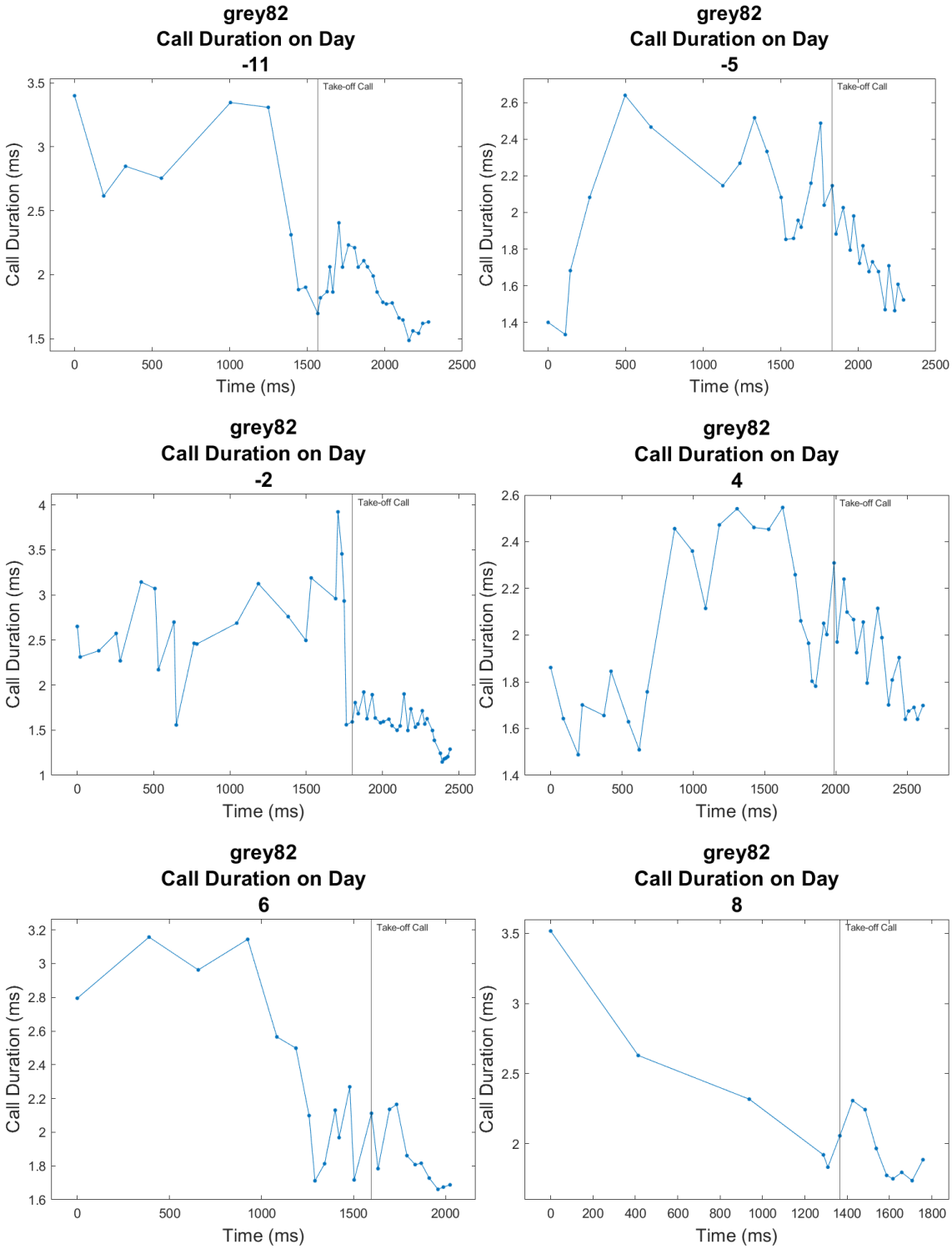

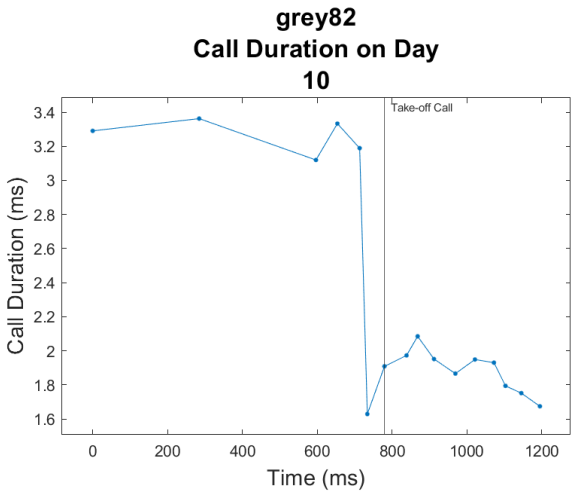
grey82
Call Duration on Day
10
Take-off Call
Call Duration (ms)
Time (ms)

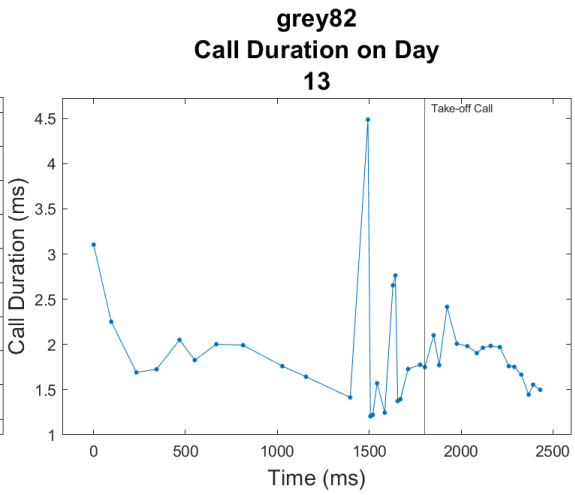
grey82
Call Duration on Day
13
Take-off Call
Call Duration (ms)
Time (ms)

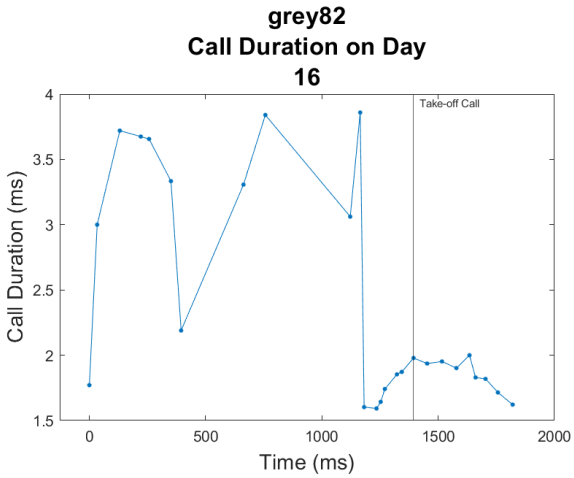
grey82
Call Duration on Day
16
Take-off Call
Call Duration (ms)
Time (ms)

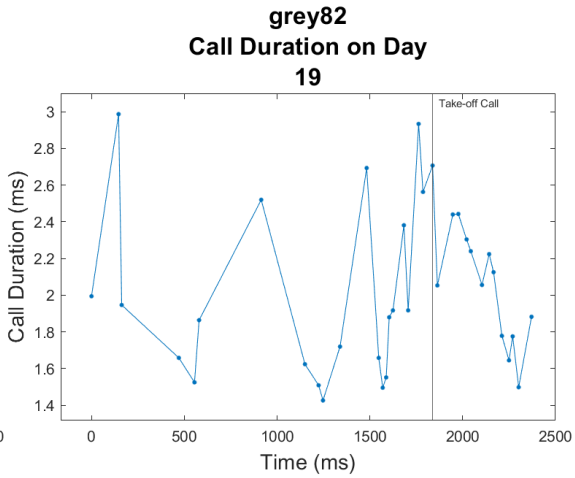
grey82
Call Duration on Day
19
Take-off Call
Call Duration (ms)
Time (ms)

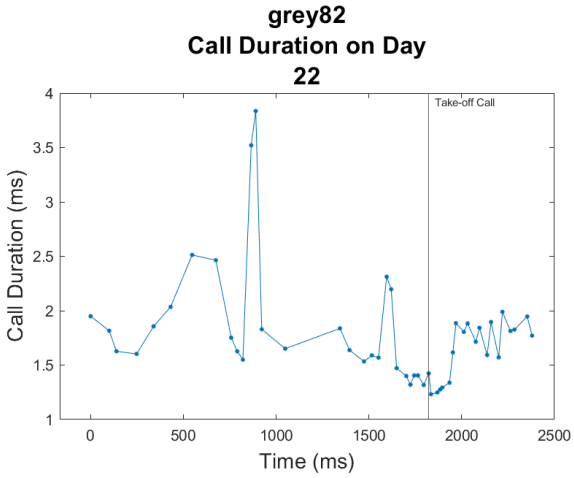
grey82
Call Duration on Day
22
Take-off Call
Call Duration (ms)
Time (ms)

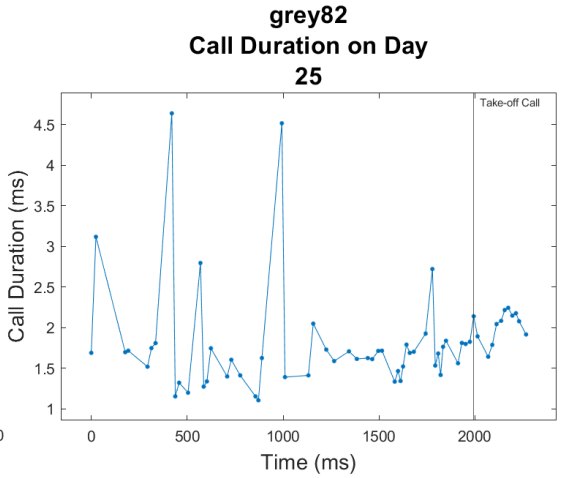
grey82
Call Duration on Day
25
Take-off Call
Call Duration (ms)
Time (ms)

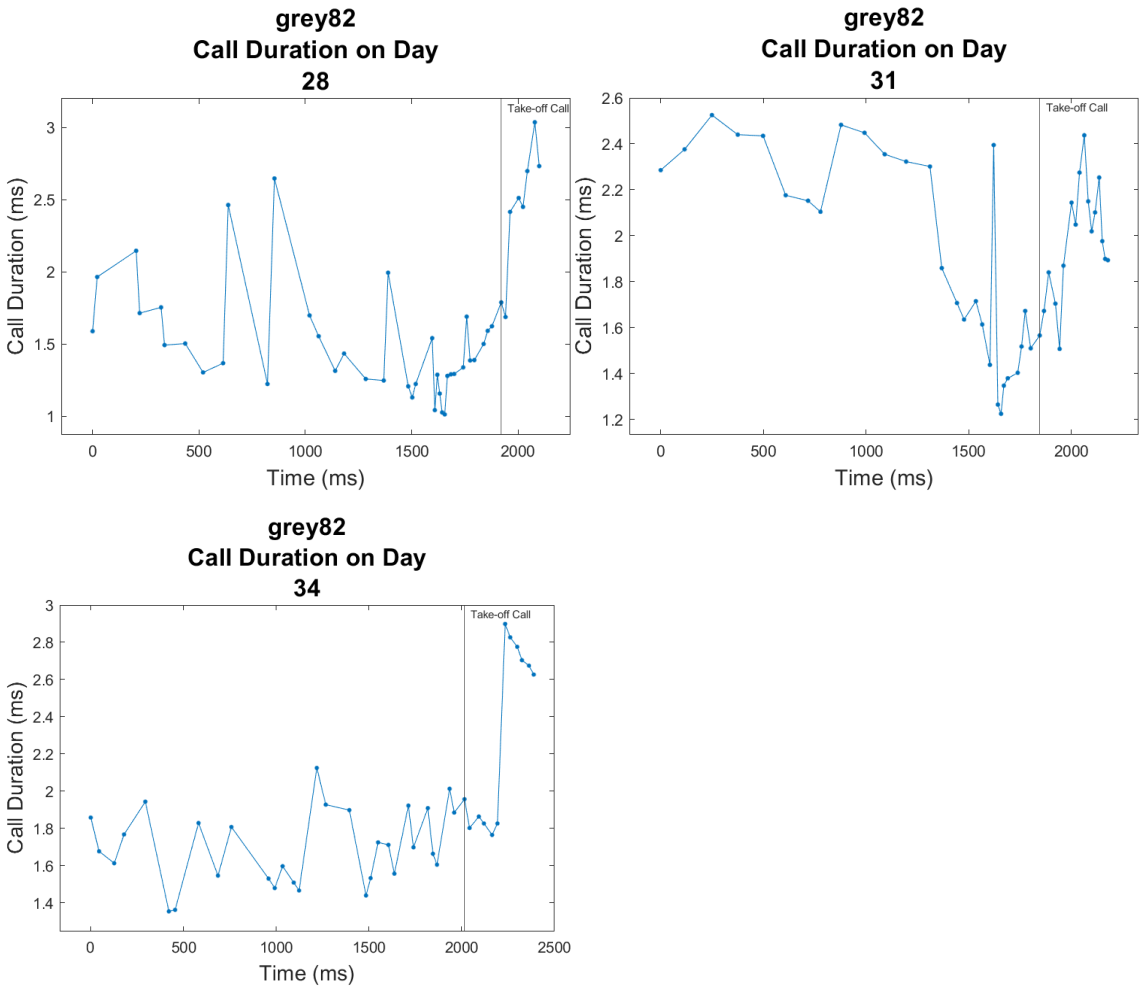

Appendix Figure 19: Grey 82 call duration plotted as a function of recording time per day. Each panel shows call durations before and after taking flight, with different panels showing data recorded on different days relative to parturition (number above panel; parturition day defined as Day 0). The take-off call is marked by a vertical line.

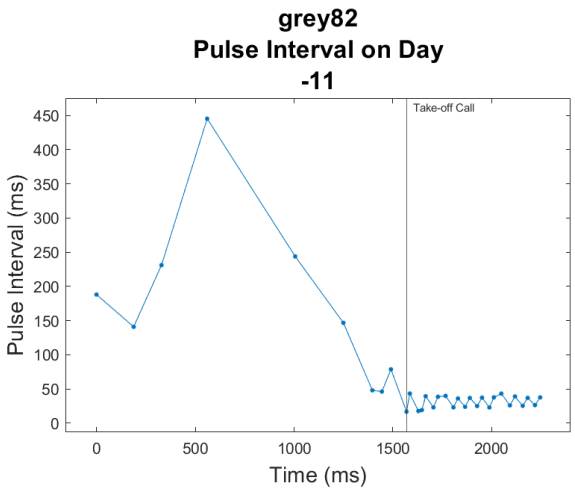
grey82
Pulse Interval on Day
-11
Take-off Call
Pulse Interval (ms)
Time (ms)

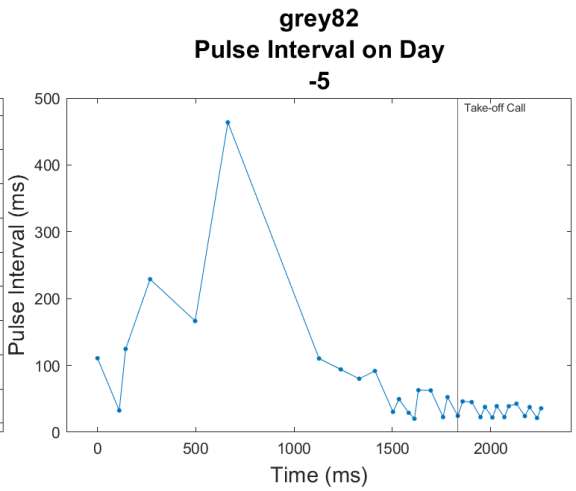
grey82
Pulse Interval on Day
-5
Take-off Call
Pulse Interval (ms)
Time (ms)

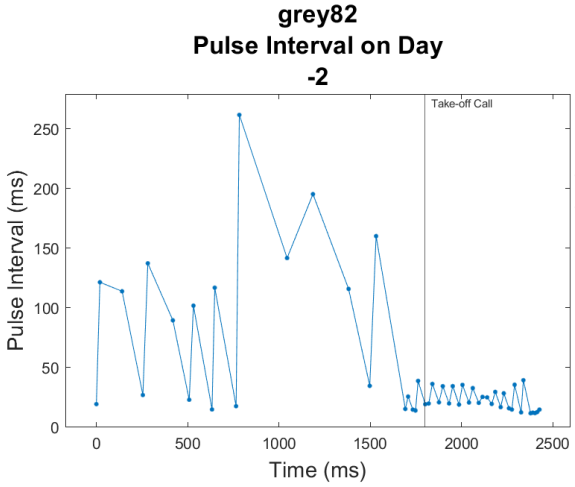
grey82
Pulse Interval on Day
-2
Take-off Call
Pulse Interval (ms)
Time (ms)

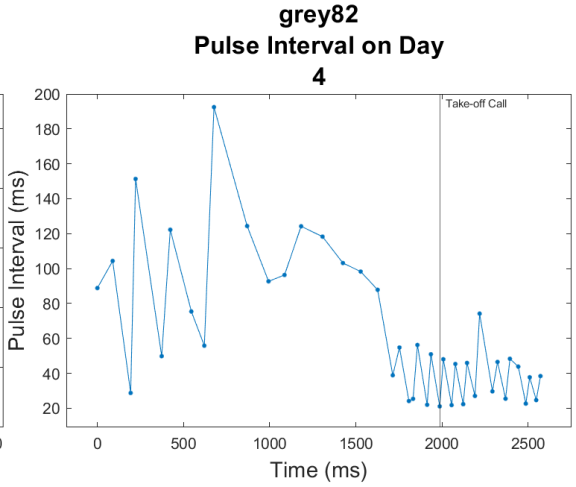
grey82
Pulse Interval on Day
4
Take-off Call
Pulse Interval (ms)
Time (ms)

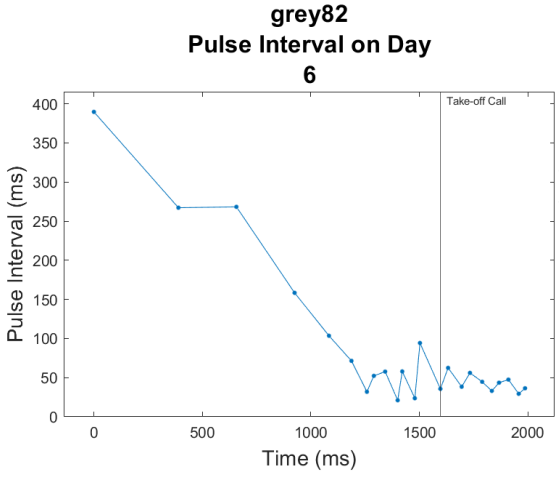
grey82
Pulse Interval on Day
6
Take-off Call
Pulse Interval (ms)
Time (ms)

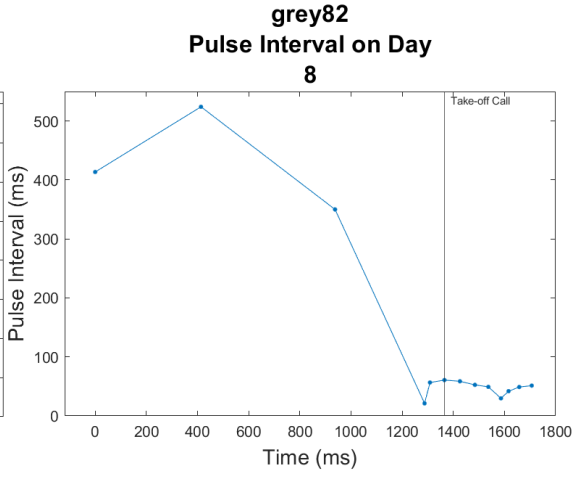
grey82
Pulse Interval on Day
8
Take-off Call
Pulse Interval (ms)
Time (ms)

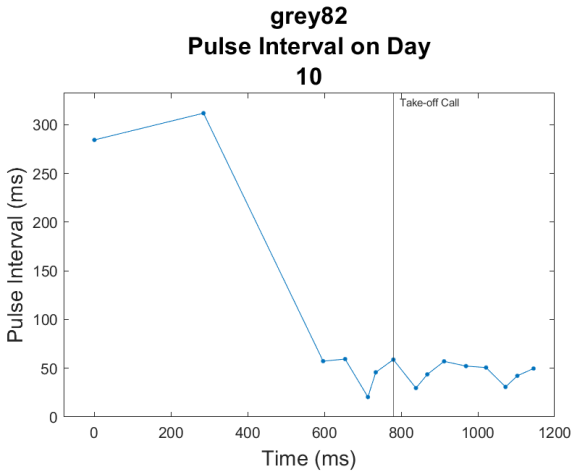
grey82
Pulse Interval on Day
10
Take-off Call
Pulse Interval (ms)
Time (ms)

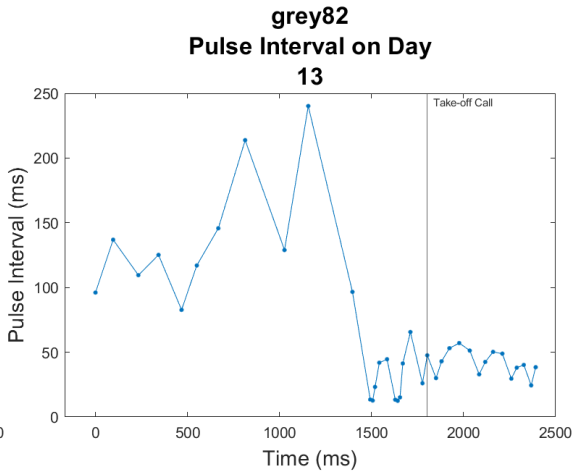
grey82
Pulse Interval on Day
13
Take-off Call
Pulse Interval (ms)
Time (ms)

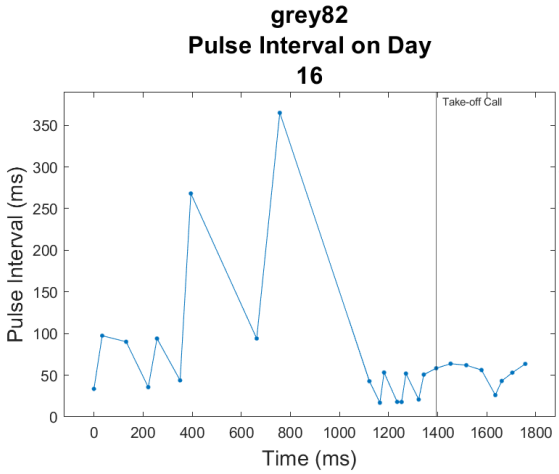
grey82
Pulse Interval on Day
16
Take-off Call
Pulse Interval (ms)
Time (ms)

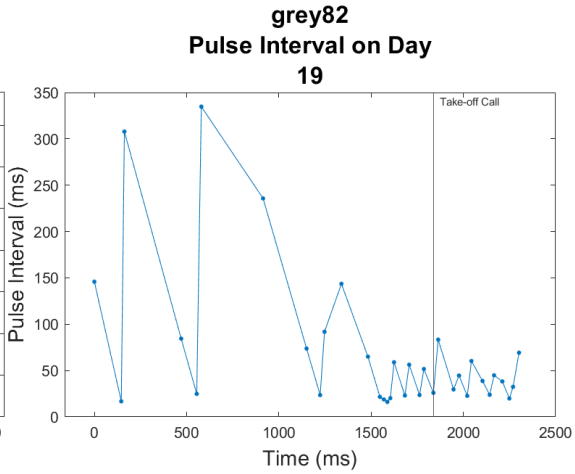
grey82
Pulse Interval on Day
19
Take-off Call
Pulse Interval (ms)
Time (ms)

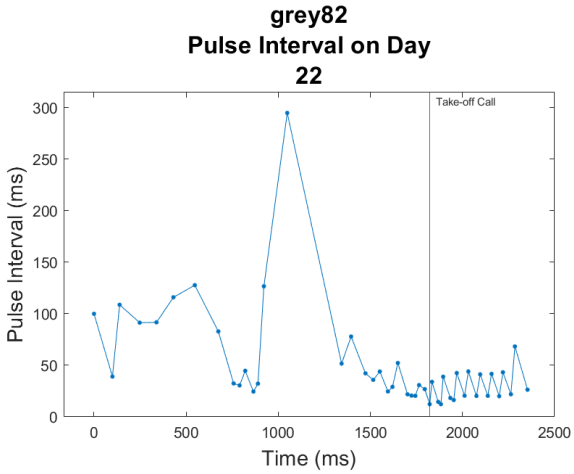
grey82
Pulse Interval on Day
22
Take-off Call
Pulse Interval (ms)
Time (ms)

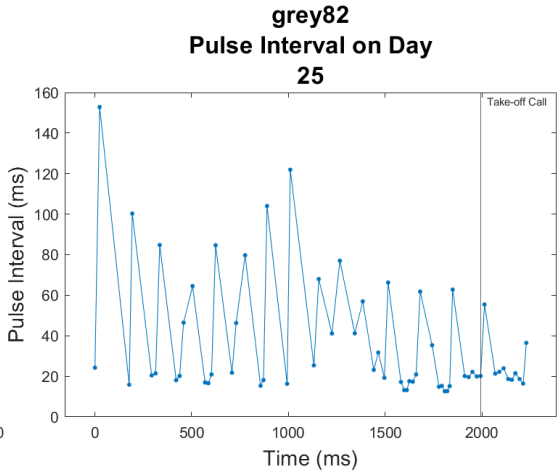
grey82
Pulse Interval on Day
25
Take-off Call
Pulse Interval (ms)
Time (ms)

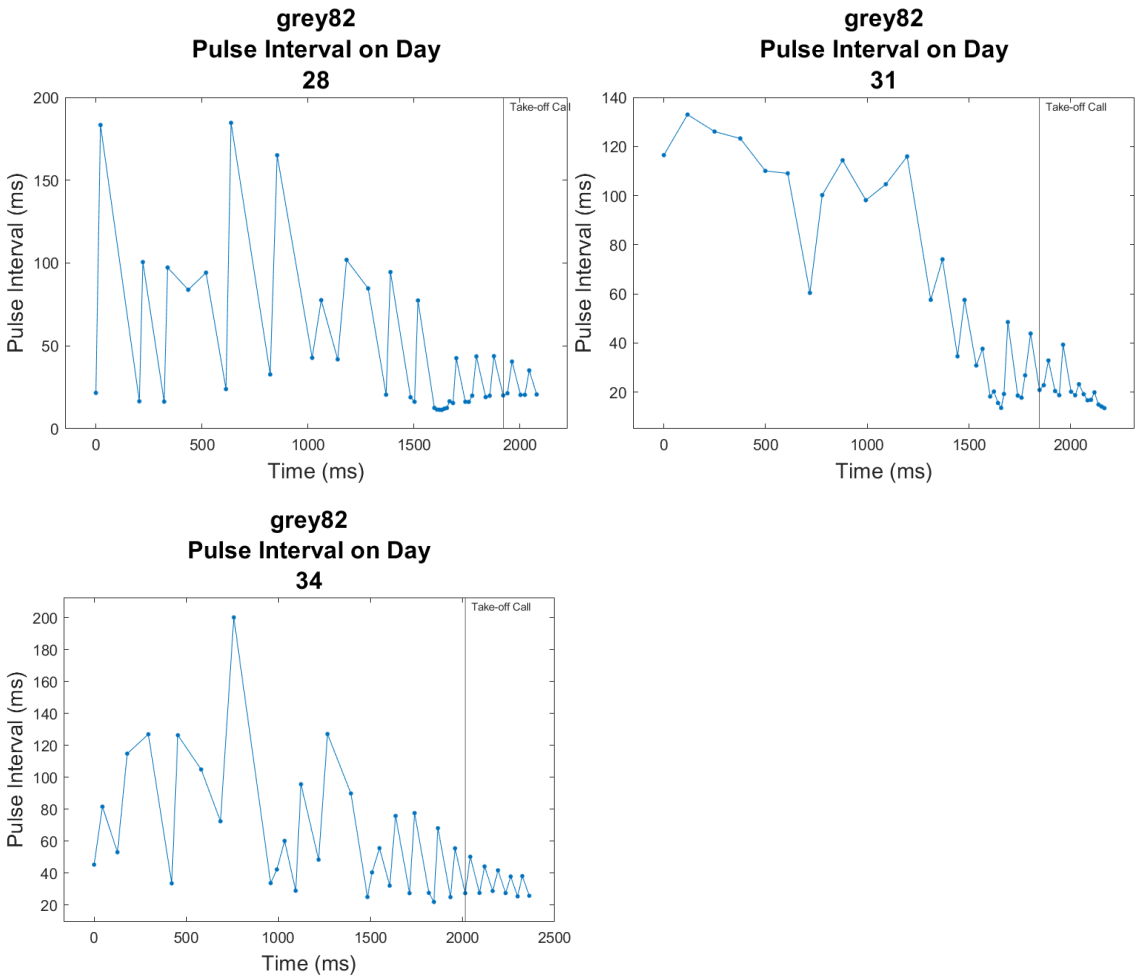

Appendix Figure 20: Grey 82 pulse interval plotted as a function of recording time per day. Each panel shows call durations before and after taking flight, with different panels showing data recorded on different days relative to parturition (number above panel; parturition day defined as Day 0). The take-off call is marked by a vertical line.

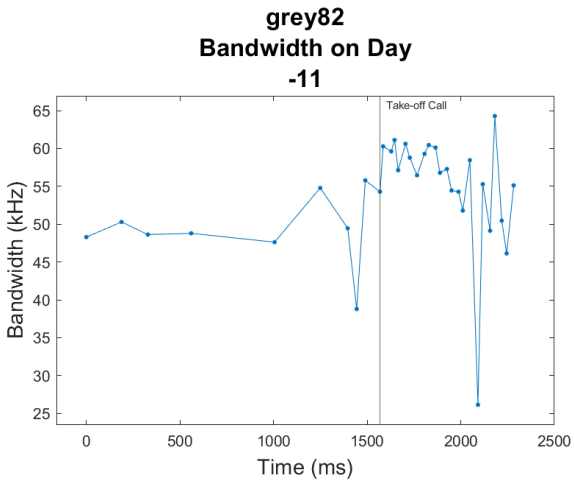
grey82
Bandwidth on Day
-11
Take-off Call
Bandwidth (kHz)
Time (ms)

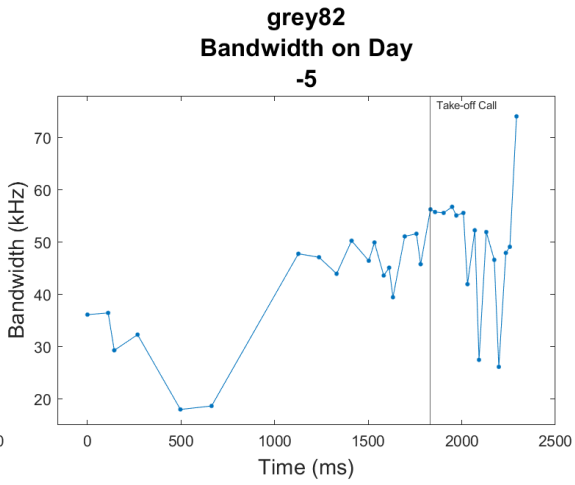
grey82
Bandwidth on Day
-5
Take-off Call
Bandwidth (kHz)
Time (ms)

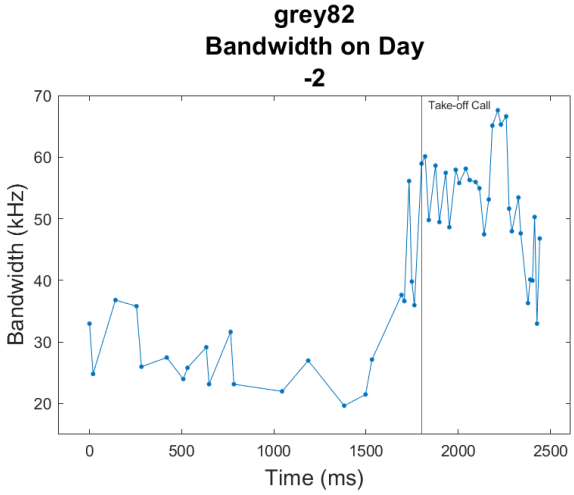
grey82
Bandwidth on Day
-2
Take-off Call
Bandwidth (kHz)
Time (ms)

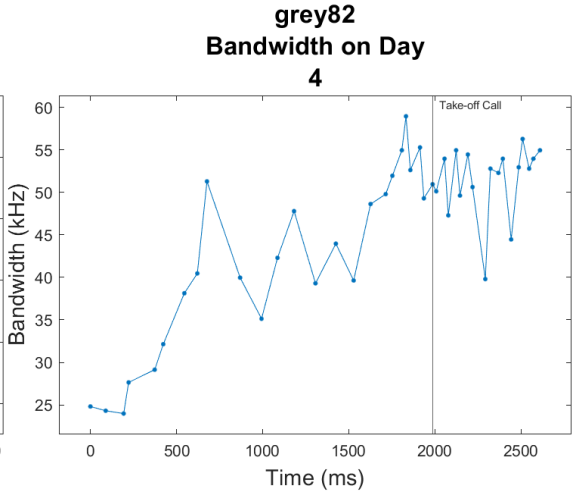
grey82
Bandwidth on Day
4
Take-off Call
Bandwidth (kHz)
Time (ms)

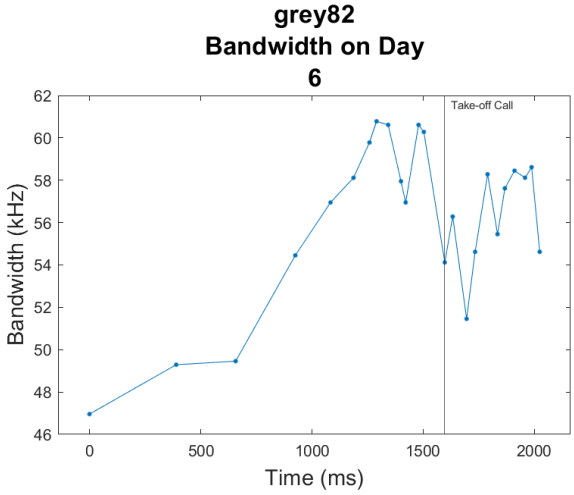
grey82
Bandwidth on Day
6
Take-off Call
Bandwidth (kHz)
Time (ms)

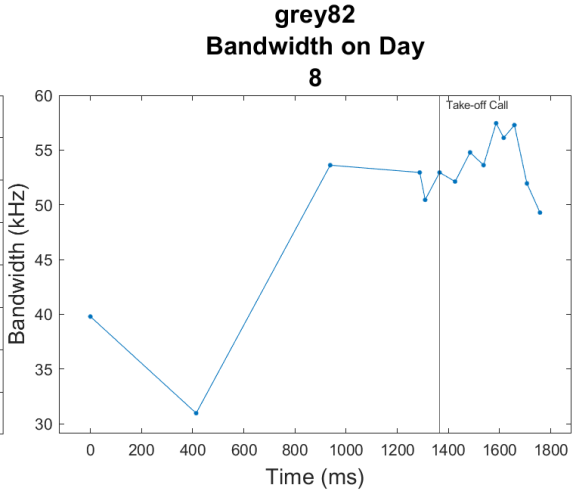
grey82
Bandwidth on Day
8
Take-off Call
Bandwidth (kHz)
Time (ms)

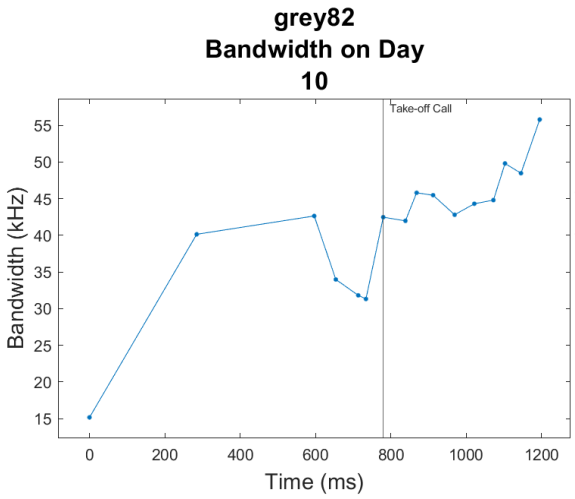
grey82
Bandwidth on Day
10
Take-off Call
Bandwidth (kHz)
Time (ms)

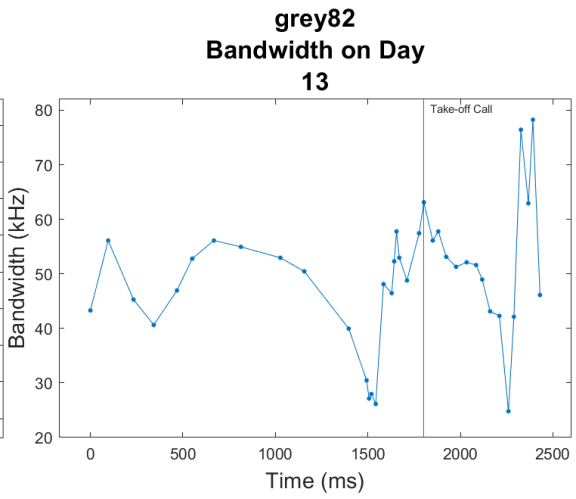
grey82
Bandwidth on Day
13
Take-off Call
Bandwidth (kHz)
Time (ms)

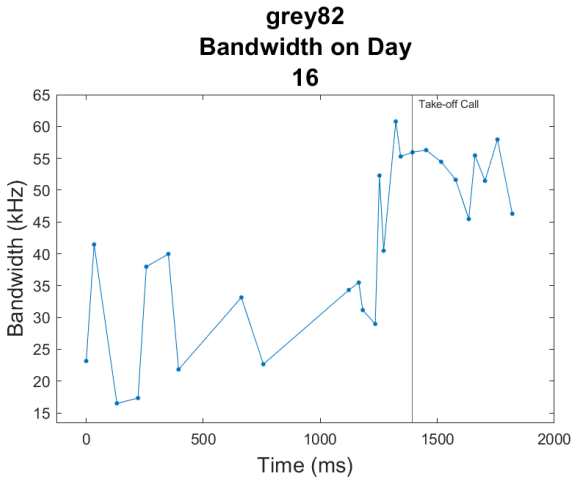
grey82
Bandwidth on Day
16
Take-off Call
Bandwidth (kHz)
Time (ms)

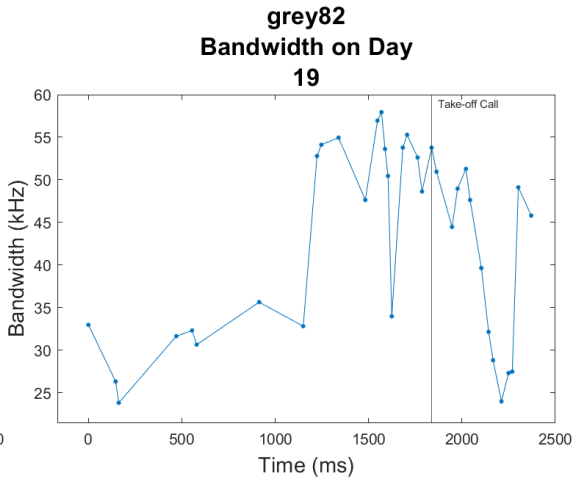
grey82
Bandwidth on Day
19
Take-off Call
Bandwidth (kHz)
Time (ms)

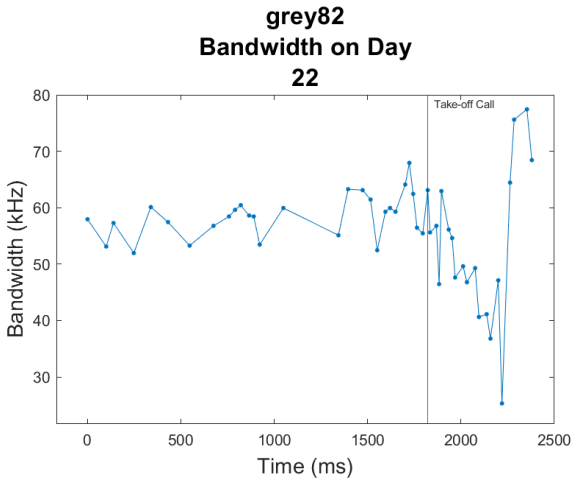
grey82
Bandwidth on Day
22
Take-off Call
Bandwidth (kHz)
Time (ms)

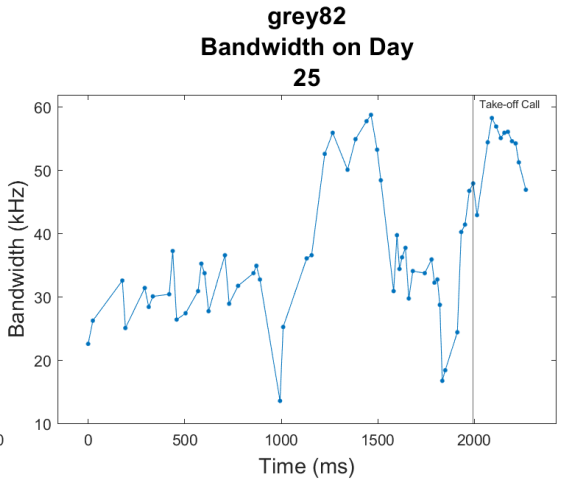
grey82
Bandwidth on Day
25
Take-off Call
Bandwidth (kHz)
Time (ms)

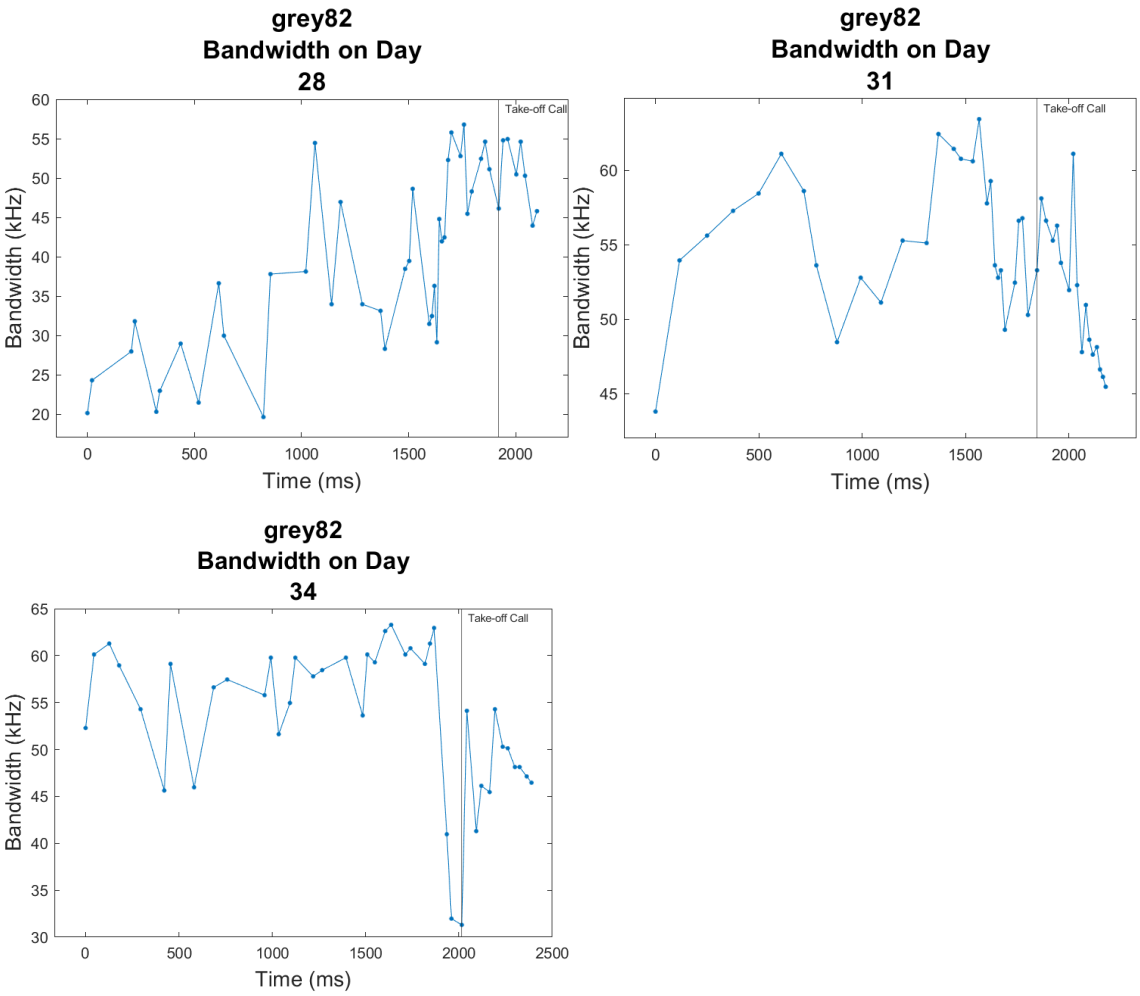

Appendix Figure 21: Grey 82 call bandwidth plotted as a function of recording time per day. Each panel shows call durations before and after taking flight, with different panels showing data recorded on different days relative to parturition (number above panel; parturition day defined as Day 0). The take-off call is marked by a vertical line.

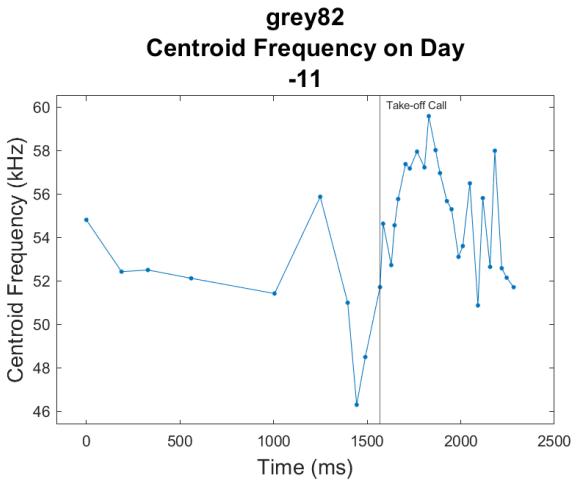
grey82
Centroid Frequency on Day
-11
Take-off Call
Centroid Frequency (kHz)
Time (ms)

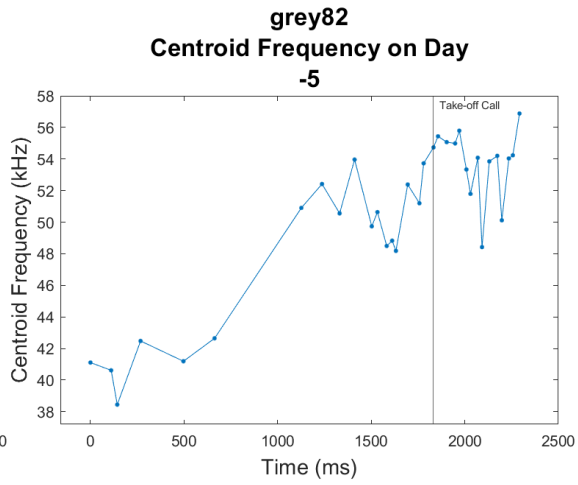
grey82
Centroid Frequency on Day
-5
Take-off Call
Centroid Frequency (kHz)
Time (ms)

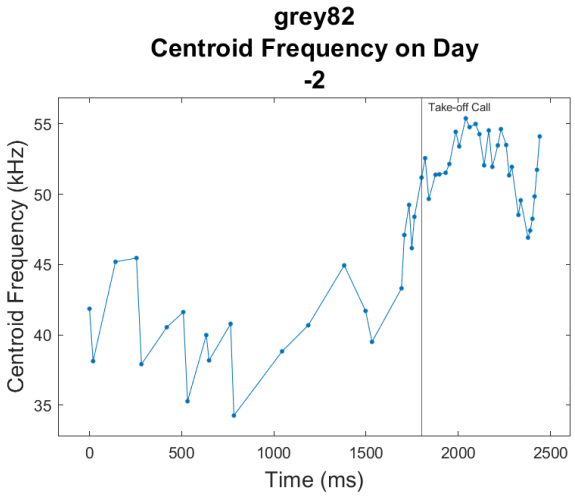
grey82
Centroid Frequency on Day
-2
Take-off Call
Centroid Frequency (kHz)
Time (ms)

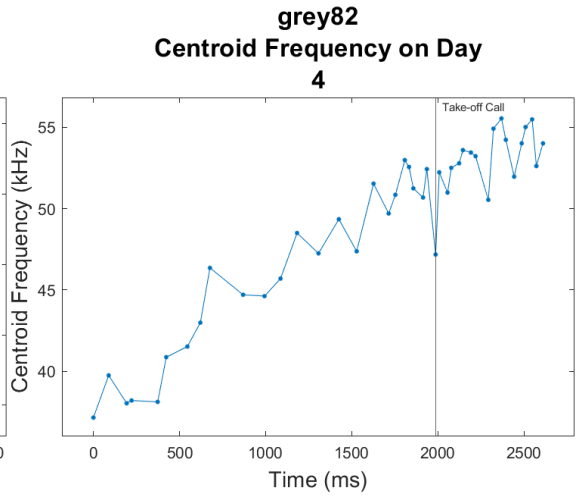
grey82
Centroid Frequency on Day
4
Take-off Call
Centroid Frequency (kHz)
Time (ms)

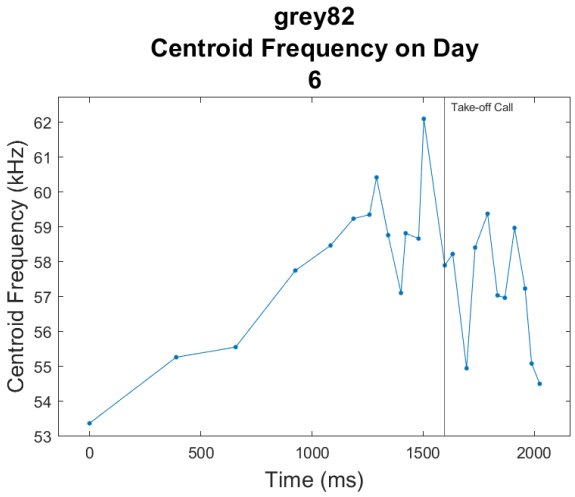
grey82
Centroid Frequency on Day
6
Take-off Call
Centroid Frequency (kHz)
Time (ms)

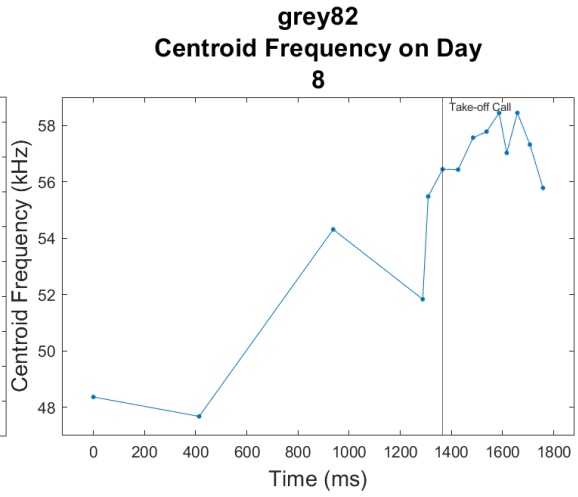
grey82
Centroid Frequency on Day
8
Take-off Call
Centroid Frequency (kHz)
Time (ms)

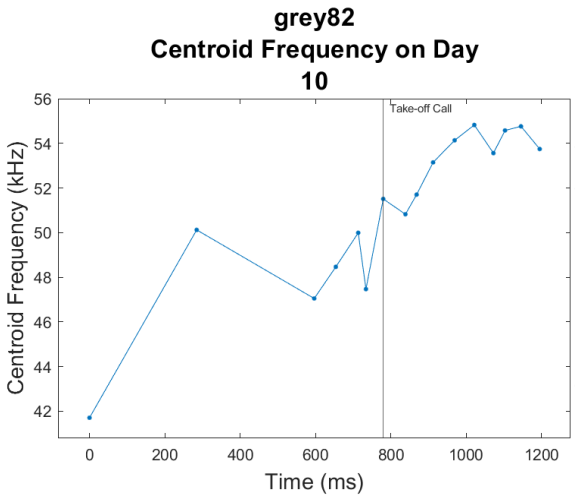
grey82
Centroid Frequency on Day
10
Take-off Call
Centroid Frequency (kHz)
Time (ms)

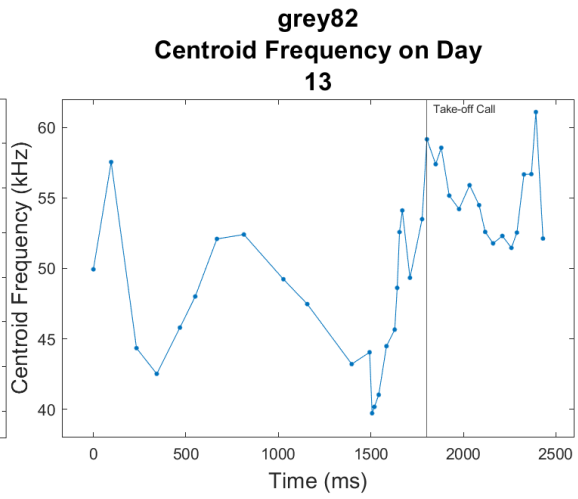
grey82
Centroid Frequency on Day
13
Take-off Call
Centroid Frequency (kHz)
Time (ms)

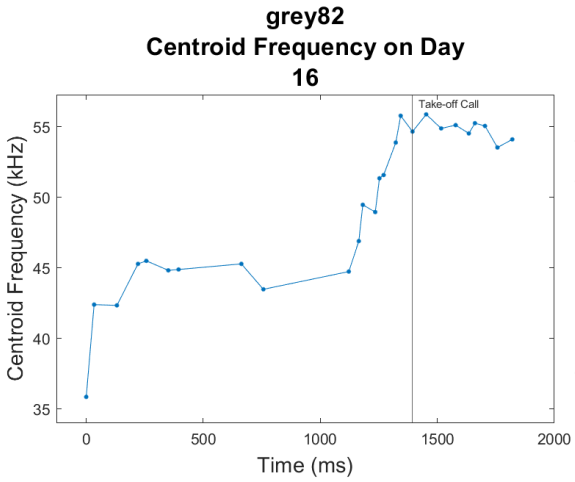
grey82
Centroid Frequency on Day
16
Take-off Call
Centroid Frequency (kHz)
Time (ms)

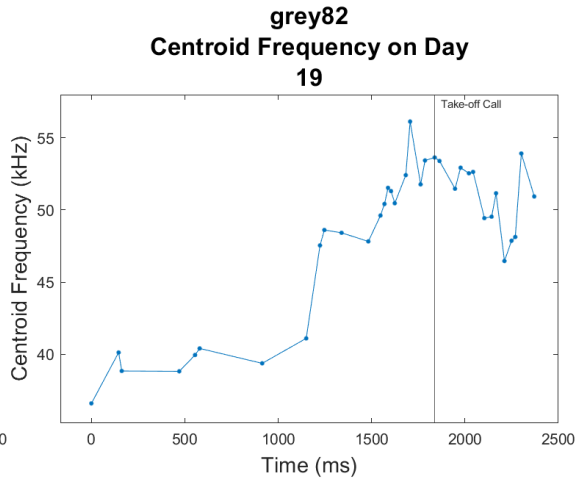
grey82
Centroid Frequency on Day
19
Take-off Call
Centroid Frequency (kHz)
Time (ms)

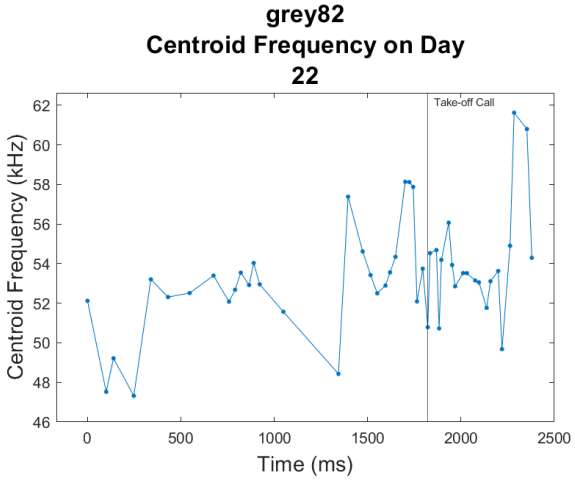
grey82
Centroid Frequency on Day
22
Take-off Call
Centroid Frequency (kHz)
Time (ms)

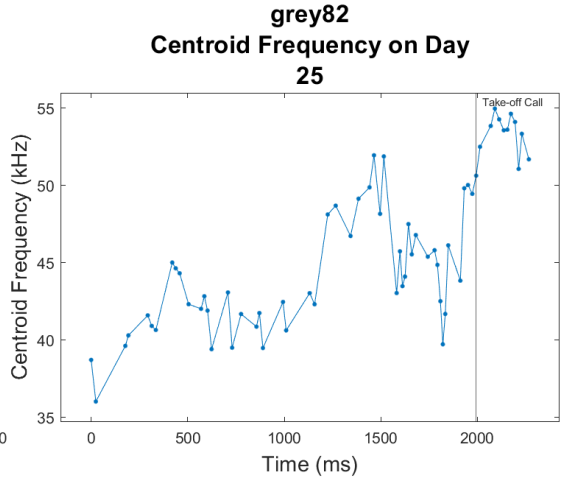
grey82
Centroid Frequency on Day
25
Take-off Call
Centroid Frequency (kHz)
Time (ms)

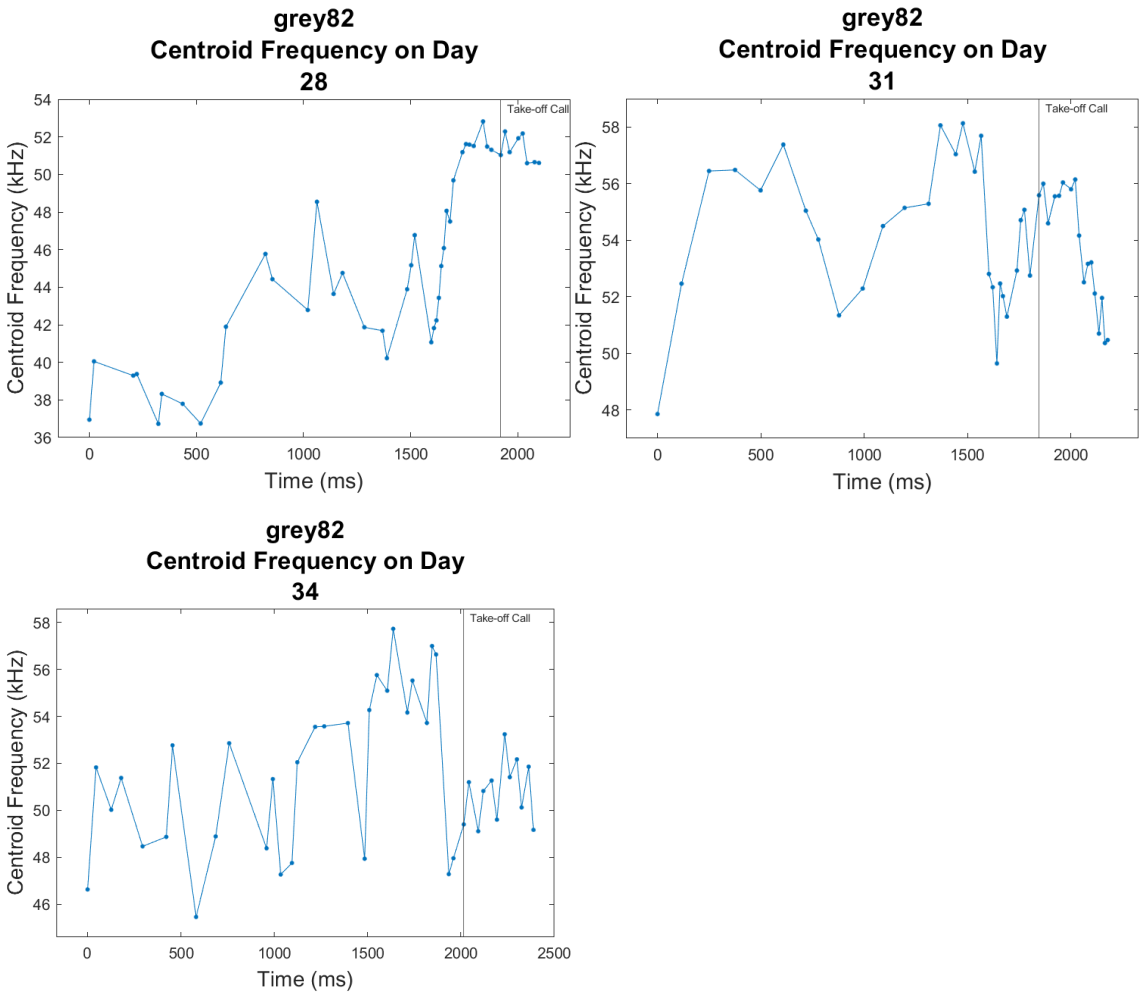

Appendix Figure 22: Grey 82 centroid frequency plotted as a function of recording time per day. Each panel shows call durations before and after taking flight, with different panels showing data recorded on different days relative to parturition (number above panel; parturition day defined as Day 0). The take-off call is marked by a vertical line.

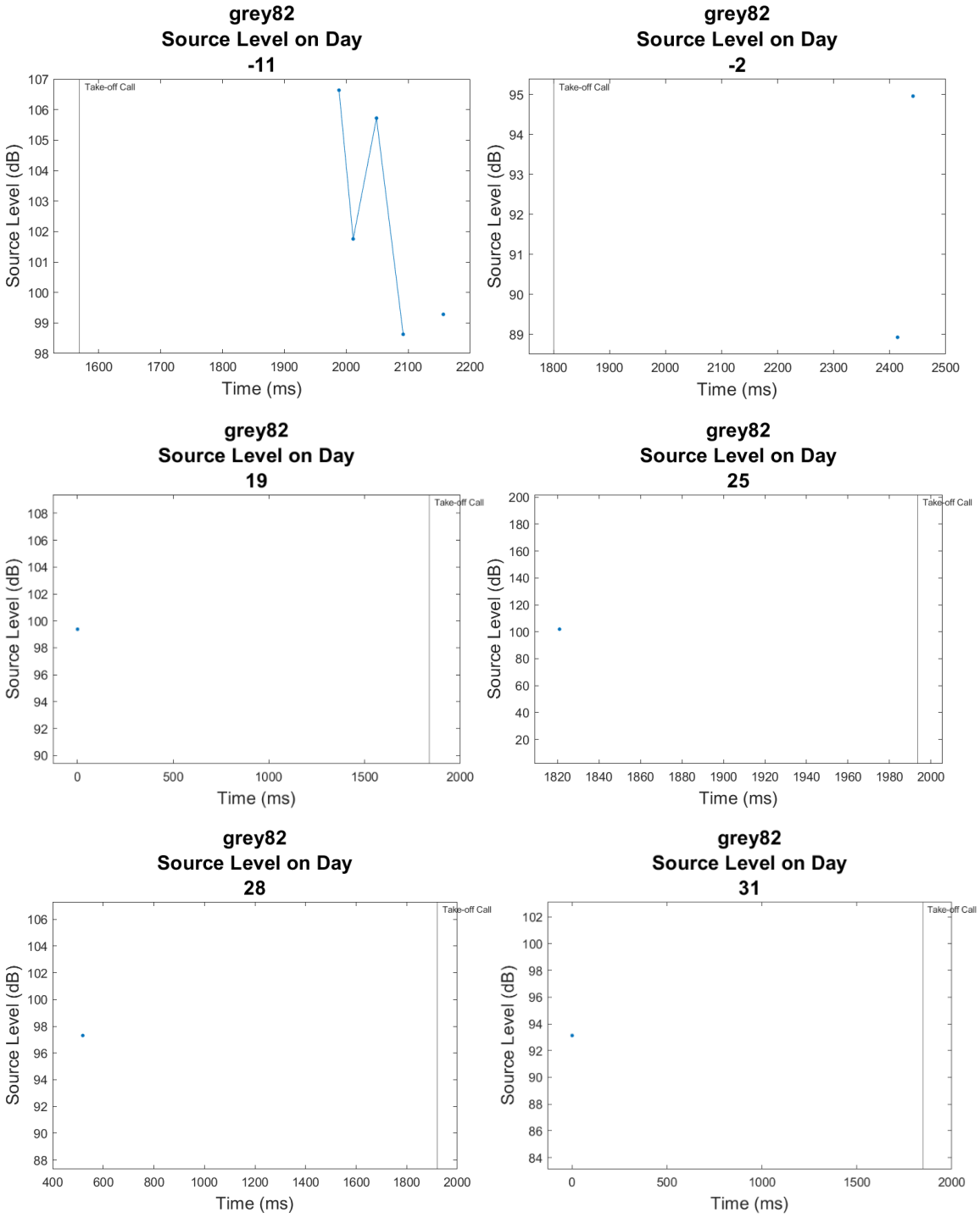

Appendix Figure 23: Grey 82 source level plotted as a function of recording time per day. Each panel shows call durations before and after taking flight, with different panels showing data recorded on different days relative to parturition (number above panel; parturition day defined as Day 0). The take-off call is marked by a vertical line.

Grey 85 Echolocation Call Characteristics Graphs

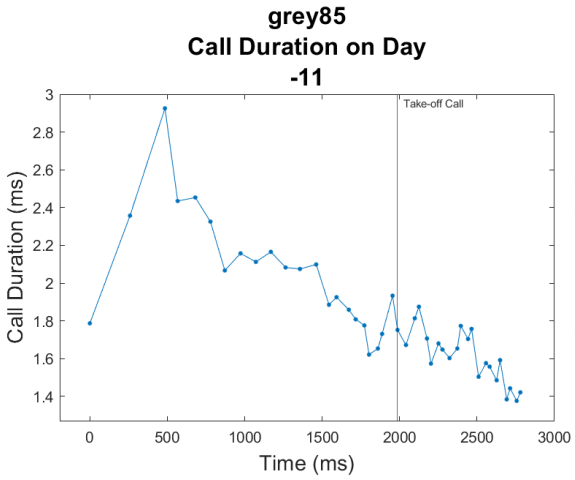

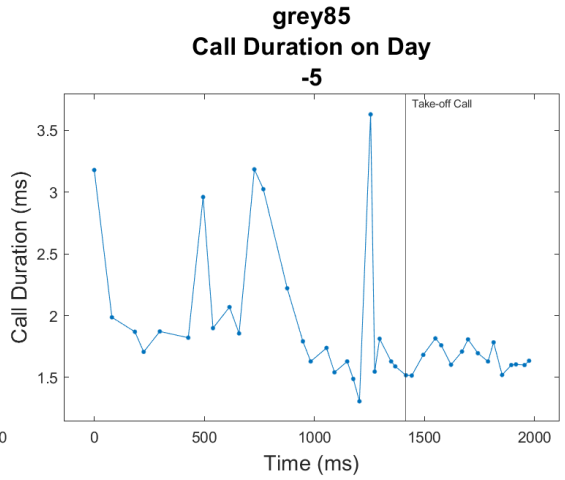

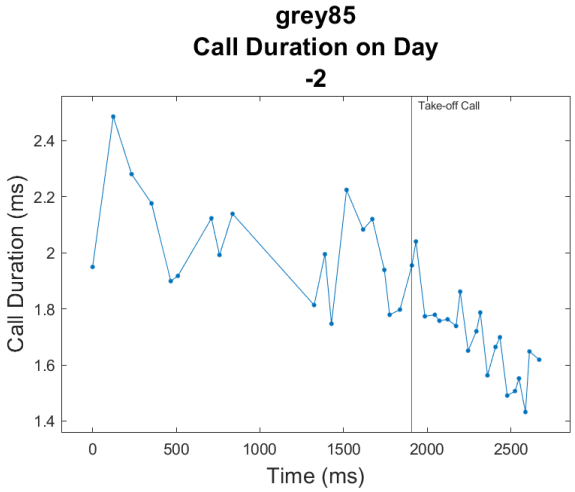

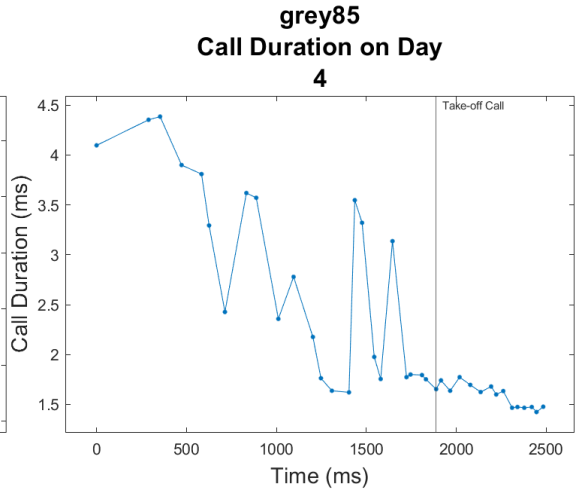

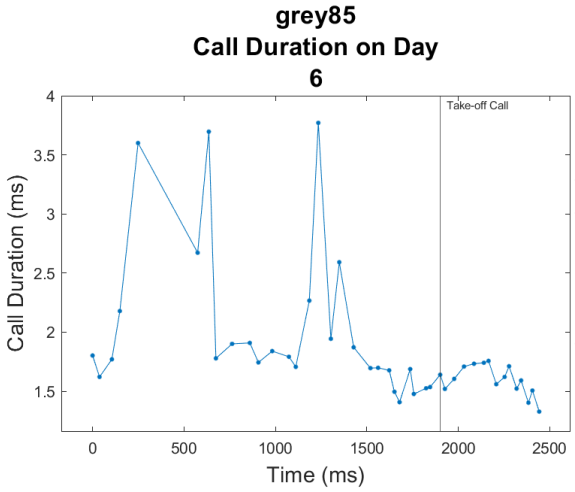

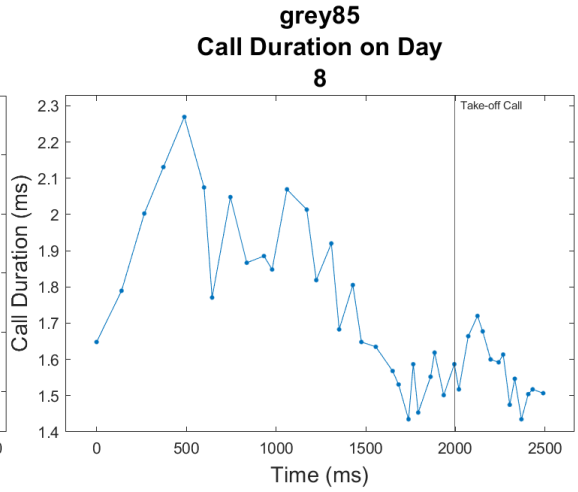

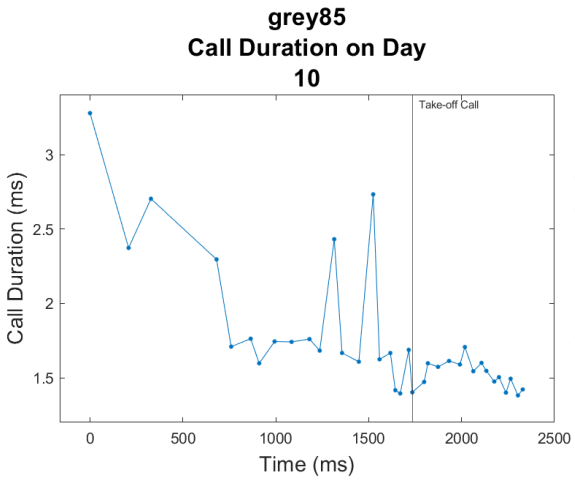
grey85
Call Duration on Day
10
Take-off Call
Call Duration (ms)
Time (ms)

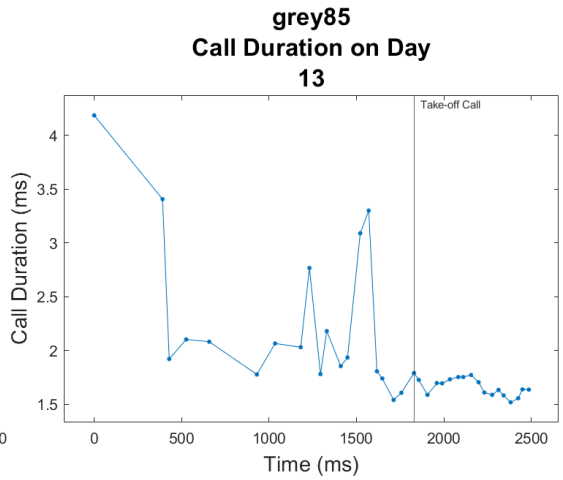
grey85
Call Duration on Day
13
Take-off Call
Call Duration (ms)
Time (ms)

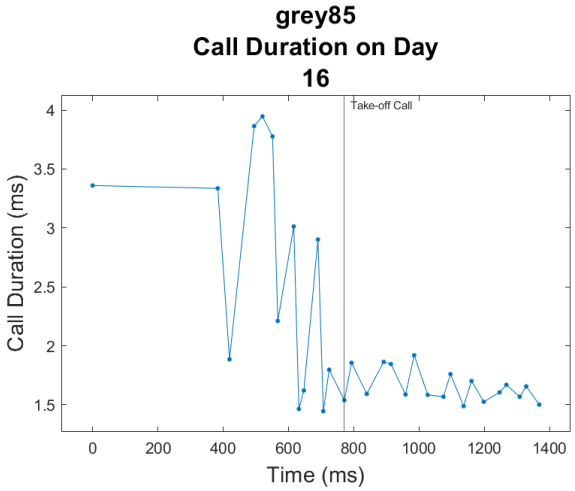
grey85
Call Duration on Day
16
Take-off Call
Call Duration (ms)
Time (ms)

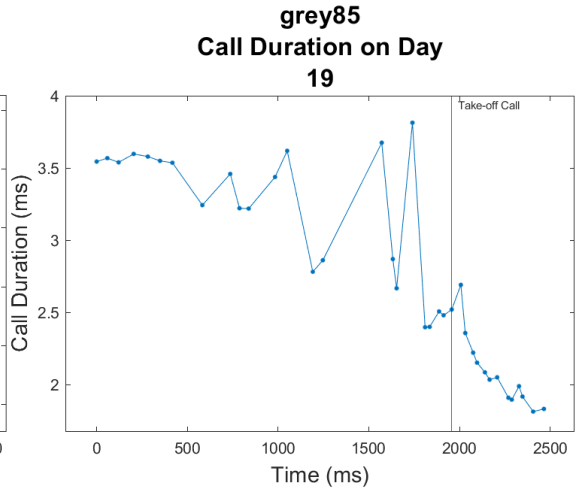
grey85
Call Duration on Day
19
Take-off Call
Call Duration (ms)
Time (ms)

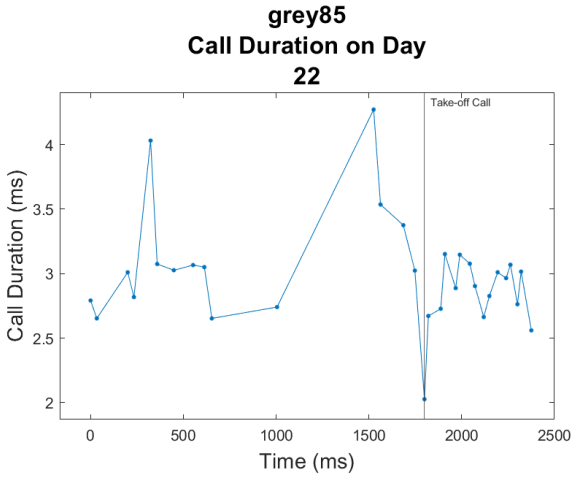
grey85
Call Duration on Day
22
Take-off Call
Call Duration (ms)
Time (ms)

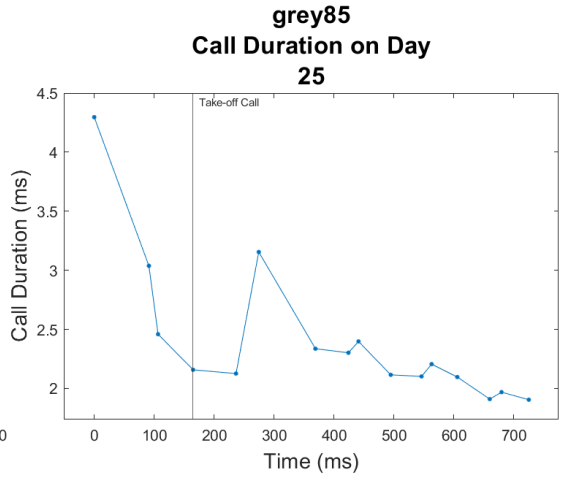
grey85
Call Duration on Day
25
Take-off Call
Call Duration (ms)
Time (ms)

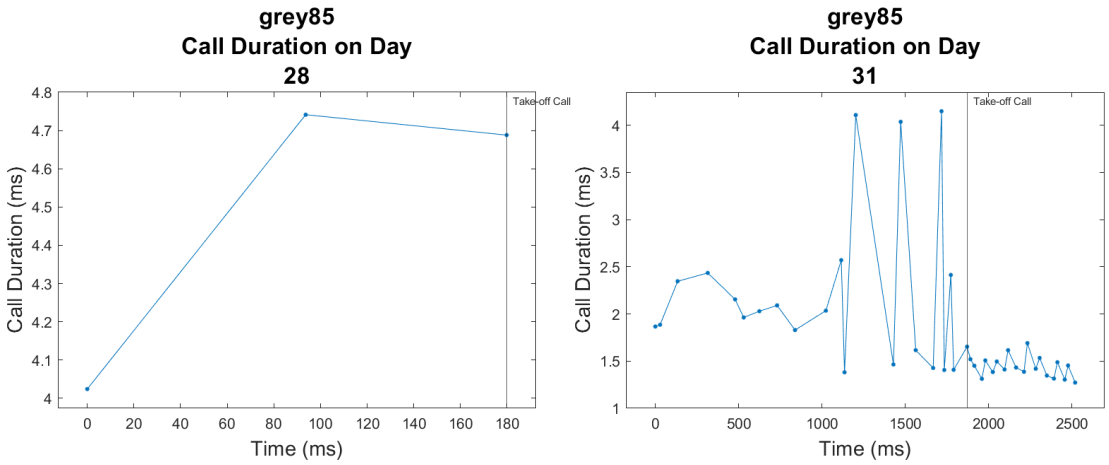

Appendix Figure 24: Grey 85 call duration plotted as a function of recording time per day. Each panel shows call durations before and after taking flight, with different panels showing data recorded on different days relative to parturition (number above panel; parturition day defined as Day 0). The take-off call is marked by a vertical line..

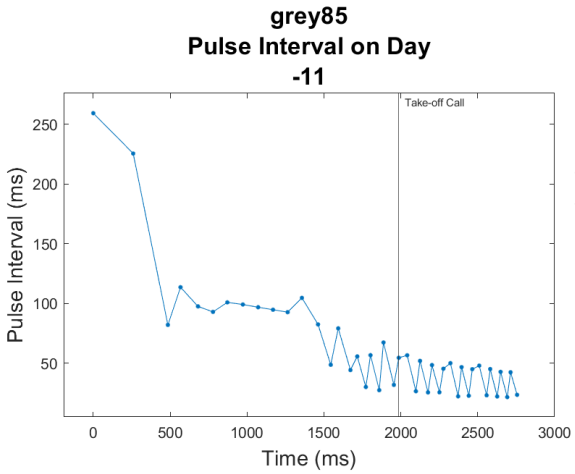
grey85
Pulse Interval on Day
-11
Take-off Call
Pulse Interval (ms)
Time (ms)

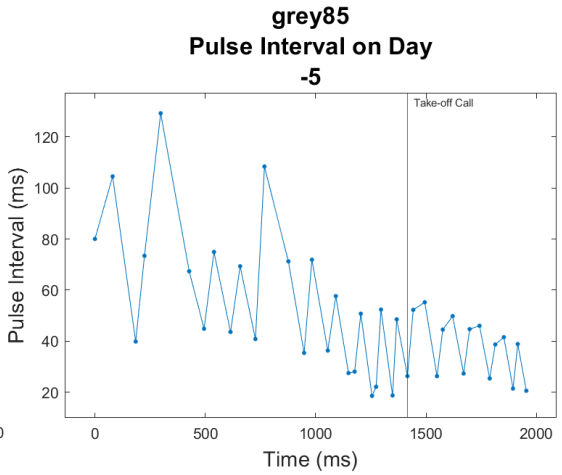
grey85
Pulse Interval on Day
-5
Take-off Call
Pulse Interval (ms)
Time (ms)

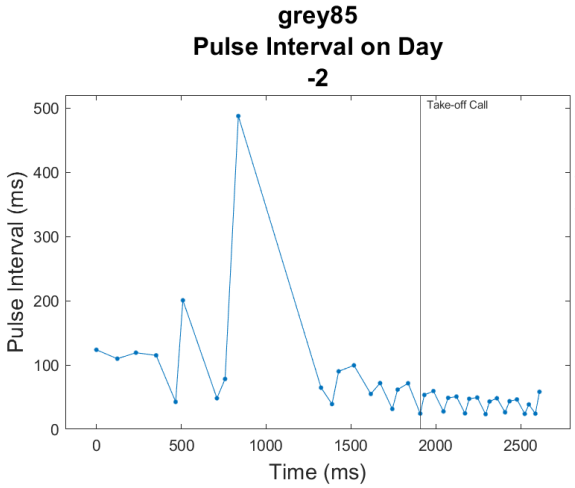
grey85
Pulse Interval on Day
-2
Take-off Call
Pulse Interval (ms)
Time (ms)

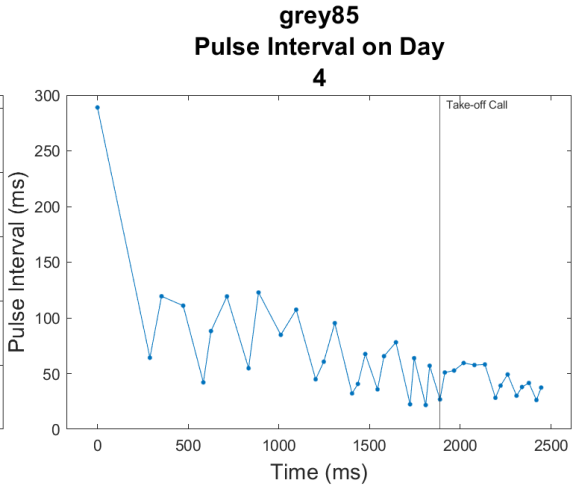
grey85
Pulse Interval on Day
4
Take-off Call
Pulse Interval (ms)
Time (ms)

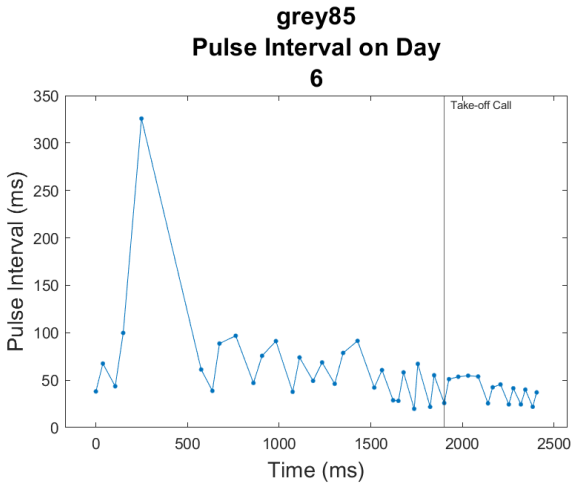
grey85
Pulse Interval on Day
6
Take-off Call
Pulse Interval (ms)
Time (ms)

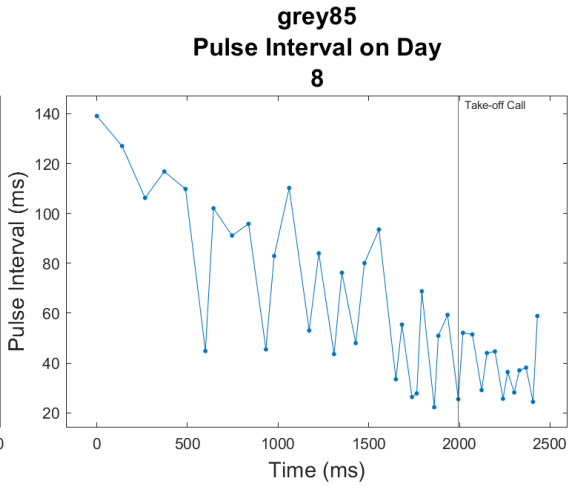
grey85
Pulse Interval on Day
8
Take-off Call
Pulse Interval (ms)
Time (ms)

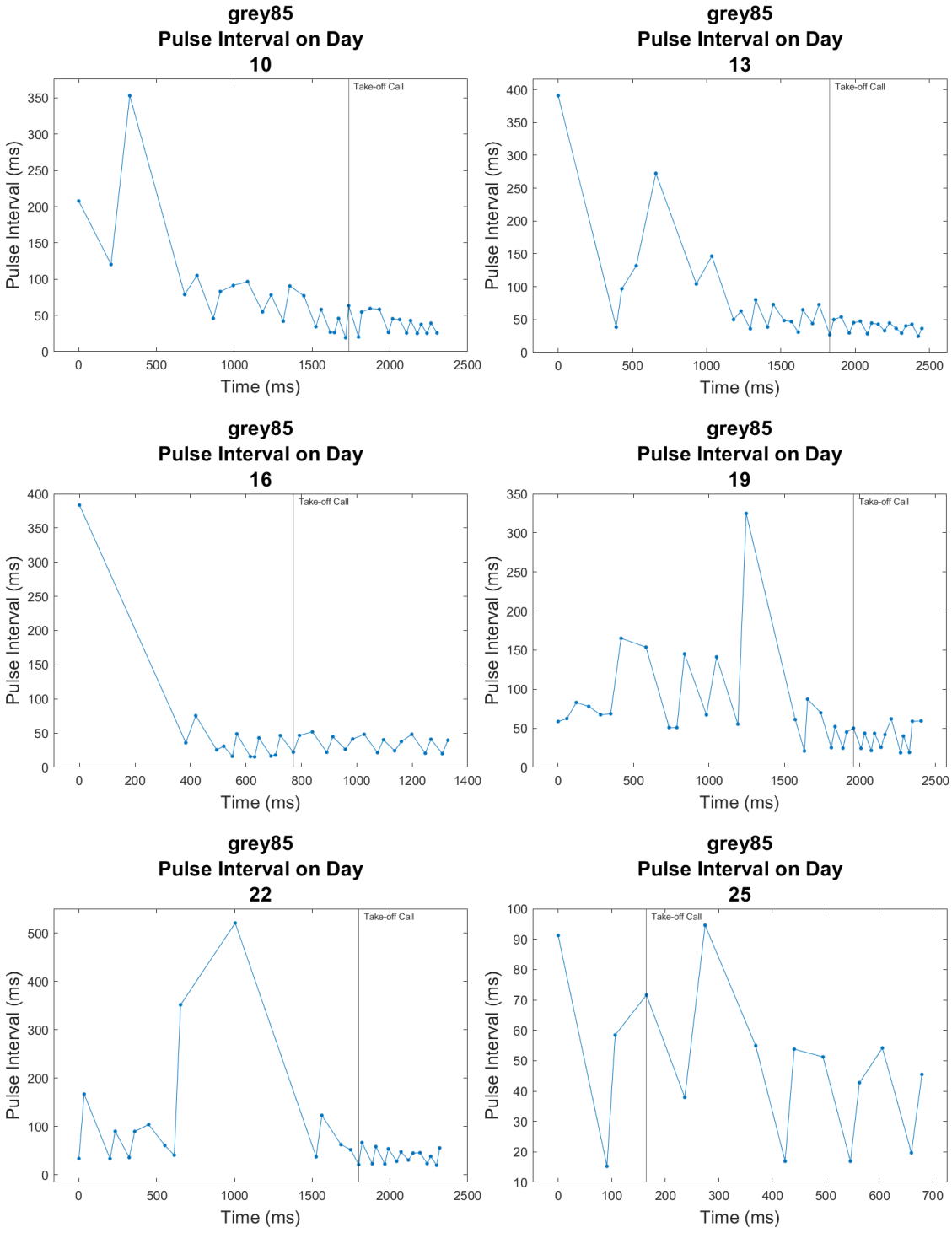
grey85
Pulse Interval on Day
10
Take-off Call
Pulse Interval (ms)
Time (ms)
grey85
Pulse Interval on Day
13
Take-off Call
Pulse Interval (ms)
Time (ms)
grey85
Pulse Interval on Day
16
Take-off Call
Pulse Interval (ms)
Time (ms)
grey85
Pulse Interval on Day
19
Take-off Call
Pulse Interval (ms)
Time (ms)
grey85
Pulse Interval on Day
22
Take-off Call
Pulse Interval (ms)
Time (ms)
grey85
Pulse Interval on Day
25
Take-off Call
Pulse Interval (ms)
Time (ms)

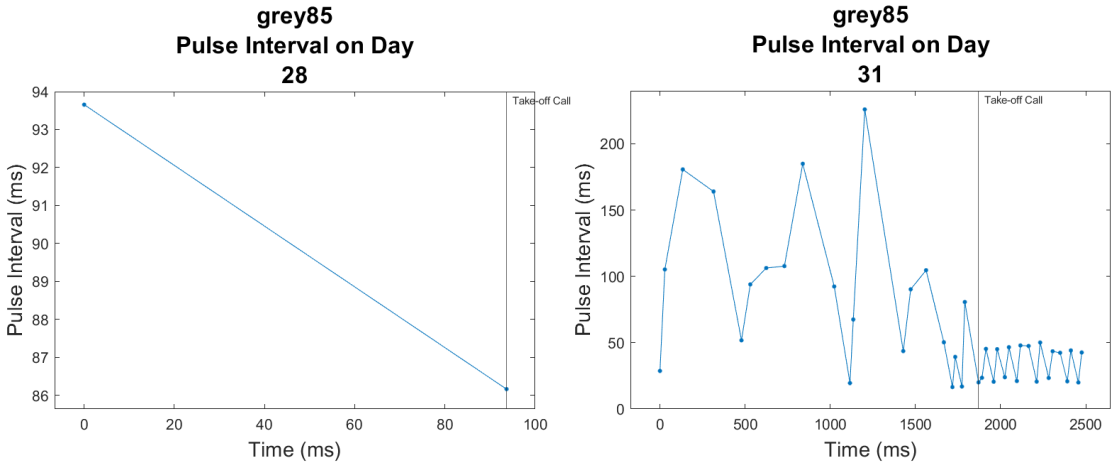

Appendix Figure 25: Grey 85 pulse interval plotted as a function of recording time per day. Each panel shows call durations before and after taking flight, with different panels showing data recorded on different days relative to parturition (number above panel; parturition day defined as Day 0). The take-off call is marked by a vertical line.

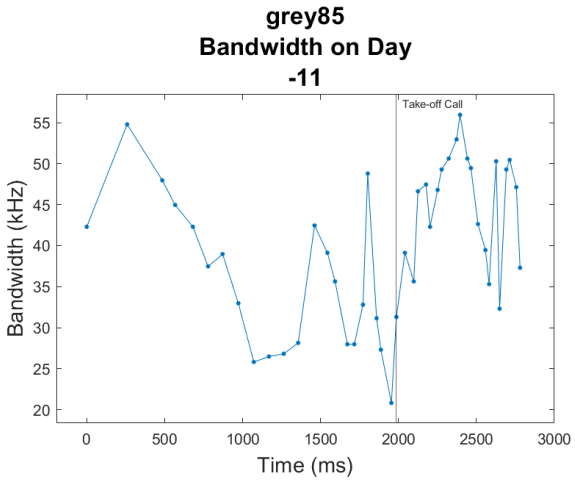
grey85
Bandwidth on Day
-11
Take-off Call
Bandwidth (kHz)
Time (ms)

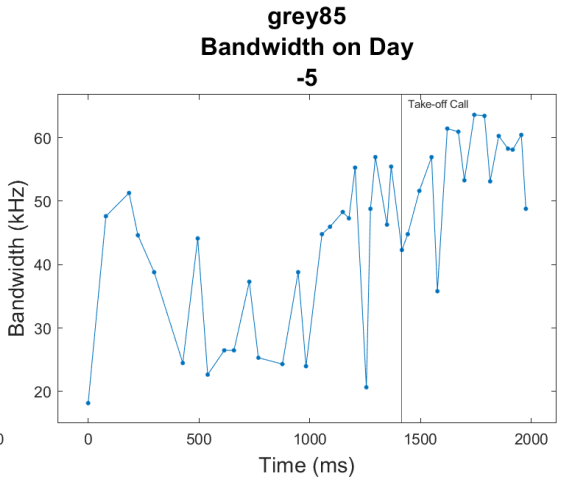
grey85
Bandwidth on Day
-5
Take-off Call
Bandwidth (kHz)
Time (ms)

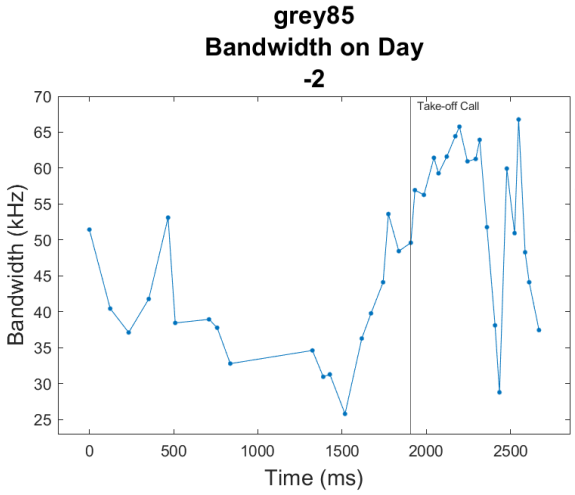
grey85
Bandwidth on Day
-2
Take-off Call
Bandwidth (kHz)
Time (ms)

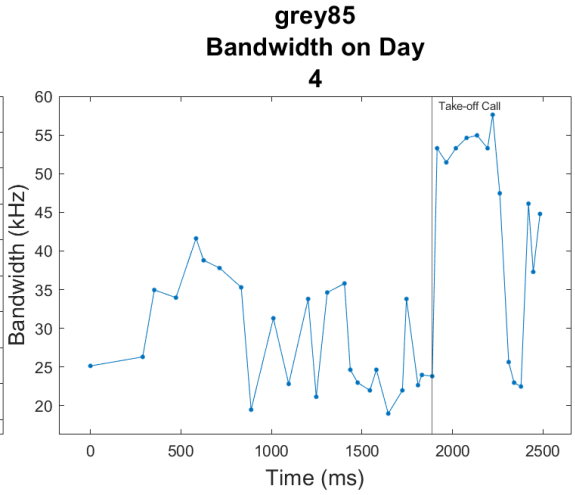
grey85
Bandwidth on Day
4
Take-off Call
Bandwidth (kHz)
Time (ms)

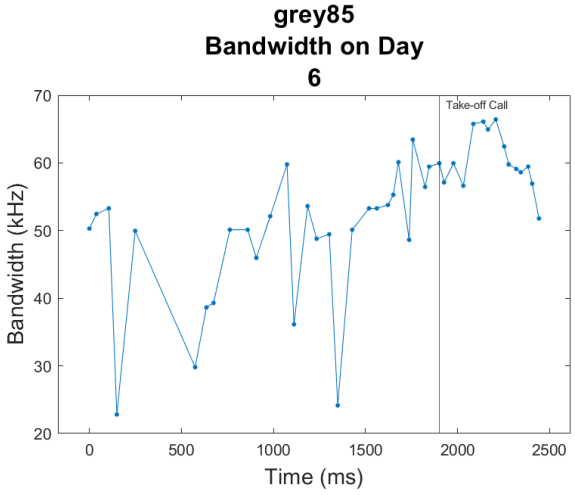
grey85
Bandwidth on Day
6
Take-off Call
Bandwidth (kHz)
Time (ms)

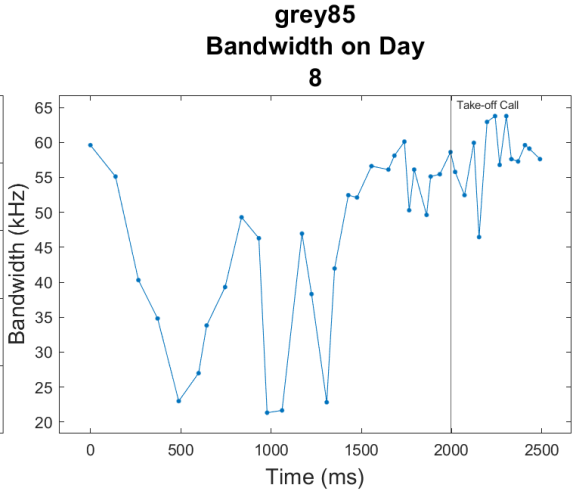
grey85
Bandwidth on Day
8
Take-off Call
Bandwidth (kHz)
Time (ms)

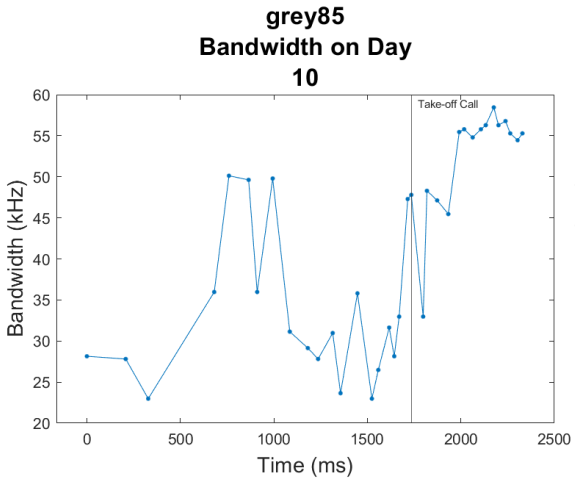
grey85
Bandwidth on Day
10
Take-off Call
Bandwidth (kHz)
Time (ms)

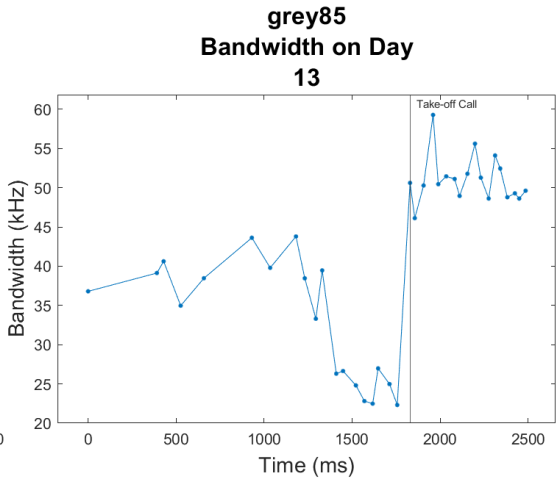
grey85
Bandwidth on Day
13
Take-off Call
Bandwidth (kHz)
Time (ms)

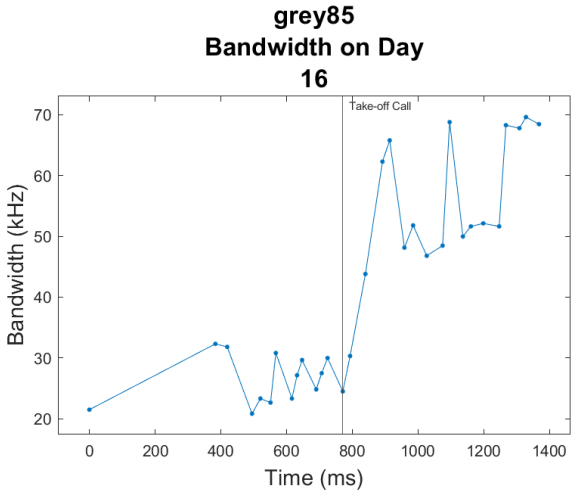
grey85
Bandwidth on Day
16
Take-off Call
Bandwidth (kHz)
Time (ms)

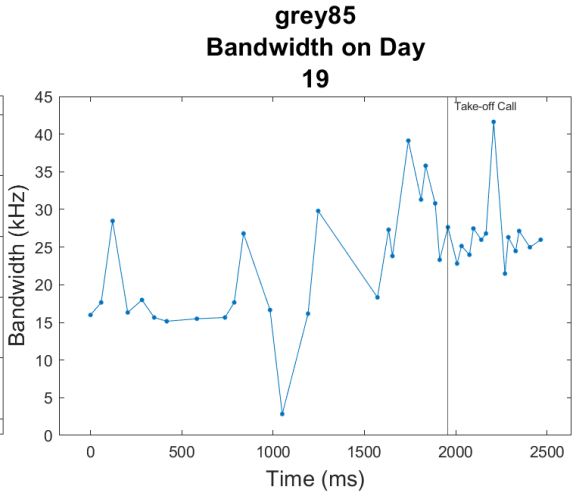
grey85
Bandwidth on Day
19
Take-off Call
Bandwidth (kHz)
Time (ms)

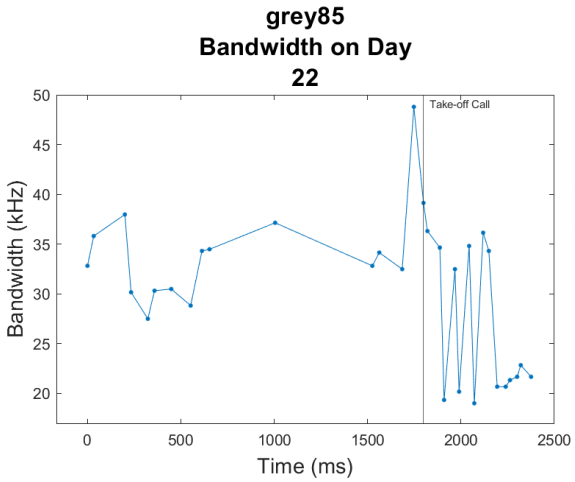
grey85
Bandwidth on Day
22
Take-off Call
Bandwidth (kHz)
Time (ms)

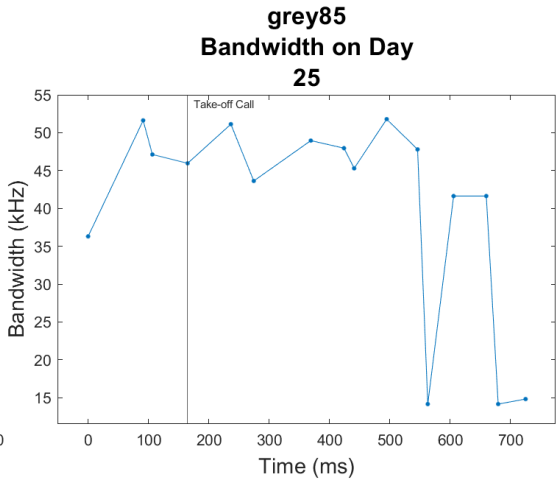
grey85
Bandwidth on Day
25
Take-off Call
Bandwidth (kHz)
Time (ms)

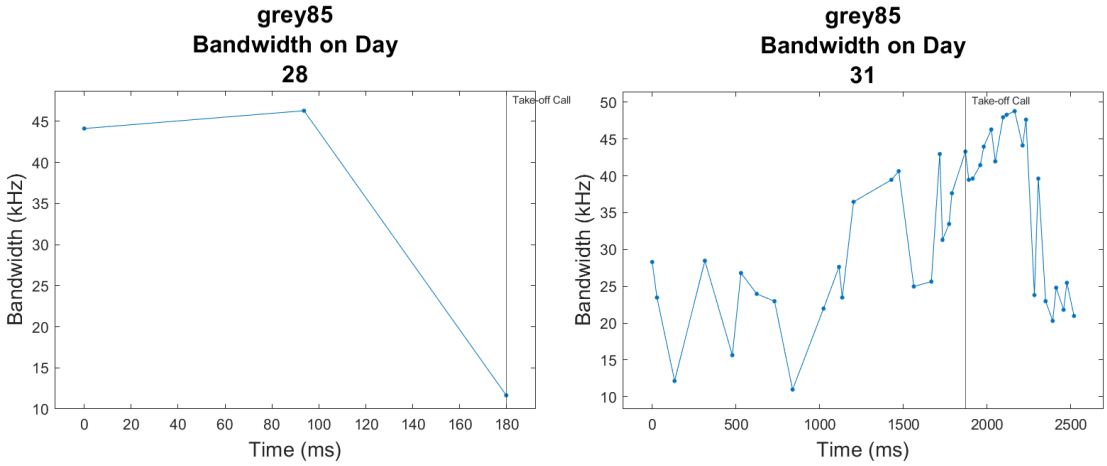

Appendix Figure 26: Grey 85 call bandwidth plotted as a function of recording time per day. Each panel shows call durations before and after taking flight, with different panels showing data recorded on different days relative to parturition (number above panel; parturition day defined as Day 0). The take-off call is marked by a vertical line.

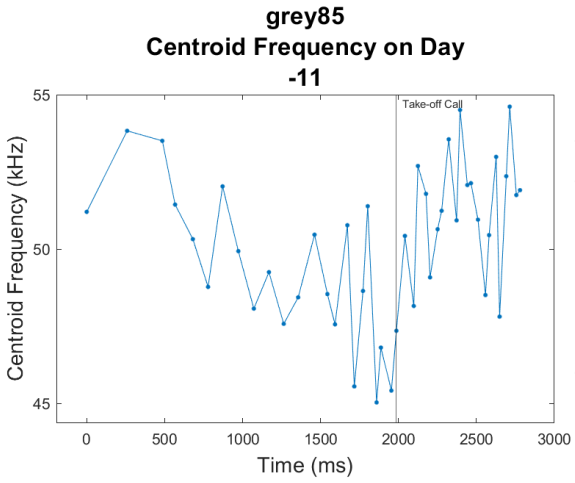
grey85
Centroid Frequency on Day
-11
Take-off Call
Centroid Frequency (kHz)
Time (ms)

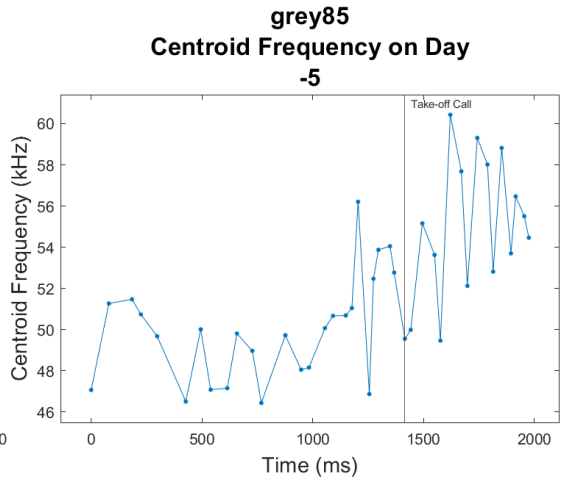
grey85
Centroid Frequency on Day
-5
Take-off Call
Centroid Frequency (kHz)
Time (ms)

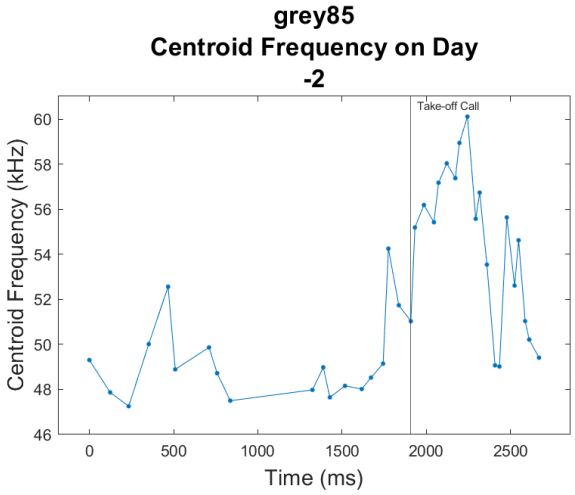
grey85
Centroid Frequency on Day
-2
Take-off Call
Centroid Frequency (kHz)
Time (ms)

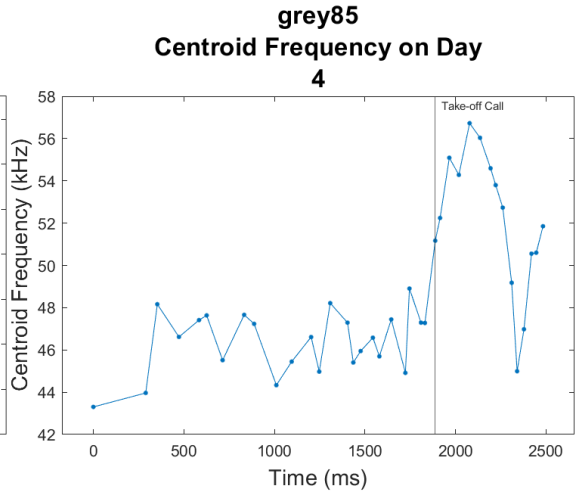
grey85
Centroid Frequency on Day
4
Take-off Call
Centroid Frequency (kHz)
Time (ms)

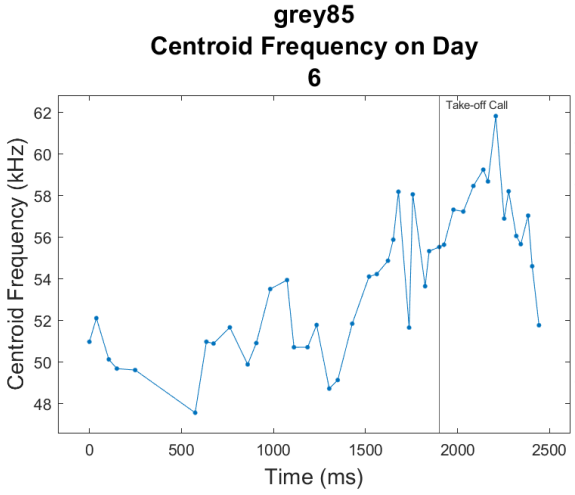
grey85
Centroid Frequency on Day
6
Take-off Call
Centroid Frequency (kHz)
Time (ms)

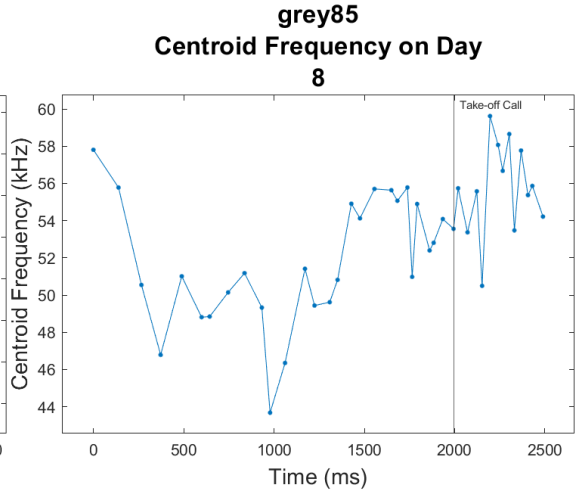
grey85
Centroid Frequency on Day
8
Take-off Call
Centroid Frequency (kHz)
Time (ms)

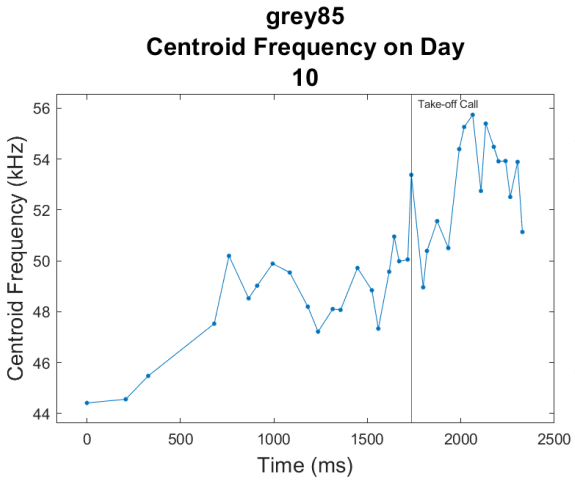
grey85
Centroid Frequency on Day
10
Take-off Call
Centroid Frequency (kHz)
Time (ms)

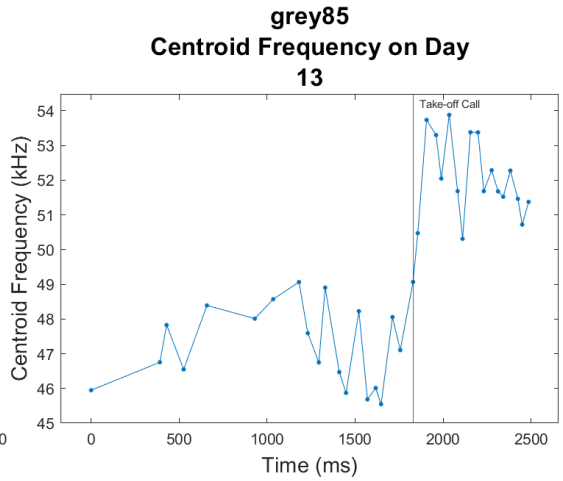
grey85
Centroid Frequency on Day
13
Take-off Call
Centroid Frequency (kHz)
Time (ms)

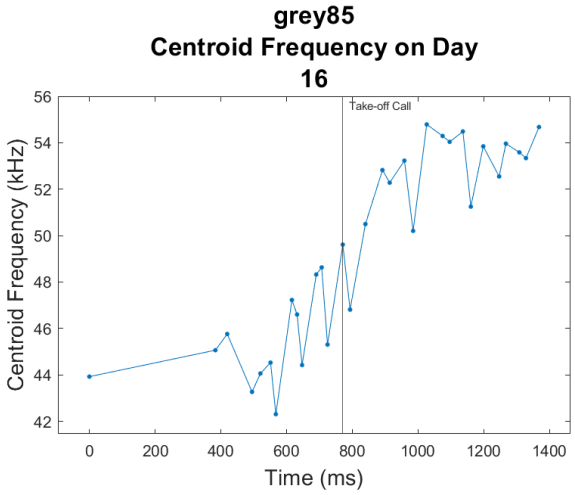
grey85
Centroid Frequency on Day
16
Take-off Call
Centroid Frequency (kHz)
Time (ms)

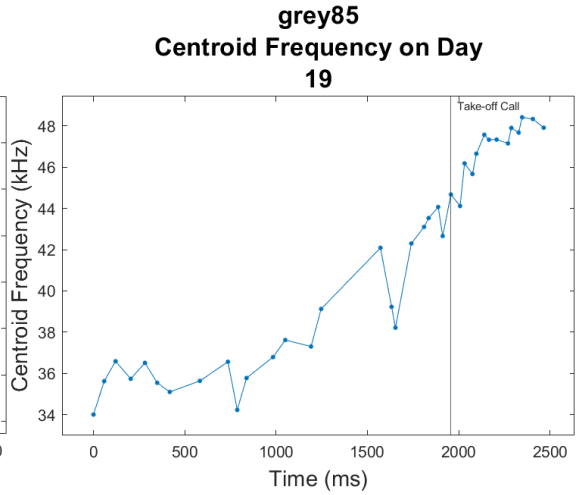
grey85
Centroid Frequency on Day
19
Take-off Call
Centroid Frequency (kHz)
Time (ms)

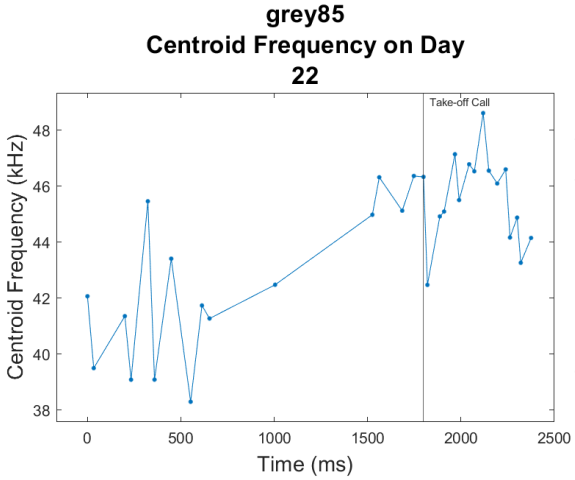
grey85
Centroid Frequency on Day
22
Take-off Call
Centroid Frequency (kHz)
Time (ms)

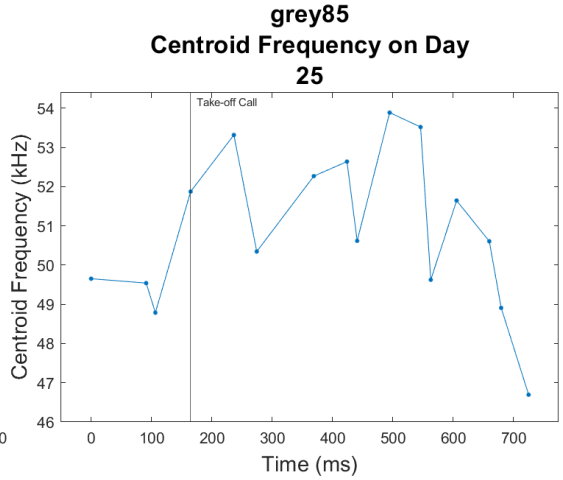
grey85
Centroid Frequency on Day
25
Take-off Call
Centroid Frequency (kHz)
Time (ms)

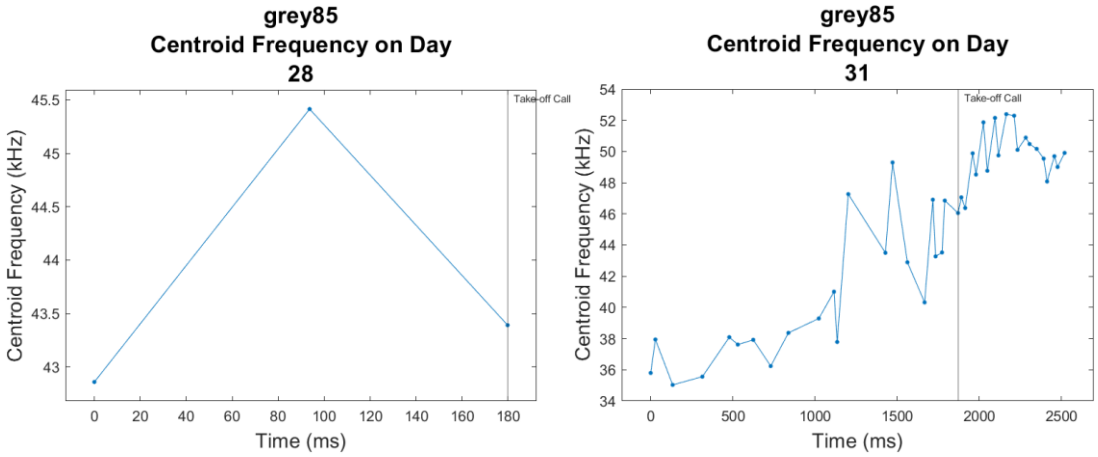

Appendix Figure 27: Grey 85 centroid frequency plotted as a function of recording time per day. Each panel shows call durations before and after taking flight, with different panels showing data recorded on different days relative to parturition (number above panel; parturition day defined as Day 0). The take-off call is marked by a vertical line.

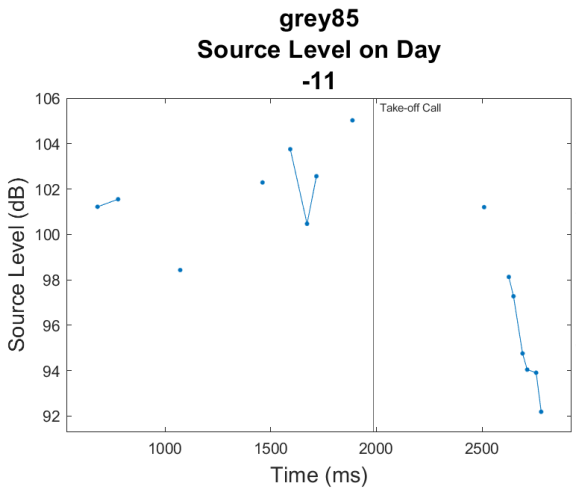
grey85
Source Level on Day
-11
Take-off Call
Source Level (dB)
Time (ms)

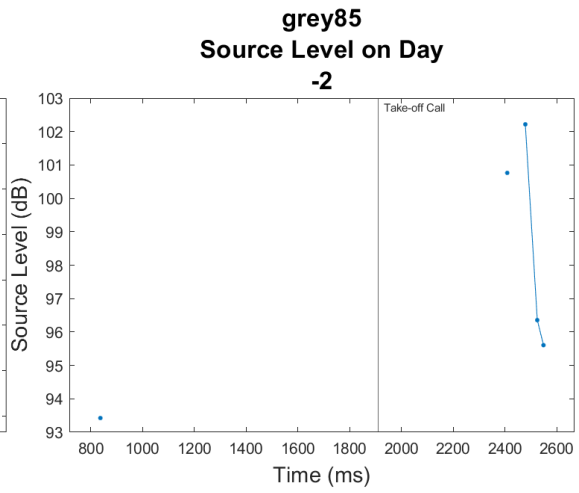
grey85
Source Level on Day
-2
Take-off Call
Source Level (dB)
Time (ms)

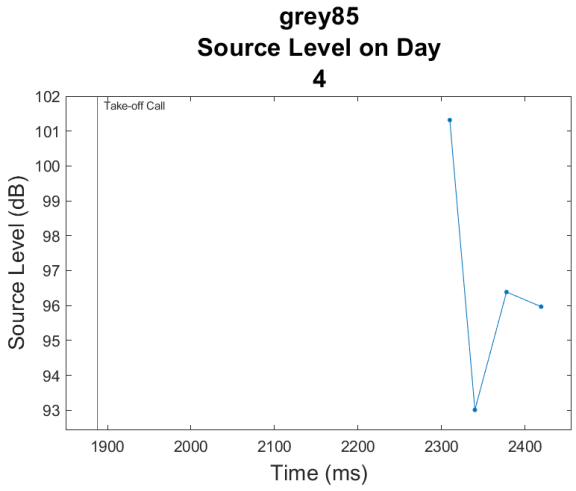
grey85
Source Level on Day
4
Take-off Call
Source Level (dB)
Time (ms)

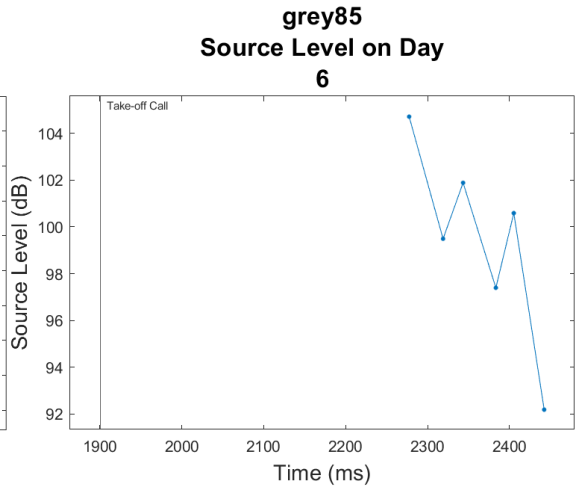
grey85
Source Level on Day
6
Take-off Call
Source Level (dB)
Time (ms)

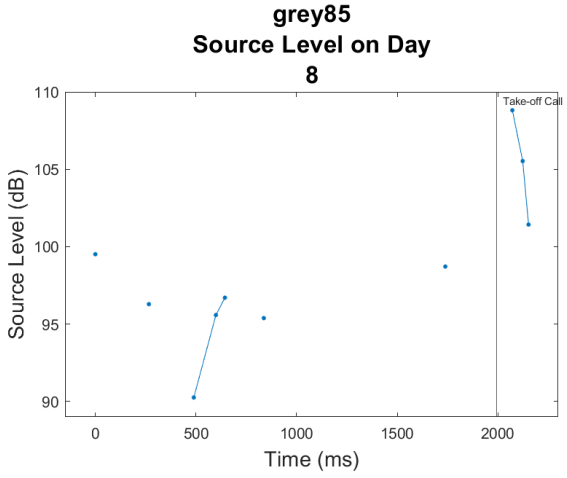
grey85
Source Level on Day
8
Take-off Call
Source Level (dB)
Time (ms)

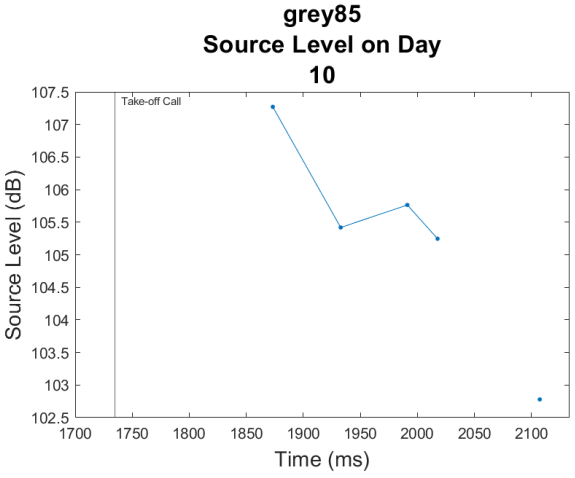
grey85
Source Level on Day
10
Take-off Call
Source Level (dB)
Time (ms)

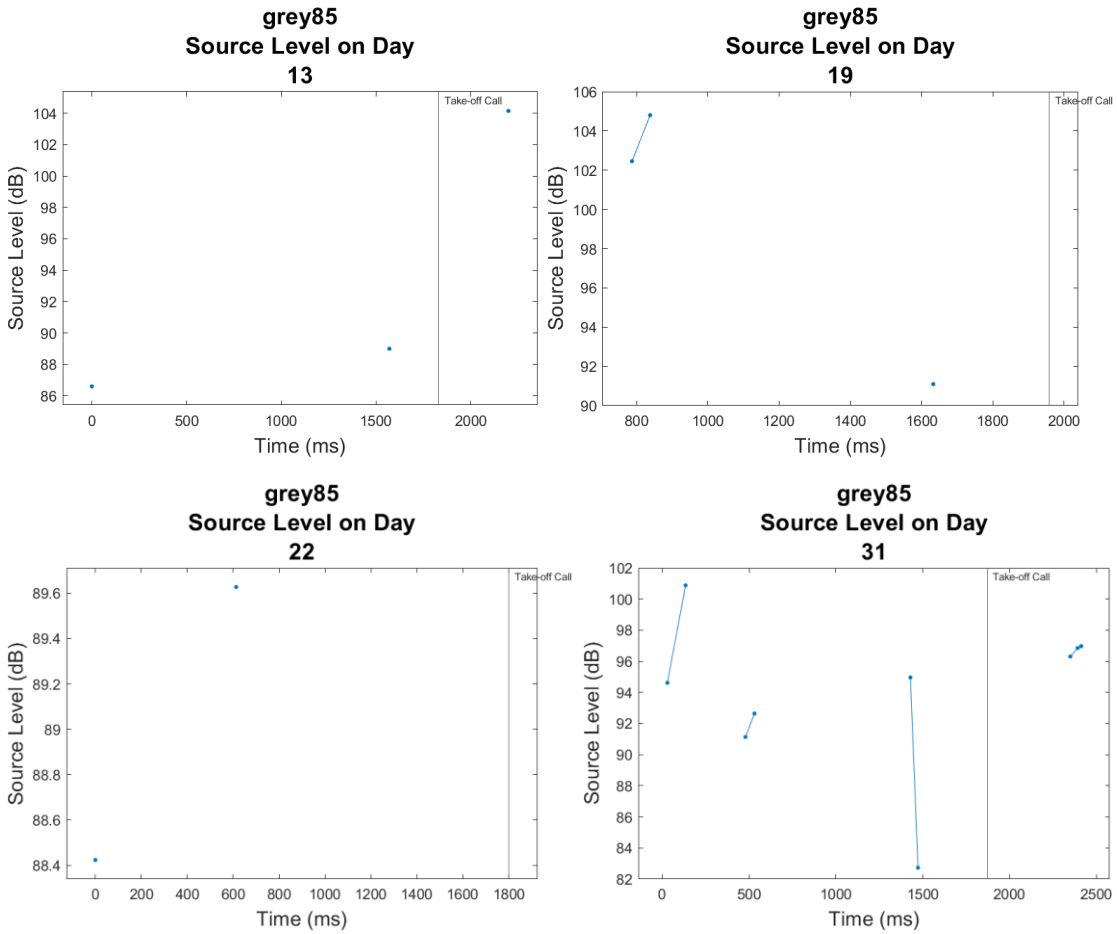

Appendix Figure 28: Grey 85 source level plotted as a function of recording time per day. Each panel shows call durations before and after taking flight, with different panels showing data recorded on different days relative to parturition (number above panel; parturition day defined as Day 0). The take-off call is marked by a vertical line.

Grey 86 Echolocation Call Characteristics Graphs

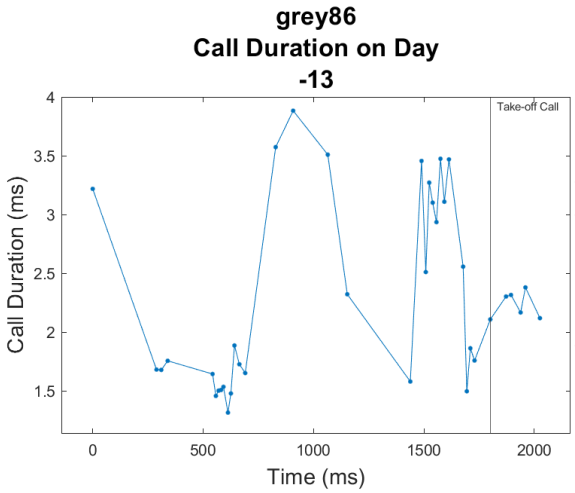

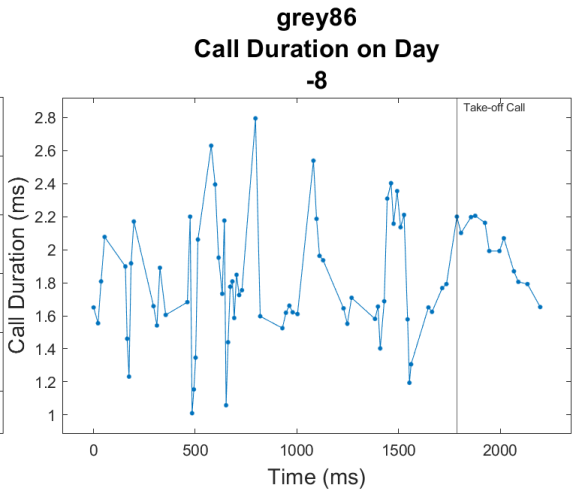

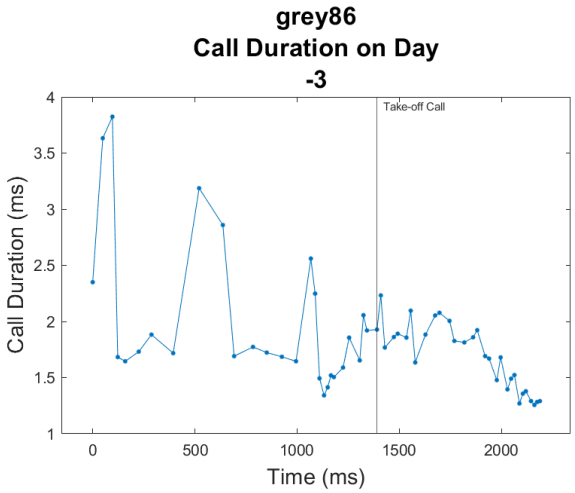

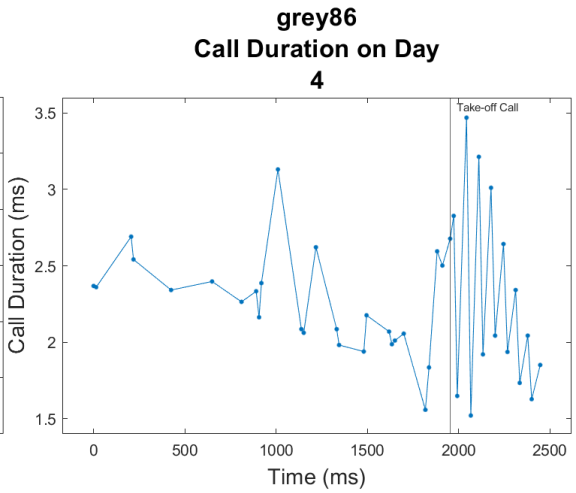

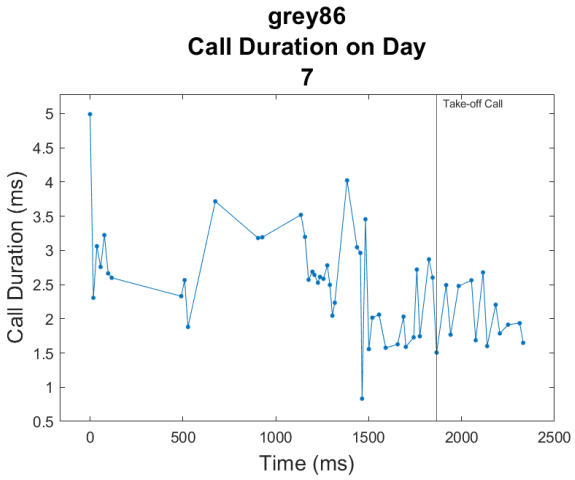

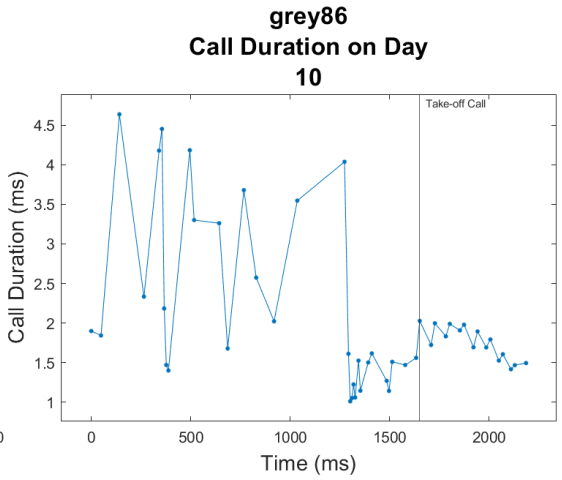

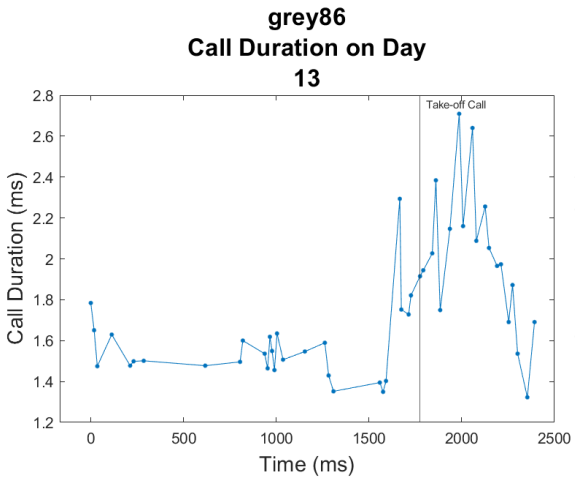
grey86
Call Duration on Day
13
Take-off Call
Call Duration (ms)
Time (ms)

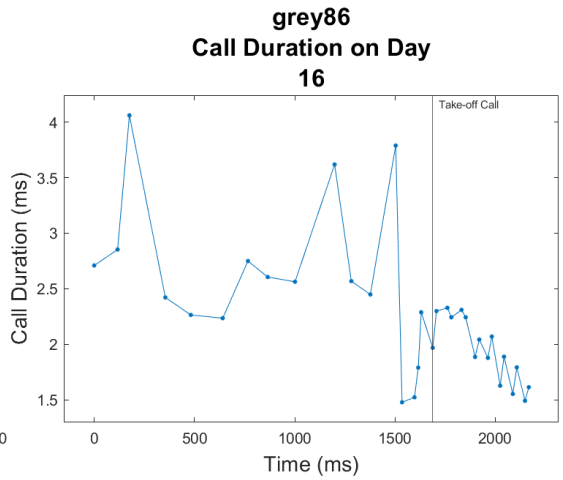
grey86
Call Duration on Day
16
Take-off Call
Call Duration (ms)
Time (ms)

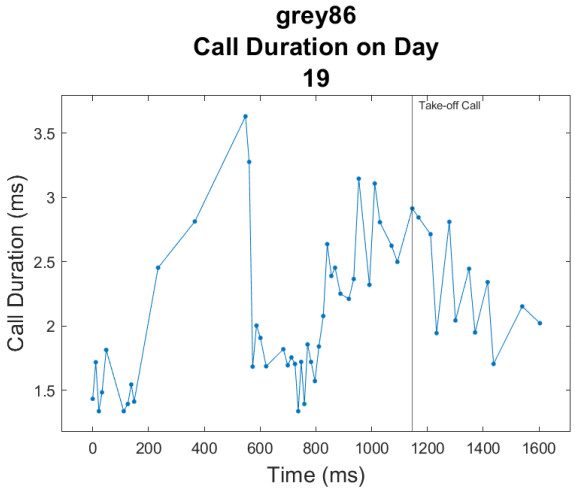
grey86
Call Duration on Day
19
Take-off Call
Call Duration (ms)
Time (ms)

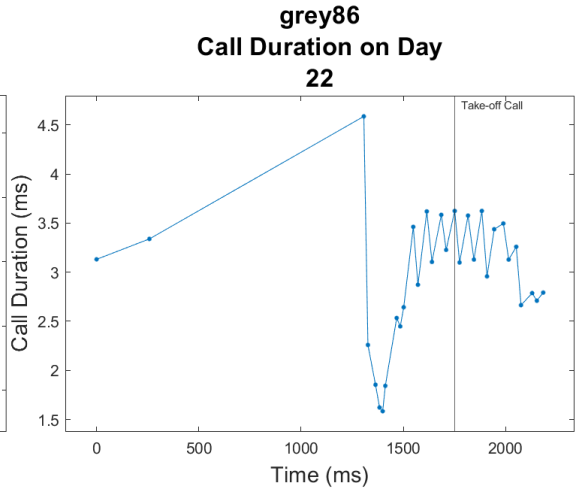
grey86
Call Duration on Day
22
Take-off Call
Call Duration (ms)
Time (ms)

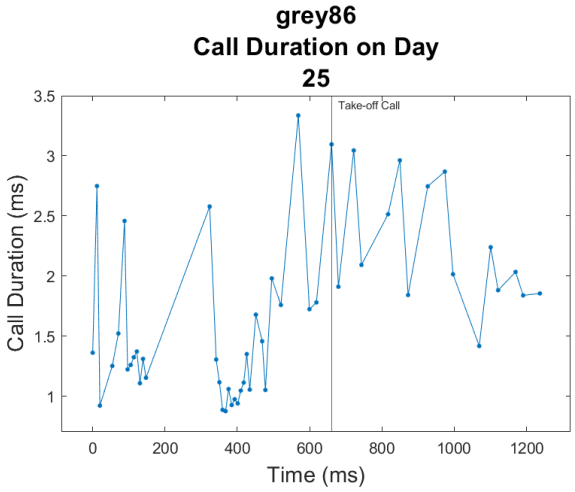
grey86
Call Duration on Day
25
Take-off Call
Call Duration (ms)
Time (ms)

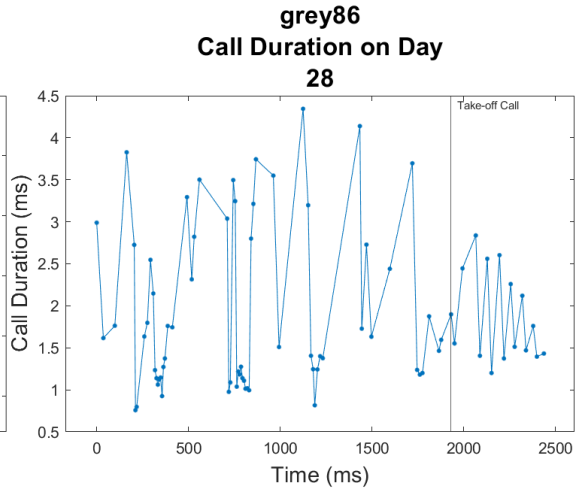
grey86
Call Duration on Day
28
Take-off Call
Call Duration (ms)
Time (ms)

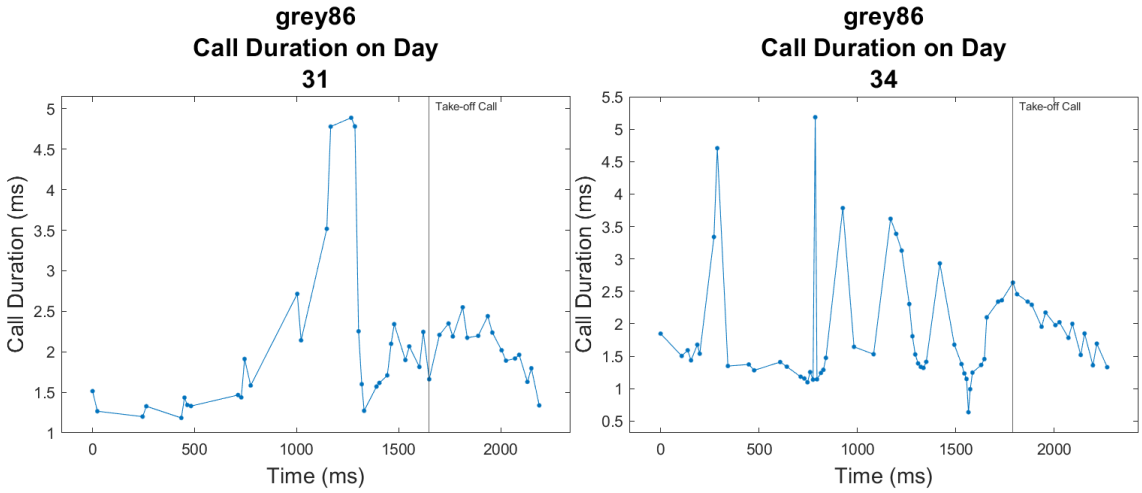

Appendix Figure 29: Grey 86 call duration plotted as a function of recording time per day. Each panel shows call durations before and after taking flight, with different panels showing data recorded on different days relative to parturition (number above panel; parturition day defined as Day 0). The take-off call is marked by a vertical line.

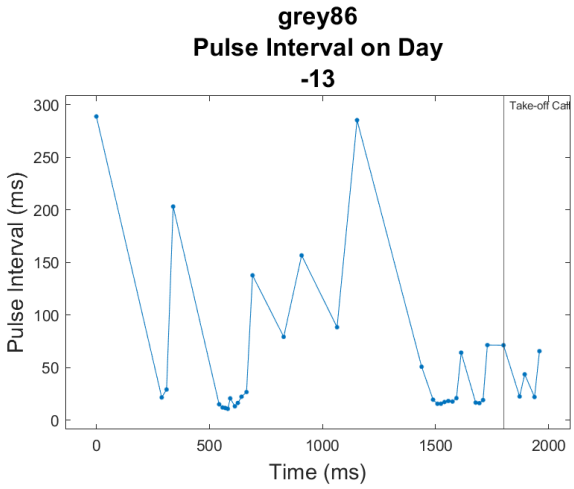
grey86
Pulse Interval on Day
-13
Take-off Call
Pulse Interval (ms)
Time (ms)

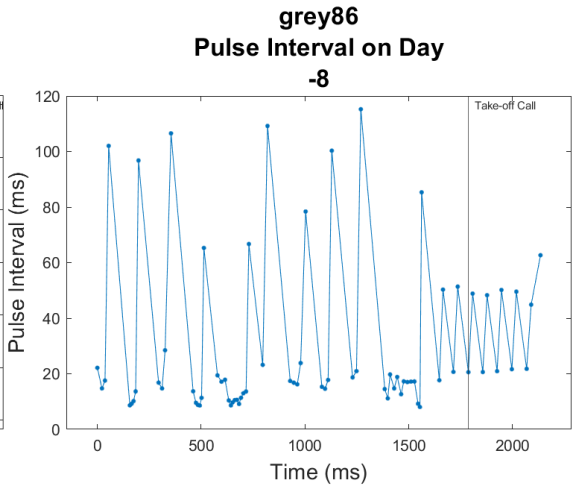
grey86
Pulse Interval on Day
-8
Take-off Call
Pulse Interval (ms)
Time (ms)

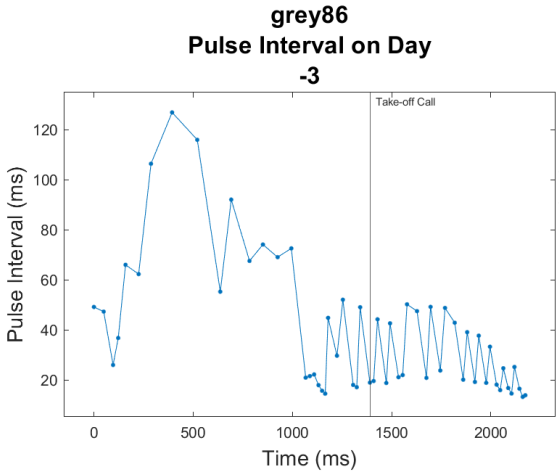
grey86
Pulse Interval on Day
-3
Take-off Call
Pulse Interval (ms)
Time (ms)

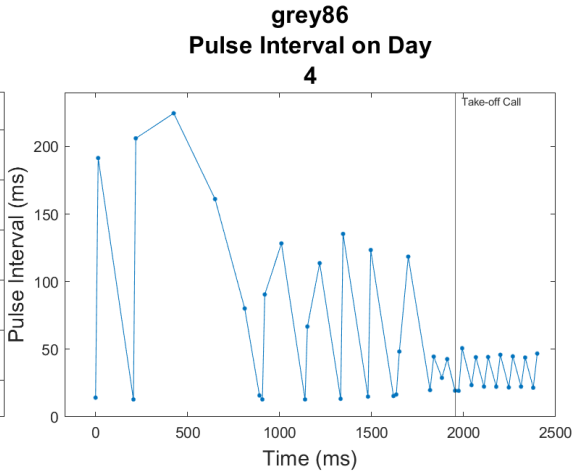
grey86
Pulse Interval on Day
4
Take-off Call
Pulse Interval (ms)
Time (ms)

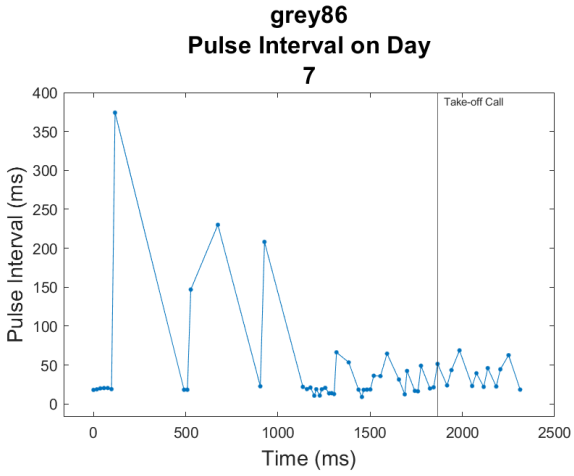
grey86
Pulse Interval on Day
7
Take-off Call
Pulse Interval (ms)
Time (ms)

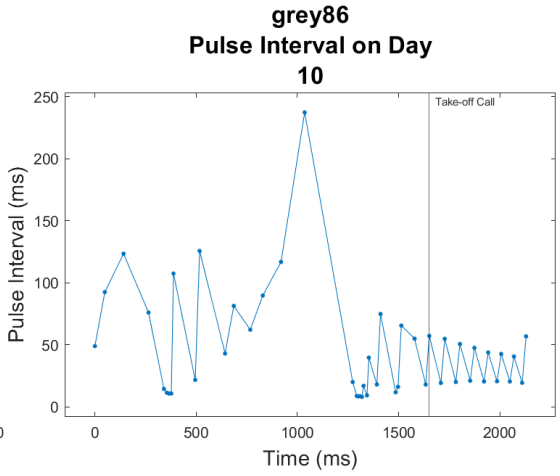
grey86
Pulse Interval on Day
10
Take-off Call
Pulse Interval (ms)
Time (ms)

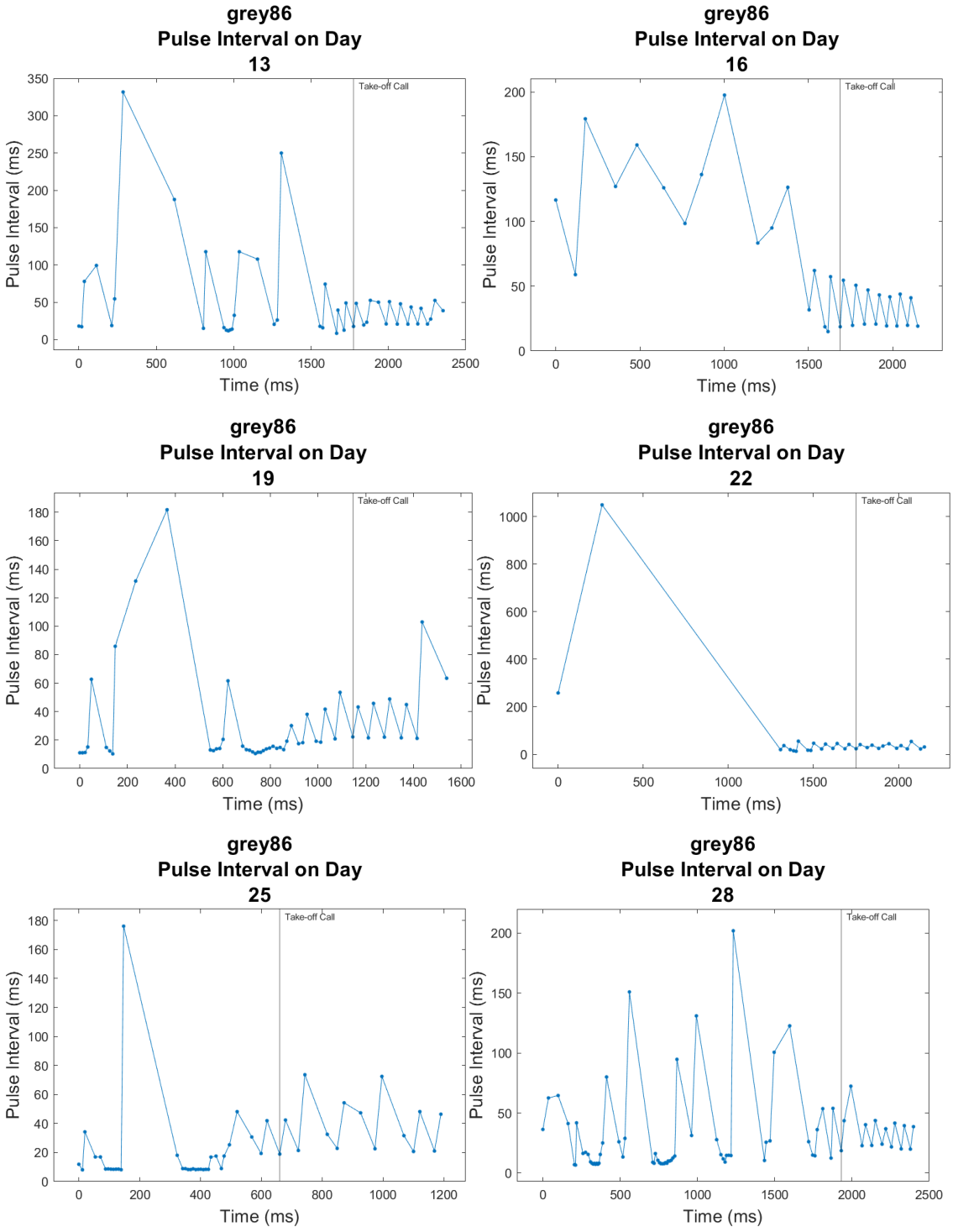
grey86
Pulse Interval on Day
13
Take-off Call
Pulse Interval (ms)
Time (ms)
grey86
Pulse Interval on Day
16
Take-off Call
Pulse Interval (ms)
Time (ms)
grey86
Pulse Interval on Day
19
Take-off Call
Pulse Interval (ms)
Time (ms)
grey86
Pulse Interval on Day
22
Take-off Call
Pulse Interval (ms)
Time (ms)
grey86
Pulse Interval on Day
25
Take-off Call
Pulse Interval (ms)
Time (ms)
grey86
Pulse Interval on Day
28
Take-off Call
Pulse Interval (ms)
Time (ms)

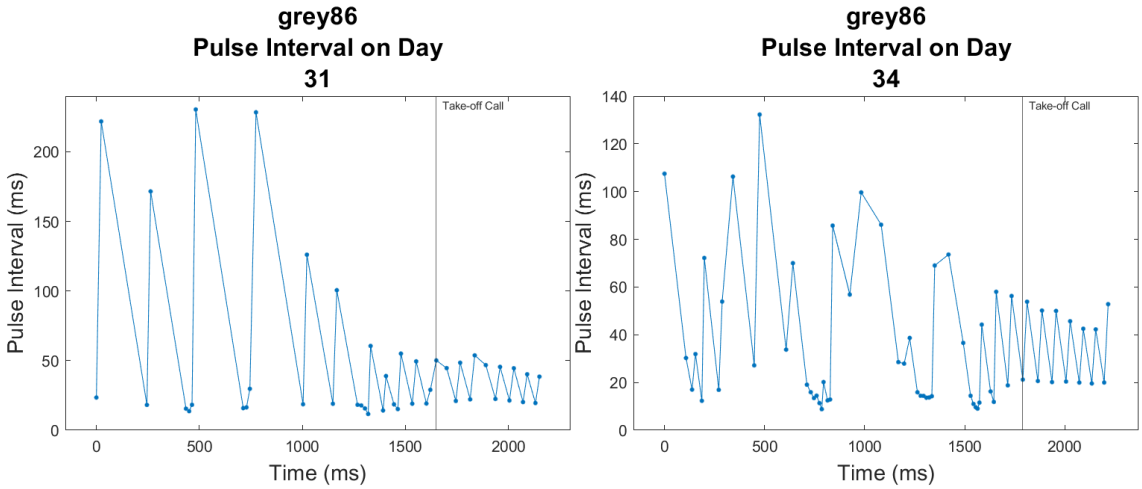

Appendix Figure 30: Grey 86 pulse interval plotted as a function of recording time per day. Each panel shows call durations before and after taking flight, with different panels showing data recorded on different days relative to parturition (number above panel; parturition day defined as Day 0). The take-off call is marked by a vertical line..

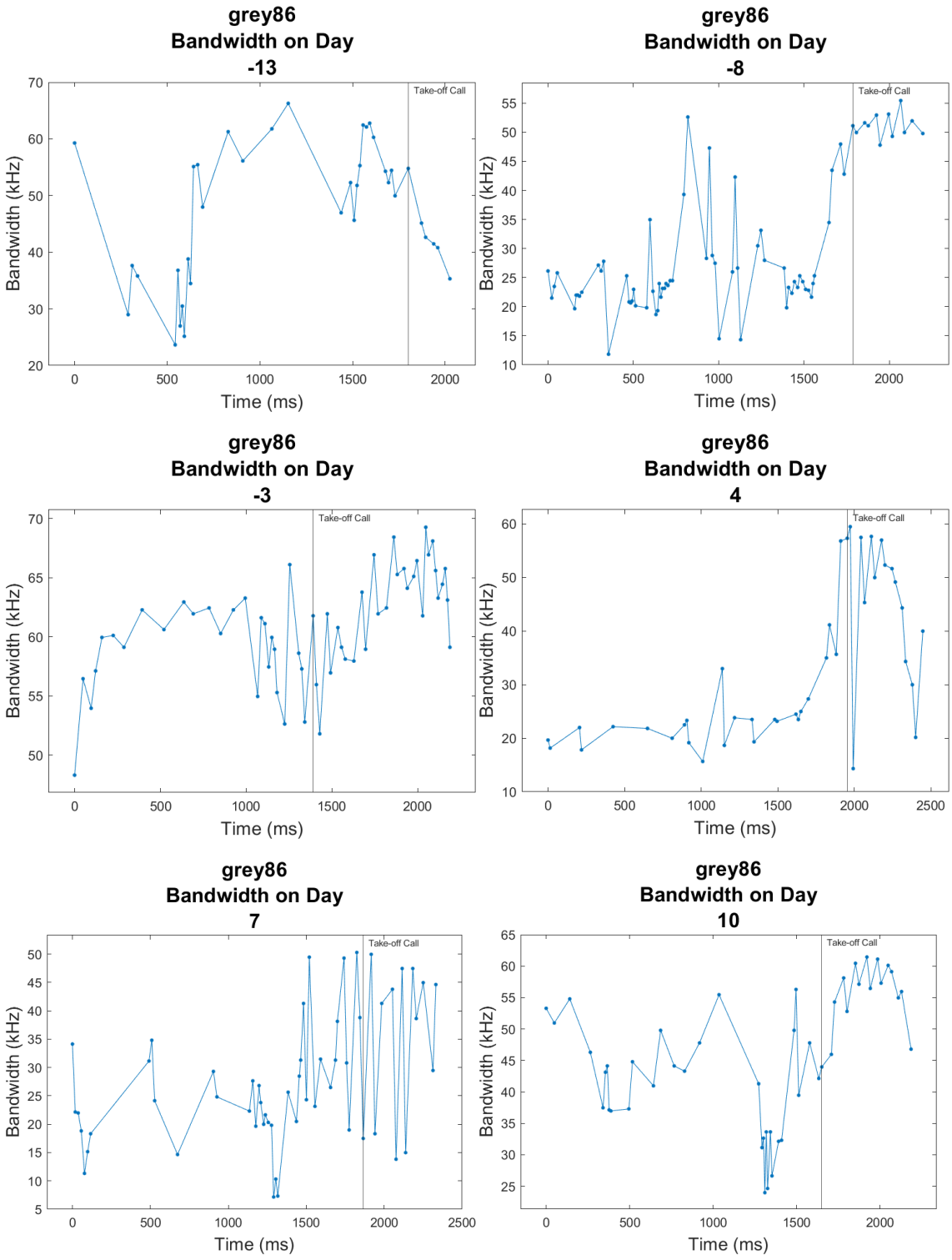
grey86
Bandwidth on Day
-13
Take-off Call
Bandwidth (kHz)
Time (ms)
grey86
Bandwidth on Day
-8
Take-off Call
Bandwidth (kHz)
Time (ms)
grey86
Bandwidth on Day
-3
Take-off Call
Bandwidth (kHz)
Time (ms)
grey86
Bandwidth on Day
4
Take-off Call
Bandwidth (kHz)
Time (ms)
grey86
Bandwidth on Day
7
Take-off Call
Bandwidth (kHz)
Time (ms)
grey86
Bandwidth on Day
10
Take-off Call
Bandwidth (kHz)
Time (ms)

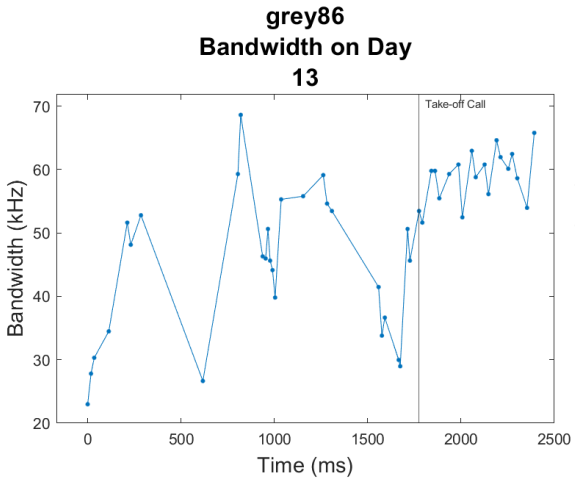
grey86
Bandwidth on Day
13
Take-off Call
Bandwidth (kHz)
Time (ms)

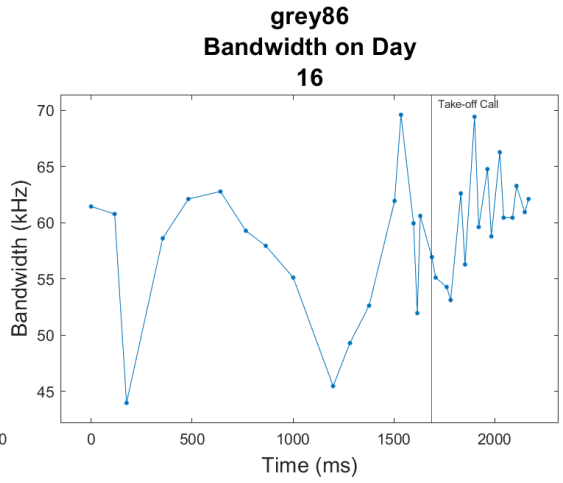
grey86
Bandwidth on Day
16
Take-off Call
Bandwidth (kHz)
Time (ms)

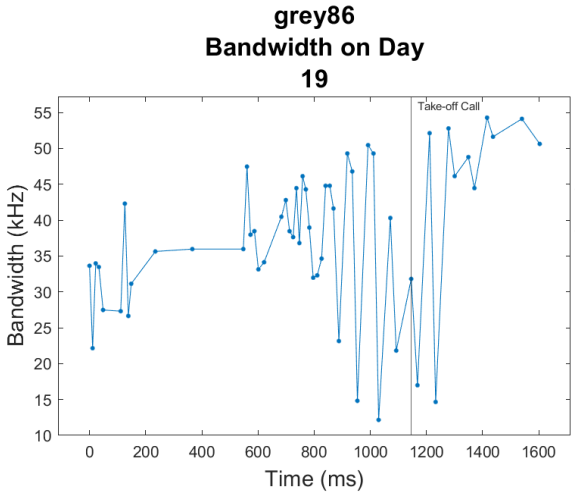
grey86
Bandwidth on Day
19
Take-off Call
Bandwidth (kHz)
Time (ms)

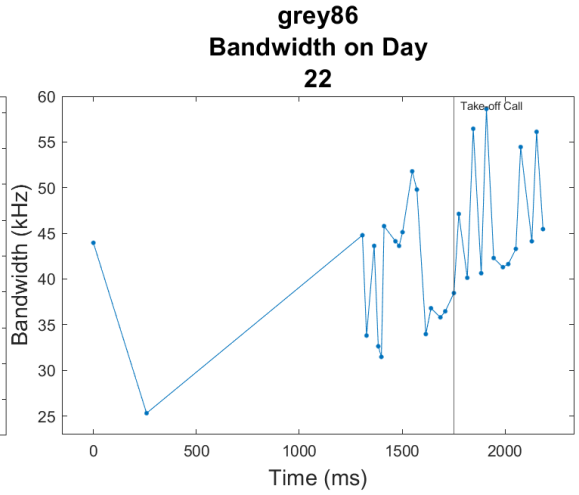
grey86
Bandwidth on Day
22
Take-off Call
Bandwidth (kHz)
Time (ms)

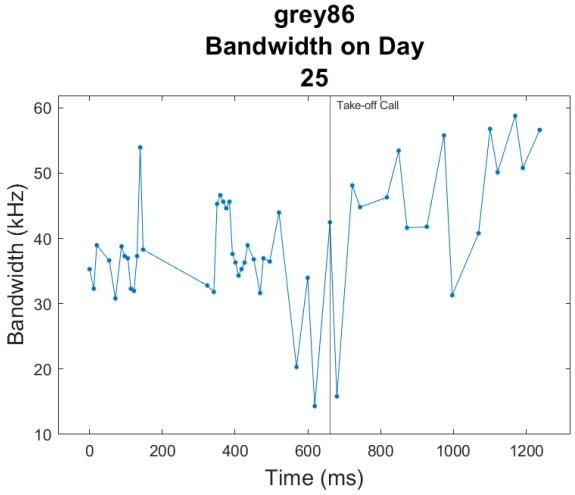
grey86
Bandwidth on Day
25
Take-off Call
Bandwidth (kHz)
Time (ms)

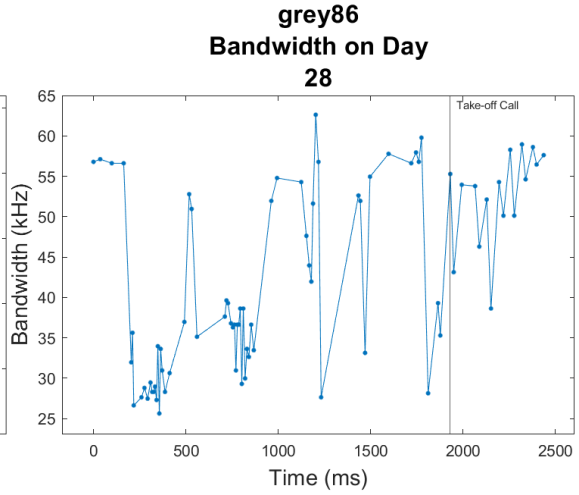
grey86
Bandwidth on Day
28
Take-off Call
Bandwidth (kHz)
Time (ms)

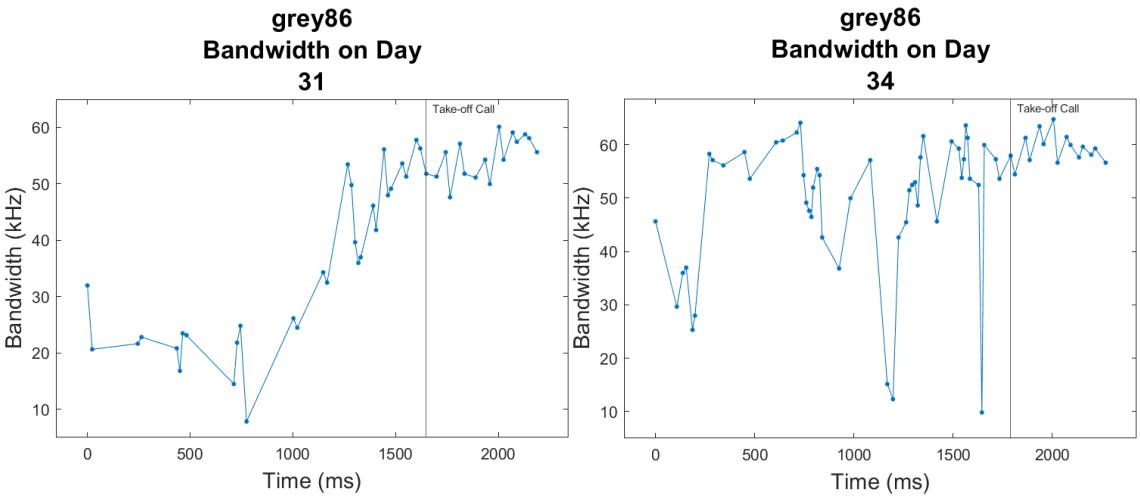

Appendix Figure 31: Grey 86 call bandwidth plotted as a function of recording time per day. Each panel shows call durations before and after taking flight, with different panels showing data recorded on different days relative to parturition (number above panel; parturition day defined as Day 0). The take-off call is marked by a vertical line..

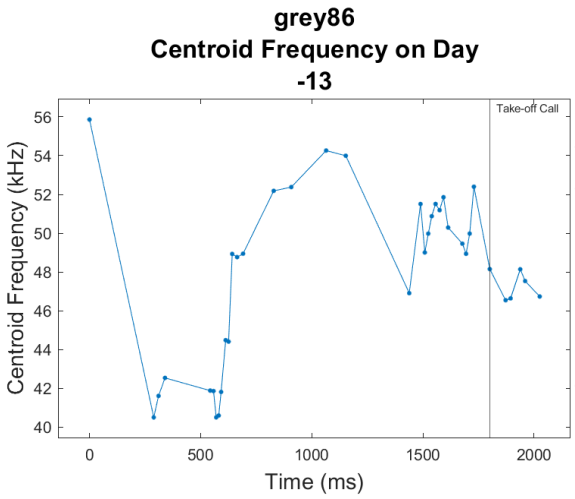
grey86
Centroid Frequency on Day
-13
Take-off Call
Centroid Frequency (kHz)
Time (ms)

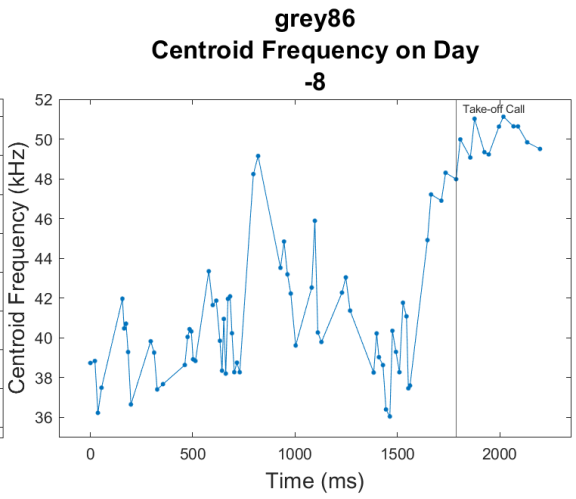
grey86
Centroid Frequency on Day
-8
Take-off Call
Centroid Frequency (kHz)
Time (ms)

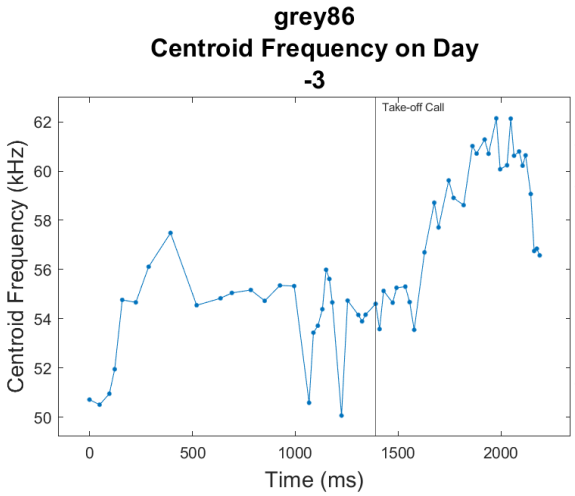
grey86
Centroid Frequency on Day
-3
Take-off Call
Centroid Frequency (kHz)
Time (ms)

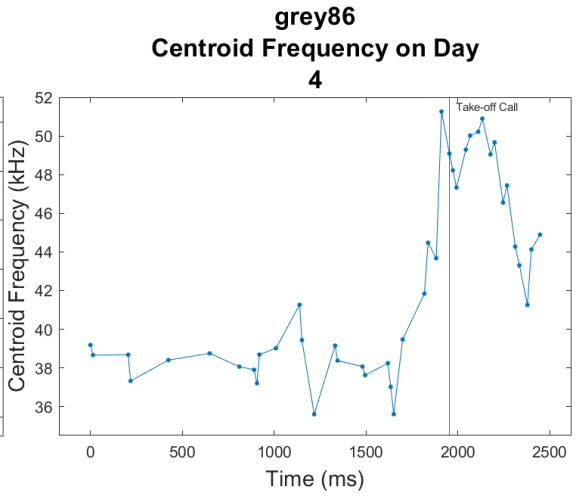
grey86
Centroid Frequency on Day
4
Take-off Call
Centroid Frequency (kHz)
Time (ms)

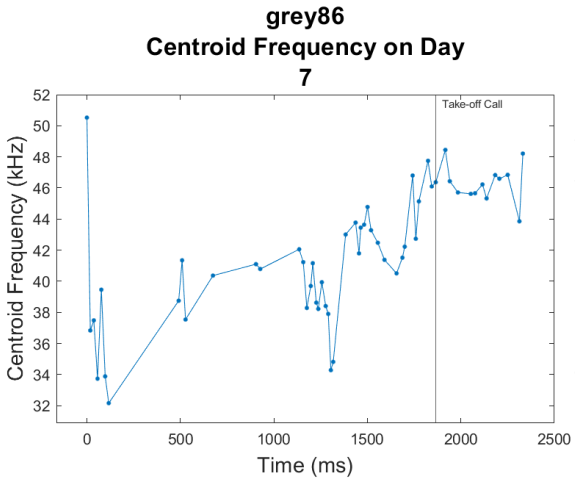
grey86
Centroid Frequency on Day
7
Take-off Call
Centroid Frequency (kHz)
Time (ms)

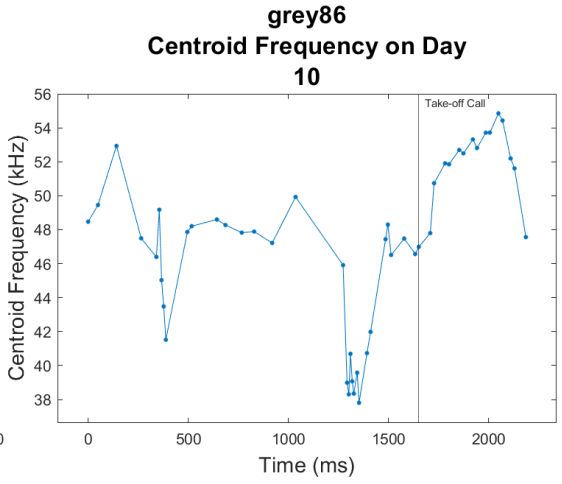
grey86
Centroid Frequency on Day
10
Take-off Call
Centroid Frequency (kHz)
Time (ms)

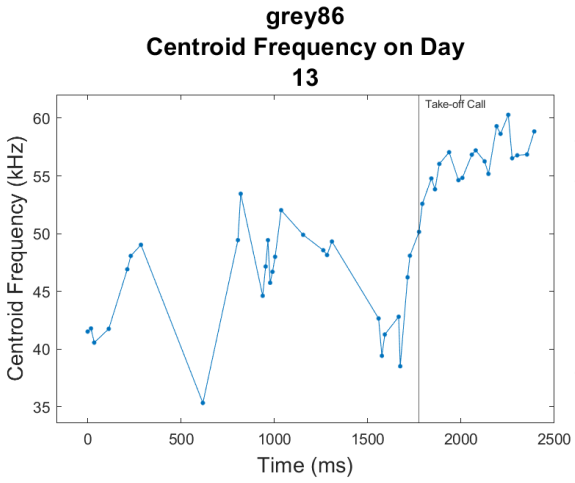
grey86
Centroid Frequency on Day
13
Take-off Call
Centroid Frequency (kHz)
Time (ms)

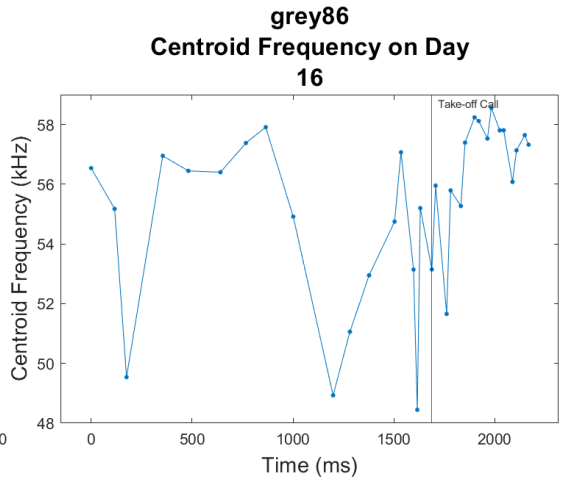
grey86
Centroid Frequency on Day
16
Take-off Call
Centroid Frequency (kHz)
Time (ms)

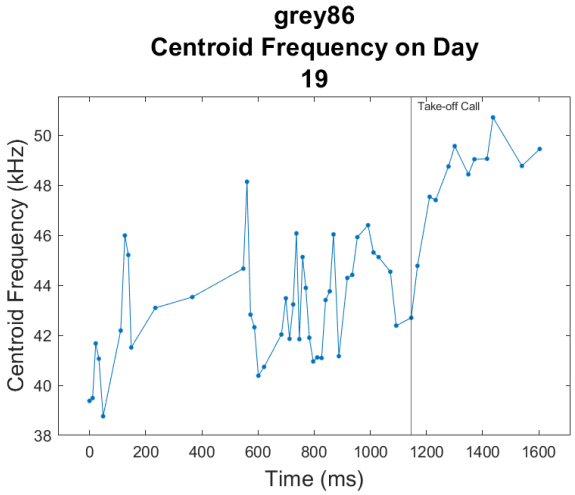
grey86
Centroid Frequency on Day
19
Take-off Call
Centroid Frequency (kHz)
Time (ms)

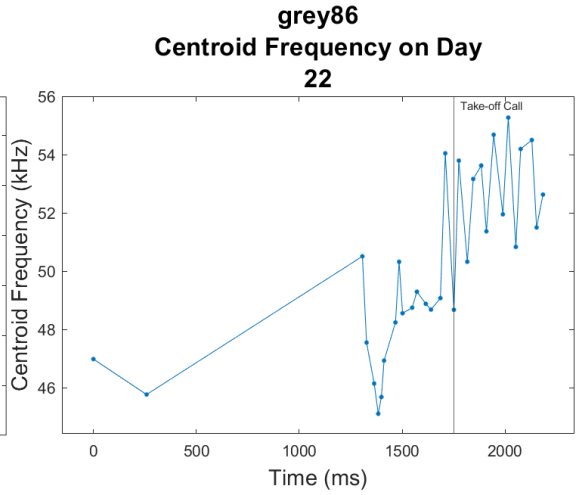
grey86
Centroid Frequency on Day
22
Take-off Call
Centroid Frequency (kHz)
Time (ms)

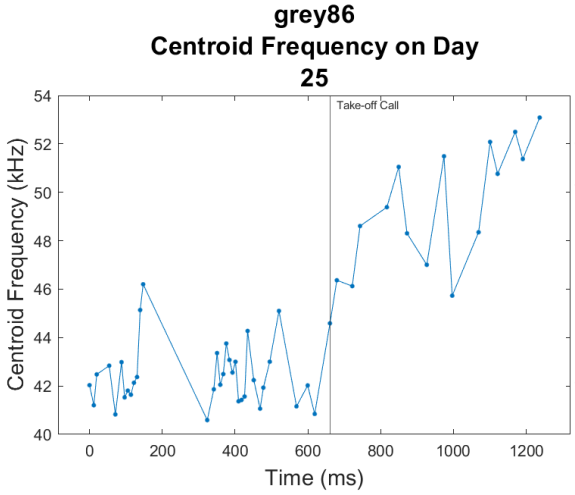
grey86
Centroid Frequency on Day
25
Take-off Call
Centroid Frequency (kHz)
Time (ms)

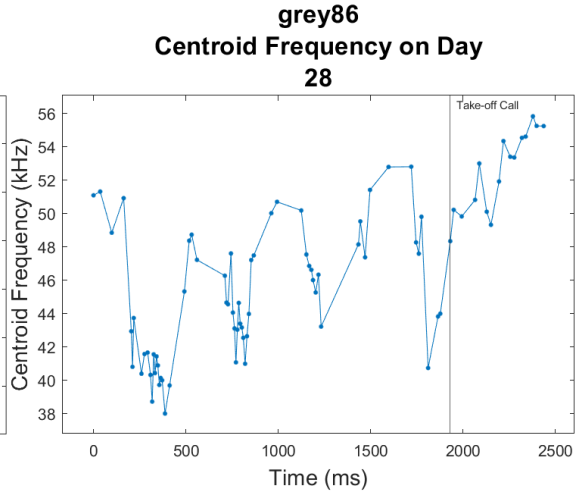
grey86
Centroid Frequency on Day
28
Take-off Call
Centroid Frequency (kHz)
Time (ms)

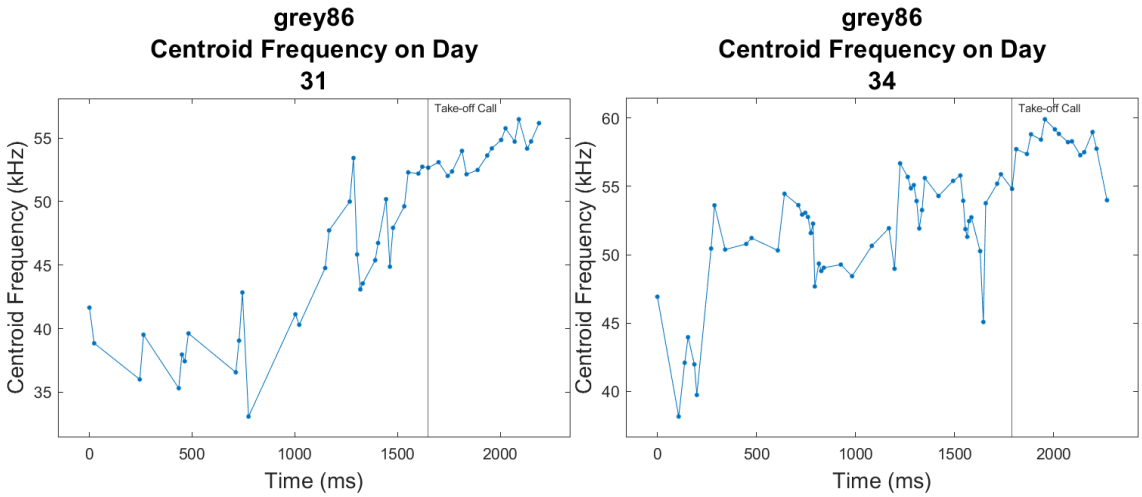

Appendix Figure 32: Grey 86 centroid frequency plotted as a function of recording time per day. Each panel shows call durations before and after taking flight, with different panels showing data recorded on different days relative to parturition (number above panel; parturition day defined as Day 0). The take-off call is marked by a vertical line.

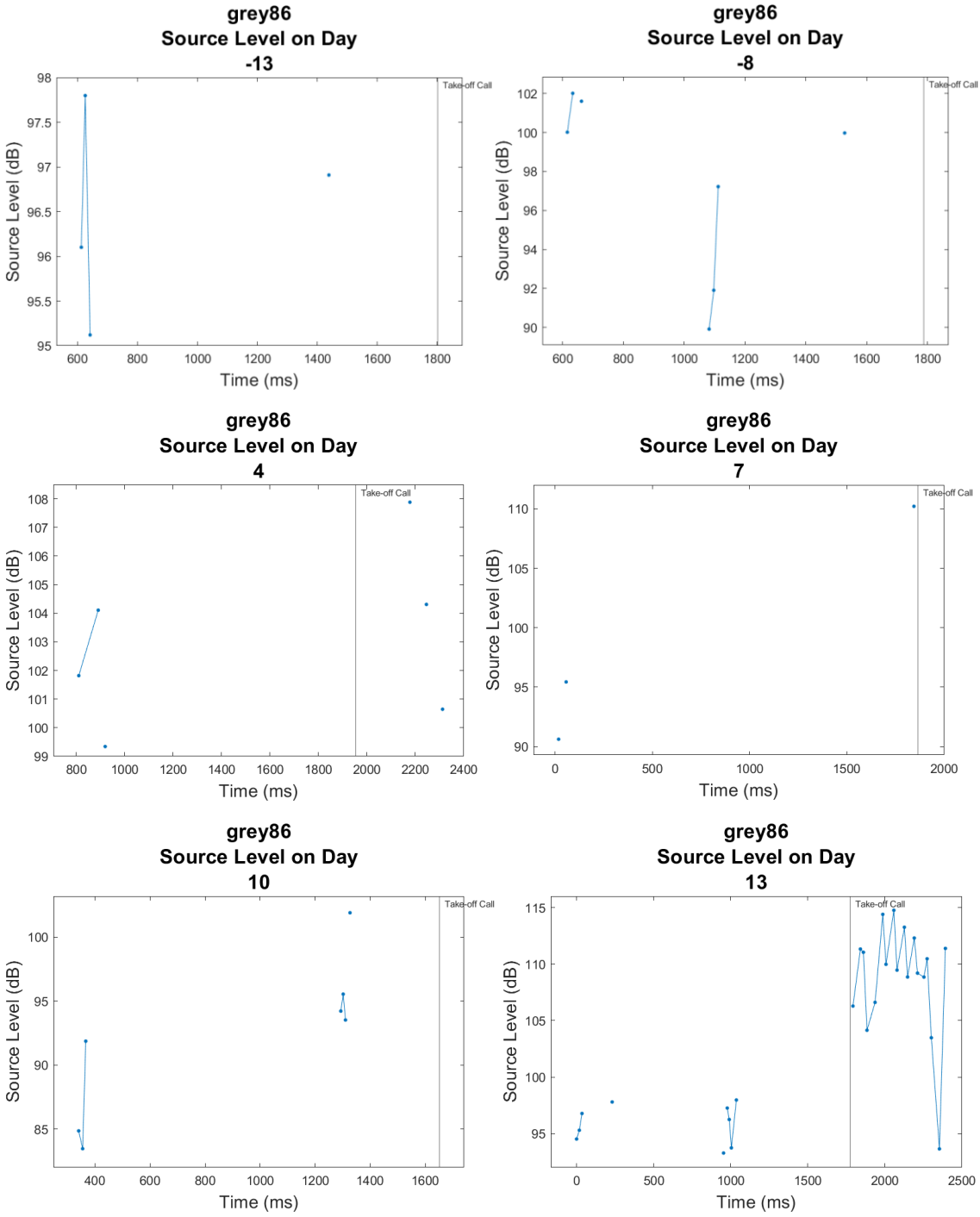
grey86
Source Level on Day
-13
Take-off Call
Source Level (dB)
Time (ms)
grey86
Source Level on Day
-8
Take-off Call
Source Level (dB)
Time (ms)
grey86
Source Level on Day
4
Take-off Call
Source Level (dB)
Time (ms)
grey86
Source Level on Day
7
Take-off Call
Source Level (dB)
Time (ms)
grey86
Source Level on Day
10
Take-off Call
Source Level (dB)
Time (ms)
grey86
Source Level on Day
13
Take-off Call
Source Level (dB)
Time (ms)

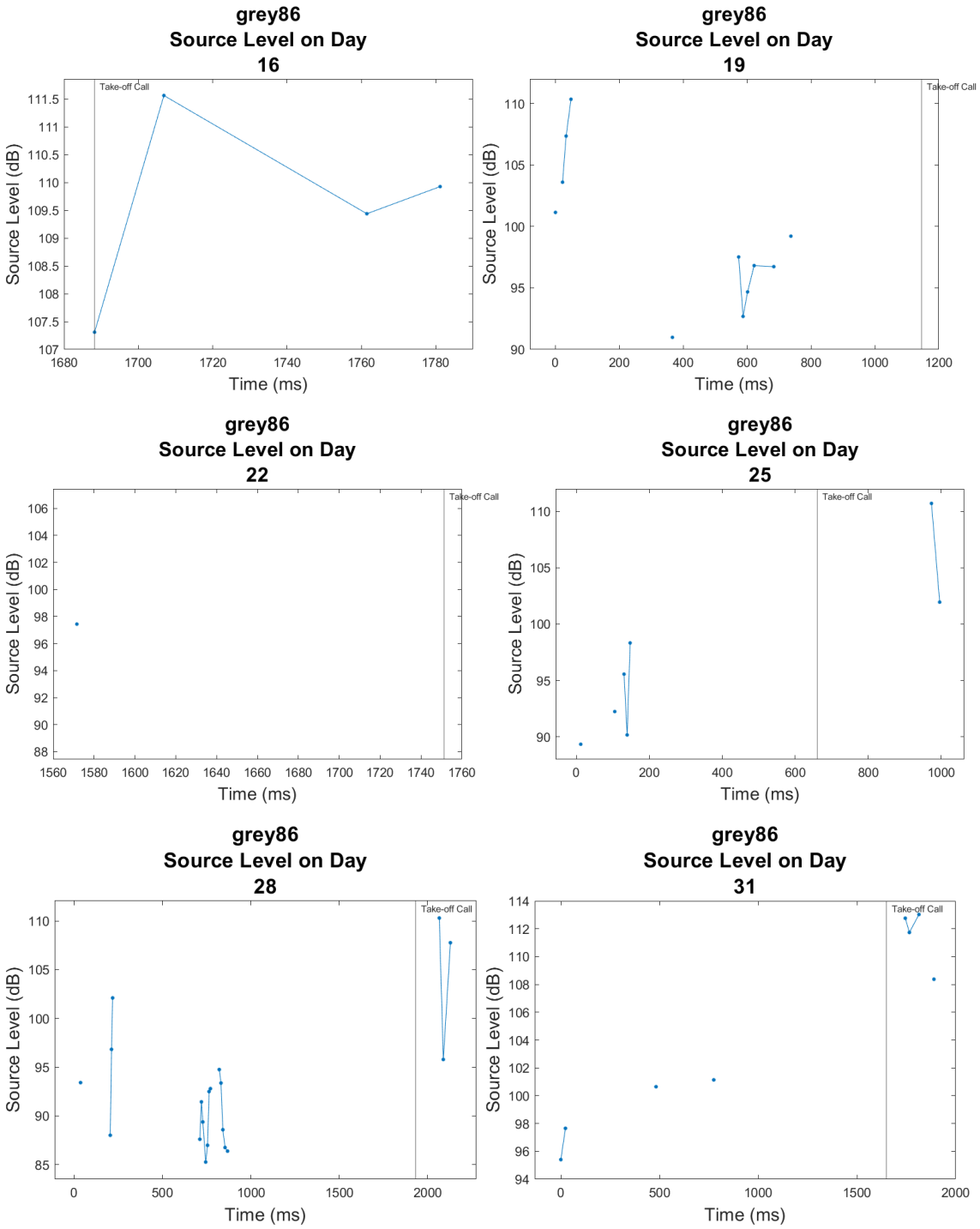
grey86
Source Level on Day
16
Take-off Call
Source Level (dB)
Time (ms)
grey86
Source Level on Day
19
Take-off Call
Source Level (dB)
Time (ms)
grey86
Source Level on Day
22
Take-off Call
Source Level (dB)
Time (ms)
grey86
Source Level on Day
25
Take-off Call
Source Level (dB)
Time (ms)
grey86
Source Level on Day
28
Take-off Call
Source Level (dB)
Time (ms)
grey86
Source Level on Day
31
Take-off Call
Source Level (dB)
Time (ms)

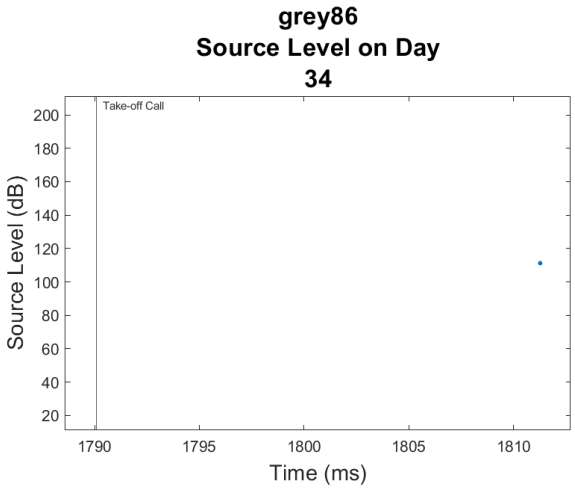

Appendix Figure 33: Grey 86 source level plotted as a function of recording time per day. Each panel shows call durations before and after taking flight, with different panels showing data recorded on different days relative to parturition (number above panel; parturition day defined as Day 0). The take-off call is marked by a vertical line.

Grey 87 Echolocation Call Characteristics Graphs

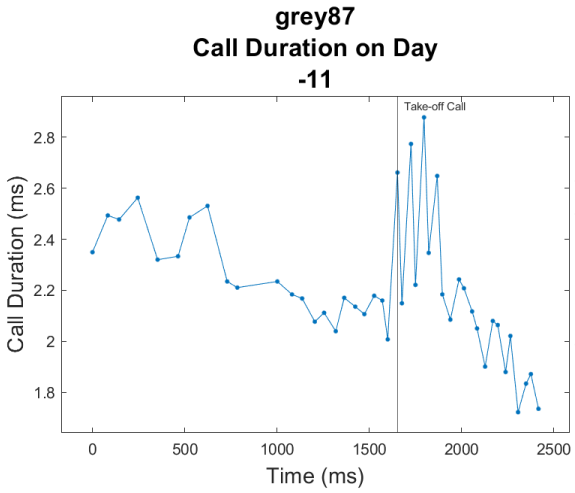

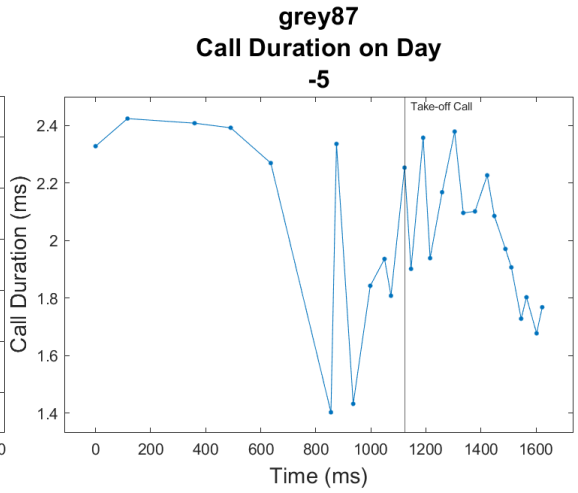

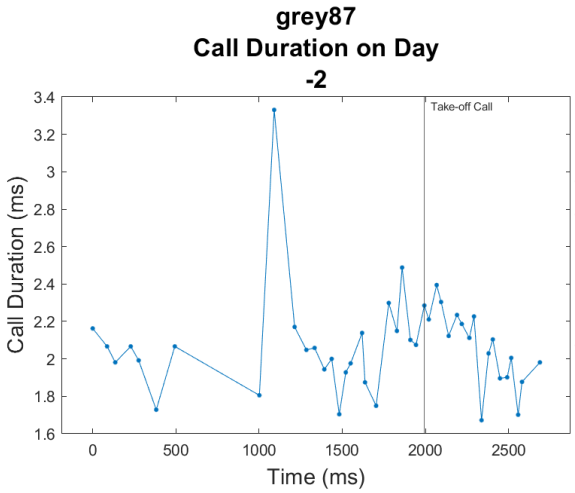

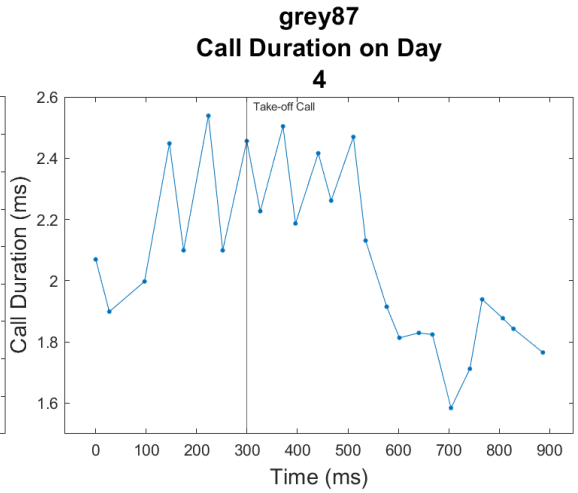

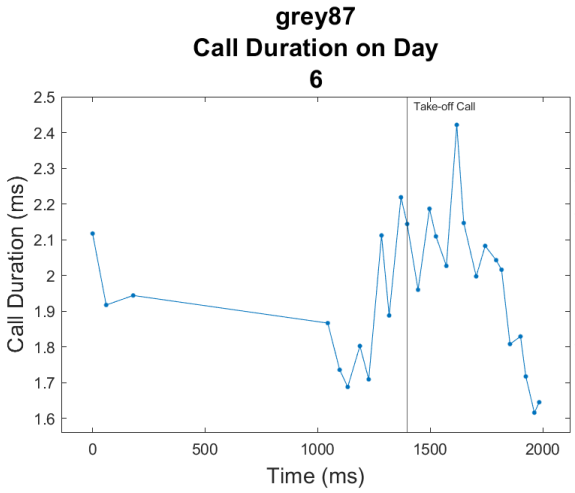

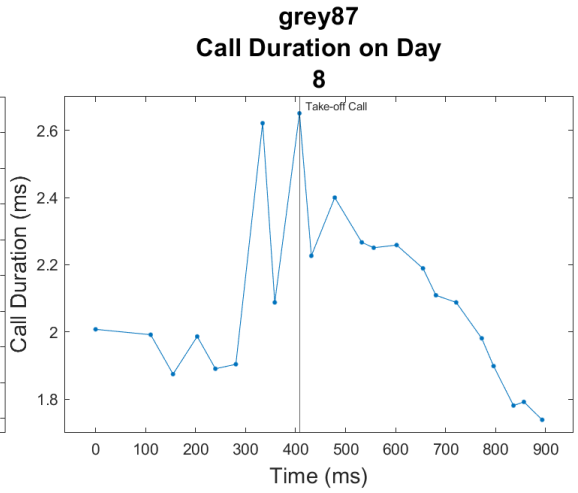

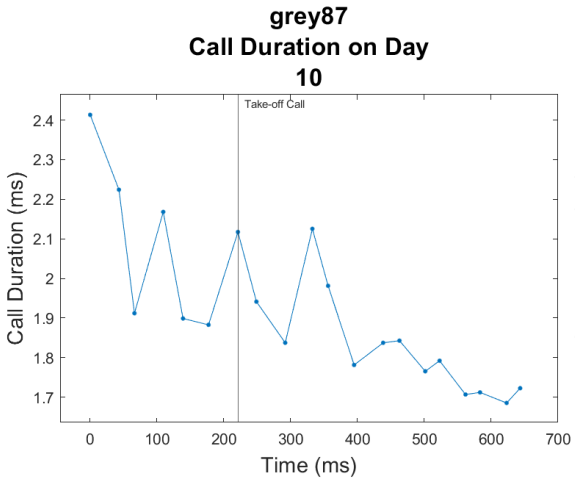
grey87
Call Duration on Day
10
Take-off Call
Call Duration (ms)
Time (ms)

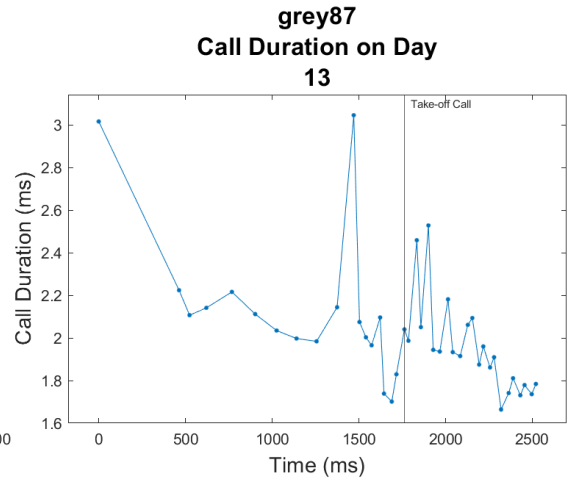
grey87
Call Duration on Day
13
Take-off Call
Call Duration (ms)
Time (ms)

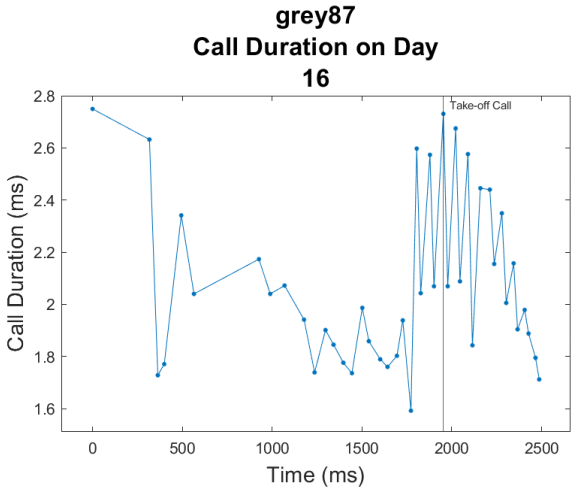
grey87
Call Duration on Day
16
Take-off Call
Call Duration (ms)
Time (ms)

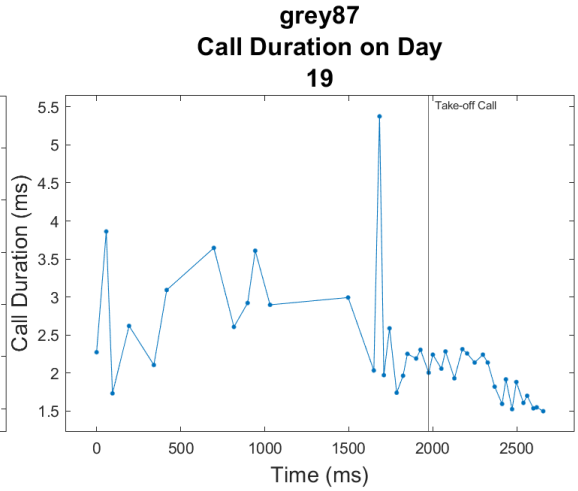
grey87
Call Duration on Day
19
Take-off Call
Call Duration (ms)
Time (ms)

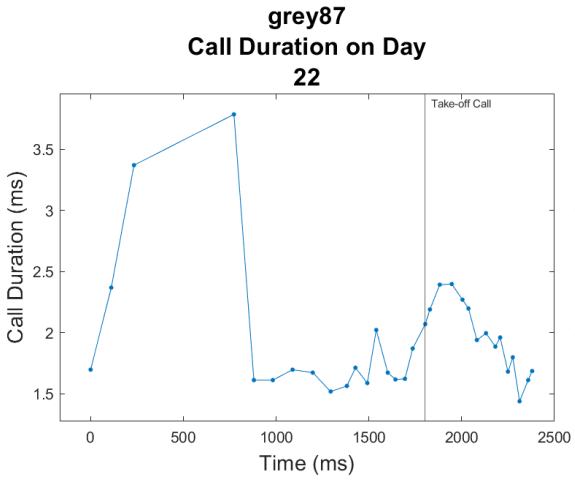
grey87
Call Duration on Day
22
Take-off Call
Call Duration (ms)
Time (ms)

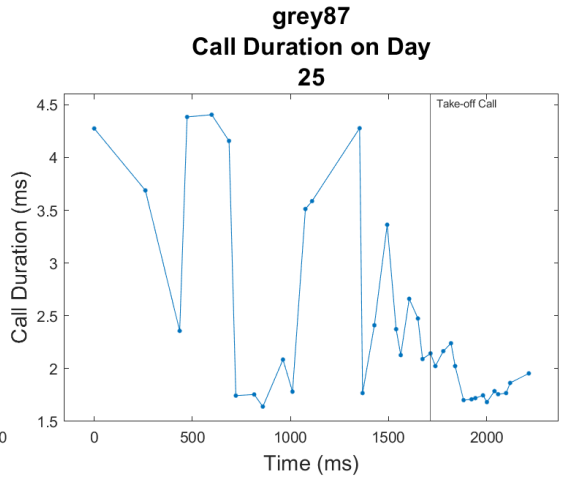
grey87
Call Duration on Day
25
Take-off Call
Call Duration (ms)
Time (ms)

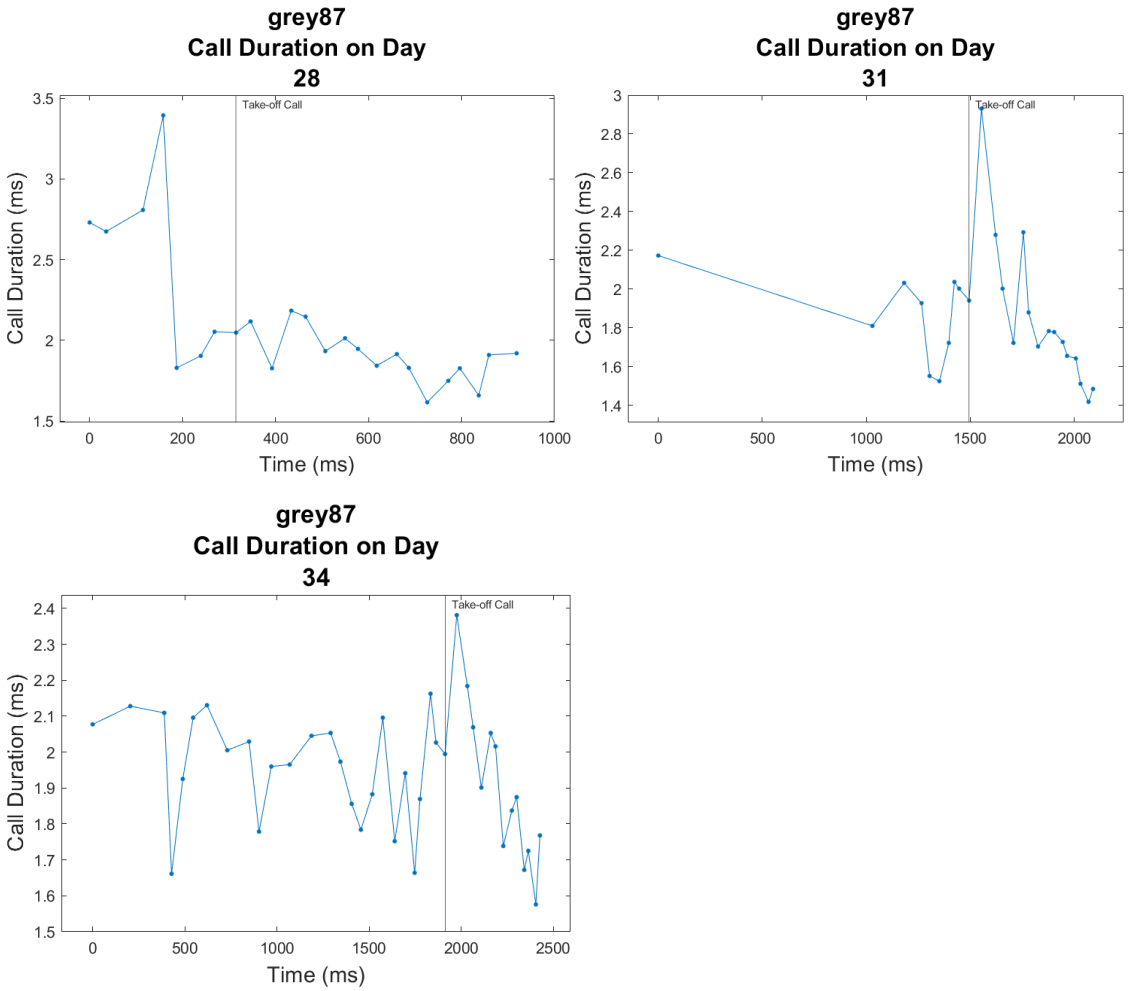

Appendix Figure 34: Grey 87 call duration plotted as a function of recording time per day. Each panel shows call durations before and after taking flight, with different panels showing data recorded on different days relative to parturition (number above panel; parturition day defined as Day 0). The take-off call is marked by a vertical line.

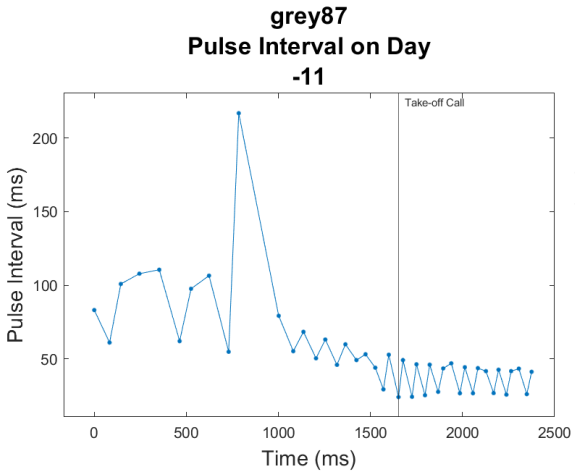
grey87
Pulse Interval on Day
-11
Take-off Call
Pulse Interval (ms)
Time (ms)

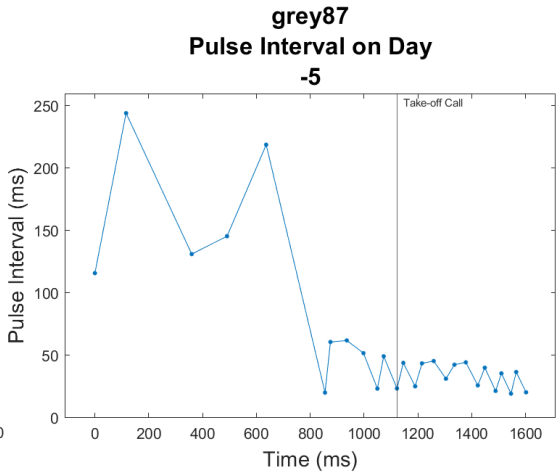
grey87
Pulse Interval on Day
-5
Take-off Call
Pulse Interval (ms)
Time (ms)

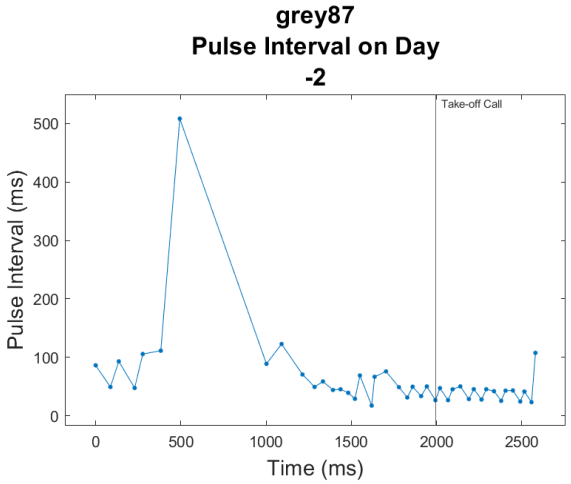
grey87
Pulse Interval on Day
-2
Take-off Call
Pulse Interval (ms)
Time (ms)

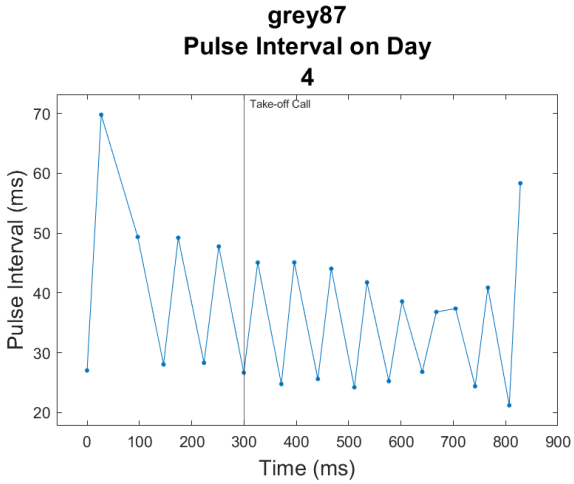
grey87
Pulse Interval on Day
4
Take-off Call
Pulse Interval (ms)
Time (ms)

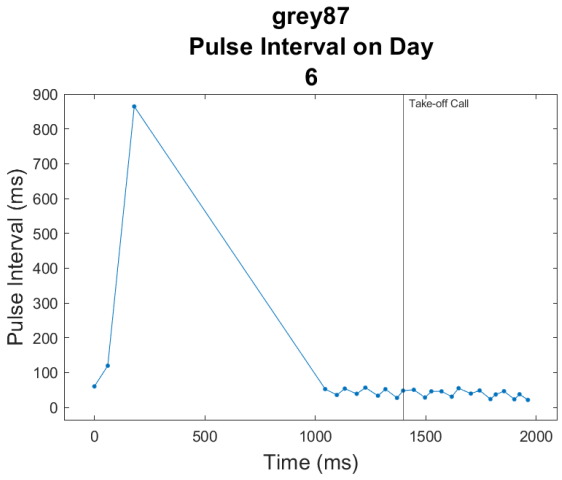
grey87
Pulse Interval on Day
6
Take-off Call
Pulse Interval (ms)
Time (ms)

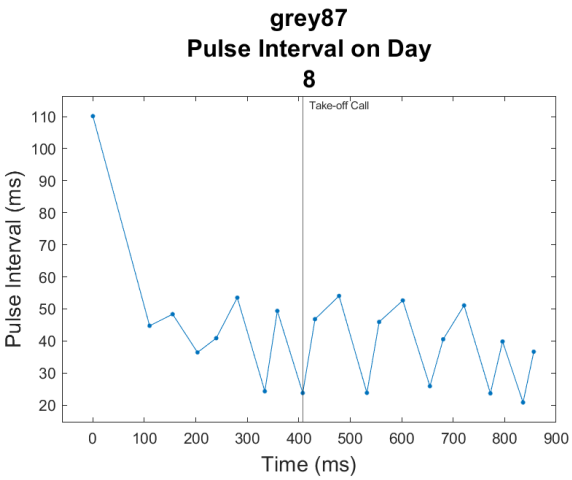
grey87
Pulse Interval on Day
8
Take-off Call
Pulse Interval (ms)
Time (ms)

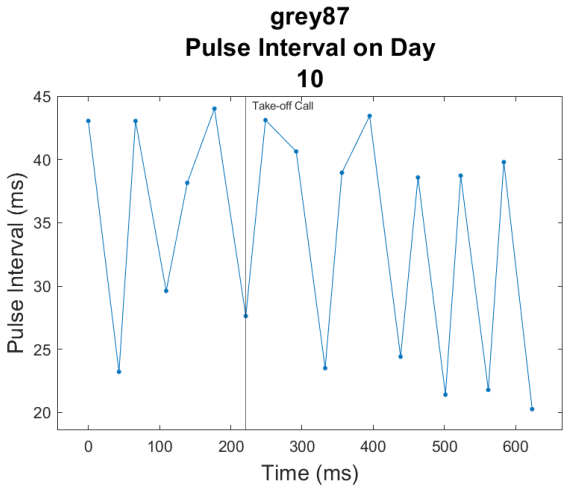
grey87
Pulse Interval on Day
10
Take-off Call
Pulse Interval (ms)
Time (ms)

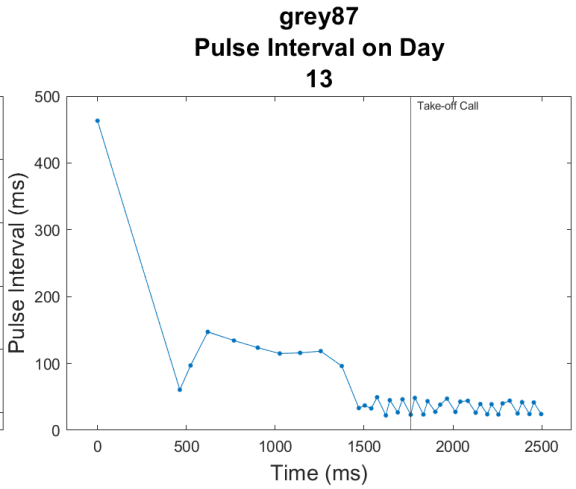
grey87
Pulse Interval on Day
13
Take-off Call
Pulse Interval (ms)
Time (ms)

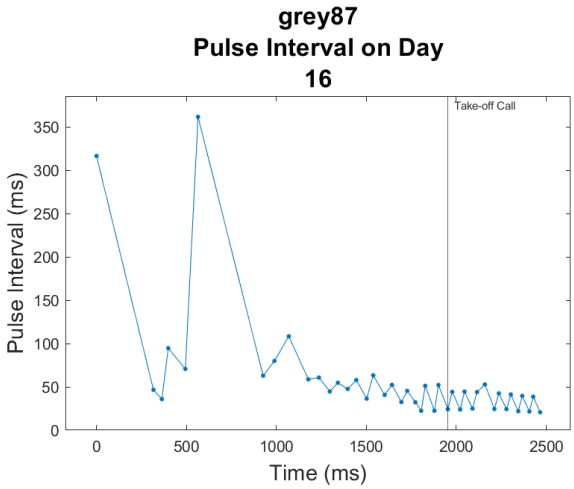
grey87
Pulse Interval on Day
16
Take-off Call
Pulse Interval (ms)
Time (ms)

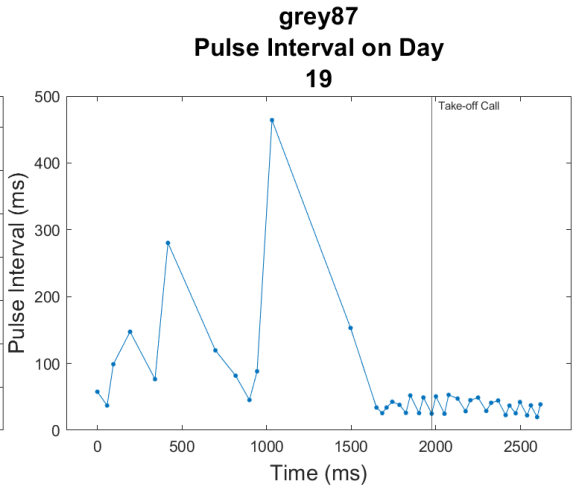
grey87
Pulse Interval on Day
19
Take-off Call
Pulse Interval (ms)
Time (ms)

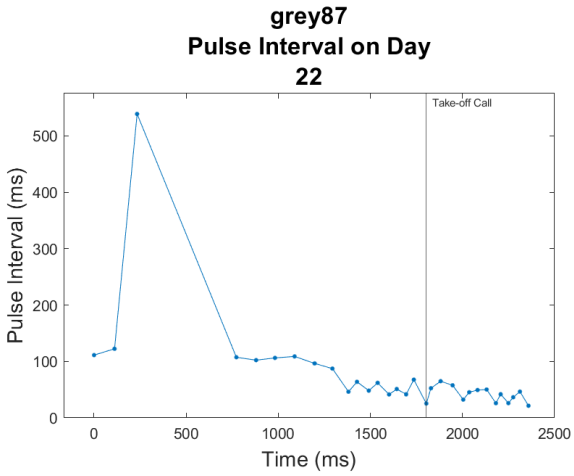
grey87
Pulse Interval on Day
22
Take-off Call
Pulse Interval (ms)
Time (ms)

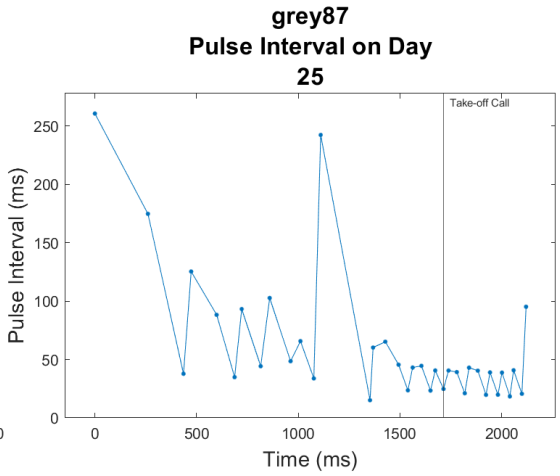
grey87
Pulse Interval on Day
25
Take-off Call
Pulse Interval (ms)
Time (ms)

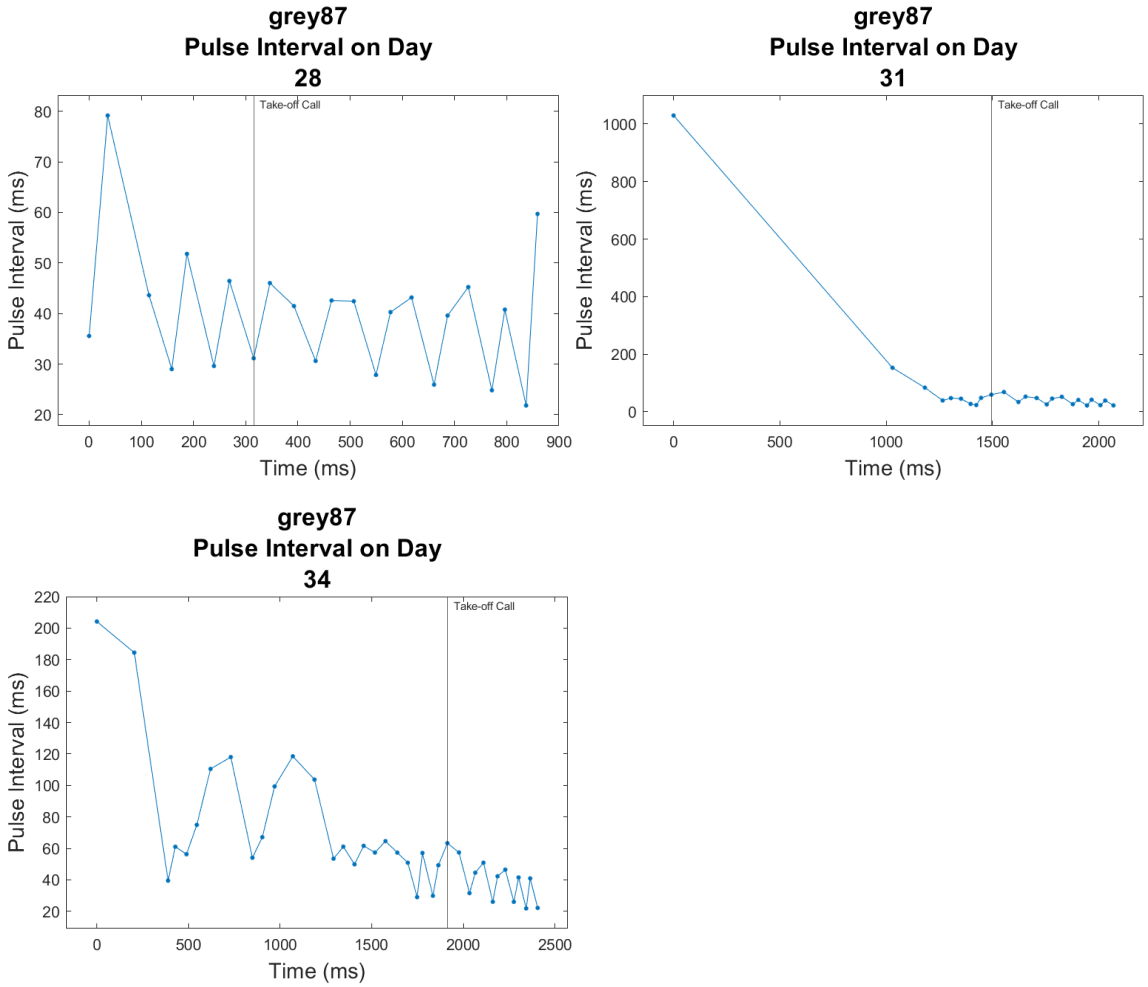

Appendix Figure 35: Grey 87 pulse interval plotted as a function of recording time per day. Each panel shows call durations before and after taking flight, with different panels showing data recorded on different days relative to parturition (number above panel; parturition day defined as Day 0). The take-off call is marked by a vertical line.

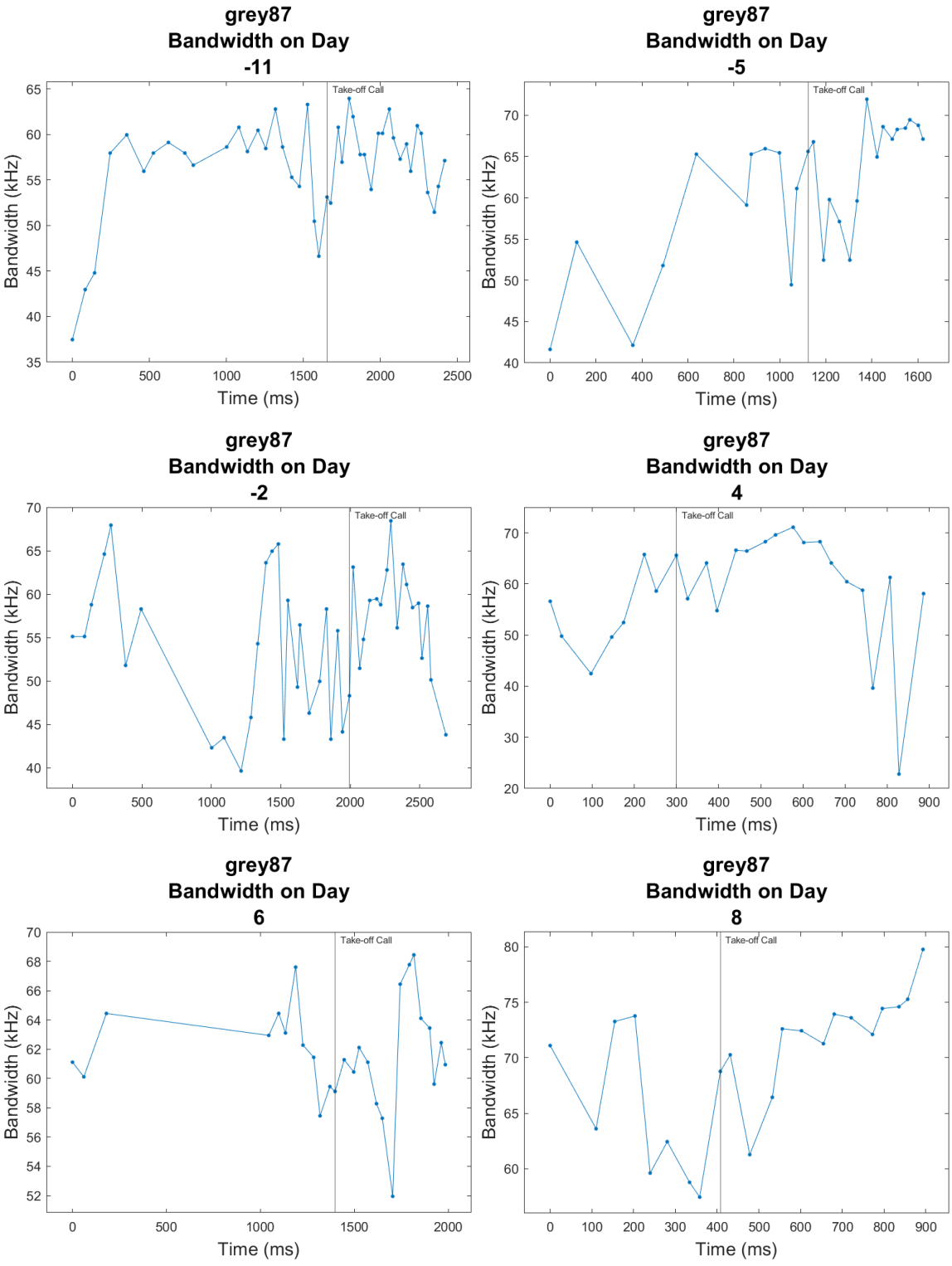
grey87
Bandwidth on Day
-11
Take-off Call
Bandwidth (kHz)
Time (ms)
grey87
Bandwidth on Day
-5
Take-off Call
Bandwidth (kHz)
Time (ms)
grey87
Bandwidth on Day
-2
Take-off Call
Bandwidth (kHz)
Time (ms)
grey87
Bandwidth on Day
4
Take-off Call
Bandwidth (kHz)
Time (ms)
grey87
Bandwidth on Day
6
Take-off Call
Bandwidth (kHz)
Time (ms)
grey87
Bandwidth on Day
8
Take-off Call
Bandwidth (kHz)
Time (ms)

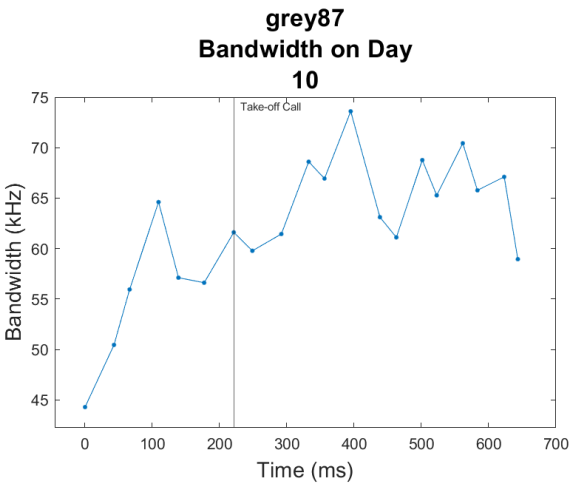
grey87
Bandwidth on Day
10
Take-off Call
Bandwidth (kHz)
Time (ms)

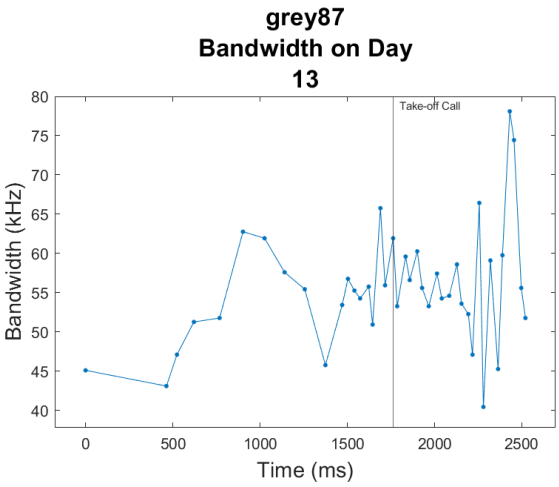
grey87
Bandwidth on Day
13
Take-off Call
Bandwidth (kHz)
Time (ms)

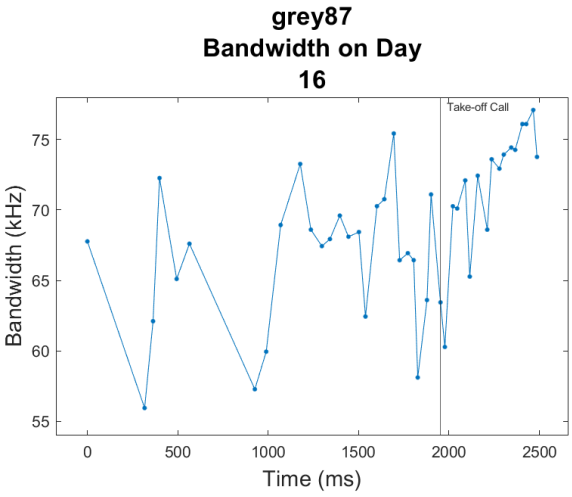
grey87
Bandwidth on Day
16
Take-off Call
Bandwidth (kHz)
Time (ms)

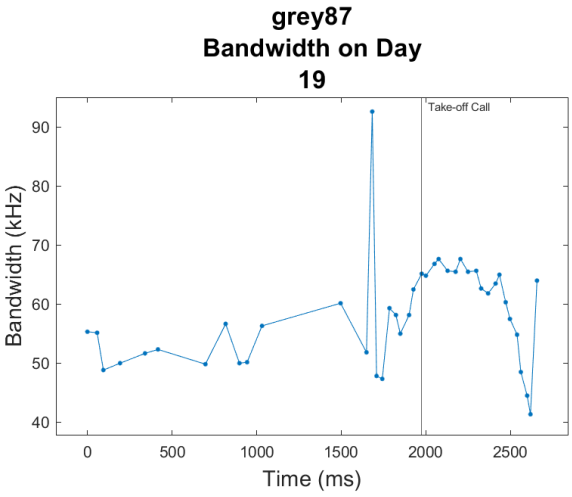
grey87
Bandwidth on Day
19
Take-off Call
Bandwidth (kHz)
Time (ms)

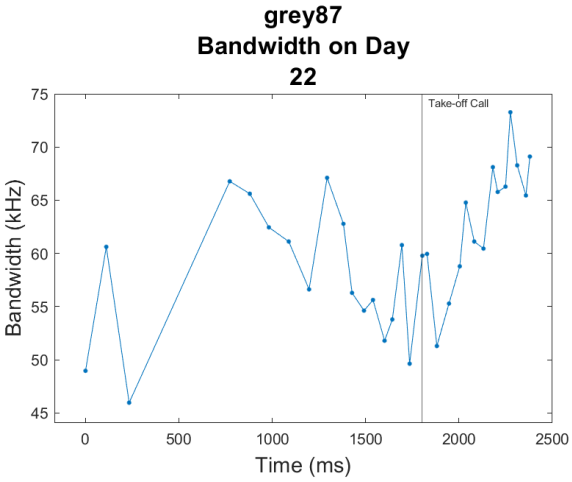
grey87
Bandwidth on Day
22
Take-off Call
Bandwidth (kHz)
Time (ms)

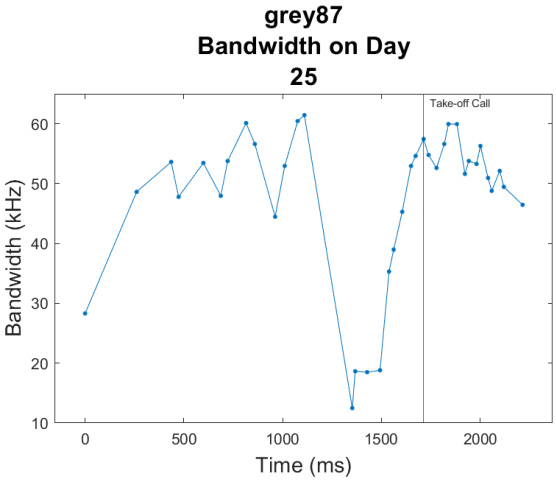
grey87
Bandwidth on Day
25
Take-off Call
Bandwidth (kHz)
Time (ms)

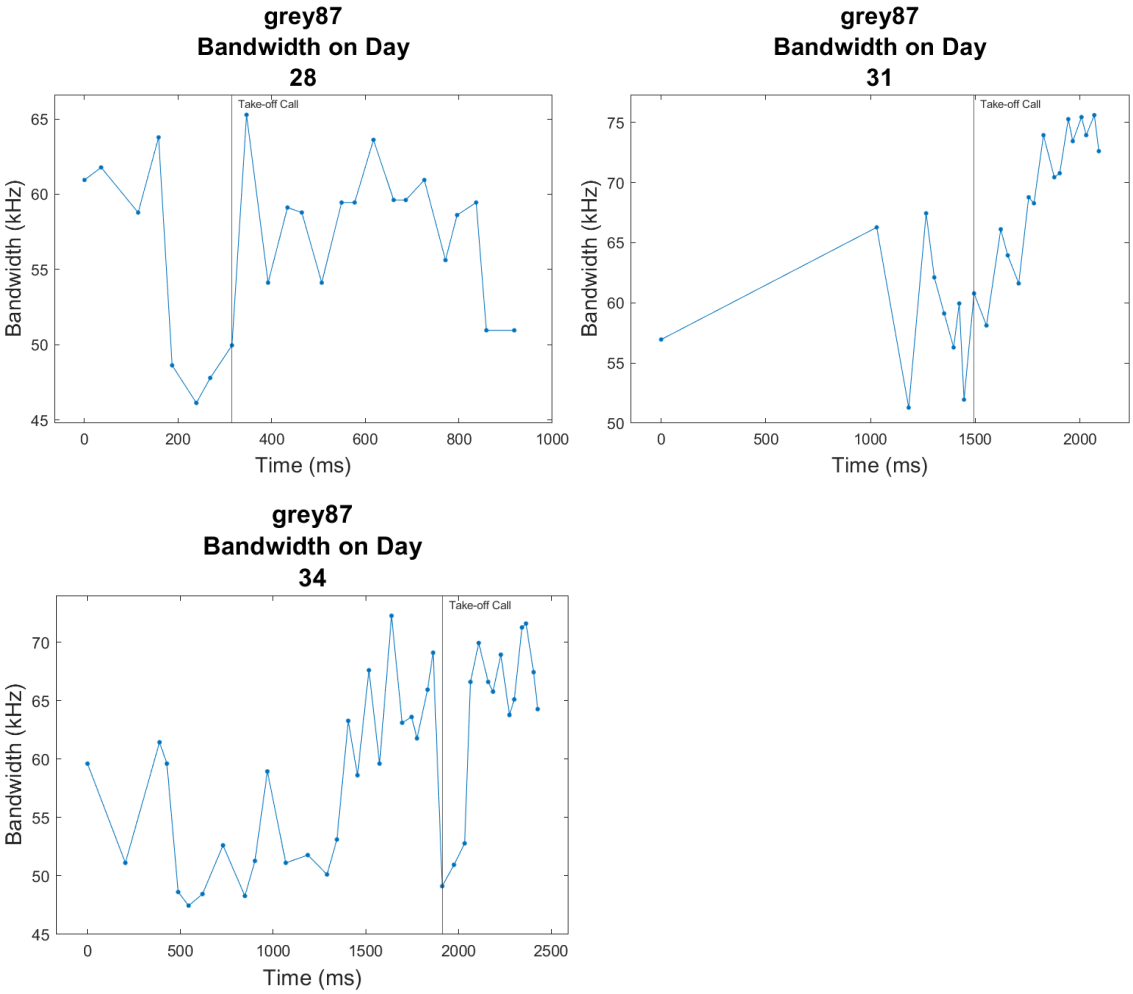

Appendix Figure 36: Grey 87 call bandwidth plotted as a function of recording time per day. Each panel shows call durations before and after taking flight, with different panels showing data recorded on different days relative to parturition (number above panel; parturition day defined as Day 0). The take-off call is marked by a vertical line.

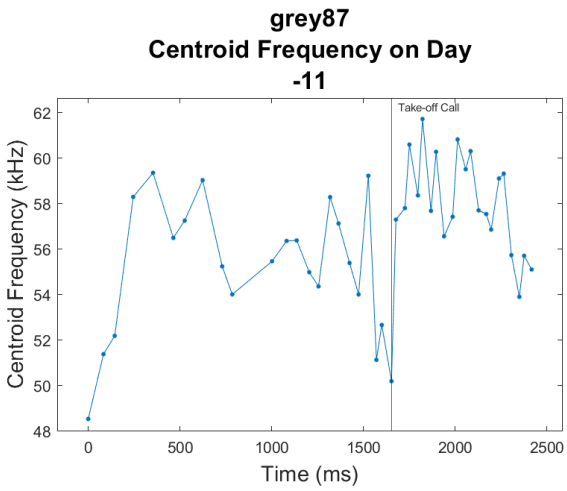
grey87
Centroid Frequency on Day
-11
Take-off Call
Centroid Frequency (kHz)
Time (ms)

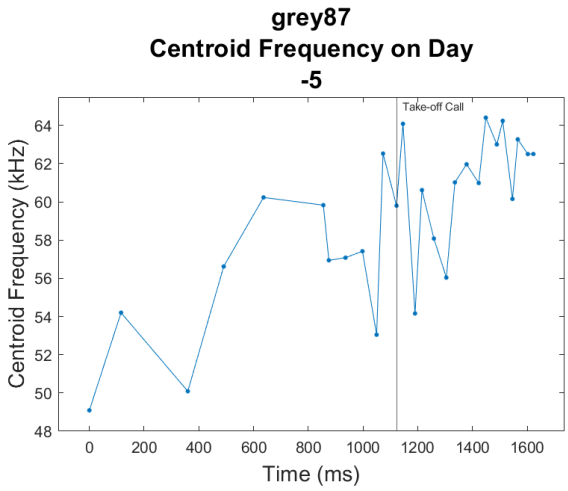
grey87
Centroid Frequency on Day
-5
Take-off Call
Centroid Frequency (kHz)
Time (ms)

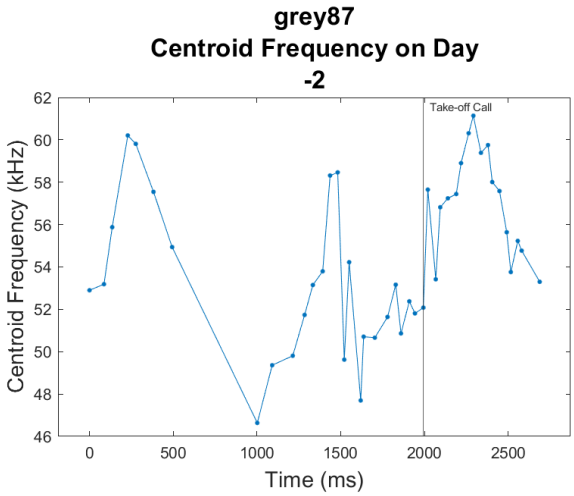
grey87
Centroid Frequency on Day
-2
Take-off Call
Centroid Frequency (kHz)
Time (ms)

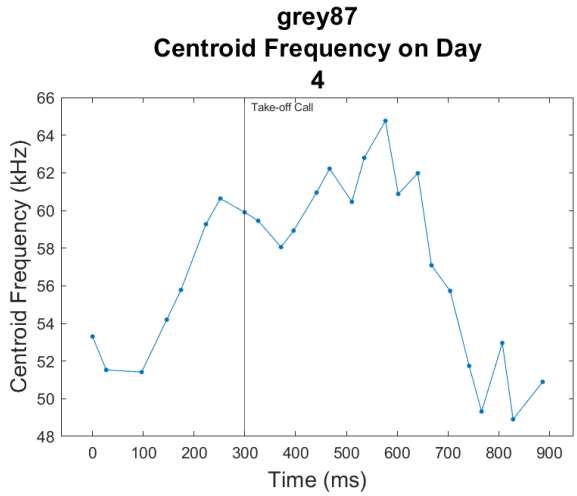
grey87
Centroid Frequency on Day
4
Take-off Call
Centroid Frequency (kHz)
Time (ms)

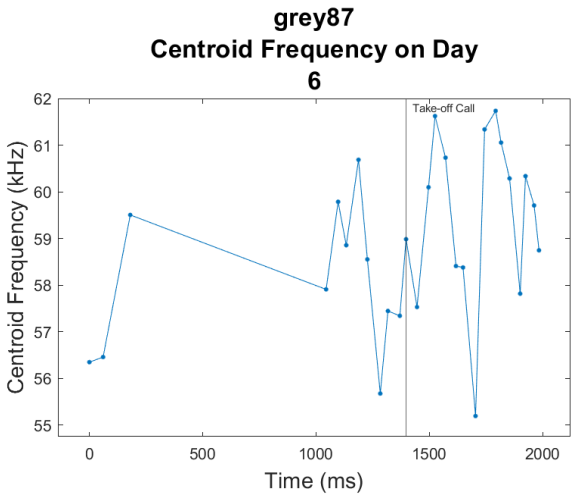
grey87
Centroid Frequency on Day
6
Take-off Call
Centroid Frequency (kHz)
Time (ms)

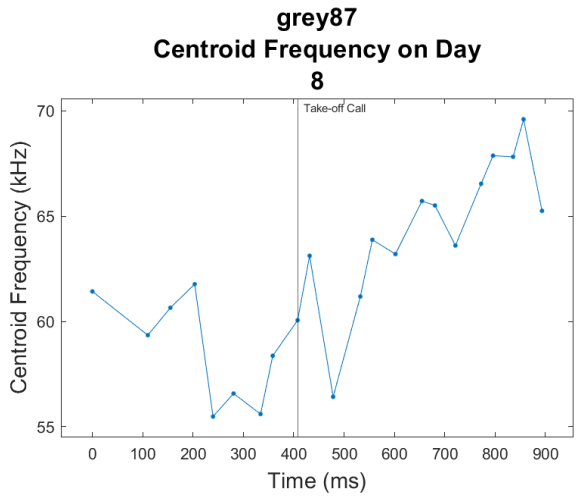
grey87
Centroid Frequency on Day
8
Take-off Call
Centroid Frequency (kHz)
Time (ms)

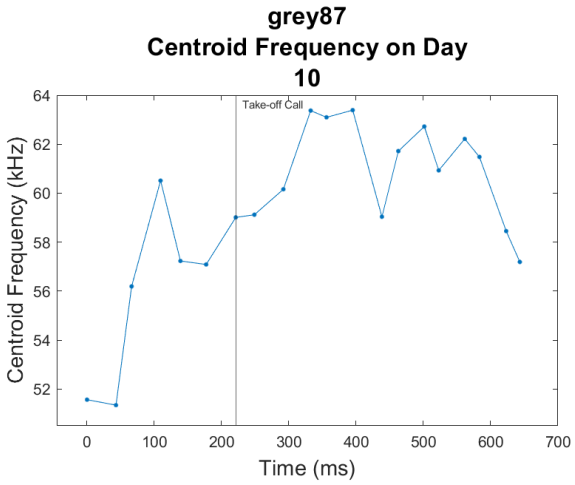
grey87
Centroid Frequency on Day
10
Take-off Call
Centroid Frequency (kHz)
Time (ms)

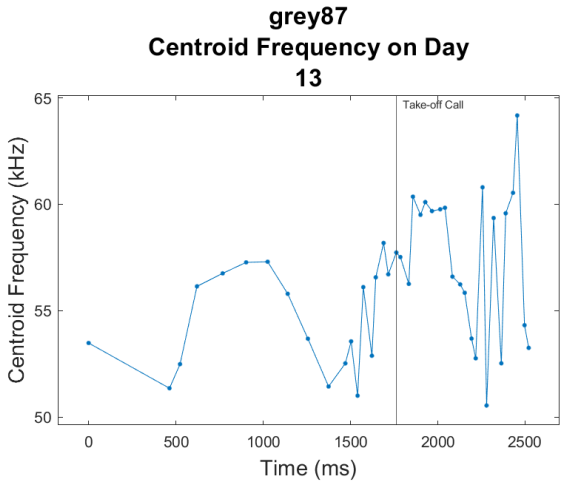
grey87
Centroid Frequency on Day
13
Take-off Call
Centroid Frequency (kHz)
Time (ms)

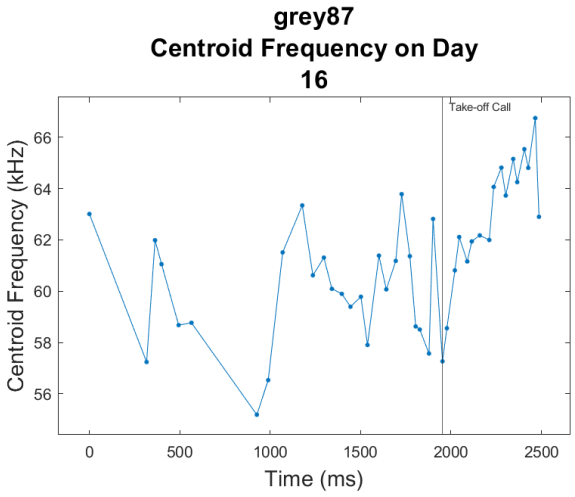
grey87
Centroid Frequency on Day
16
Take-off Call
Centroid Frequency (kHz)
Time (ms)

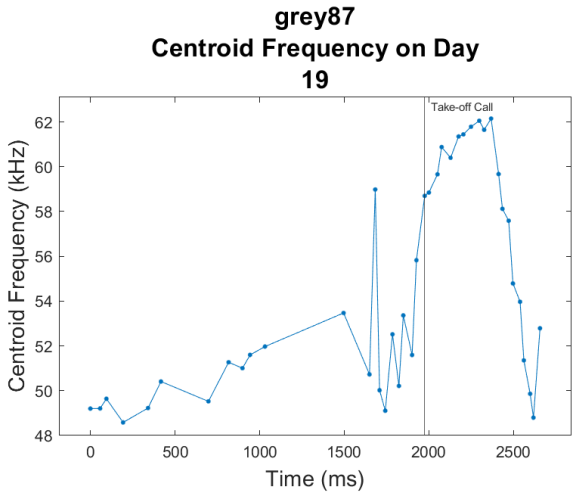
grey87
Centroid Frequency on Day
19
Take-off Call
Centroid Frequency (kHz)
Time (ms)

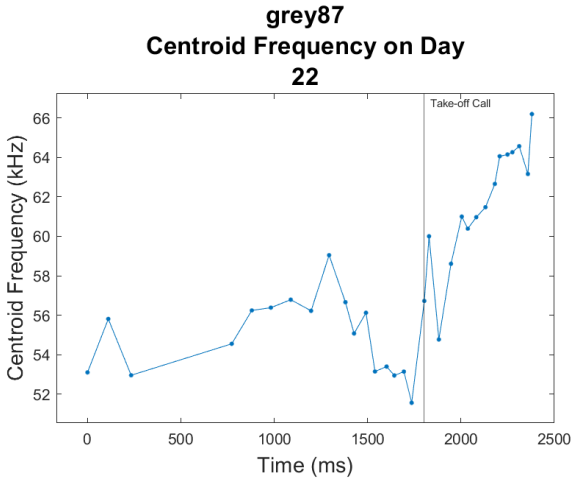
grey87
Centroid Frequency on Day
22
Take-off Call
Centroid Frequency (kHz)
Time (ms)

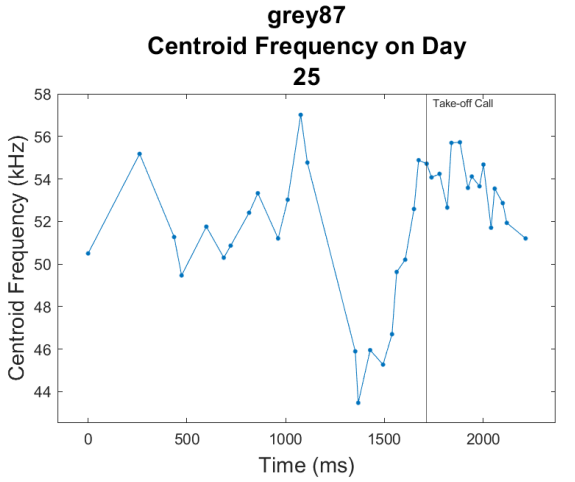
grey87
Centroid Frequency on Day
25
Take-off Call
Centroid Frequency (kHz)
Time (ms)

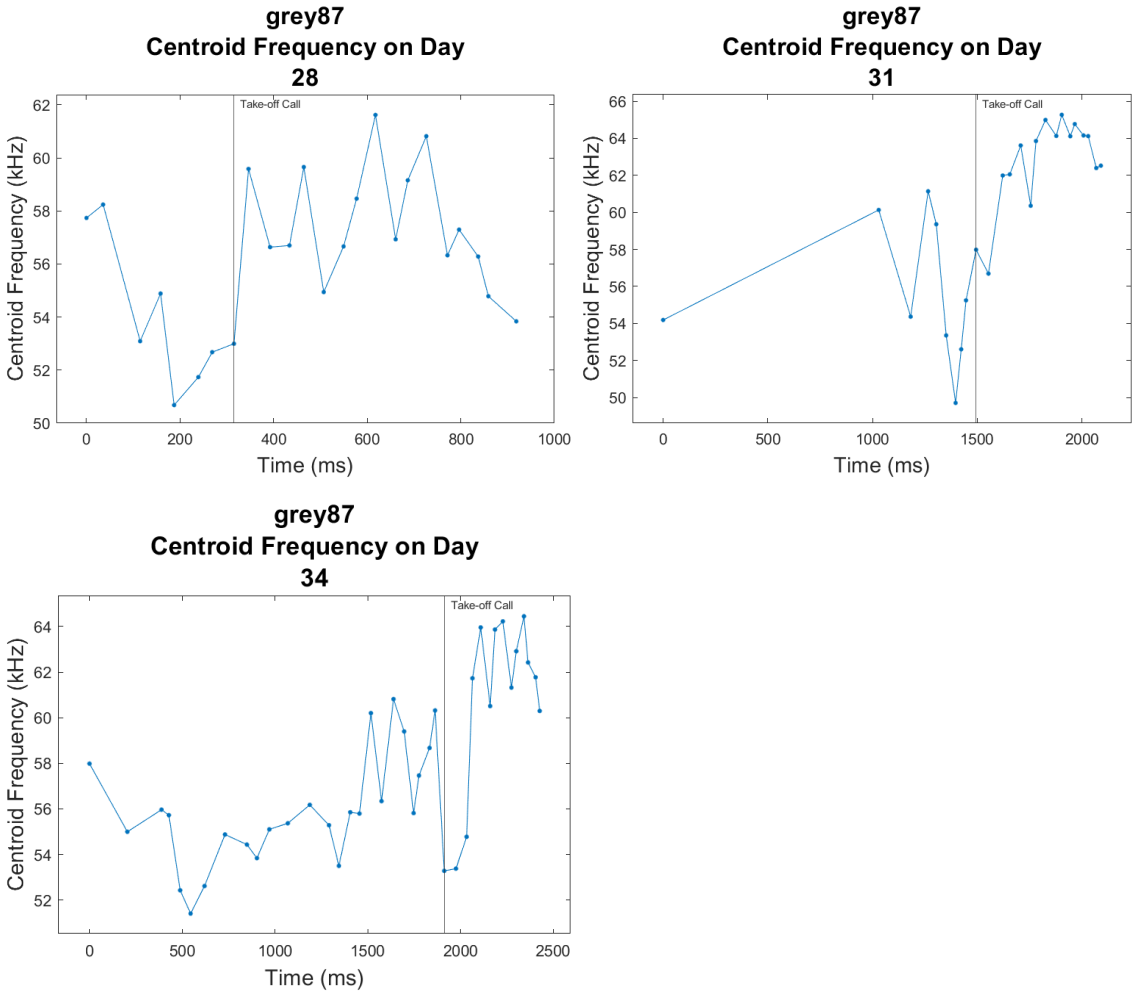

Appendix Figure 37: Grey 87 centroid frequency plotted as a function of recording time per day. Each panel shows call durations before and after taking flight, with different panels showing data recorded on different days relative to parturition (number above panel; parturition day defined as Day 0). The take-off call is marked by a vertical line.

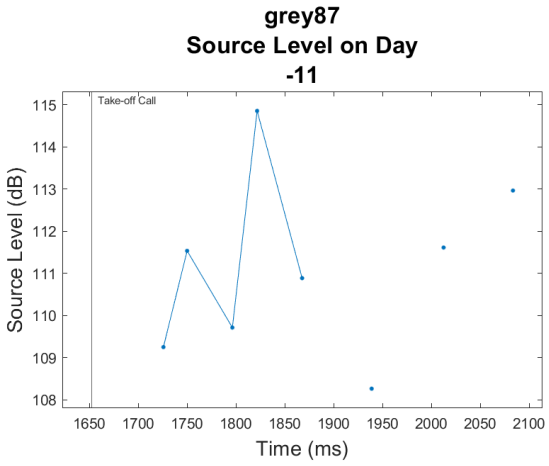
grey87
Source Level on Day
-11
Take-off Call
Source Level (dB)
Time (ms)

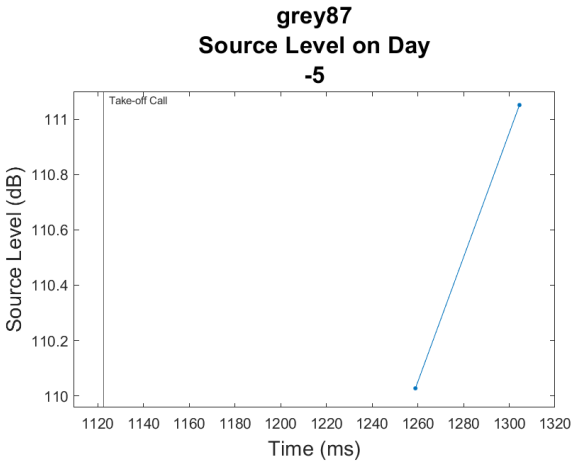
grey87
Source Level on Day
-5
Take-off Call
Source Level (dB)
Time (ms)

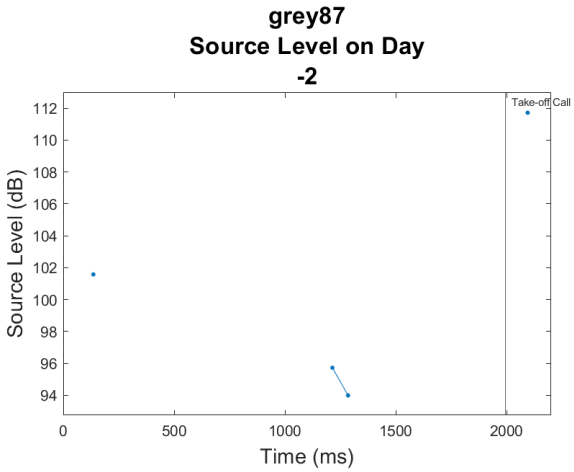
grey87
Source Level on Day
-2
Take-off Call
Source Level (dB)
Time (ms)

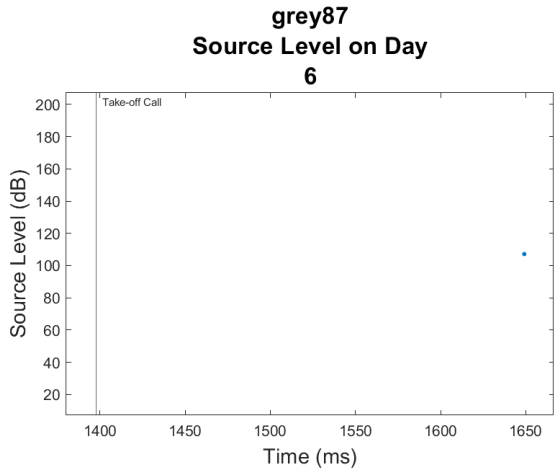
grey87
Source Level on Day
6
Take-off Call
Source Level (dB)
Time (ms)

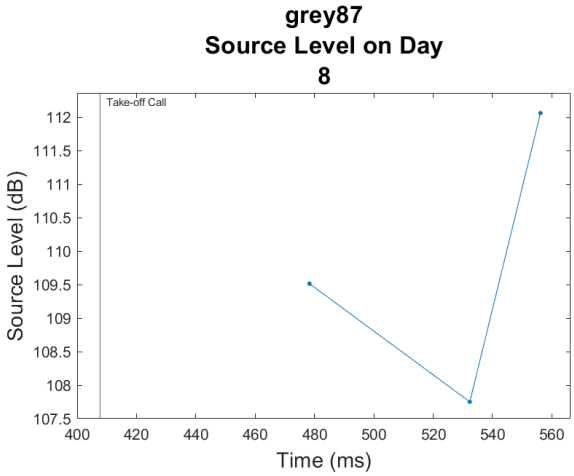
grey87
Source Level on Day
8
Take-off Call
Source Level (dB)
Time (ms)

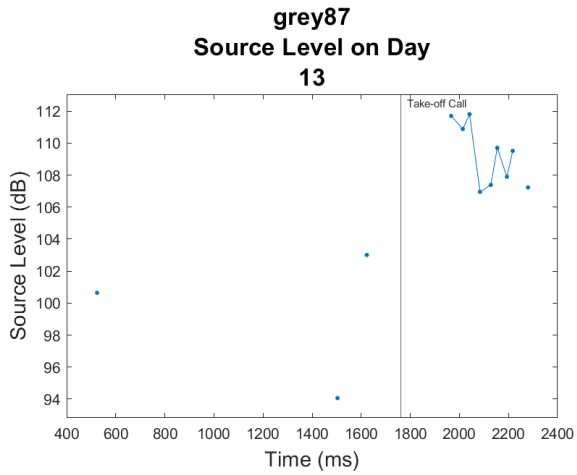
grey87
Source Level on Day
13
Take-off Call
Source Level (dB)
Time (ms)

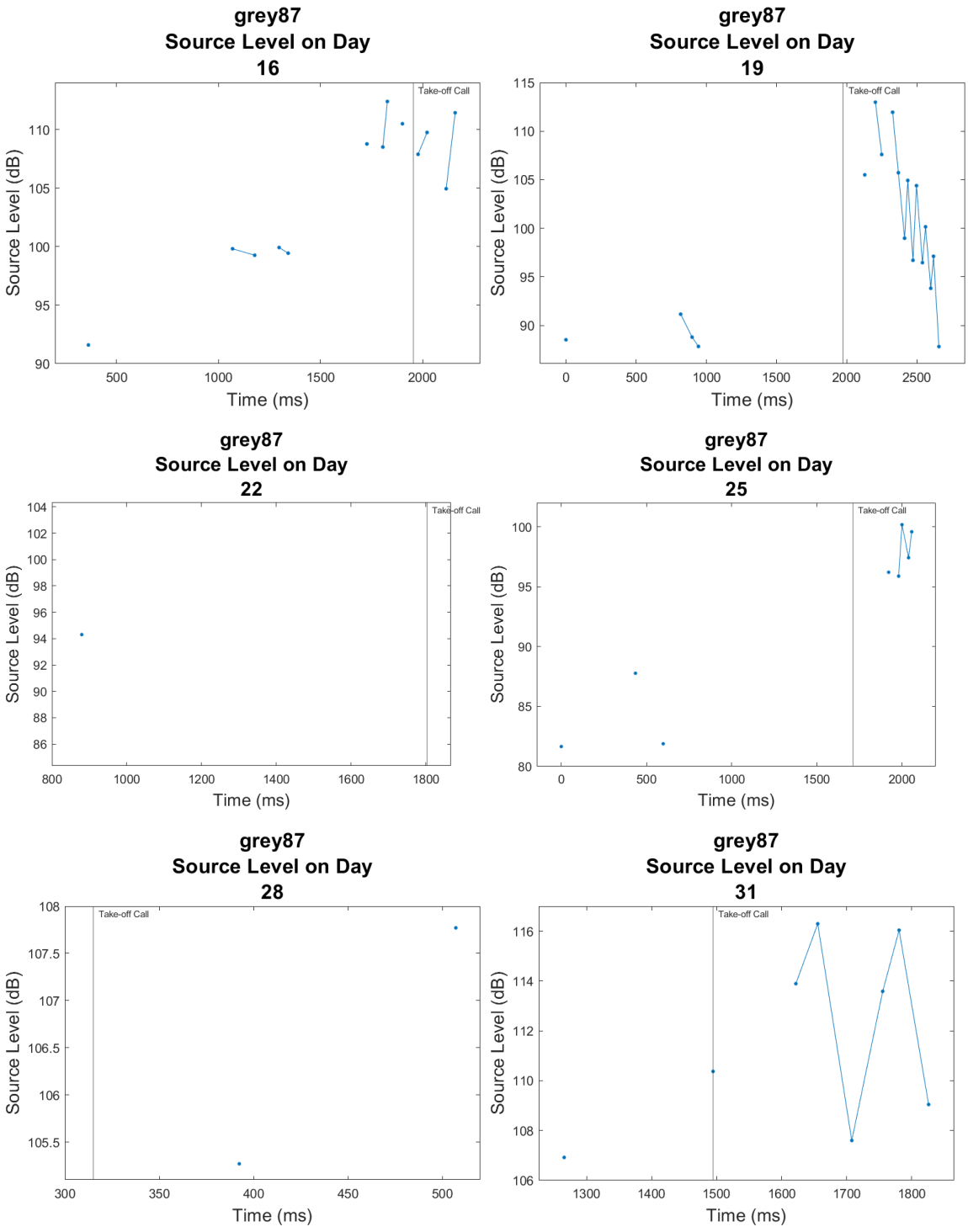
grey87
Source Level on Day
16
Take-off Call
Source Level (dB)
Time (ms)
grey87
Source Level on Day
19
Take-off Call
Source Level (dB)
Time (ms)
grey87
Source Level on Day
22
Take-off Call
Source Level (dB)
Time (ms)
grey87
Source Level on Day
25
Take-off Call
Source Level (dB)
Time (ms)
grey87
Source Level on Day
28
Take-off Call
Source Level (dB)
Time (ms)
grey87
Source Level on Day
31
Take-off Call
Source Level (dB)
Time (ms)

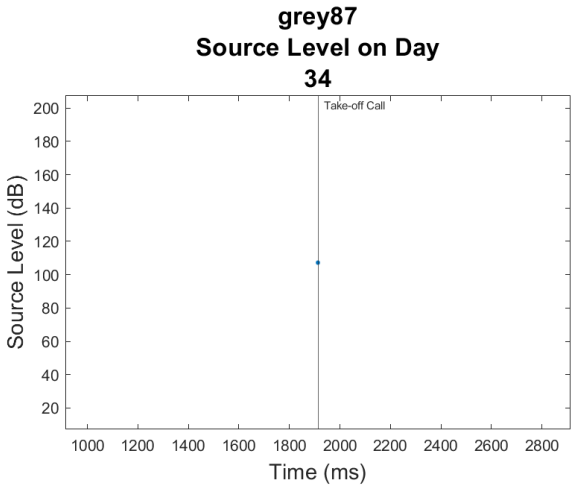

Appendix Figure 38: Grey 87 source level plotted as a function of recording time per day. Each panel shows call durations before and after taking flight, with different panels showing data recorded on different days relative to parturition (number above panel; parturition day defined as Day 0). The take-off call is marked by a vertical line.

Grey 88 Echolocation Call Characteristics Graphs

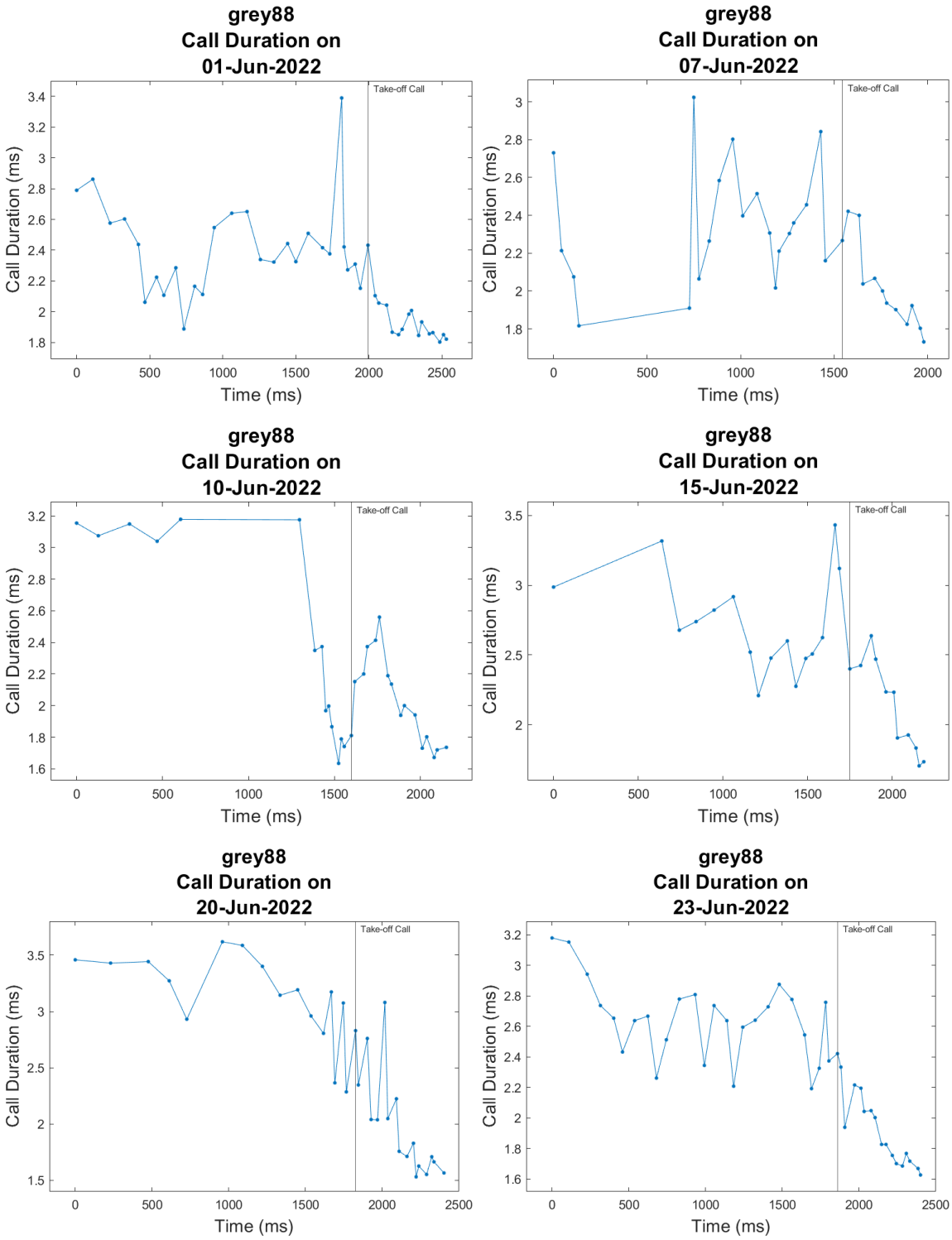

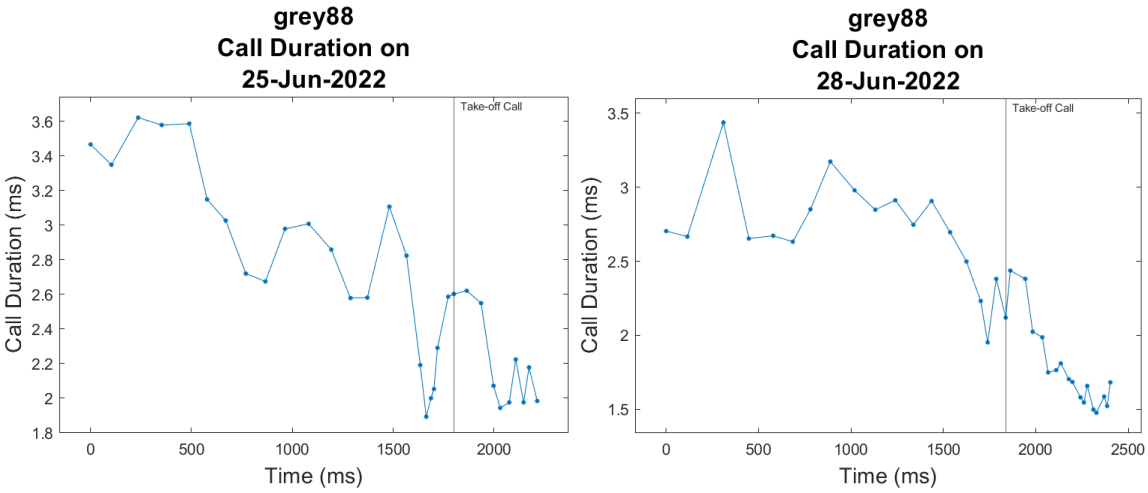

Appendix Figure 39: Grey 88 call duration plotted as a function of recording time per recording date. Each panel shows call durations before and after taking flight, with different panels showing data recorded on different recording dates. The take-off call is marked by a vertical line.

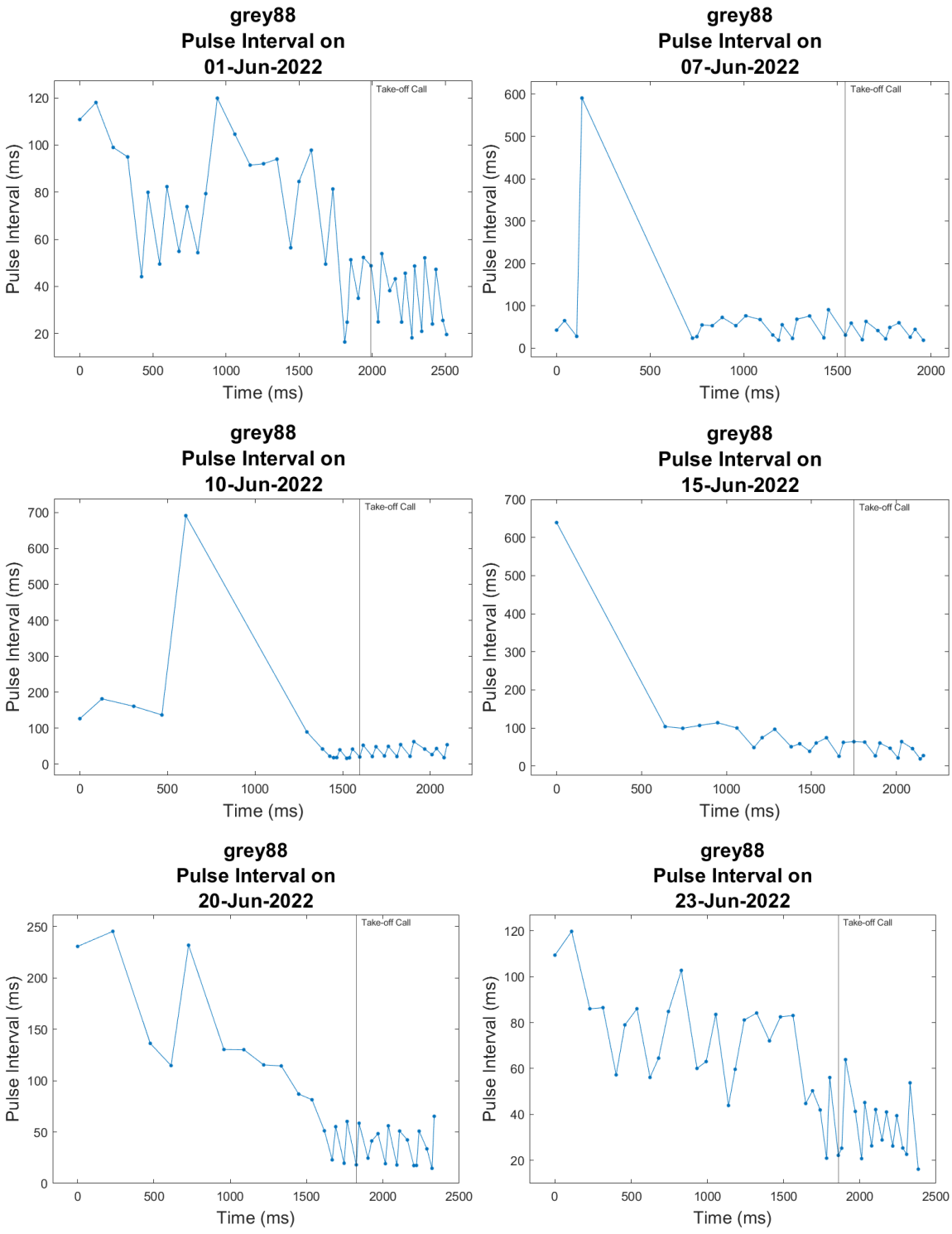
grey88
Pulse Interval on
01-Jun-2022
Take-off Call
Pulse Interval (ms)
Time (ms)
grey88
Pulse Interval on
07-Jun-2022
Take-off Call
Pulse Interval (ms)
Time (ms)
grey88
Pulse Interval on
10-Jun-2022
Take-off Call
Pulse Interval (ms)
Time (ms)
grey88
Pulse Interval on
15-Jun-2022
Take-off Call
Pulse Interval (ms)
Time (ms)
grey88
Pulse Interval on
20-Jun-2022
Take-off Call
Pulse Interval (ms)
Time (ms)
grey88
Pulse Interval on
23-Jun-2022
Take-off Call
Pulse Interval (ms)
Time (ms)

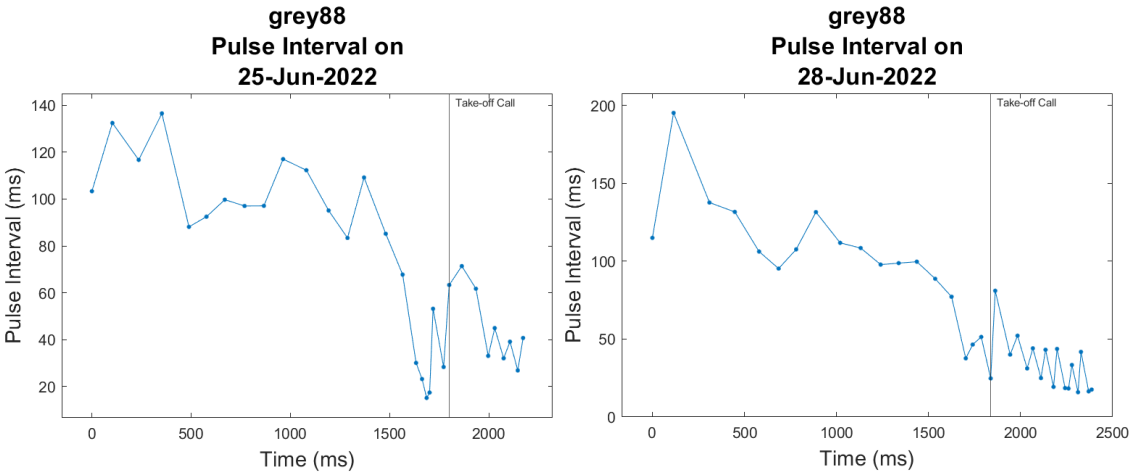

Appendix Figure 40: Grey 88 pulse interval plotted as a function of recording time per recording date. Each panel shows call durations before and after taking flight, with different panels showing data recorded on different recording dates. The take-off call is marked by a vertical line.

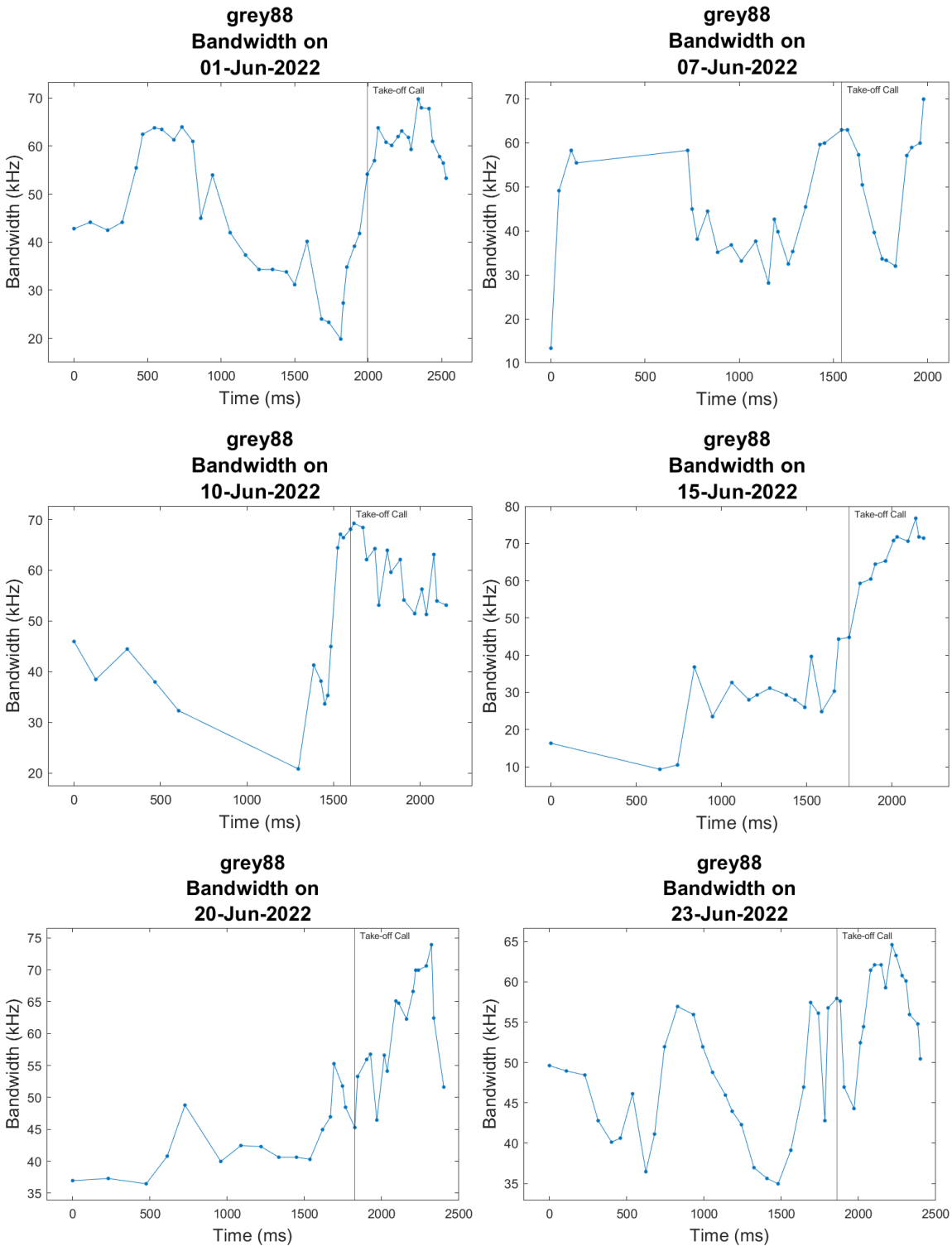
grey88
Bandwidth on
01-Jun-2022
Take-off Call
Bandwidth (kHz)
Time (ms)
grey88
Bandwidth on
07-Jun-2022
Take-off Call
Bandwidth (kHz)
Time (ms)
grey88
Bandwidth on
10-Jun-2022
Take-off Call
Bandwidth (kHz)
Time (ms)
grey88
Bandwidth on
15-Jun-2022
Take-off Call
Bandwidth (kHz)
Time (ms)
grey88
Bandwidth on
20-Jun-2022
Take-off Call
Bandwidth (kHz)
Time (ms)
grey88
Bandwidth on
23-Jun-2022
Take-off Call
Bandwidth (kHz)
Time (ms)

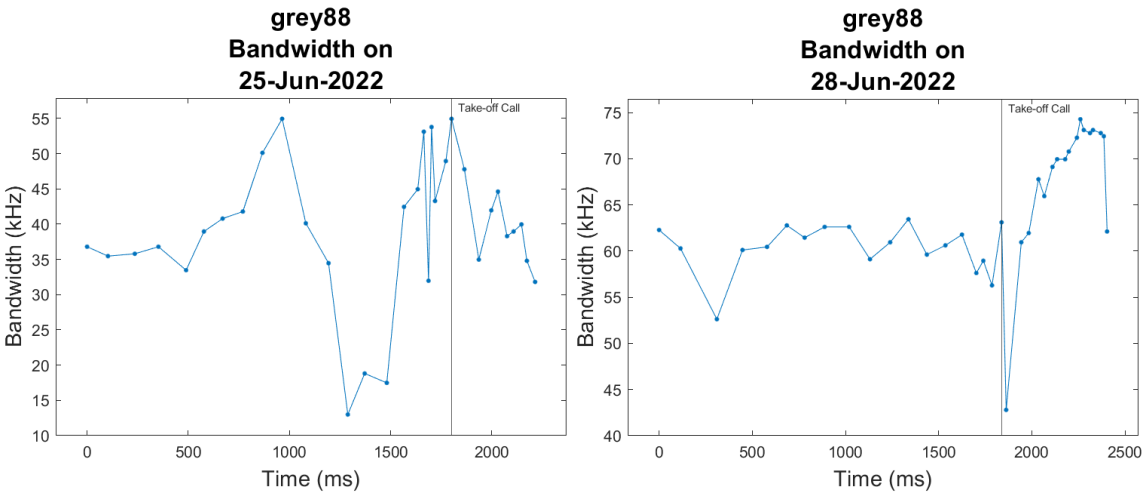

Appendix Figure 41: Grey 88 call bandwidth plotted as a function of recording time per recording date. Each panel shows call durations before and after taking flight, with different panels showing data recorded on different recording dates. The take-off call is marked by a vertical line.

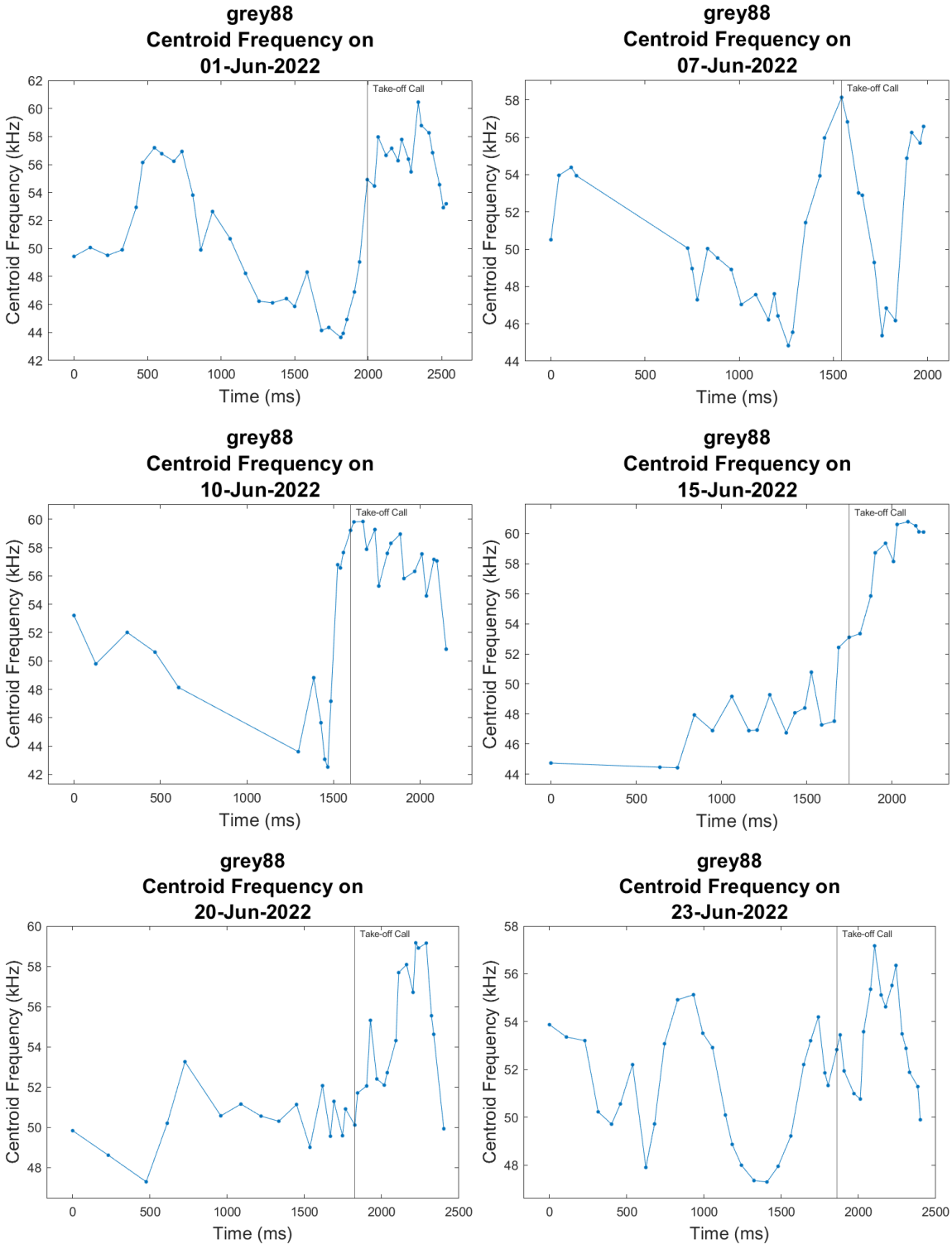
grey88
Centroid Frequency on
01-Jun-2022
Take-off Call
Centroid Frequency (kHz)
Time (ms)
grey88
Centroid Frequency on
07-Jun-2022
Take-off Call
Centroid Frequency (kHz)
Time (ms)
grey88
Centroid Frequency on
10-Jun-2022
Take-off Call
Centroid Frequency (kHz)
Time (ms)
grey88
Centroid Frequency on
15-Jun-2022
Take-off Call
Centroid Frequency (kHz)
Time (ms)
grey88
Centroid Frequency on
20-Jun-2022
Take-off Call
Centroid Frequency (kHz)
Time (ms)
grey88
Centroid Frequency on
23-Jun-2022
Take-off Call
Centroid Frequency (kHz)
Time (ms)

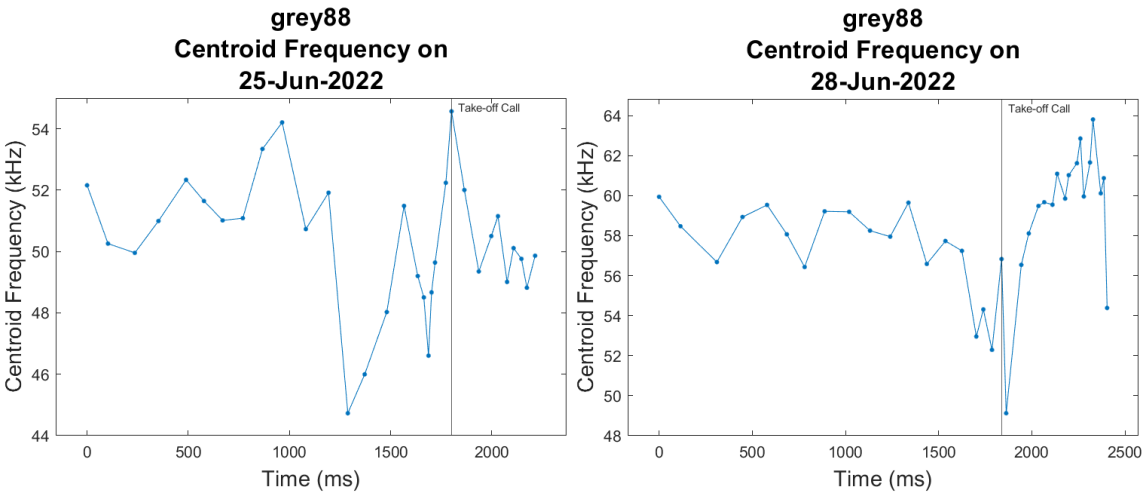

Appendix Figure 42: Grey 88 centroid frequency plotted as a function of recording time per recording date. Each panel shows call durations before and after taking flight, with different panels showing data recorded on different recording dates. The take-off call is marked by a vertical line.

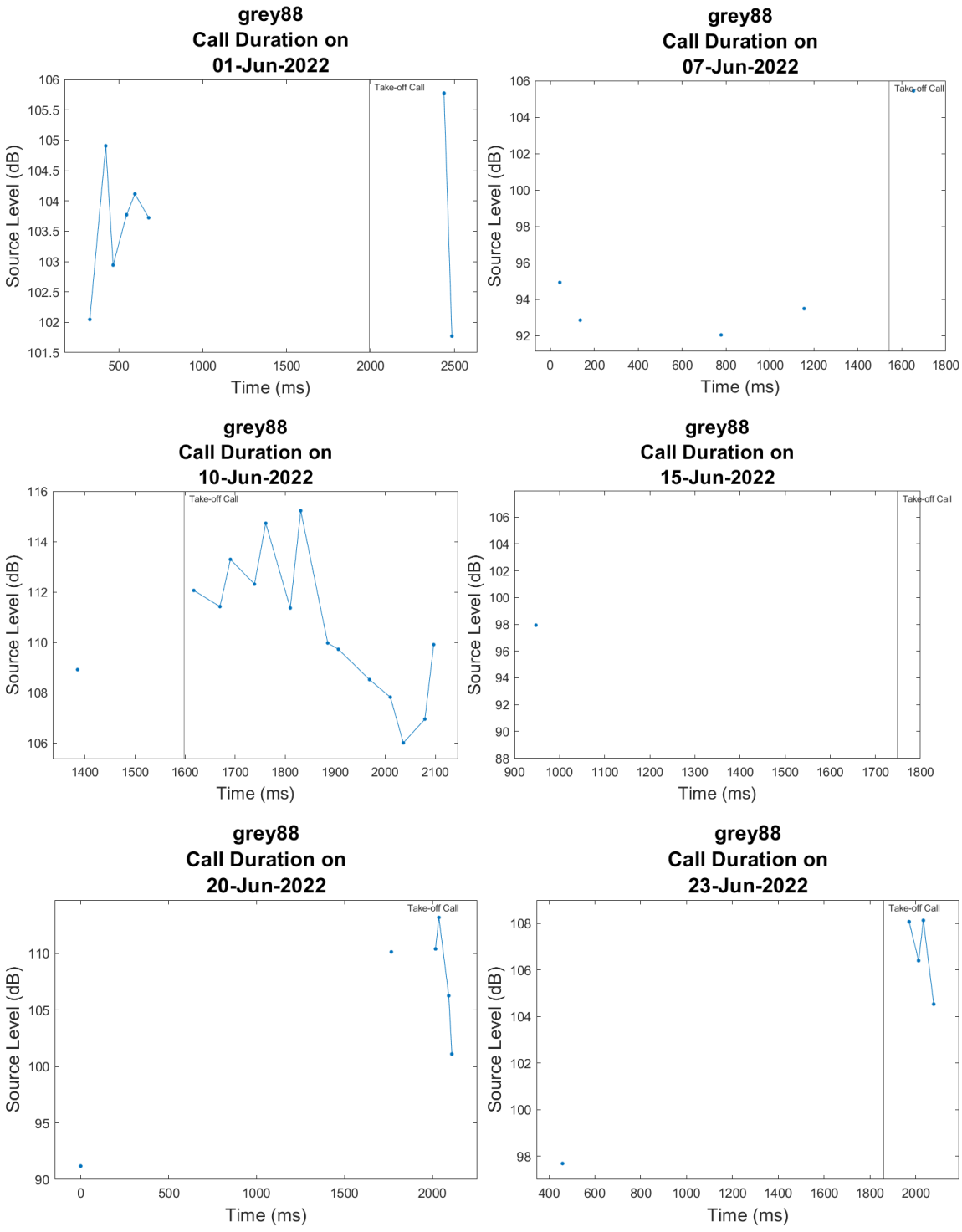
grey88
Call Duration on
01-Jun-2022
Take-off Call
Source Level (dB)
Time (ms)
grey88
Call Duration on
07-Jun-2022
Take-off Call
Source Level (dB)
Time (ms)
grey88
Call Duration on
10-Jun-2022
Take-off Call
Source Level (dB)
Time (ms)
grey88
Call Duration on
15-Jun-2022
Take-off Call
Source Level (dB)
Time (ms)
grey88
Call Duration on
20-Jun-2022
Take-off Call
Source Level (dB)
Time (ms)
grey88
Call Duration on
23-Jun-2022
Take-off Call
Source Level (dB)
Time (ms)

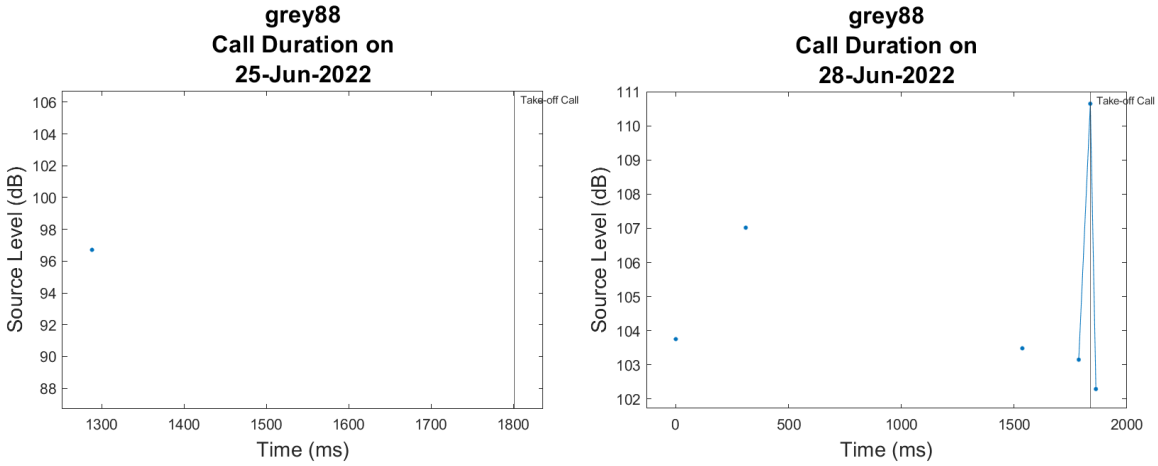

Appendix Figure 43: Grey 88 source level plotted as a function of recording time per recording date. Each panel shows call durations before and after taking flight, with different panels showing data recorded on different recording dates. The take-off call is marked by a vertical line.

Grey 92 Echolocation Call Characteristics Graphs

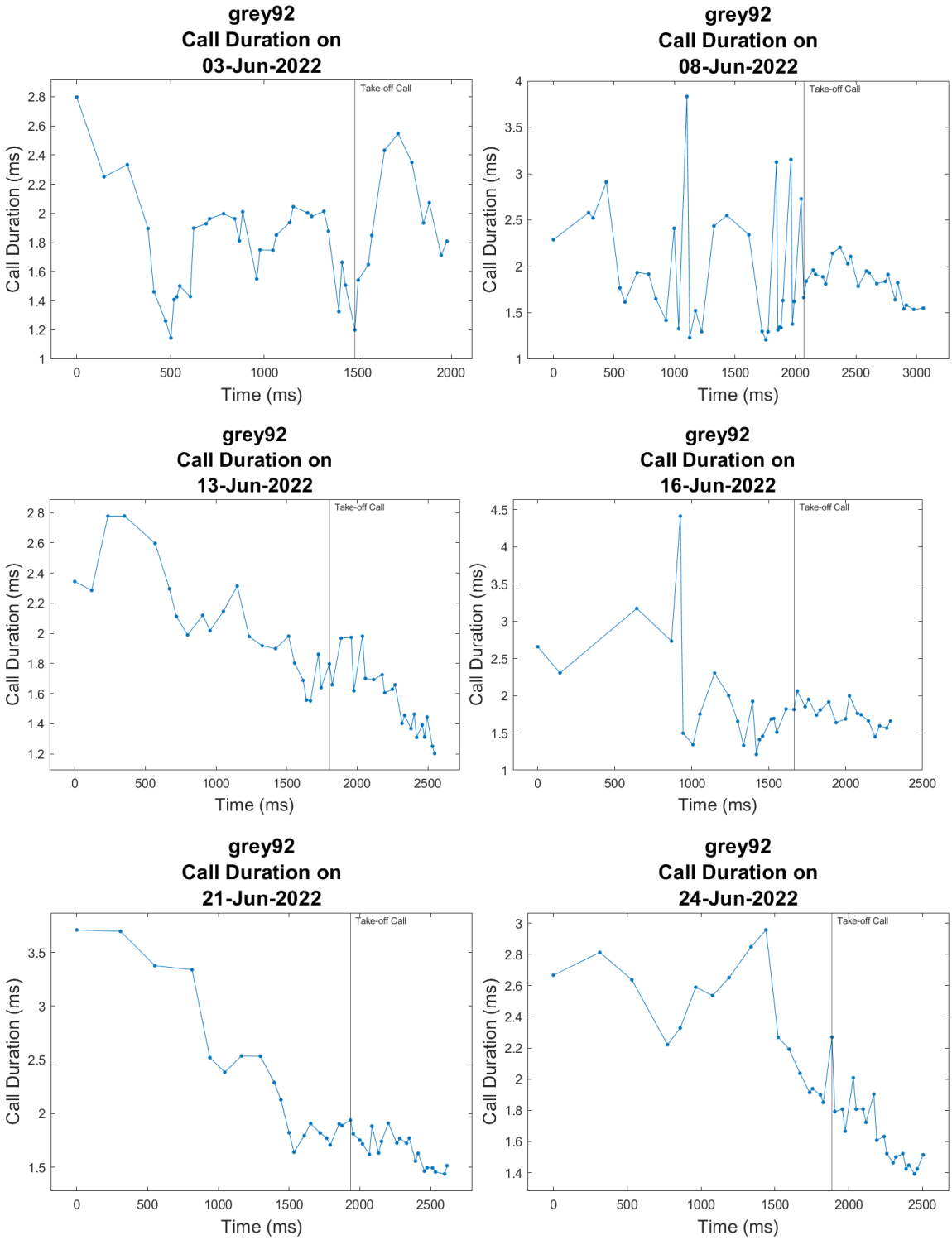

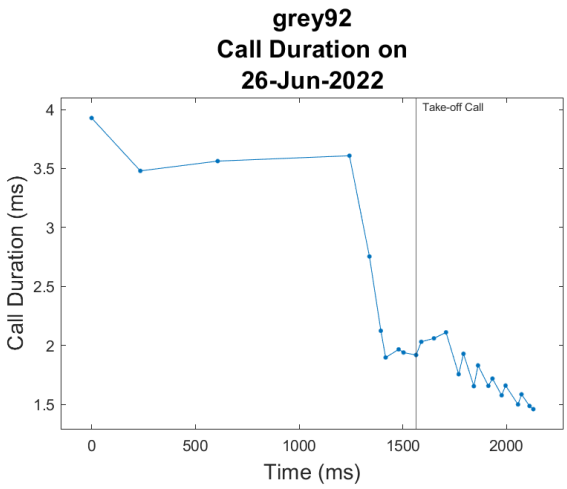
grey92
Call Duration on
26-Jun-2022
Take-off Call
Call Duration (ms)
Time (ms)

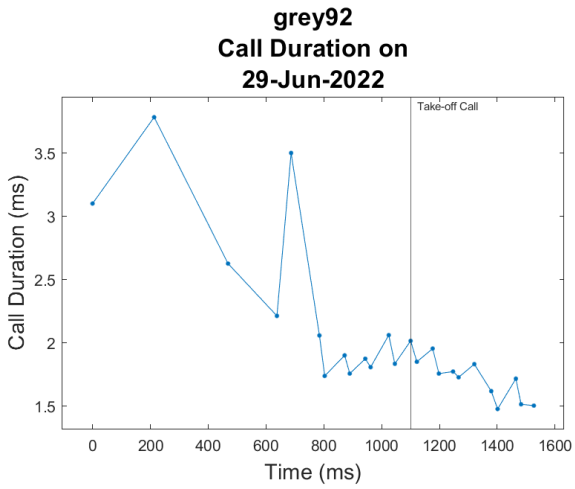
grey92
Call Duration on
29-Jun-2022
Take-off Call
Call Duration (ms)
Time (ms)

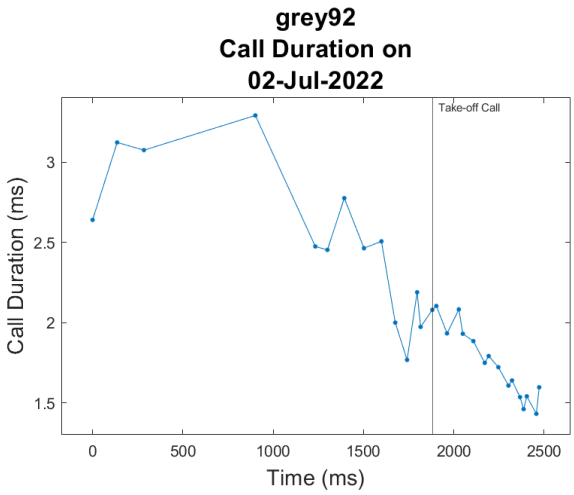
grey92
Call Duration on
02-Jul-2022
Take-off Call
Call Duration (ms)
Time (ms)

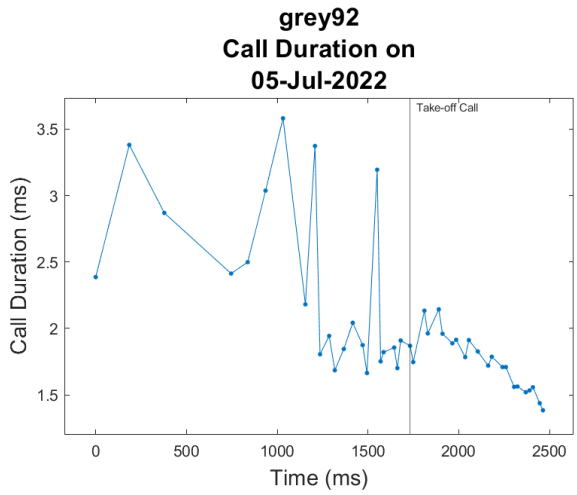
grey92
Call Duration on
05-Jul-2022
Take-off Call
Call Duration (ms)
Time (ms)

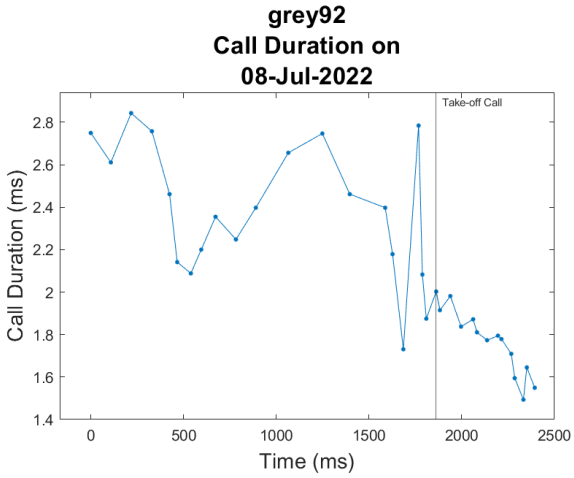
grey92
Call Duration on
08-Jul-2022
Take-off Call
Call Duration (ms)
Time (ms)

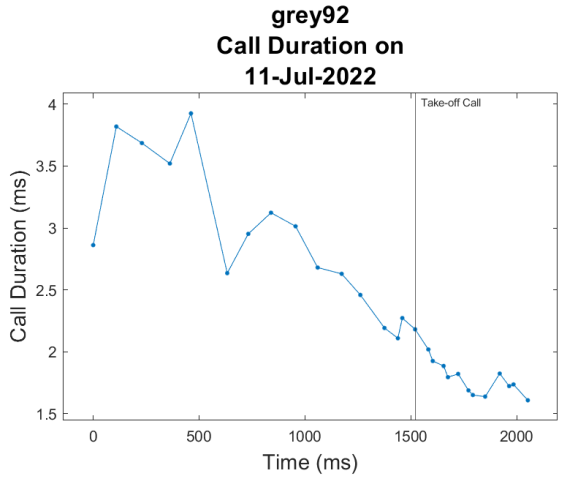
grey92
Call Duration on
11-Jul-2022
Take-off Call
Call Duration (ms)
Time (ms)

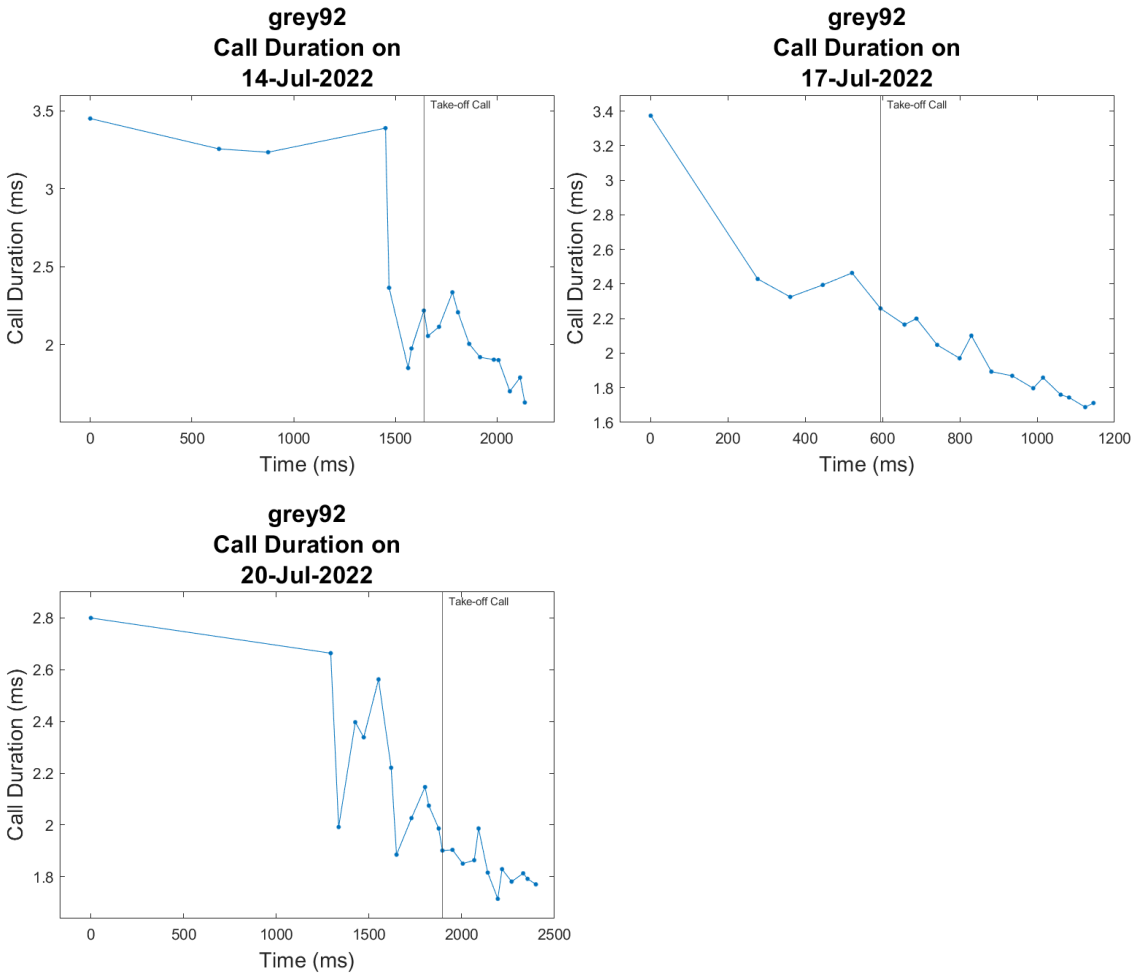

Appendix Figure 44: Grey 92 call duration plotted as a function of recording time per recording date. Each panel shows call durations before and after taking flight, with different panels showing data recorded on different recording dates. The take-off call is marked by a vertical line.

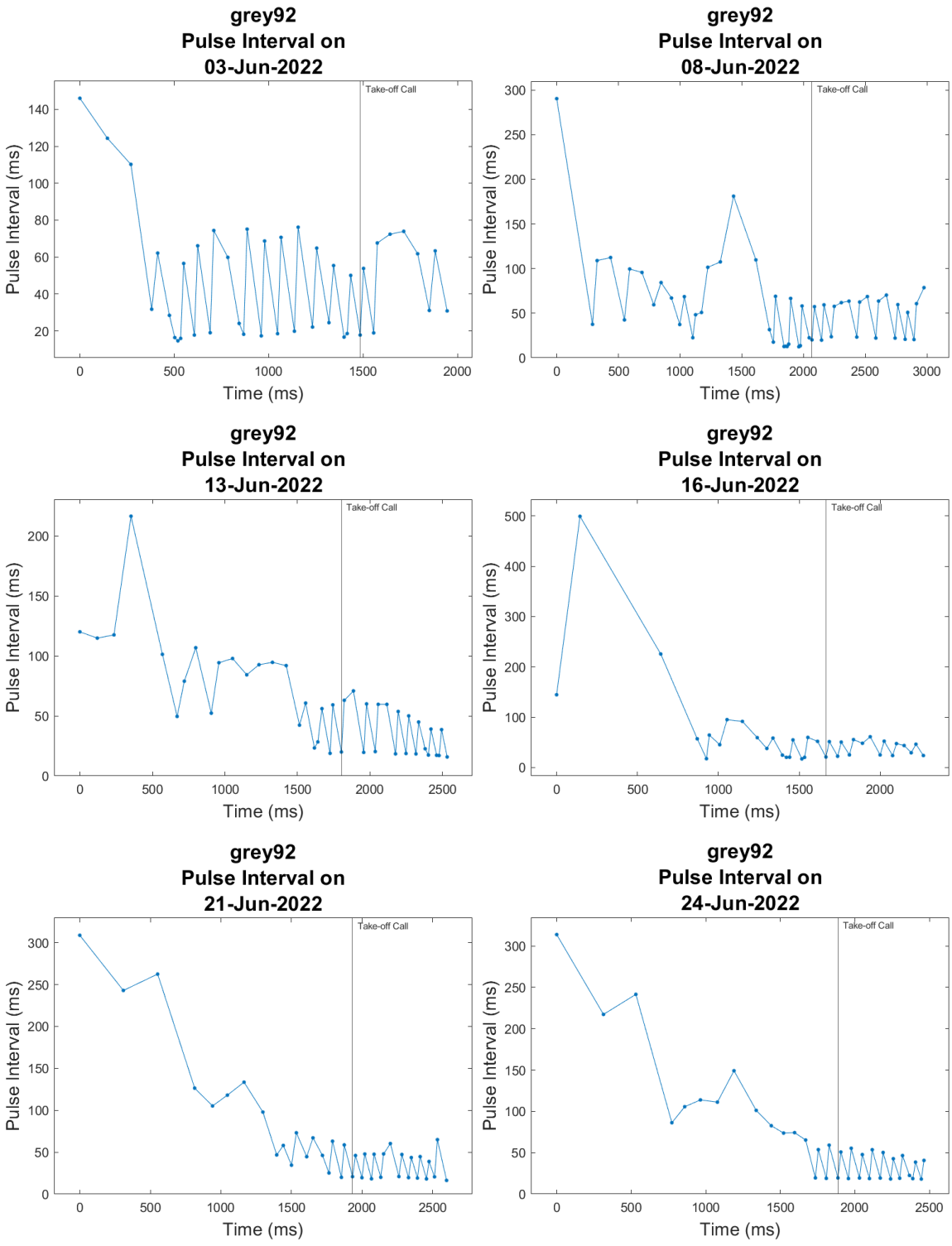
grey92
Pulse Interval on
03-Jun-2022
Take-off Call
Pulse Interval (ms)
Time (ms)
grey92
Pulse Interval on
08-Jun-2022
Take-off Call
Pulse Interval (ms)
Time (ms)
grey92
Pulse Interval on
13-Jun-2022
Take-off Call
Pulse Interval (ms)
Time (ms)
grey92
Pulse Interval on
16-Jun-2022
Take-off Call
Pulse Interval (ms)
Time (ms)
grey92
Pulse Interval on
21-Jun-2022
Take-off Call
Pulse Interval (ms)
Time (ms)
grey92
Pulse Interval on
24-Jun-2022
Take-off Call
Pulse Interval (ms)
Time (ms)

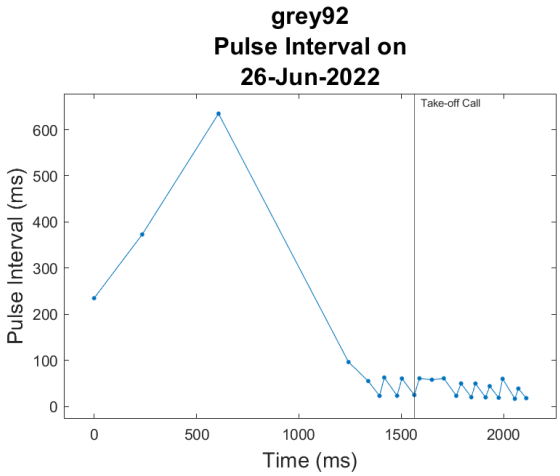
grey92
Pulse Interval on
26-Jun-2022
Take-off Call
Pulse Interval (ms)
Time (ms)

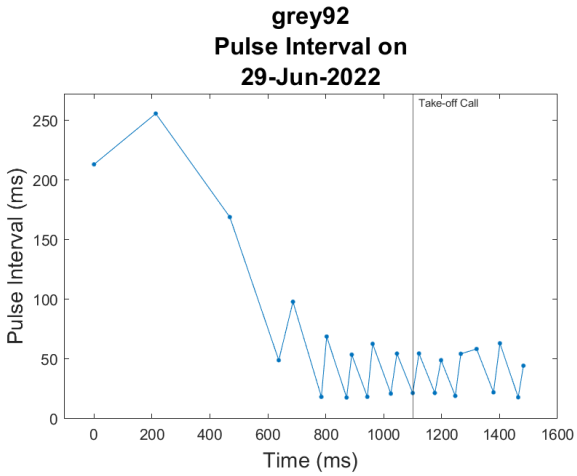
grey92
Pulse Interval on
29-Jun-2022
Take-off Call
Pulse Interval (ms)
Time (ms)

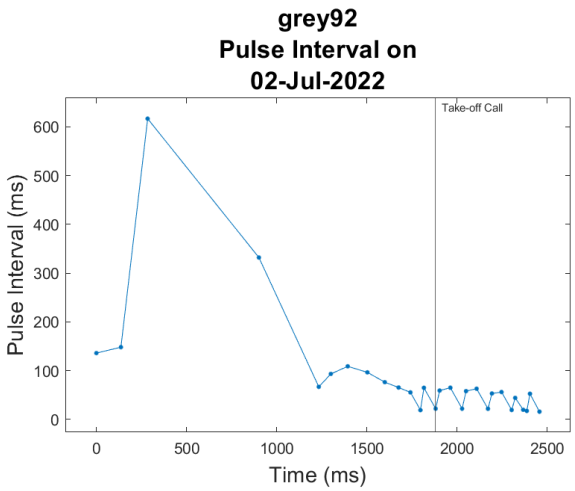
grey92
Pulse Interval on
02-Jul-2022
Take-off Call
Pulse Interval (ms)
Time (ms)

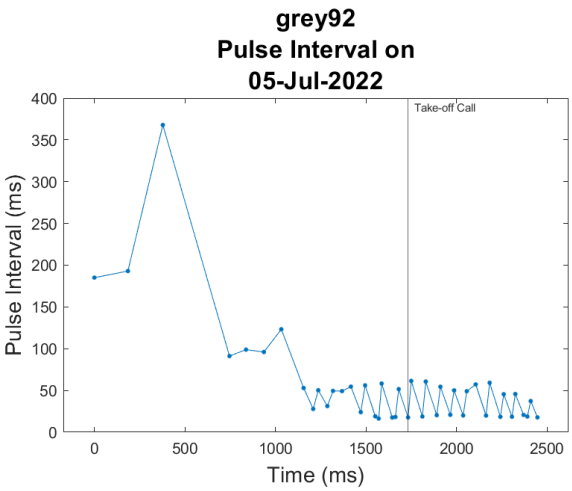
grey92
Pulse Interval on
05-Jul-2022
Take-off Call
Pulse Interval (ms)
Time (ms)

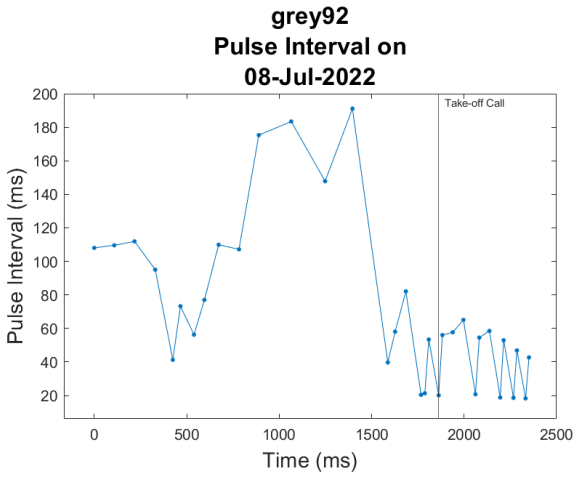
grey92
Pulse Interval on
08-Jul-2022
Take-off Call
Pulse Interval (ms)
Time (ms)

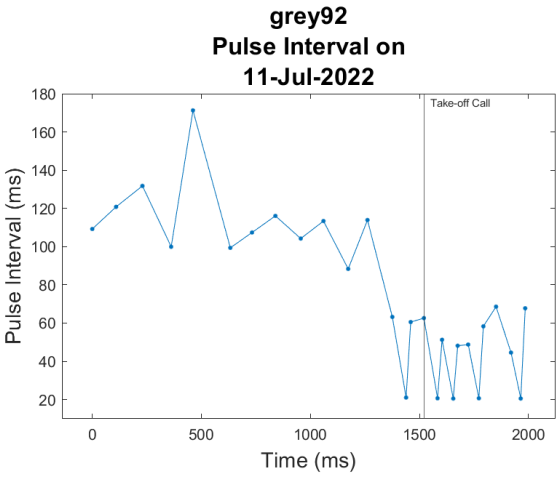
grey92
Pulse Interval on
11-Jul-2022
Take-off Call
Pulse Interval (ms)
Time (ms)

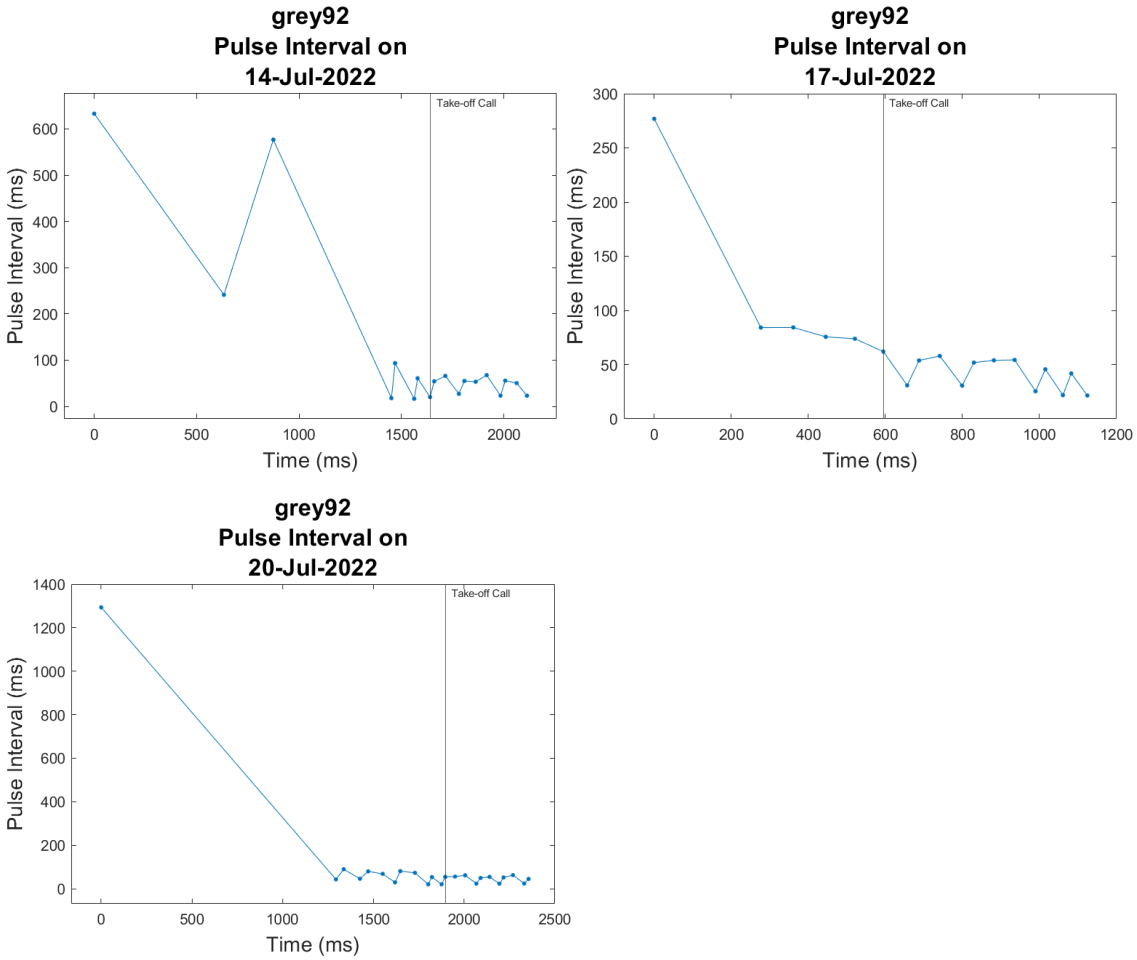

Appendix Figure 45: Grey 92 pulse interval plotted as a function of recording time per recording date. Each panel shows call durations before and after taking flight, with different panels showing data recorded on different recording dates. The take-off call is marked by a vertical line.

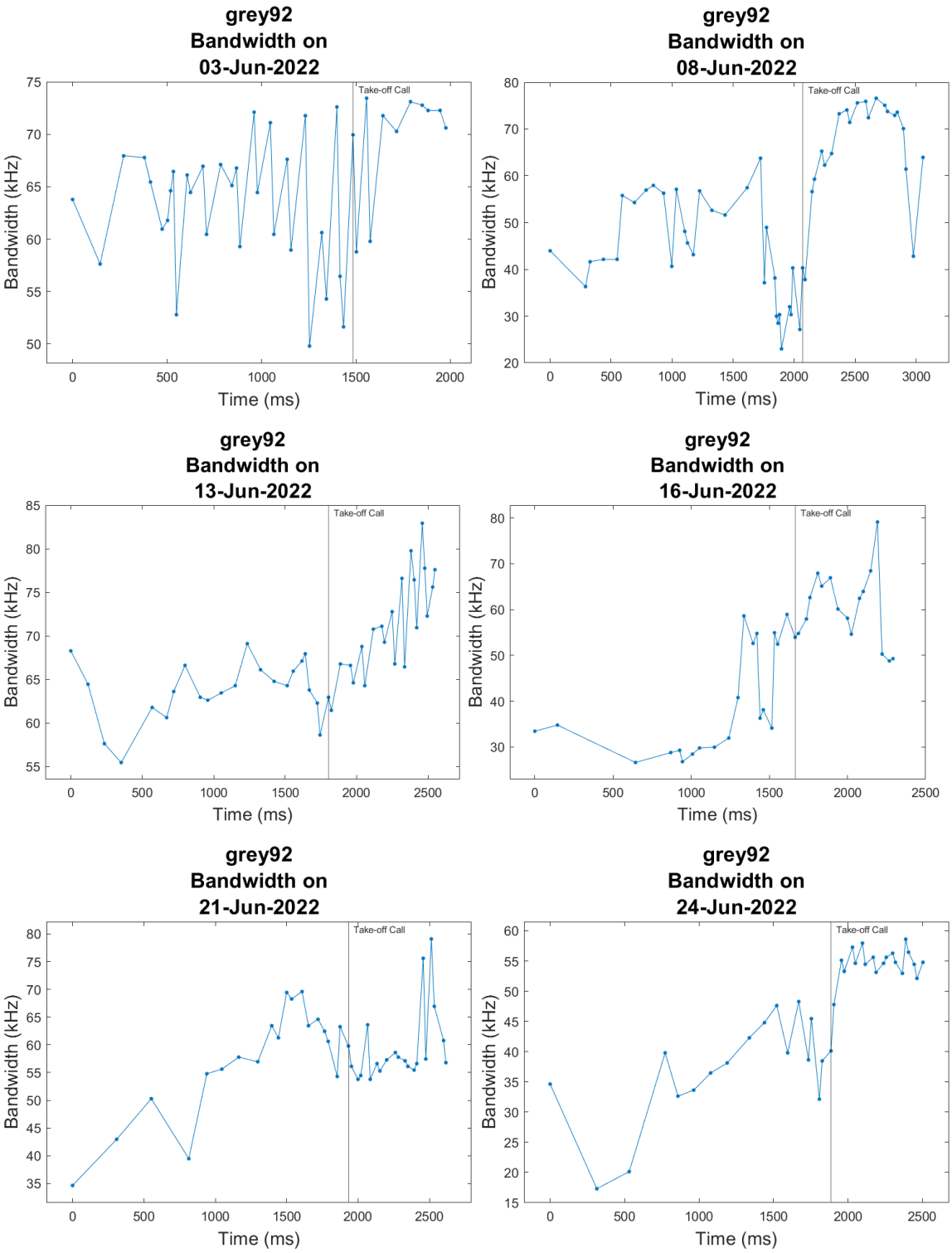
grey92
Bandwidth on
03-Jun-2022
Take-off Call
Bandwidth (kHz)
Time (ms)
grey92
Bandwidth on
08-Jun-2022
Take-off Call
Bandwidth (kHz)
Time (ms)
grey92
Bandwidth on
13-Jun-2022
Take-off Call
Bandwidth (kHz)
Time (ms)
grey92
Bandwidth on
16-Jun-2022
Take-off Call
Bandwidth (kHz)
Time (ms)
grey92
Bandwidth on
21-Jun-2022
Take-off Call
Bandwidth (kHz)
Time (ms)
grey92
Bandwidth on
24-Jun-2022
Take-off Call
Bandwidth (kHz)
Time (ms)

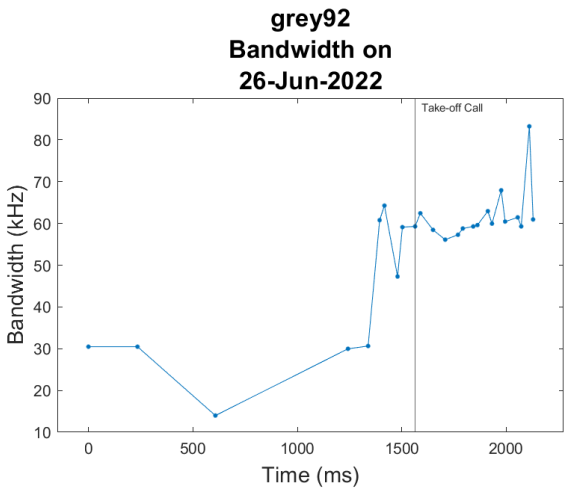
grey92
Bandwidth on
26-Jun-2022
Take-off Call
Bandwidth (kHz)
Time (ms)

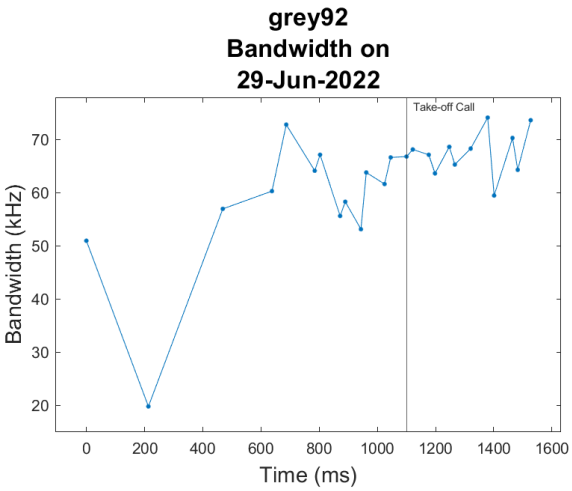
grey92
Bandwidth on
29-Jun-2022
Take-off Call
Bandwidth (kHz)
Time (ms)

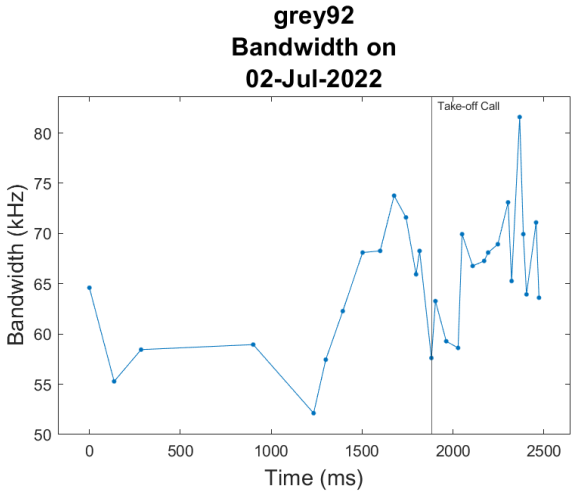
grey92
Bandwidth on
02-Jul-2022
Take-off Call
Bandwidth (kHz)
Time (ms)

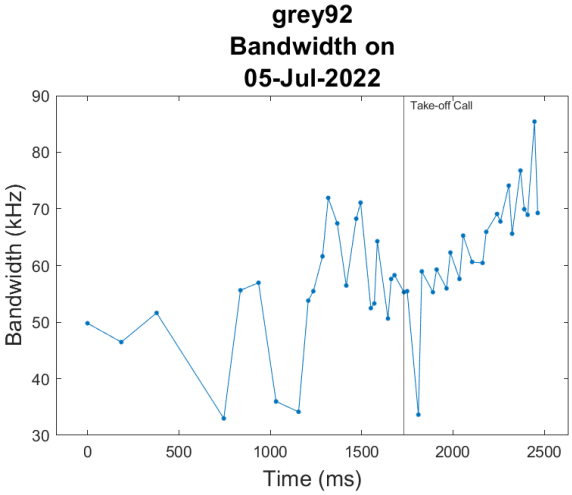
grey92
Bandwidth on
05-Jul-2022
Take-off Call
Bandwidth (kHz)
Time (ms)

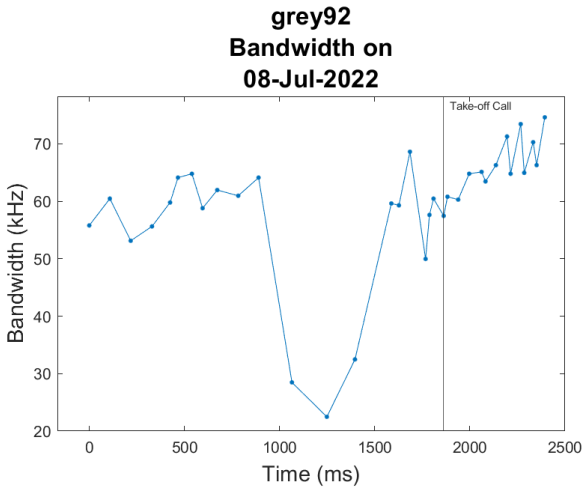
grey92
Bandwidth on
08-Jul-2022
Take-off Call
Bandwidth (kHz)
Time (ms)

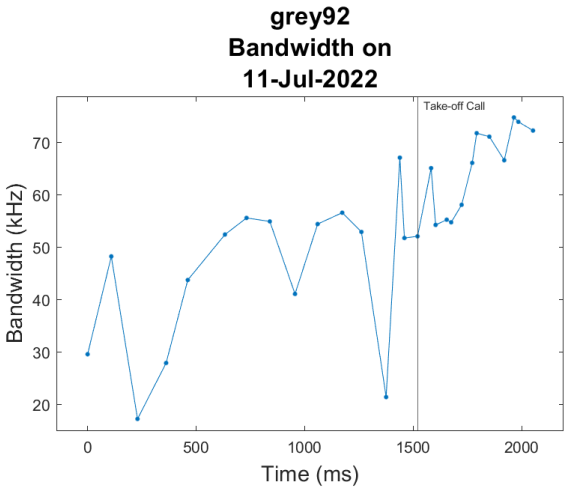
grey92
Bandwidth on
11-Jul-2022
Take-off Call
Bandwidth (kHz)
Time (ms)

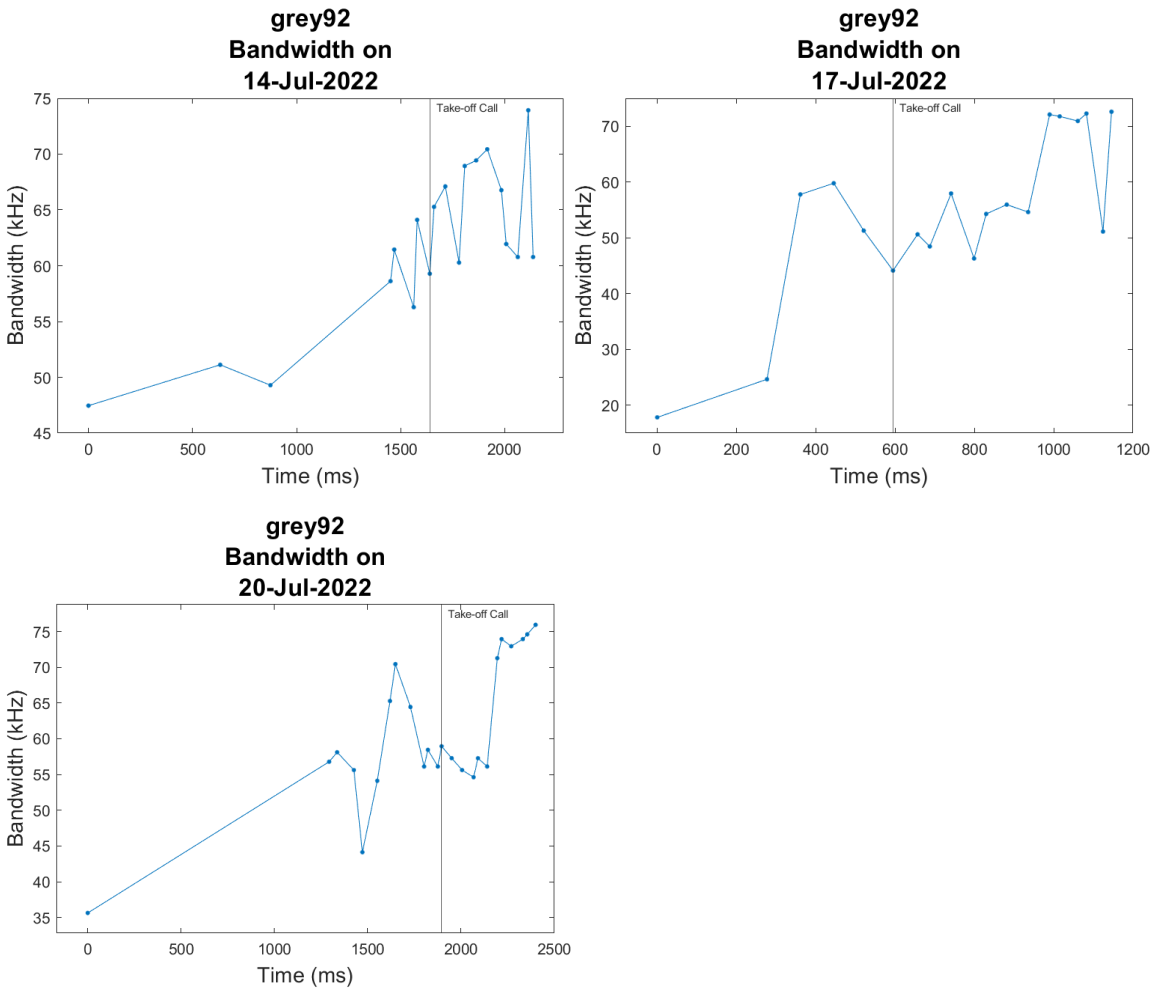

Appendix Figure 46: Grey 92 call bandwidth plotted as a function of recording time per recording date. Each panel shows call durations before and after taking flight, with different panels showing data recorded on different recording dates. The take-off call is marked by a vertical line.

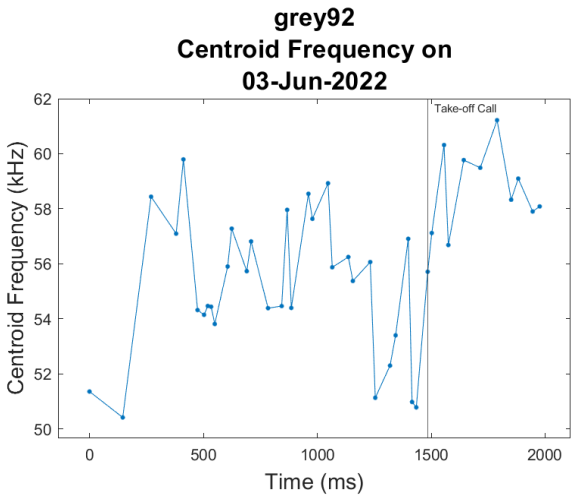
grey92
Centroid Frequency on
03-Jun-2022
Take-off Call
Centroid Frequency (kHz)
Time (ms)

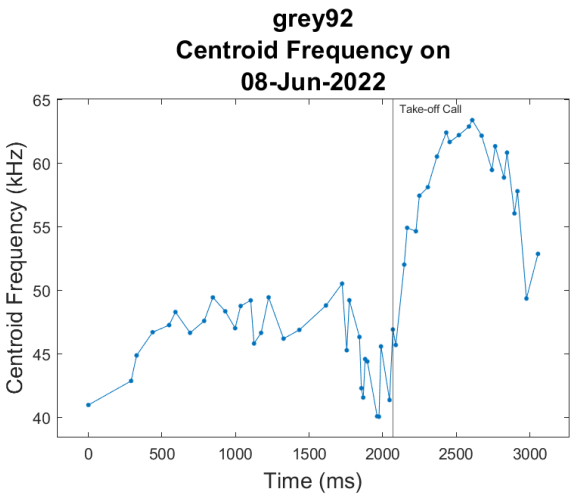
grey92
Centroid Frequency on
08-Jun-2022
Take-off Call
Centroid Frequency (kHz)
Time (ms)

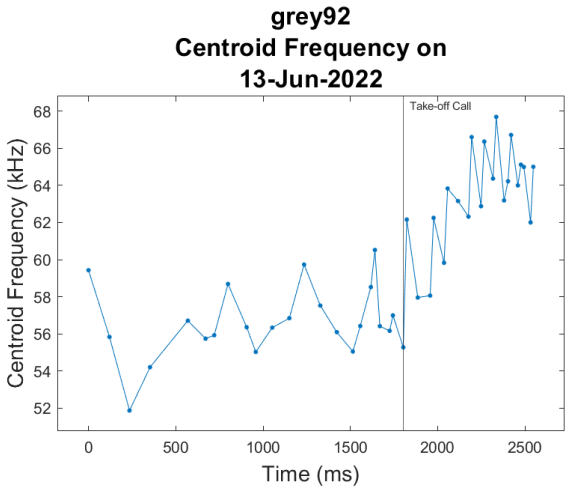
grey92
Centroid Frequency on
13-Jun-2022
Take-off Call
Centroid Frequency (kHz)
Time (ms)

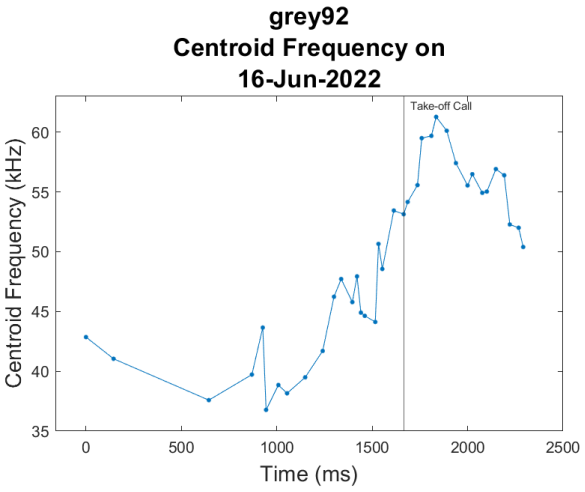
grey92
Centroid Frequency on
16-Jun-2022
Take-off Call
Centroid Frequency (kHz)
Time (ms)

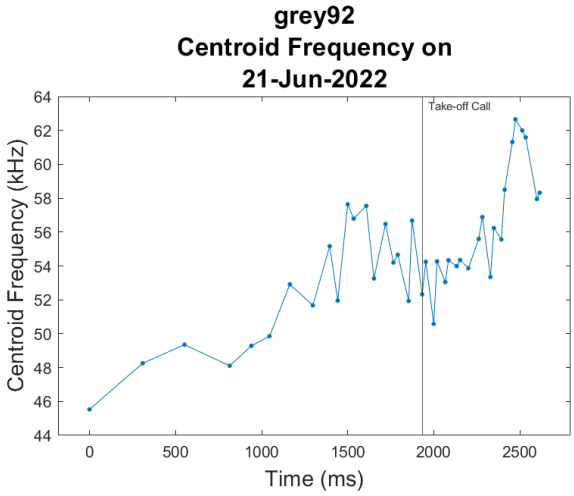
grey92
Centroid Frequency on
21-Jun-2022
Take-off Call
Centroid Frequency (kHz)
Time (ms)

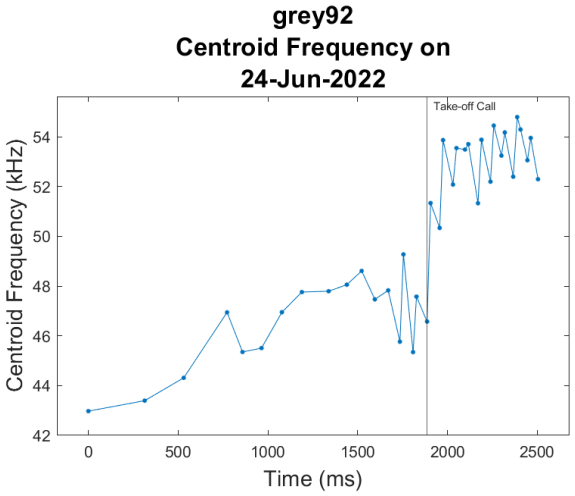
grey92
Centroid Frequency on
24-Jun-2022
Take-off Call
Centroid Frequency (kHz)
Time (ms)

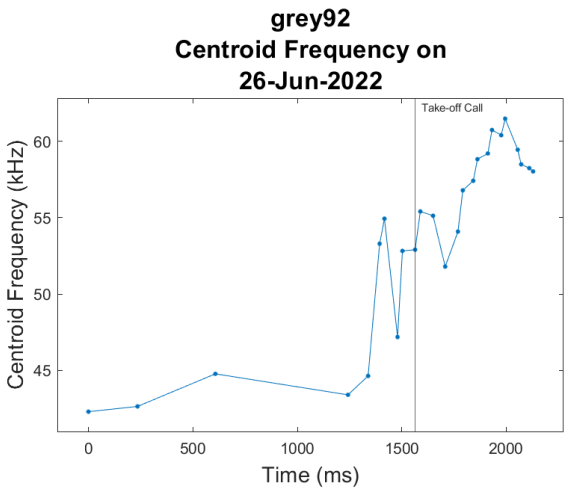
grey92
Centroid Frequency on
26-Jun-2022
Take-off Call
Centroid Frequency (kHz)
Time (ms)

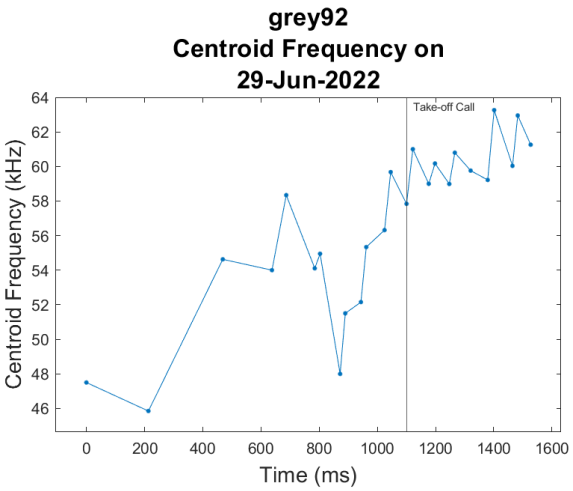
grey92
Centroid Frequency on
29-Jun-2022
Take-off Call
Centroid Frequency (kHz)
Time (ms)

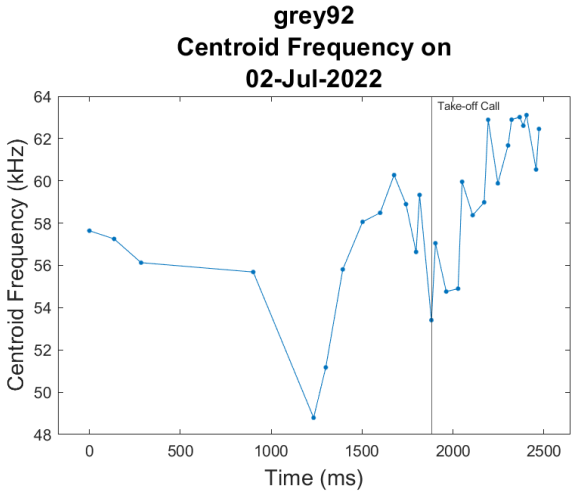
grey92
Centroid Frequency on
02-Jul-2022
Take-off Call
Centroid Frequency (kHz)
Time (ms)

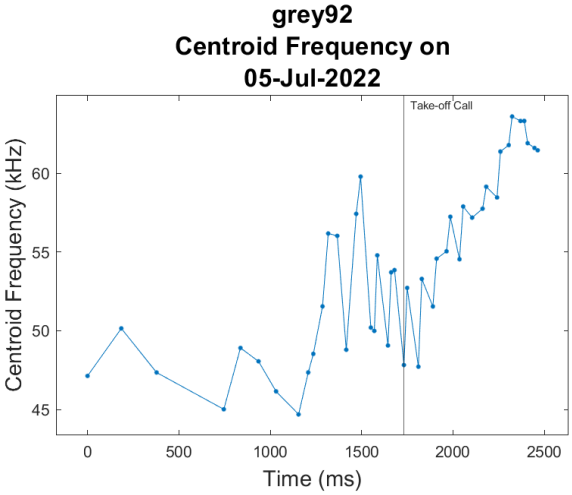
grey92
Centroid Frequency on
05-Jul-2022
Take-off Call
Centroid Frequency (kHz)
Time (ms)

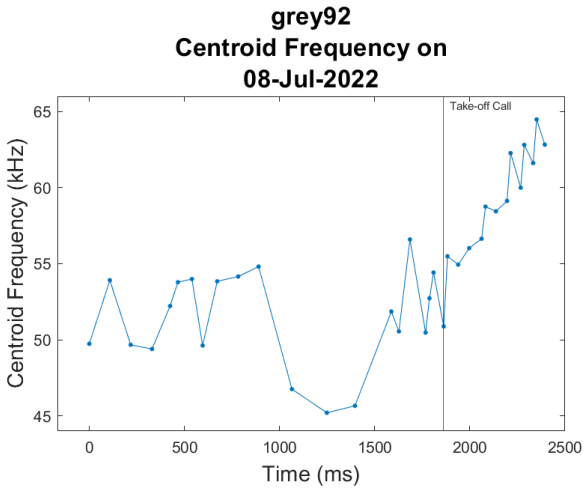
grey92
Centroid Frequency on
08-Jul-2022
Take-off Call
Centroid Frequency (kHz)
Time (ms)

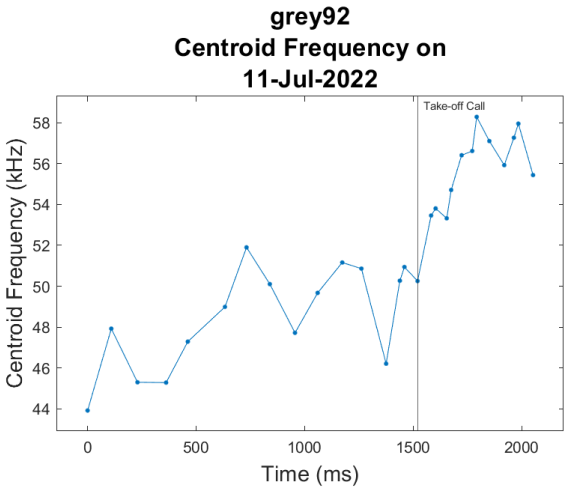
grey92
Centroid Frequency on
11-Jul-2022
Take-off Call
Centroid Frequency (kHz)
Time (ms)

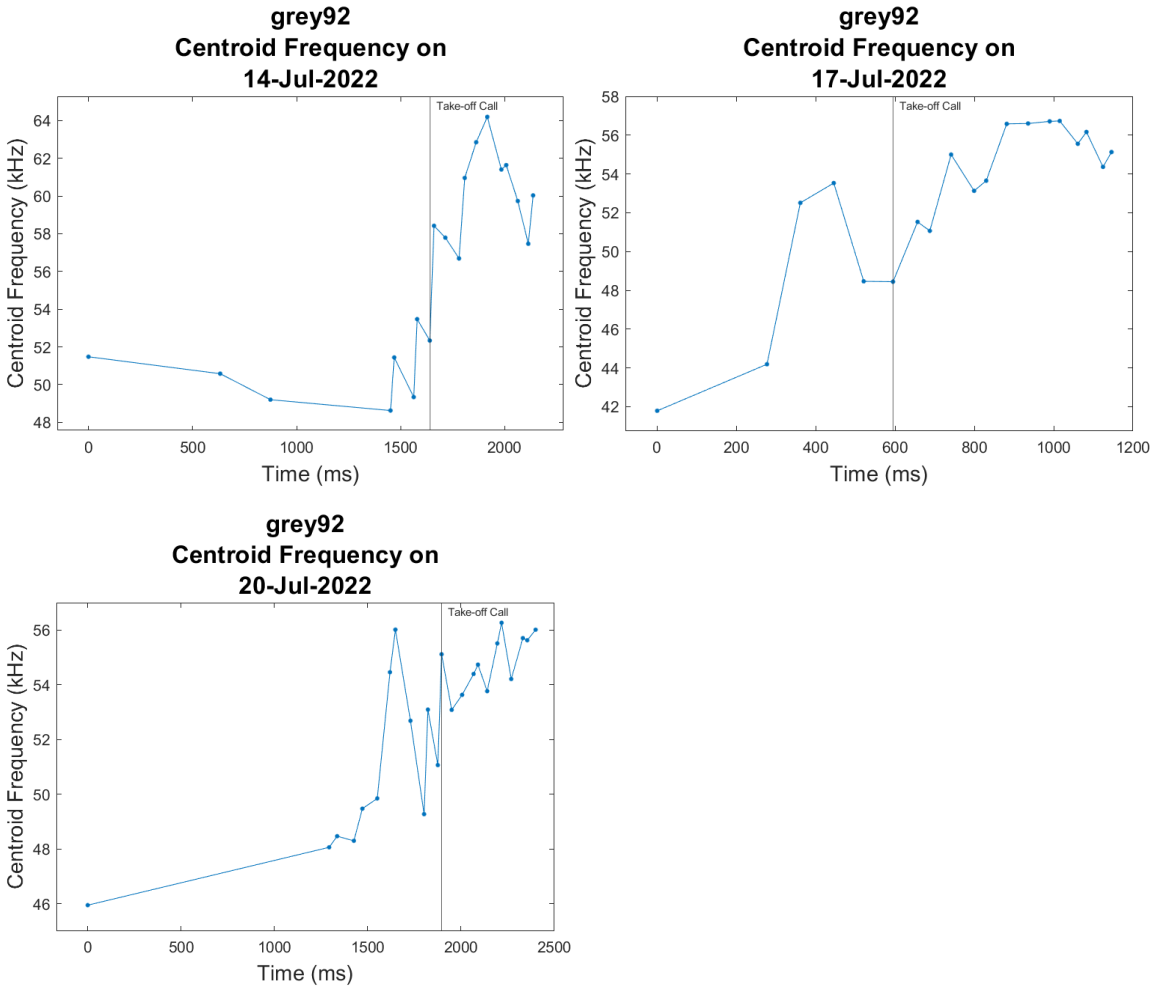

Appendix Figure 47: Grey 92 centroid frequency plotted as a function of time per recording date. Each panel shows call durations before and after taking flight, with different panels showing data recorded on different recording dates. The take-off call is marked by a vertical line.

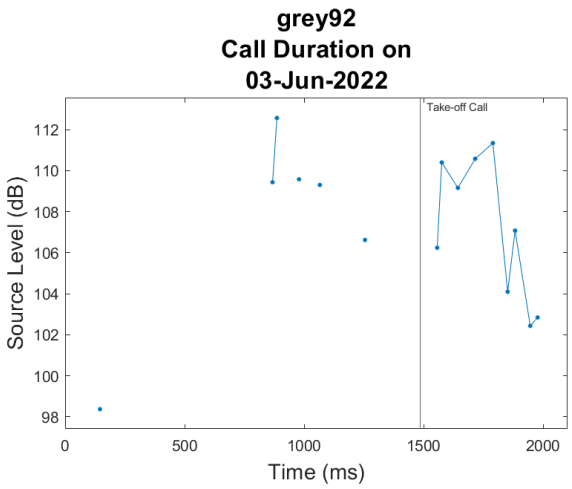
grey92
Call Duration on
03-Jun-2022
Take-off Call
Source Level (dB)
Time (ms)

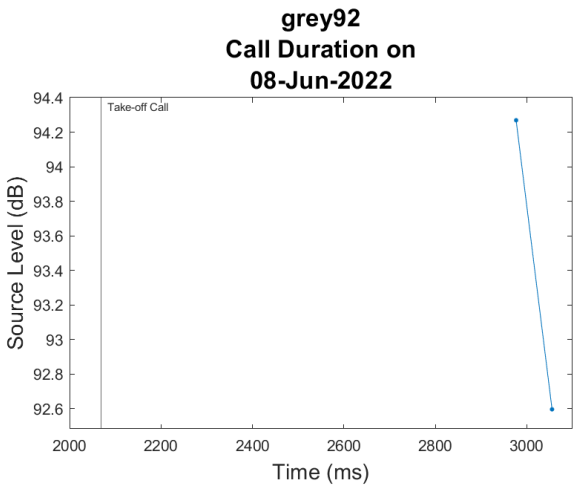
grey92
Call Duration on
08-Jun-2022
Take-off Call
Source Level (dB)
Time (ms)

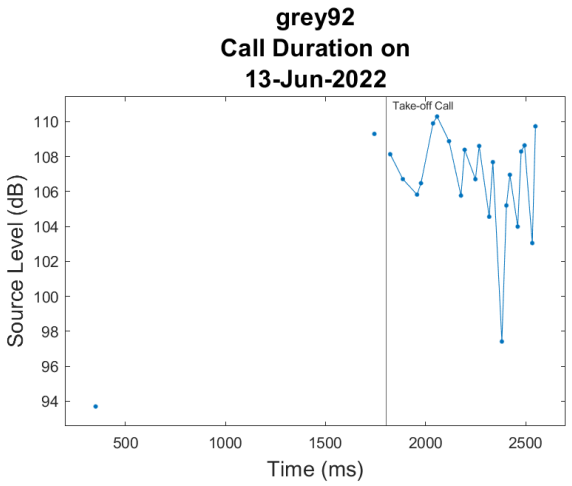
grey92
Call Duration on
13-Jun-2022
Take-off Call
Source Level (dB)
Time (ms)

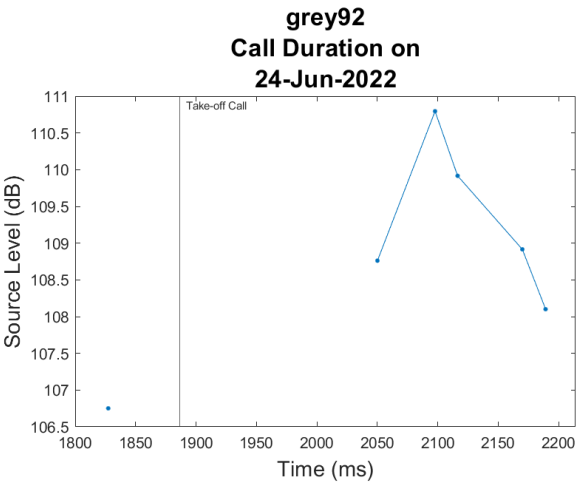
grey92
Call Duration on
24-Jun-2022
Take-off Call
Source Level (dB)
Time (ms)

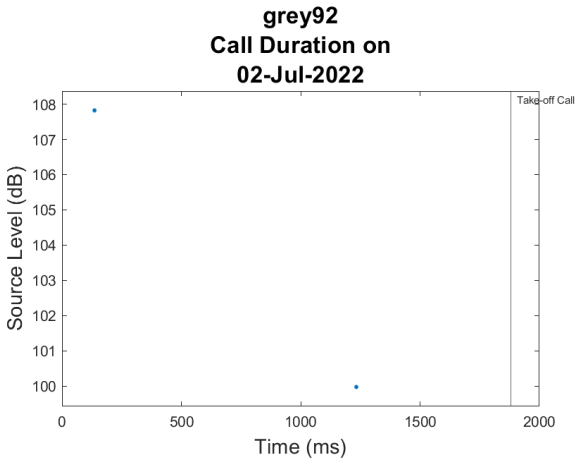
grey92
Call Duration on
02-Jul-2022
Take-off Call
Source Level (dB)
Time (ms)

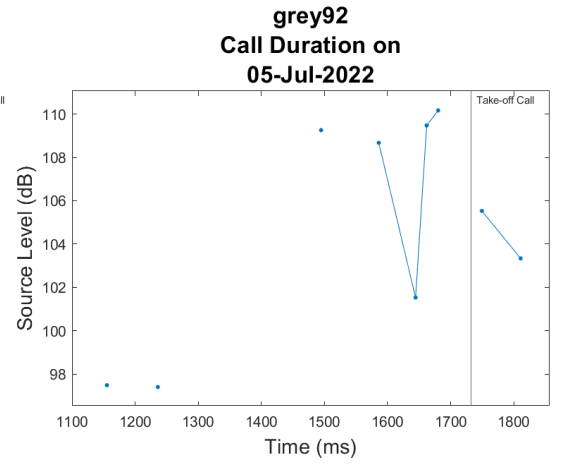
grey92
Call Duration on
05-Jul-2022
Take-off Call
Source Level (dB)
Time (ms)

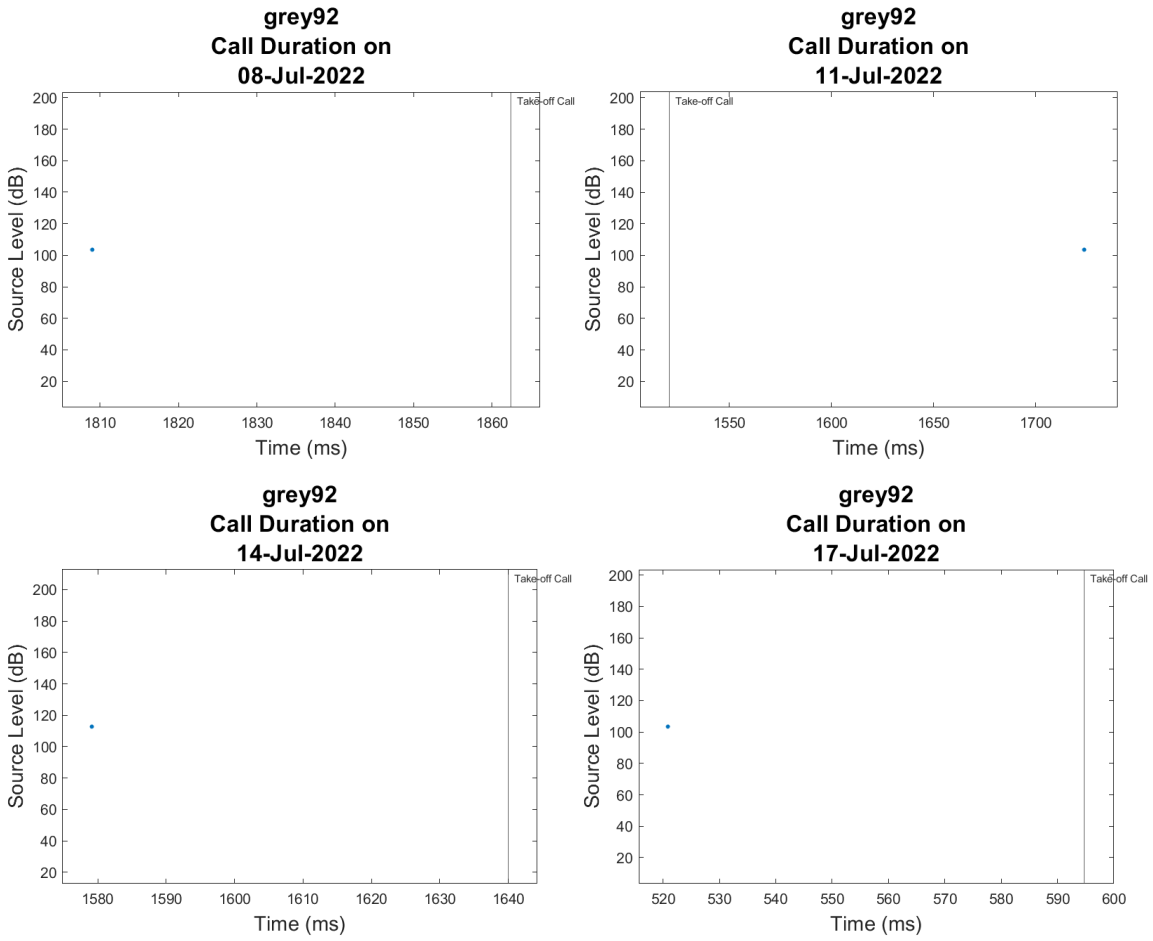

Appendix Figure 48: Grey 92 source level plotted as a function of recording time per recording date. Each panel shows call durations before and after taking flight, with different panels showing data recorded on different recording dates. The take-off call is marked by a vertical line.

Grey 94 Echolocation Call Characteristics Graphs

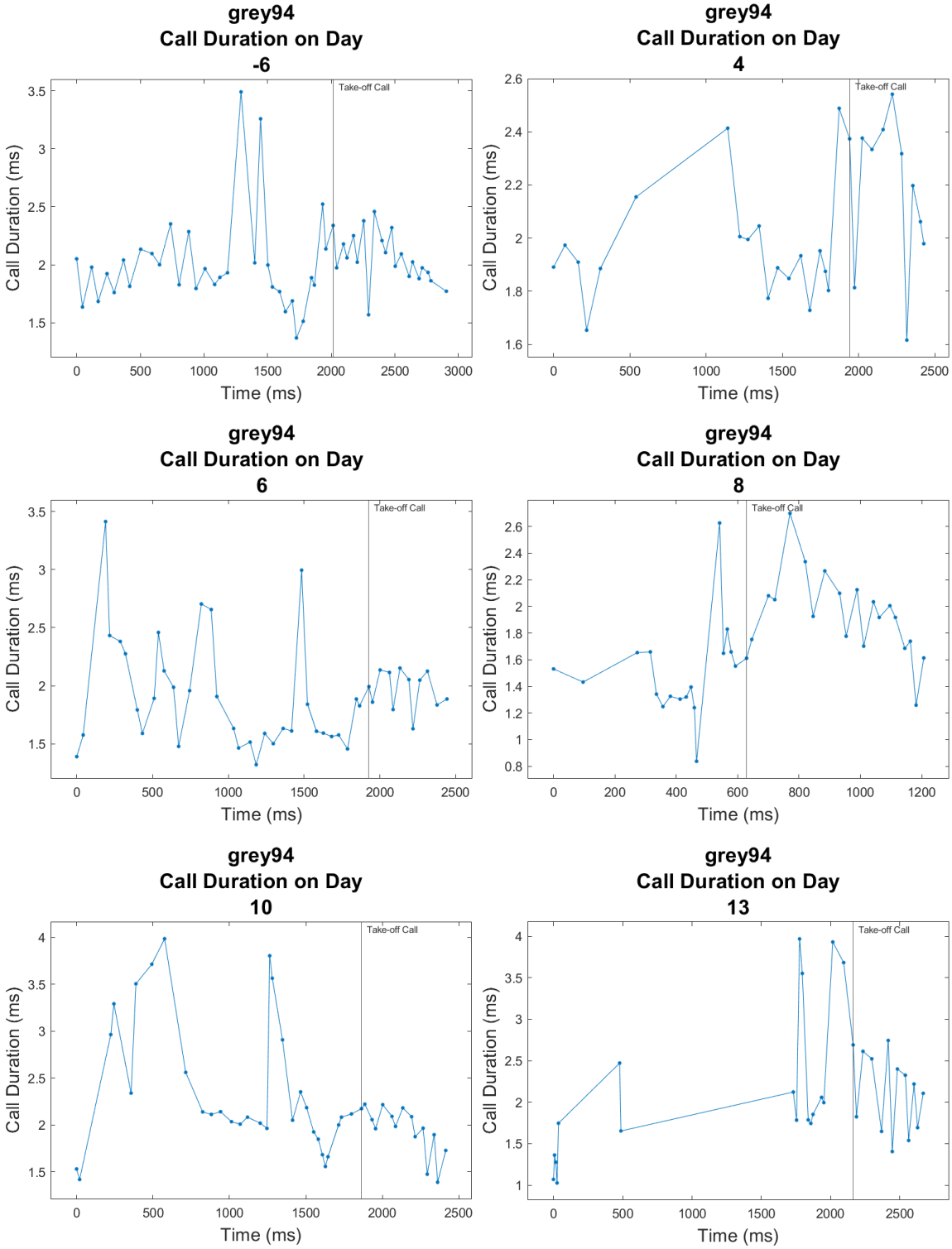

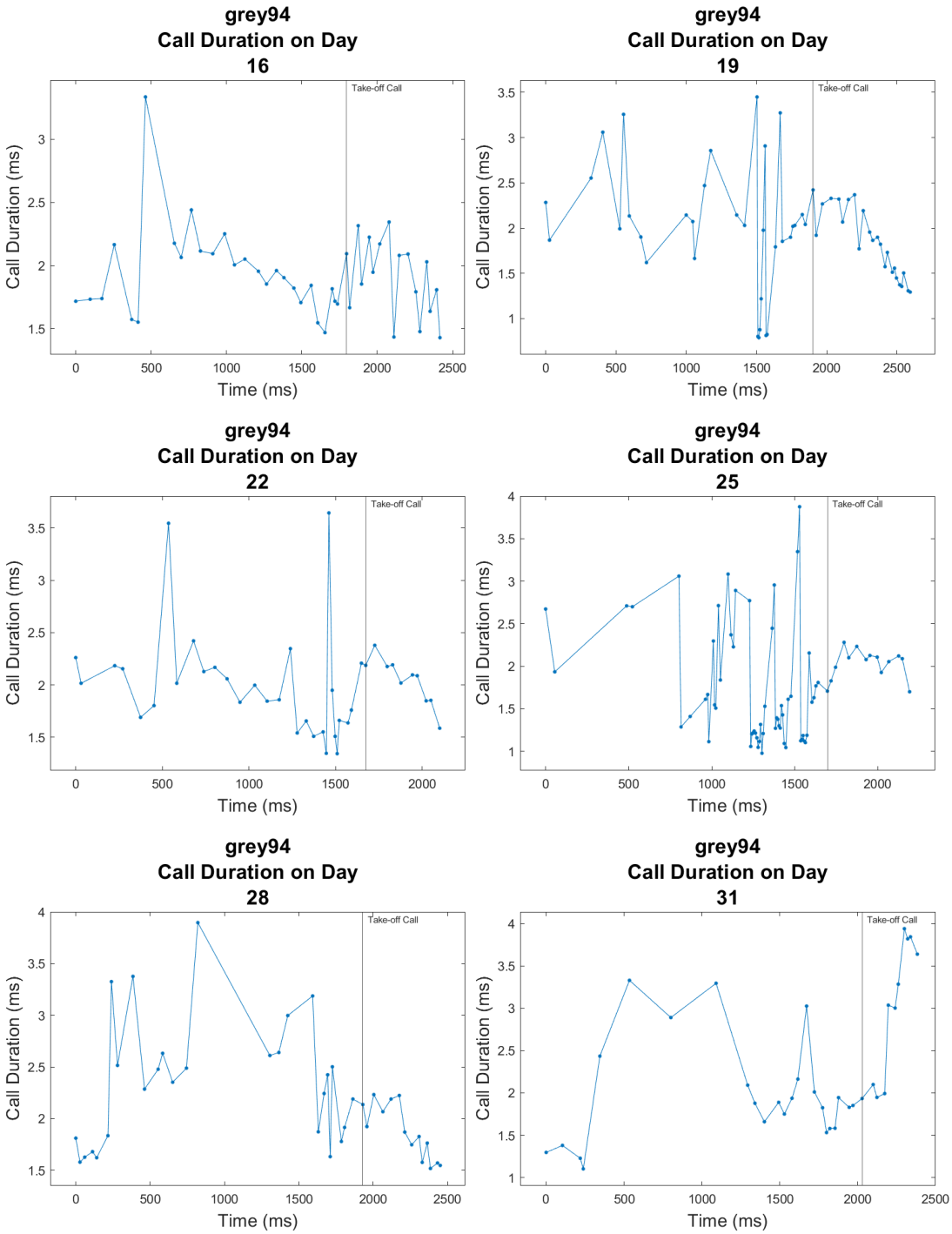

Appendix Figure 49: Grey 94 call duration plotted as a function of recording time per day. Each panel shows call durations before and after taking flight, with different panels showing data recorded on different days relative to parturition (number above panel; parturition day defined as Day 0). The take-off call is marked by a vertical line.

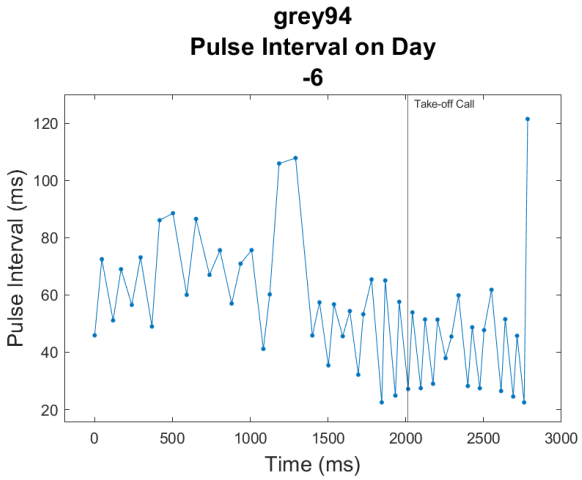
grey94
Pulse Interval on Day
-6
Take-off Call
Pulse Interval (ms)
Time (ms)

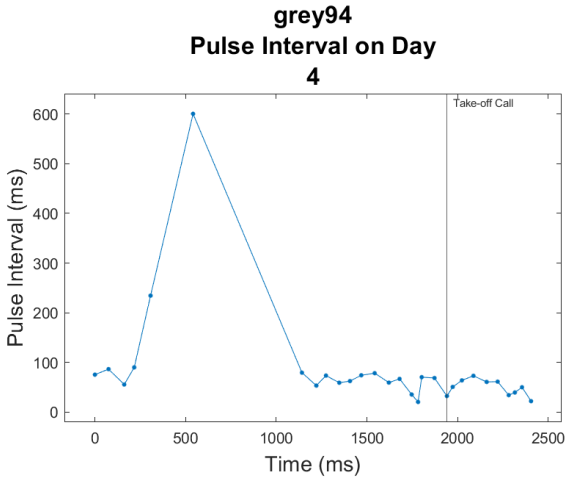
grey94
Pulse Interval on Day
4
Take-off Call
Pulse Interval (ms)
Time (ms)

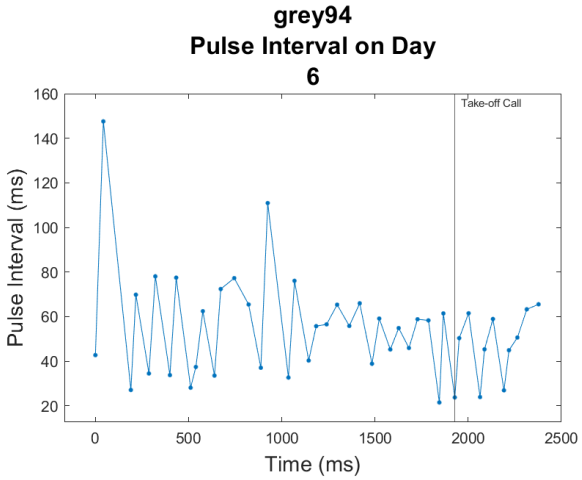
grey94
Pulse Interval on Day
6
Take-off Call
Pulse Interval (ms)
Time (ms)

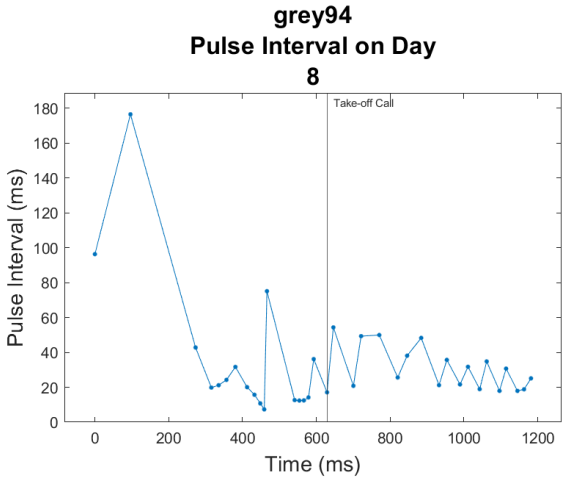
grey94
Pulse Interval on Day
8
Take-off Call
Pulse Interval (ms)
Time (ms)

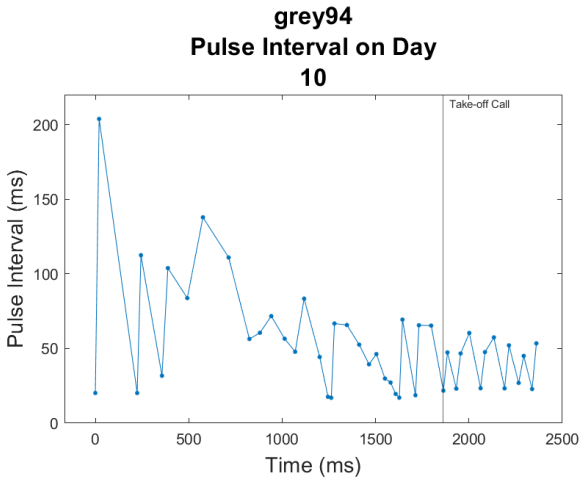
grey94
Pulse Interval on Day
10
Take-off Call
Pulse Interval (ms)
Time (ms)

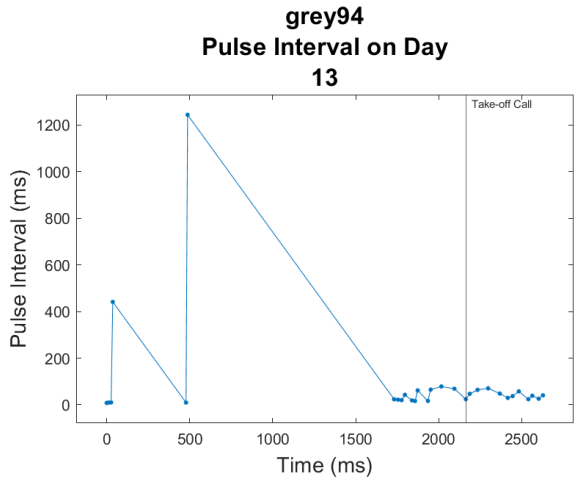
grey94
Pulse Interval on Day
13
Take-off Call
Pulse Interval (ms)
Time (ms)

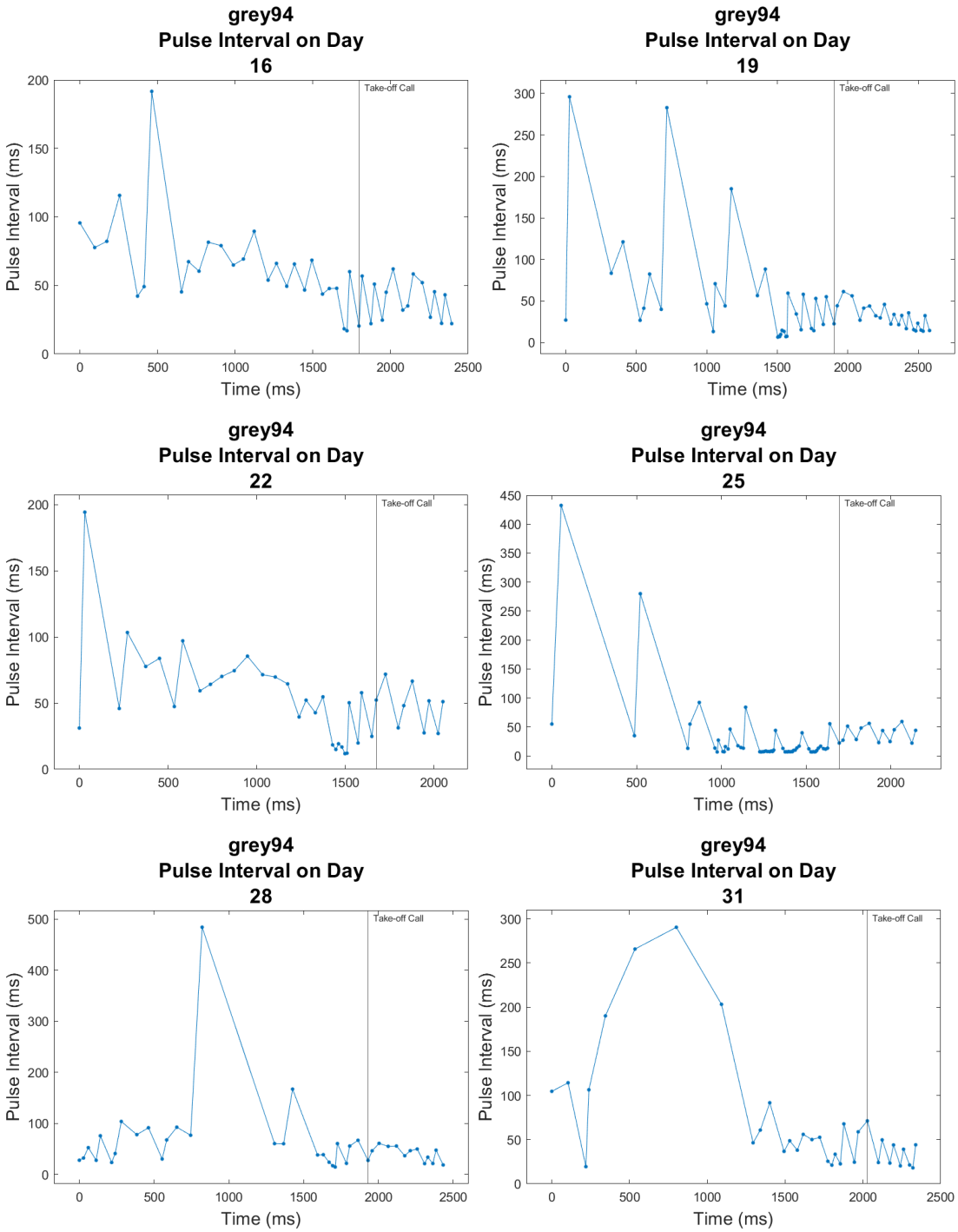

Appendix Figure 50: Grey 94 pulse interval plotted as a function of recording time per day. Each panel shows call durations before and after taking flight, with different panels showing data recorded on different days relative to parturition (number above panel; parturition day defined as Day 0). The take-off call is marked by a vertical line.

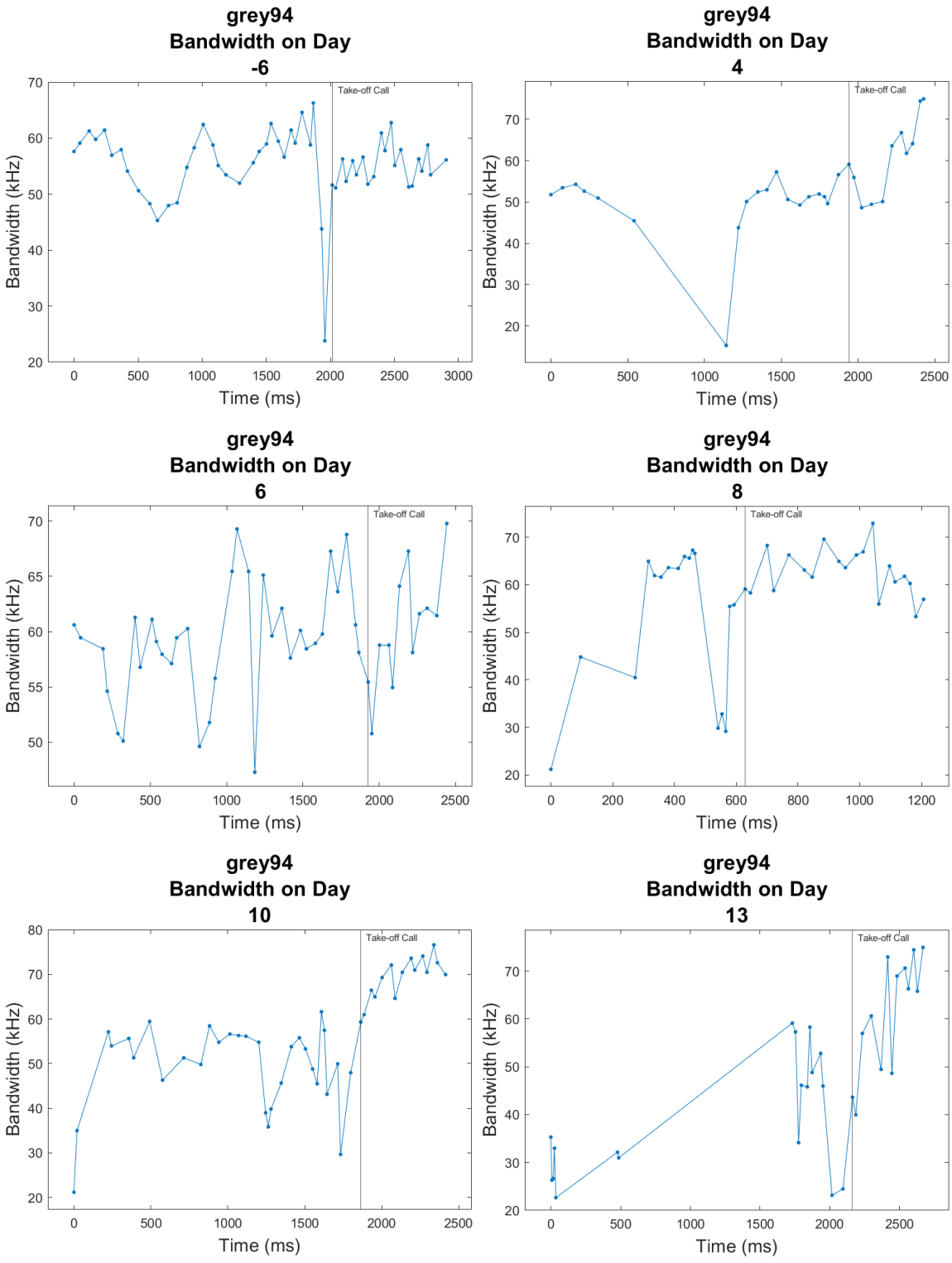
grey94
Bandwidth on Day
-6
Take-off Call
Bandwidth (kHz)
Time (ms)
grey94
Bandwidth on Day
4
Take-off Call
Bandwidth (kHz)
Time (ms)
grey94
Bandwidth on Day
6
Take-off Call
Bandwidth (kHz)
Time (ms)
grey94
Bandwidth on Day
8
Take-off Call
Bandwidth (kHz)
Time (ms)
grey94
Bandwidth on Day
10
Take-off Call
Bandwidth (kHz)
Time (ms)
grey94
Bandwidth on Day
13
Take-off Call
Bandwidth (kHz)
Time (ms)

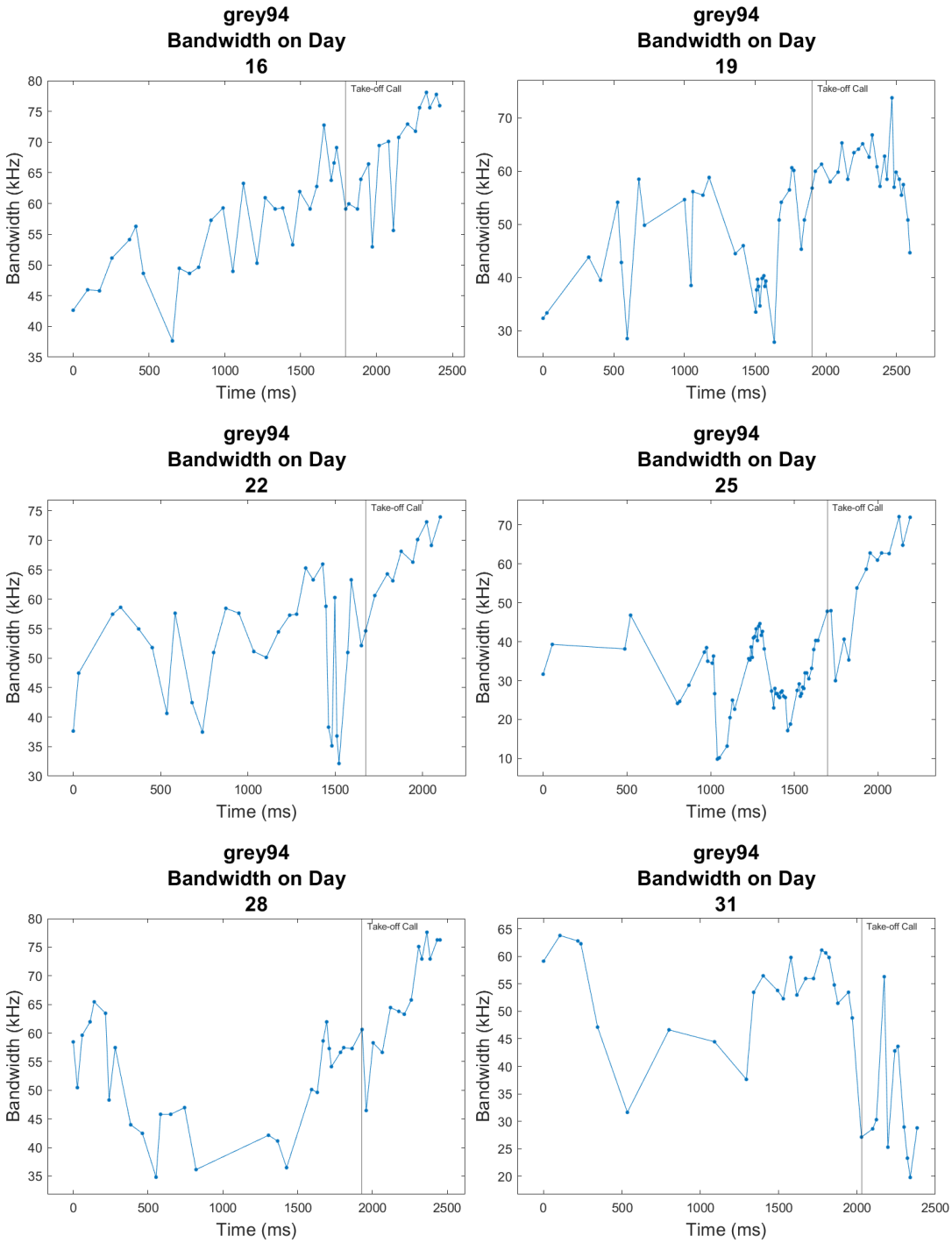

Appendix Figure 51: Grey 94 call bandwidth plotted as a function of recording time per day. Each panel shows call durations before and after taking flight, with different panels showing data recorded on different days relative to parturition (number above panel; parturition day defined as Day 0). The take-off call is marked by a vertical line.

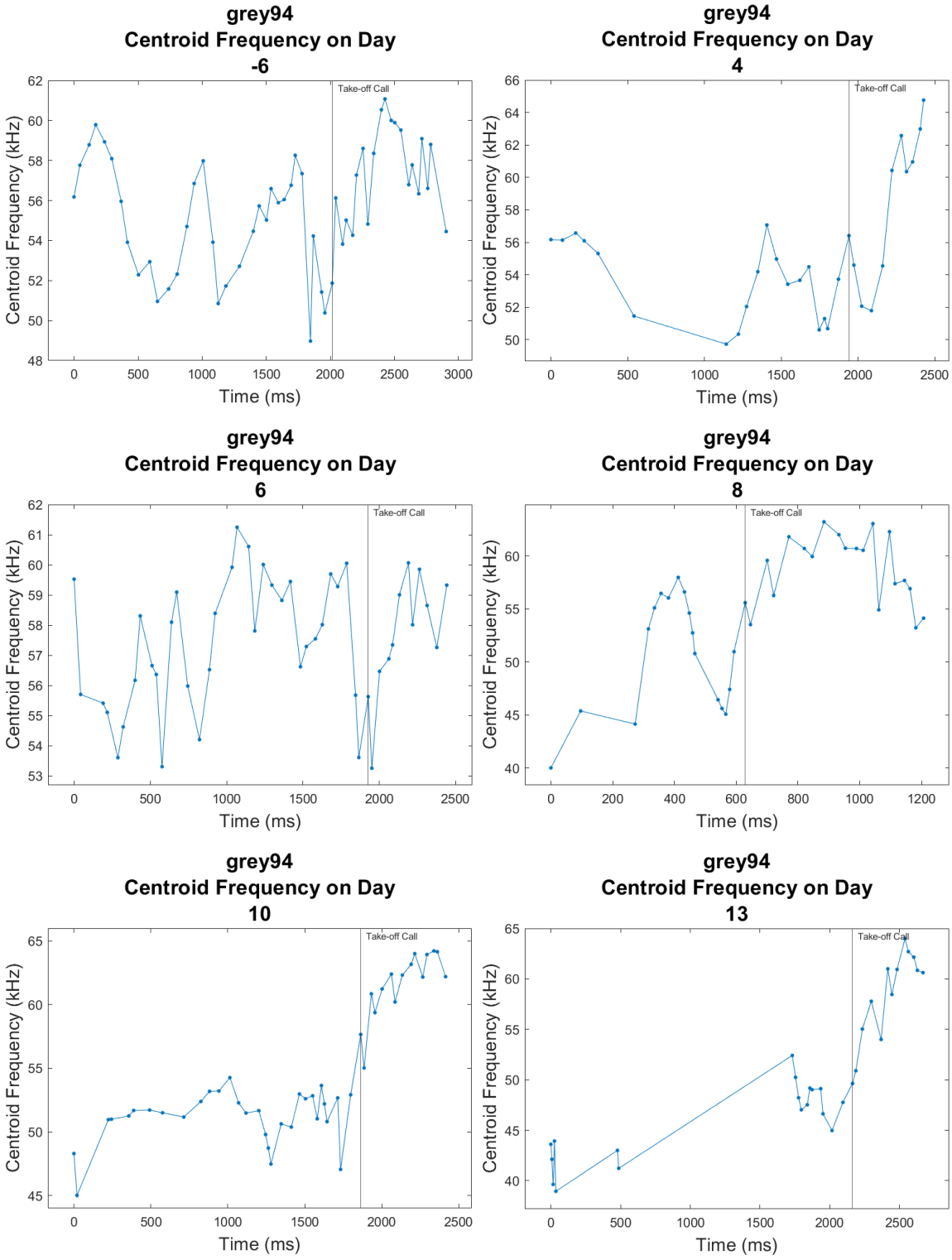
grey94
Centroid Frequency on Day -6
grey94
Centroid Frequency on Day 4
grey94
Centroid Frequency on Day 6
grey94
Centroid Frequency on Day 8
grey94
Centroid Frequency on Day 10
grey94
Centroid Frequency on Day 13
Take-off Call
Centroid Frequency (kHz)
Time (ms)

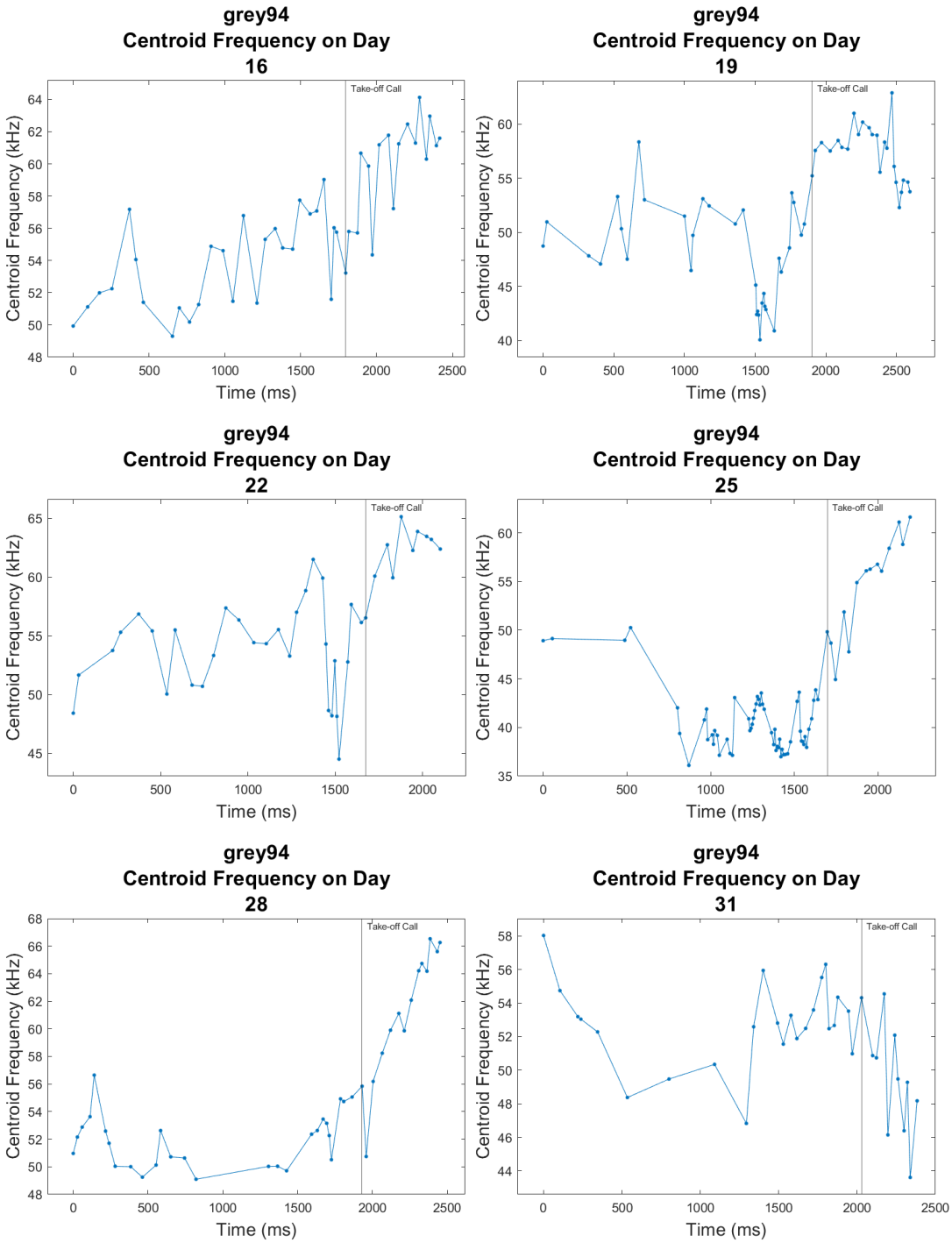

Appendix Figure 52: Grey 94 centroid frequency plotted as a function of recording time per day. Each panel shows call durations before and after taking flight, with different panels showing data recorded on different days relative to parturition (number above panel; parturition day defined as Day 0). The take-off call is marked by a vertical line.

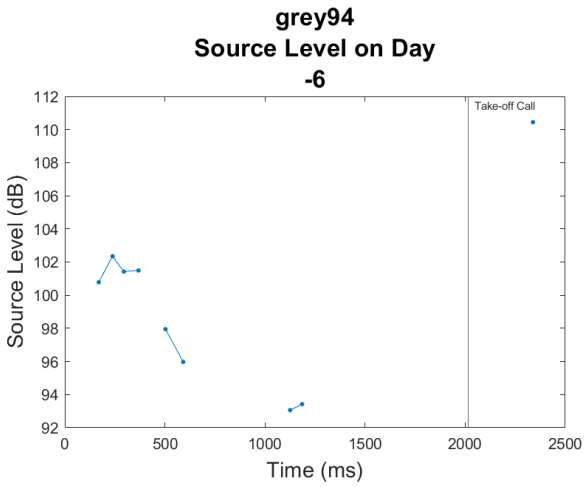
grey94
Source Level on Day
-6
Take-off Call
Source Level (dB)
Time (ms)

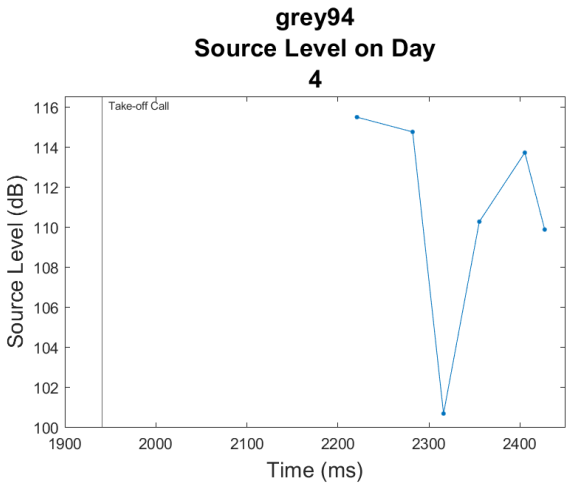
grey94
Source Level on Day
4
Take-off Call
Source Level (dB)
Time (ms)

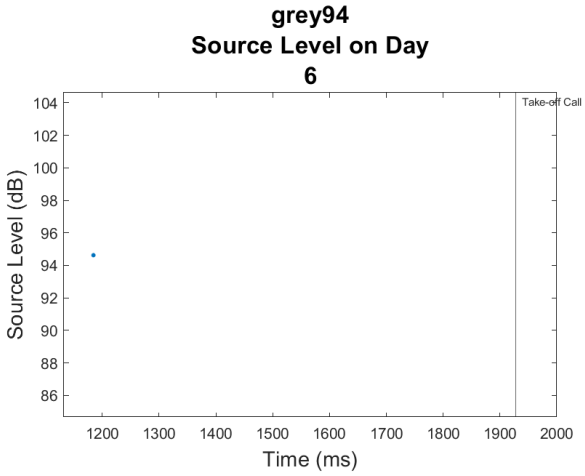
grey94
Source Level on Day
6
Take-off Call
Source Level (dB)
Time (ms)

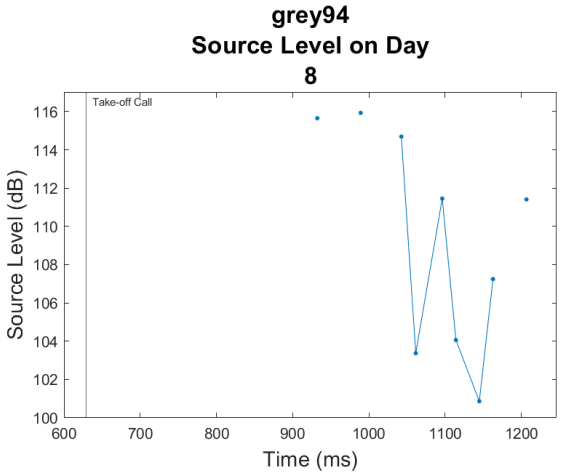
grey94
Source Level on Day
8
Take-off Call
Source Level (dB)
Time (ms)

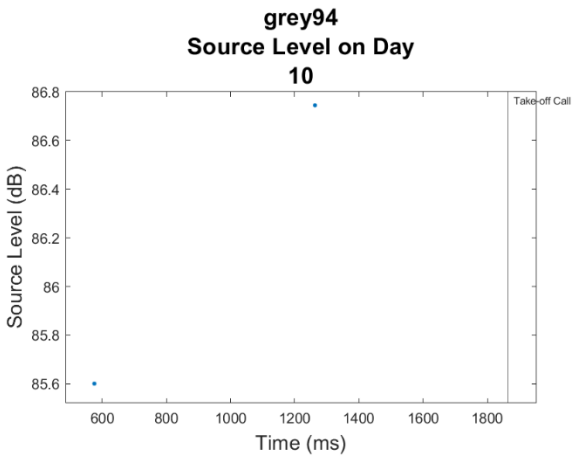
grey94
Source Level on Day
10
Take-off Call
Source Level (dB)
Time (ms)

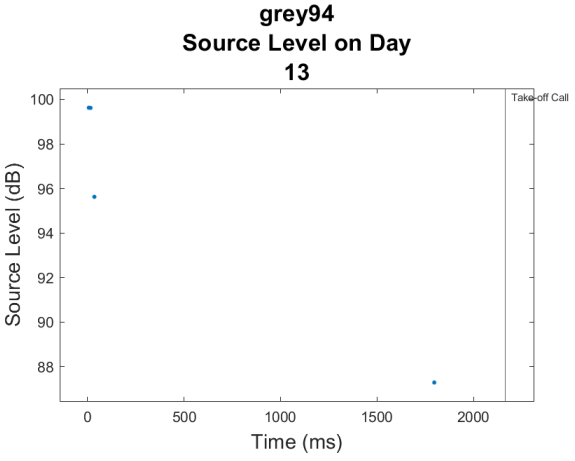
grey94
Source Level on Day
13
Take-off Call
Source Level (dB)
Time (ms)

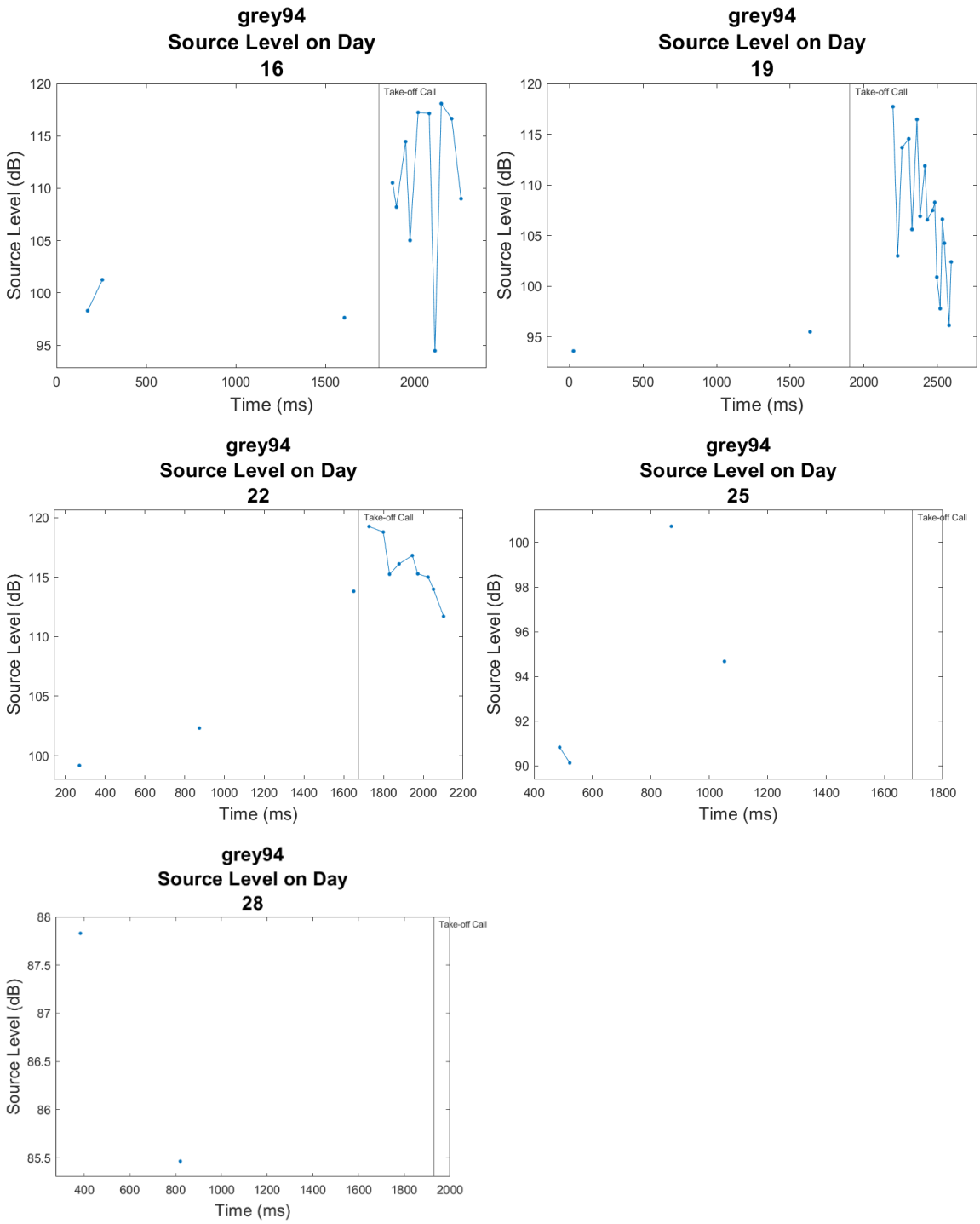

Appendix Figure 53: Grey 94 source level plotted as a function of recording time per day. Each panel shows call durations before and after taking flight, with different panels showing data recorded on different days relative to parturition (number above panel; parturition day defined as Day 0). The take-off call is marked by a vertical line.

Grey 97 Echolocation Call Characteristics Graphs

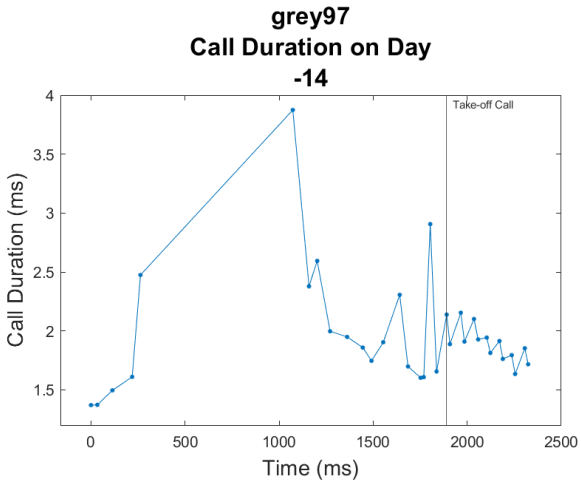

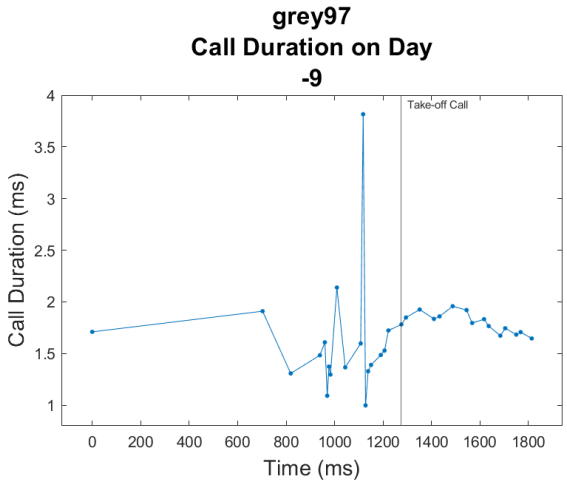

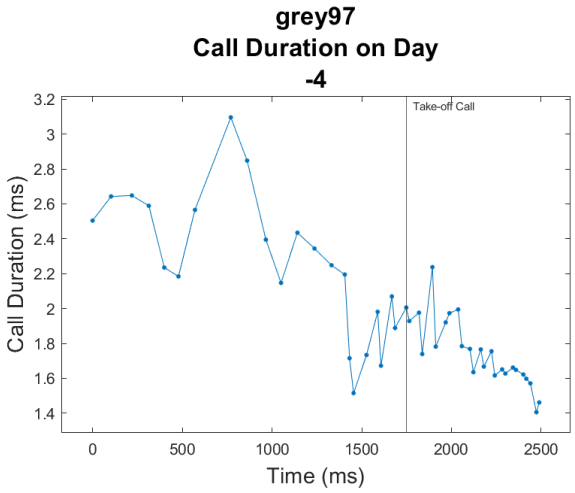

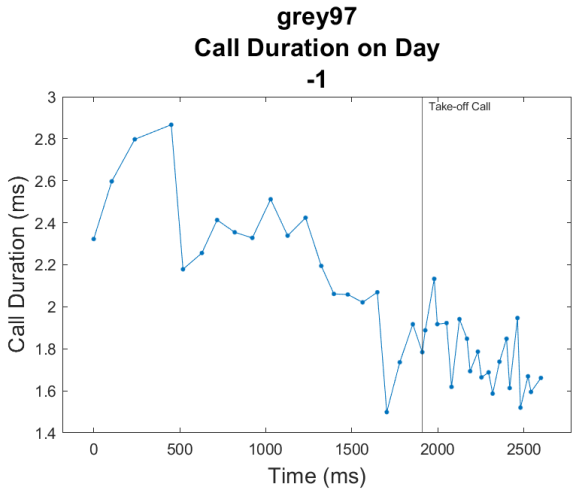

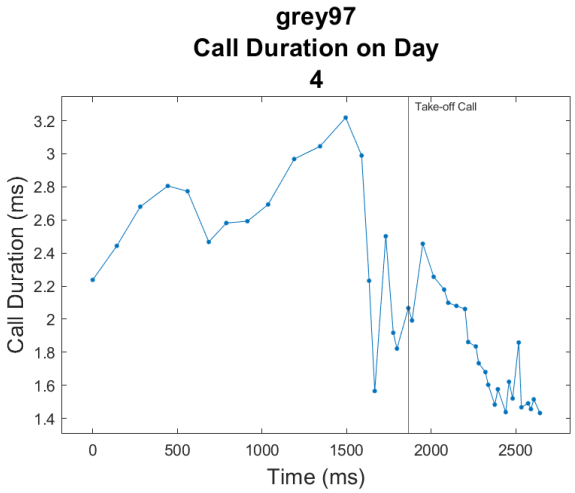

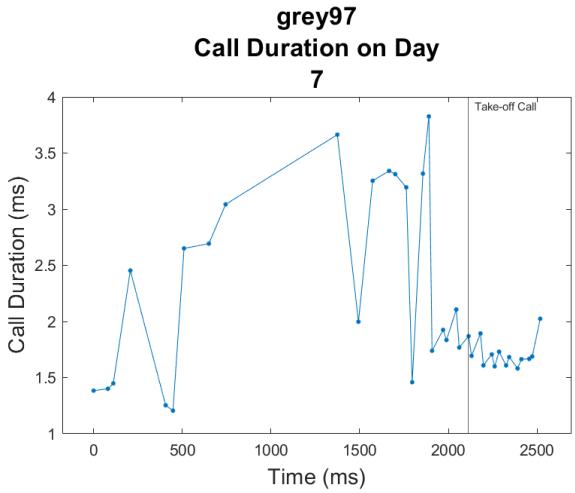

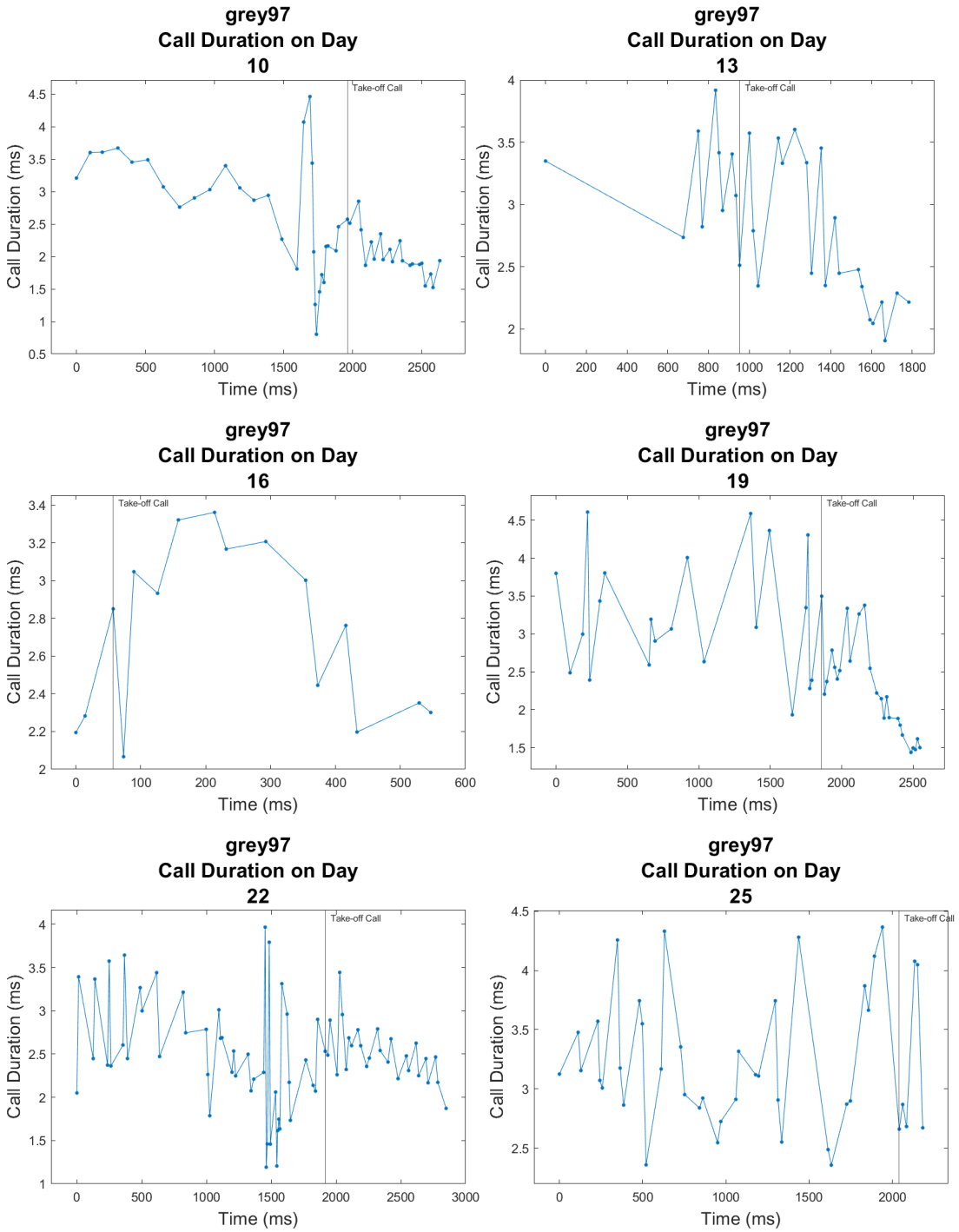

Appendix Figure 54: Grey 97 call duration plotted as a function of recording time per day. Each panel shows call durations before and after taking flight, with different panels showing data recorded on different days relative to parturition (number above panel; parturition day defined as Day 0). The take-off call is marked by a vertical line.

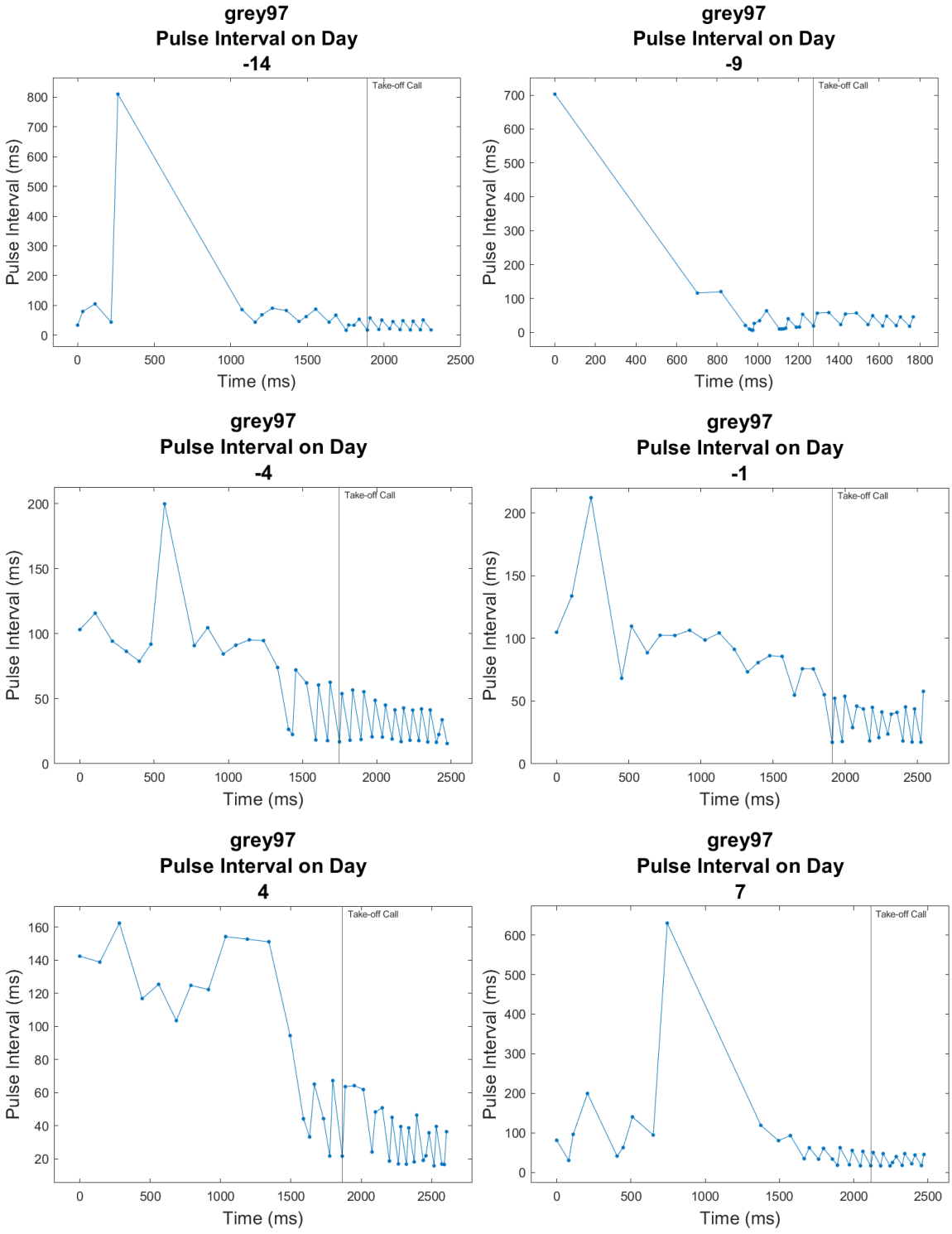
grey97
Pulse Interval on Day
-14
Take-off Call
Pulse Interval (ms)
Time (ms)
grey97
Pulse Interval on Day
-9
Take-off Call
Pulse Interval (ms)
Time (ms)
grey97
Pulse Interval on Day
-4
Take-off Call
Pulse Interval (ms)
Time (ms)
grey97
Pulse Interval on Day
-1
Take-off Call
Pulse Interval (ms)
Time (ms)
grey97
Pulse Interval on Day
4
Take-off Call
Pulse Interval (ms)
Time (ms)
grey97
Pulse Interval on Day
7
Take-off Call
Pulse Interval (ms)
Time (ms)

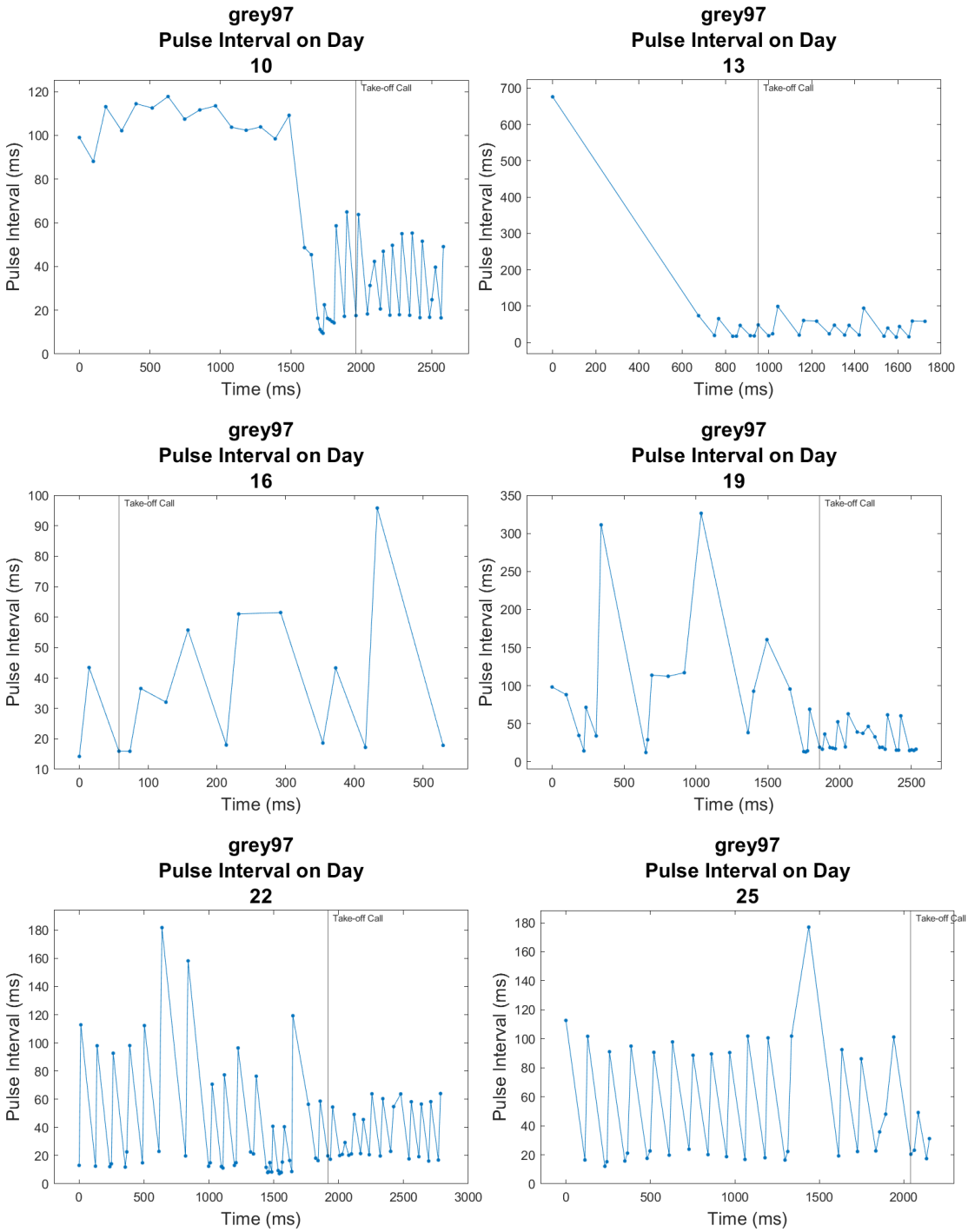

Appendix Figure 55: Grey 97 pulse interval plotted as a function of recording time per day. Each panel shows call durations before and after taking flight, with different panels showing data recorded on different days relative to parturition (number above panel; parturition day defined as Day 0). The take-off call is marked by a vertical line.

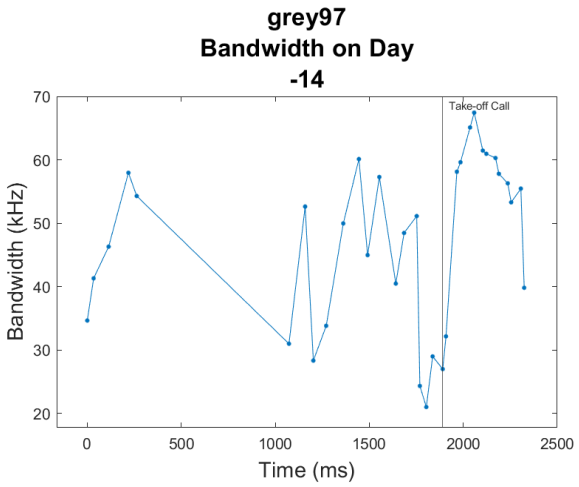
grey97
Bandwidth on Day
-14
Take-off Call
Bandwidth (kHz)
Time (ms)

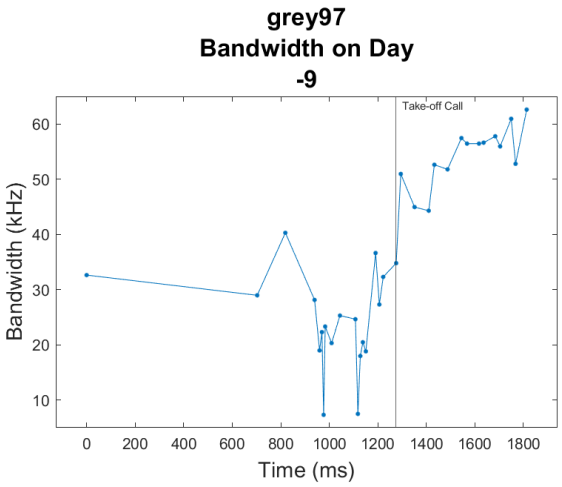
grey97
Bandwidth on Day
-9
Take-off Call
Bandwidth (kHz)
Time (ms)

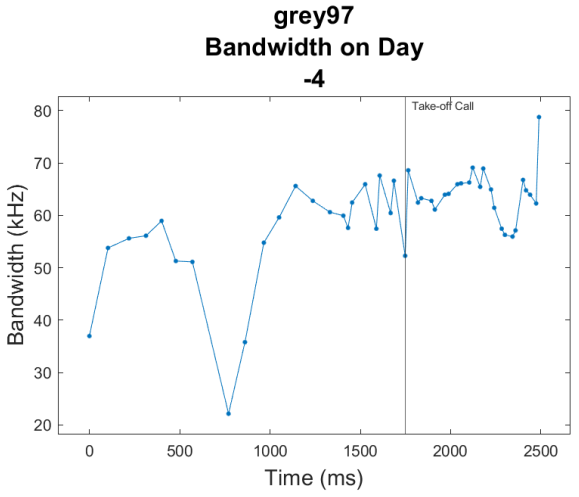
grey97
Bandwidth on Day
-4
Take-off Call
Bandwidth (kHz)
Time (ms)

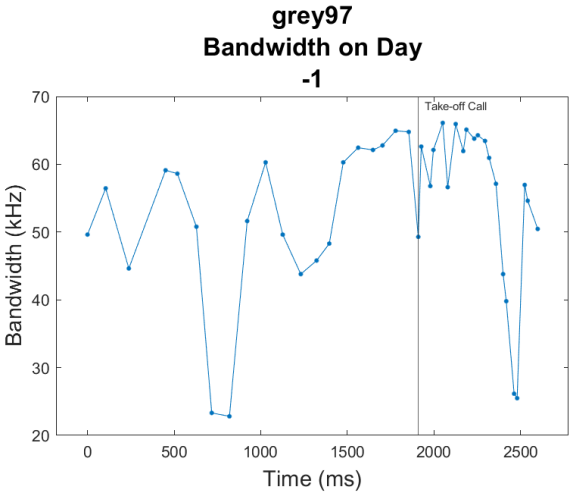
grey97
Bandwidth on Day
-1
Take-off Call
Bandwidth (kHz)
Time (ms)

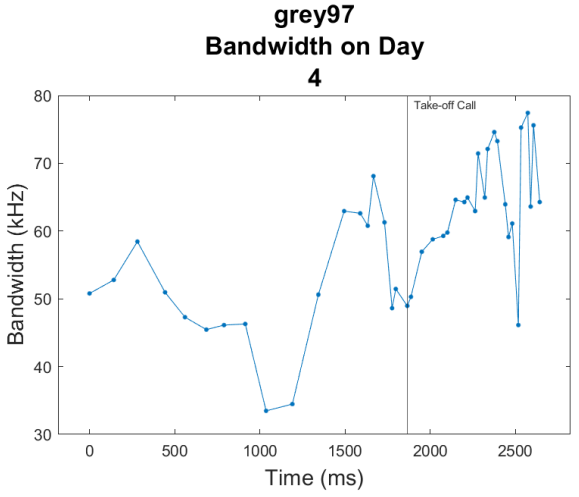
grey97
Bandwidth on Day
4
Take-off Call
Bandwidth (kHz)
Time (ms)

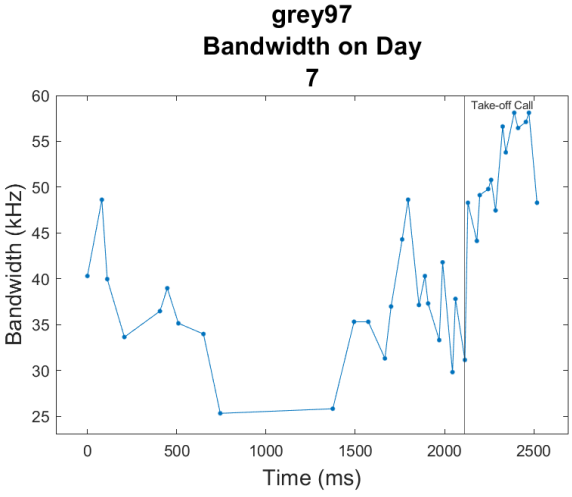
grey97
Bandwidth on Day
7
Take-off Call
Bandwidth (kHz)
Time (ms)

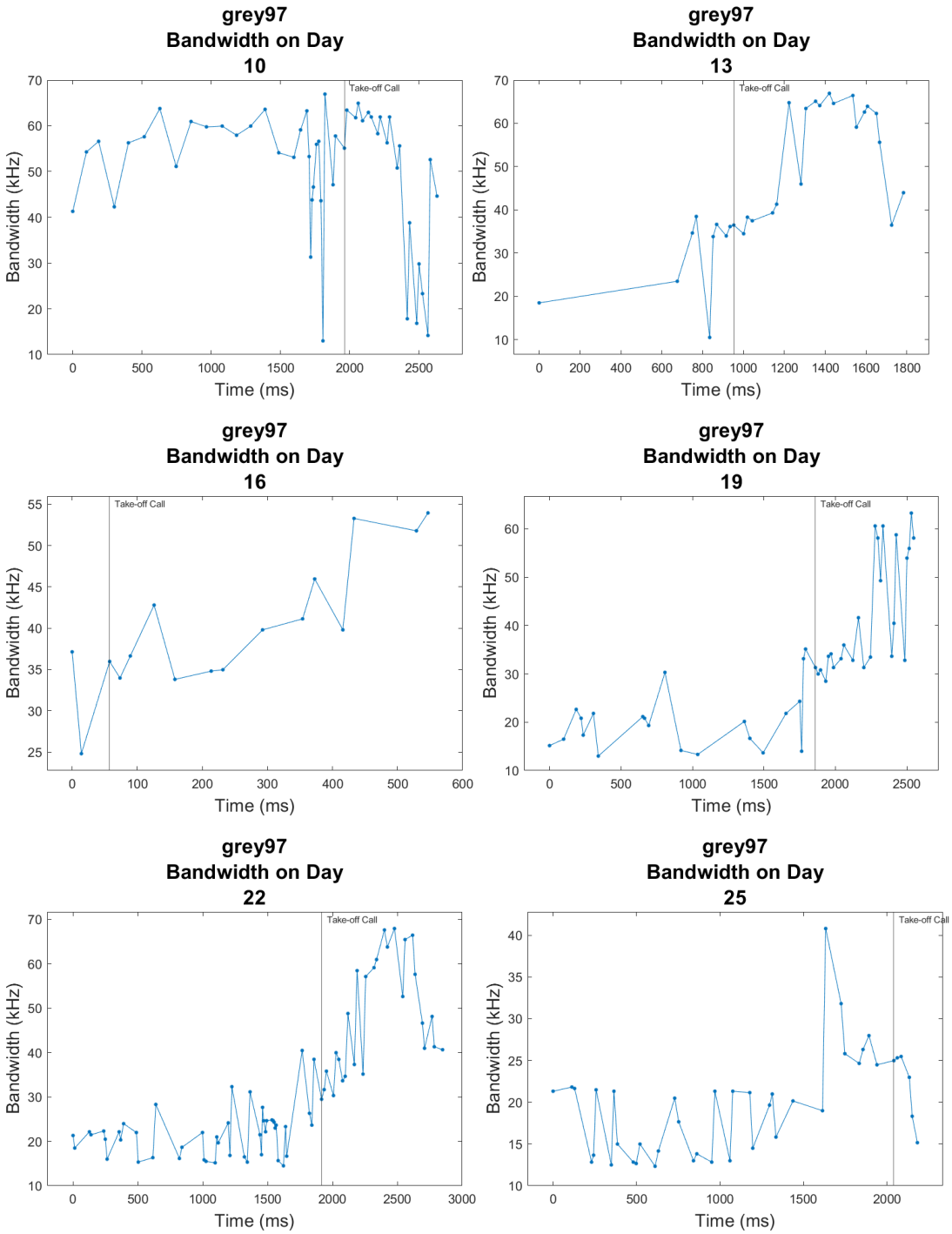

Appendix Figure 56: Grey 97 call bandwidth plotted as a function of recording time per day. Each panel shows call durations before and after taking flight, with different panels showing data recorded on different days relative to parturition (number above panel; parturition day defined as Day 0). The take-off call is marked by a vertical line.

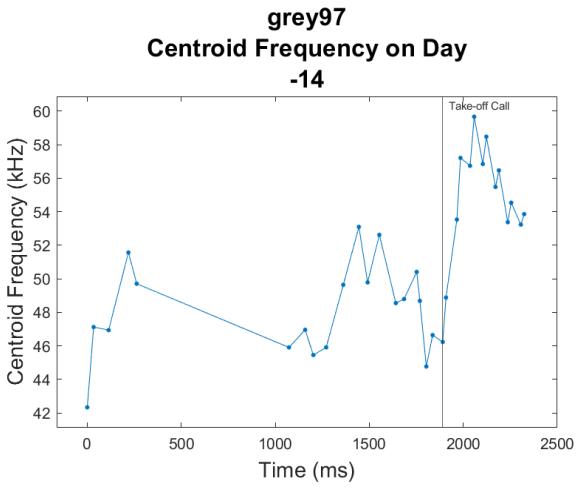
grey97
Centroid Frequency on Day
-14
Take-off Call
Centroid Frequency (kHz)
Time (ms)

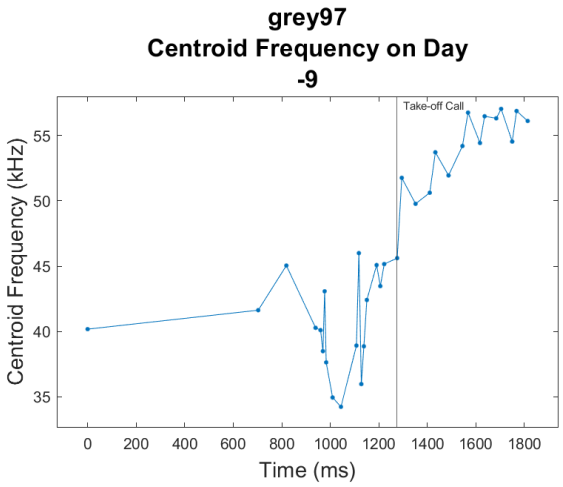
grey97
Centroid Frequency on Day
-9
Take-off Call
Centroid Frequency (kHz)
Time (ms)

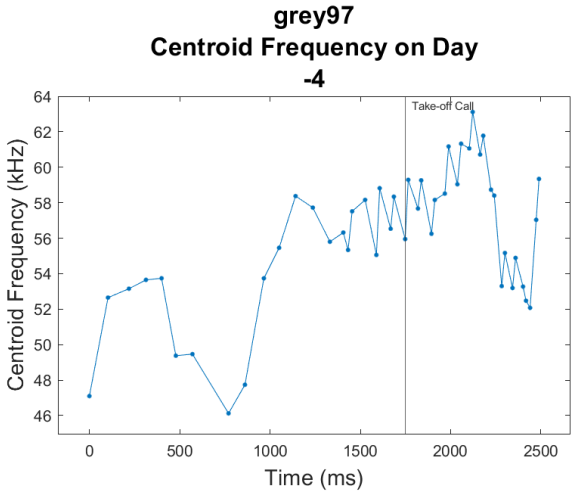
grey97
Centroid Frequency on Day
-4
Take-off Call
Centroid Frequency (kHz)
Time (ms)

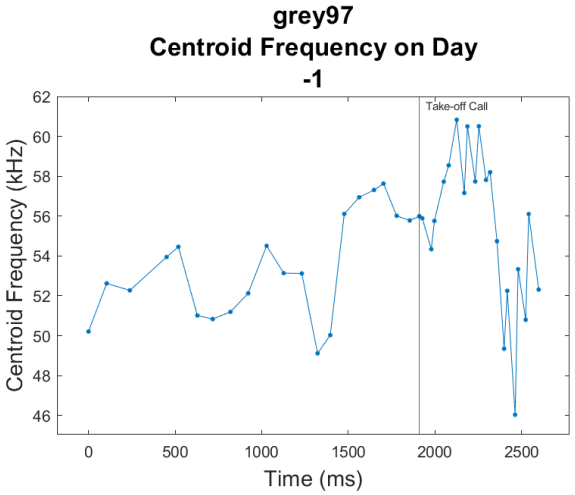
grey97
Centroid Frequency on Day
-1
Take-off Call
Centroid Frequency (kHz)
Time (ms)

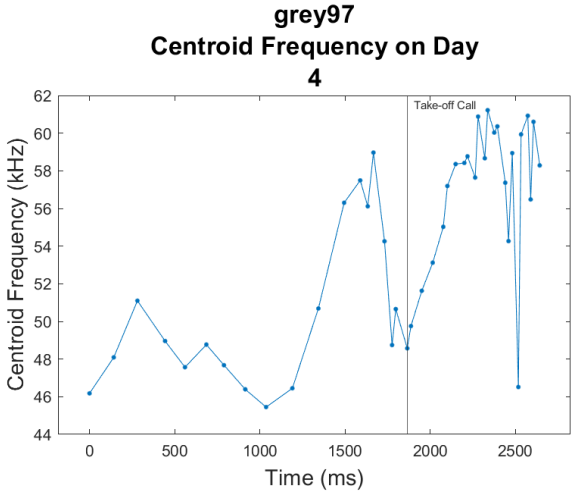
grey97
Centroid Frequency on Day
4
Take-off Call
Centroid Frequency (kHz)
Time (ms)

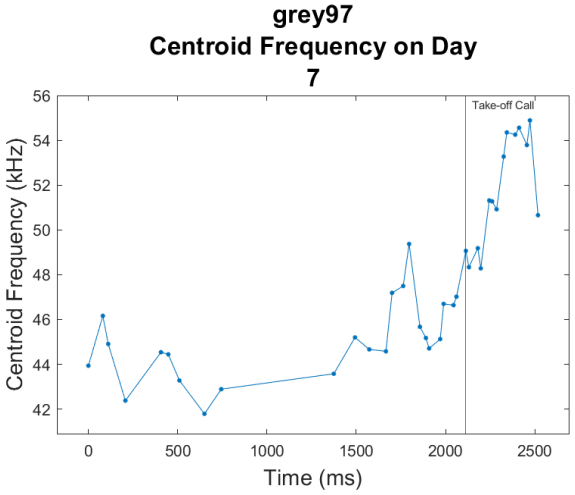
grey97
Centroid Frequency on Day
7
Take-off Call
Centroid Frequency (kHz)
Time (ms)

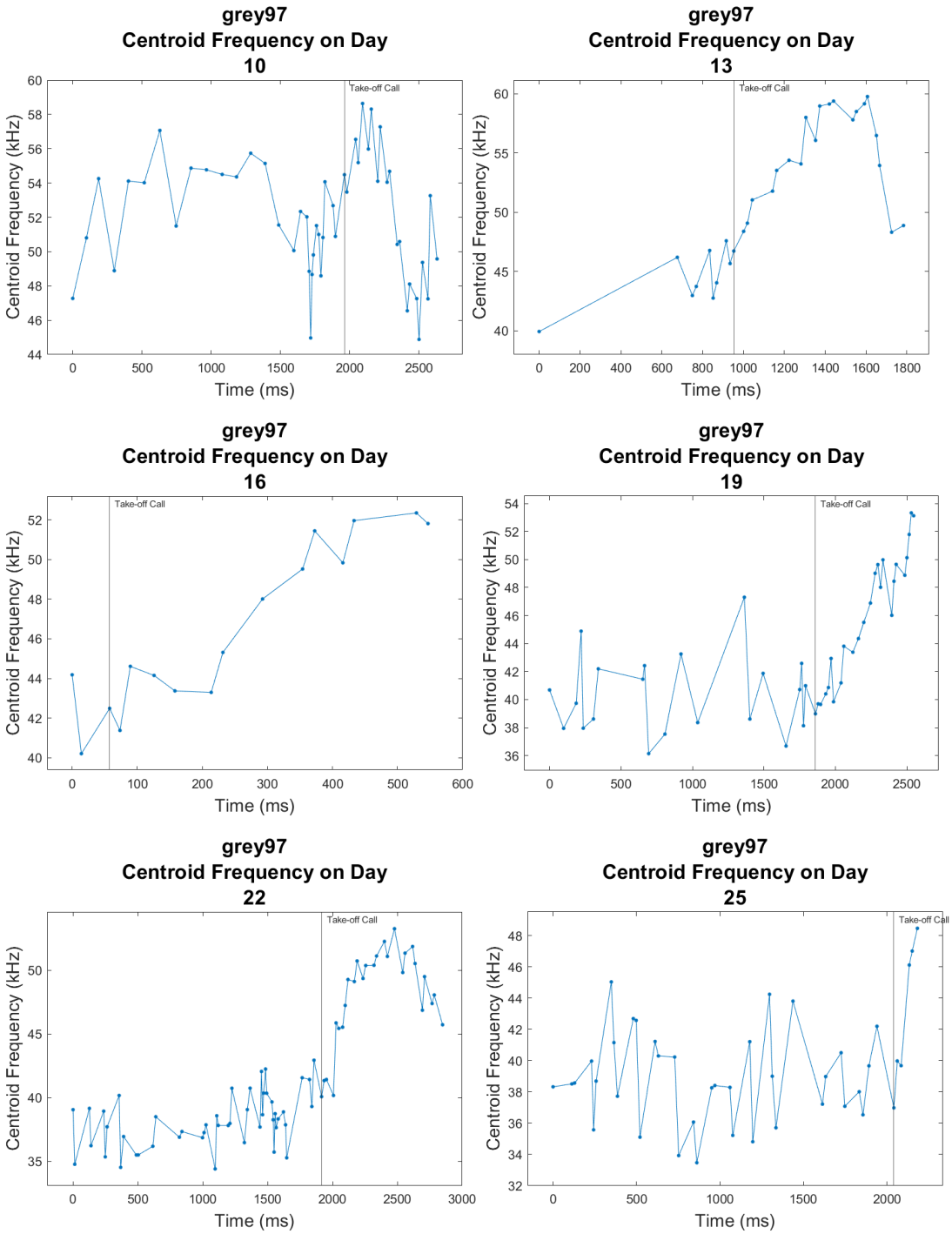

Appendix Figure 57: Grey 97 centroid frequency plotted as a function of recording time per day. Each panel shows call durations before and after taking flight, with different panels showing data recorded on different days relative to parturition (number above panel; parturition day defined as Day 0). The take-off call is marked by a vertical line.

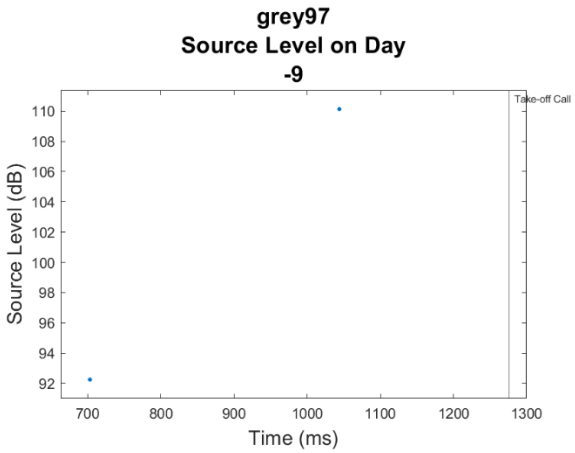
grey97
Source Level on Day
-9
Take-off Call
Source Level (dB)
Time (ms)

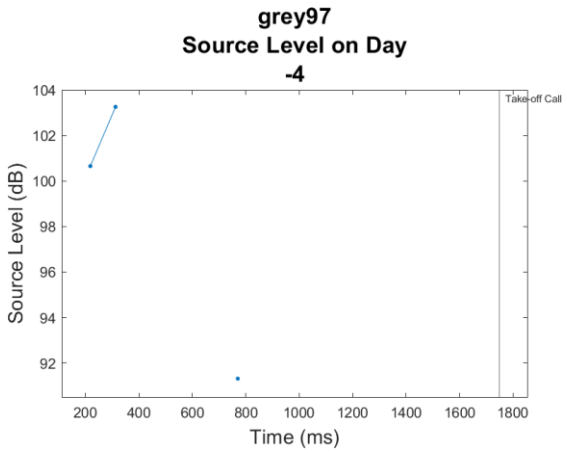
grey97
Source Level on Day
-4
Take-off Call
Source Level (dB)
Time (ms)

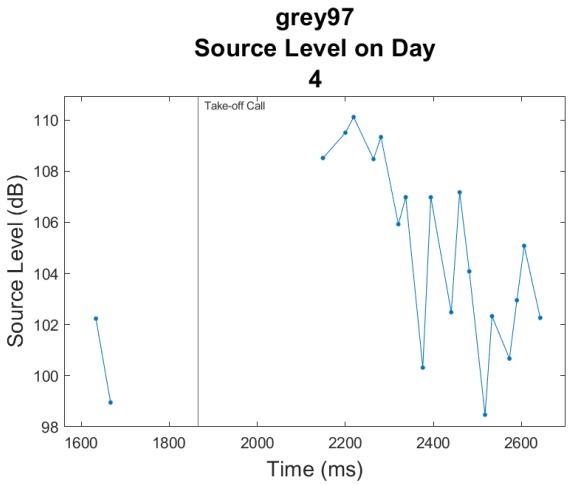
grey97
Source Level on Day
4
Take-off Call
Source Level (dB)
Time (ms)

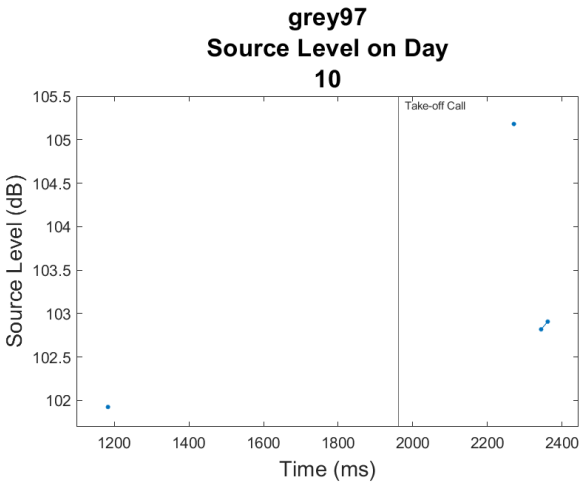
grey97
Source Level on Day
10
Take-off Call
Source Level (dB)
Time (ms)

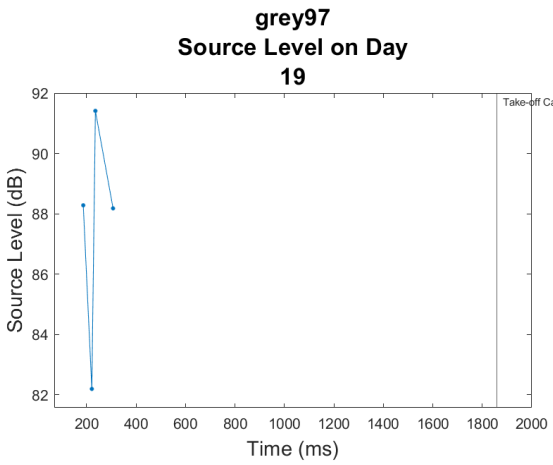
grey97
Source Level on Day
19
Take-off Call
Source Level (dB)
Time (ms)

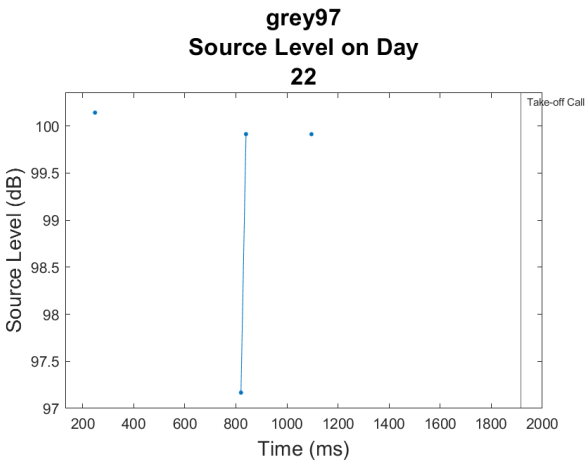
grey97
Source Level on Day
22
Take-off Call
Source Level (dB)
Time (ms)

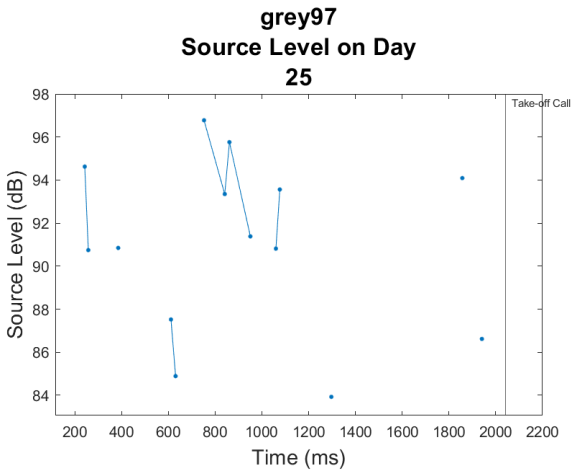

Appendix Figure 58: Grey 97 source level plotted as a function of recording time per day. Each panel shows call durations before and after taking flight, with different panels showing data recorded on different days relative to parturition (number above panel; parturition day defined as Day 0). The take-off call is marked by a vertical line.